ED730-LH

N° d'Ordre :041

THÈSE DE DOCTORAT

Présentée pour l'obtention du grade de

DOCTEUR DE L'UNIVERSITÉ DE LOMÉ

Ecole Doctorale Lettres et Humanités ED730-LH

West African Science Service Centre on Climate Change and Adapted Land Use

Domaine : Sciences de l'Homme et de la Société

Mention : Changement Climatique et Sécurité Humaine

Spécialité : Changement Climatique et Gestion des Risques de Catastrophes

Par

AKA Kadio Saint Rodrigue

YAM PRODUCTION RISKS ANALYSIS FOR FOOD SECURITY UNDER CLIMATE CHANGE IN GONTOUGO REGION (CÔTE D'IVOIRE), WEST AFRICA

Soutenue publiquement le 27 mars 2025 devant le jury composé de :

AKPAGANA Koffi	Professeur Titulaire	Université de Lomé	**Président du jury**
NANEMA Kiswendsida Romaric	Maître de Conférences	Université Joseph Ki-Zerbo, Burkina Faso	**Examinateur**
AGBOKA Komi	Maître de Conférences	Université de Lomé	**Examinateur**
AKPAVI Ben Semihinva	Professeur Titulaire	Université de Lomé	**Directeur de thèse**
DIBI N'da Hyppolite	Maître de Conférences	Université Félix Houphouët-Boigny, Côte d'Ivoire	**Co-Directeur**
Katharina LÖHR	Docteur	Centre Leibniz pour la recherche sur les paysages agricoles (ZALF), Allemagne	**Co-Directeur**

YAM PRODUCTION RISKS ANALYSIS FOR FOOD SECURITY UNDER CLIMATE CHANGE IN GONTOUGO REGION (CÔTE D'IVOIRE), WEST AFRICA

DOCTORAL DISSERTATION

By

Kadio Saint Rodrigue AKA

Supervised by

Sêmihinva Ben AKPAVI
Full Professor, University of Lomé, Togo

Co-Supervised by

Hyppolite N'da DIBI
Associate Professor, Félix Houphouët-Boigny University, Côte d'Ivoire

Katharina LÖHR
Doctor, Leibniz-Centre for Agricultural Landscape Research (ZALF), Germany.
Humboldt Universität zu Berlin, Germany.

UNIVERSITY OF LOMÉ
FACULTY OF HUMANITIES AND SOCIAL SCIENCES
WASCAL
Climate Change and Disaster Risk Management

Juillet, 2025

DEDICATION

In life, there are always those who believe in us, cheer us and support us through thick and thin in all our endeavours.
To them, I dedicate this thesis.

My thoughts are with the ALMIGHTY GOD, the Lord JESUS CHRIST, creator of heaven and earth, of the visible and invisible universe and of all that exists.

To:

My Mum, BINDE Ettien Blandine. My perpetual source of inspiration. Her love and everyday blessings continue to urge me ahead in life;

My Father, who never stopped praying for me from afar. His support and prayers for me were with me right to the end.

My uncle, BINDE Jacques. Brought me to his home in Abidjan, where I was educated from CM2 to BAC and later completed part of my university studies. I am forever thankful to him;

My uncle, BINDE Claver. Always there in my worst moments, lending a helping hand and guiding me forward. He believes in me and is always willing to provide me with the resources I need to succeed;

My mentor, KONAN Frédéric. An extremely valuable person to me. He reached out to me directly from his heart when we initially met. He is an unwavering support for me. His persistent prayer life, wisdom, and professional expertise have been passed down to me. What could be more natural than to devote my loyalty to him and perpetuate these incomparable values?

ACKNOWLEDGEMENTS

First of all, I am grateful to Almighty God for my life, his blessings, his love, and for providing me with the intellect, wisdom and vision to grasp the topic discussed in this PhD. The PhD is an intense test of reading and writing, two elements in which I have improved and surpassed myself enormously during this doctoral journey. It was an arduous exercise, fraught with pitfalls and doubts. Yet some people encouraged and supported us, whether willingly or unwittingly. I want to take this opportunity to thank everyone who helped us accomplish this project; without them, this PhD would not have been possible.

I would particularly express my deepest gratefulness to the **West African Science Service Centre on Climate Change and Adapted Land Use (WASCAL)** program and the **German Federal Ministry of Education and Research (BMBF)** for their financial support through the WASCAL scholarship.

I would also like to thank the **University of Lomé**, headed by **Professor Adama Mawulé KPODAR**, for welcoming us into the Wascal-Togo program Climate Change and Disaster Risk Management through the Doctoral School of Arts and Humanities.

I am thankful to **Professor Komi AGBOKA**, **Director of WASCAL-Togo**, and his team for providing us with the tools and assistance we needed to accomplish this program. Their commitment to perfection has been very inspiring.

Regarding technical and academic supervision, I was lucky enough to have worked with **Professor AKPAVI Ben Sêmihinva** from the **University of Lomé** as my **main supervisor**. He is a big-hearted man who knows how to promote people and make himself available for any need. Thank you very much, Professor, for your wise advice and support throughout this doctoral research.

My gratitude also extends to **Professor DIBI N'Da Hyppolite**, my **co-supervisor** from the **University Félix Houphouët-Boigny** of Abidjan. He is like a father to me. He introduced me to research at the University Centre for Research and Application in Remote Sensing (CURAT) in Abidjan, where I got my first Master's degree alongside him. He has made a significant contribution to the achievement of this thesis. Thank you so much, Professor, for your scientific rigour, observations and suggestions that have contributed to improving the content of this book.

I am thankful to my **German co-supervisor, Dr. Katharina LÖHR**, for inviting me to their research centre at the **Leibniz Centre for Agricultural Landscape Research (ZALF)**. She and her team at the SUSLand group assisted me in understanding scientific techniques, as well as providing assistance and practical guidance in fulfilling many of the thesis's aims. Thank you very much, Doctor, for your weekly meetings and regular updates on my progress during my time in Germany till the completion of my dissertation.

A special thanks to my company, the **National Office for Technical Studies and Development (BNETD)** through the **Center for Geographic and Digital Information (CIGN)** in Abidjan, Côte d'Ivoire, which greatly contributed to facilitating access to data collection in the field at a certain time and which was comprehensive in permitted me to complete my thesis. We would also like to thank the National Rural Development Support Agency (**ANADER**) in Bondoukou and Tanda for helping us connect with farmers in the field. We are grateful to Houphouët-Boigny National Polytechnic Institute of Yamoussoukro (**INPHB**) for their support in analyzing soil samples in their soil laboratory. The same goes for **3A Environmental Solutions Ltd. in Sunyani, Ghana**, for hosting me as an intern for advanced training and data analysis.

I thank **Ahou Clarisse KOFFI, Moctar TRAORE, and Ayman OBENG Manu** for their support in designing methods and data collection from the field. I also extend my thanks to **Christ Herbert KOFFI, Kassoum OUATTARA, Kouamé Donald KOUMAN, Zié Adama OUATTARA, Dr Fulgence KOUAME, Dr Hgazat Valerie KOUAME and Venance KOUADIO** for their near and far support, and especially for everything they have and continue to provide me. God bless you for reaching out to me at an appropriate moment.

I acknowledge the support of **colleagues of this fifth batch of WASCAL-Togo** not forgetting my parents, particularly my elder sister **Esther KOFFI and her husband Barthelemy BROU from Abengourou**, and my younger sister **Marie Noelle**. God bless all of you!

Finally, I would like to say a special word of thanks to all the people for their diverse support, prayers, and constant encouragement, and to those, I did not mention, please accept my sincere gratitude.

LIST OF CONTENTS

ABSTRACT

Yam, a staple food crop in Côte d'Ivoire, is the main source of livelihood for many inhabitants in the Gontougo region. Changes and variations in climate have significant impacts on its productivity. Soil depletion, variations in cropping seasons and dropping down of some agronomic practices due to climatic variability, varieties not adapted to the current climate and growing up of perennial crops such as cashews which dominating the landscape, are the main issues confronting the yam sector in the Gontougo region. This research aims to examine yam production risks and adaptive methods implemented by farmers using different methods. Firsly, we computed LULC changes and examined the vegetation healthy (NDVI) using Landsat 8 images and evaluate their effect on land surface temperature (LST). The Pearson correlation between the two parameters indicated that LST is hot when vegetation is low (strong negative coorelation) and the LULC classes forest and annual crops loose 48.13% and 65.14%, respectively of their areas for the benefit of perennial crops from 2015 to 2022. In the next step, a total of eight composite soil samples were collected ranging from 0 – 40 cm horizon on the yams farming in Tanda's and Bondoukou's department which are respectively forest and savannah zones and underwent physicochemical analysis. We discovered that soil under savannah is mainly coarse sandy (52.61%) as opposed to soil under forest which is less coarse sandy (41.63%). By computing some climate indices and surveyed communities, we discovered that yam farmers are mostly worried about rain uncertainties, decreasing of suitable land to grow and surface temperatures due to the decline of vegetation. The effects are felt most in Bondoukou's department (92.48%) than in Tanda's department (61%). Finally, the climate change scenarios coupled model intercomparison project phase 6 (CMIP6) historical and future model data including ssp2-4.5 and ssp5-8.5 have been used in the statistical Multiple Linear Regression model. The results of the simulations were carried out over 30 years (2025 - 2054) and indicate that both climate scenarios (ssp2-4.5; ssp5-8.5) show that yam yields will be lower than in the reference period. Yield variations could vary between -10% to -45% depending on the climate scenario. Effective and robust adaptation strategies, agricultural innovation, and substantial investment will be crucial to mitigate these negative impacts and sustain yam production in the face of rapid climate change.

Keywords: yam production, land surface temperature, agro-climatological risks, yield predicting, food security.

RÉSUMÉ

L'igname, culture vivrière de base en Côte d'Ivoire, est le principal moyen de subsistance de nombreux habitants de la région de Gontougo. Les changements et les variations climatiques ont des répercussions importantes sur sa productivité. L'épuisement des sols, les variations des saisons culturales et l'abandon de certaines pratiques agronomiques en raison de la variabilité climatique, les variétés non adaptées au climat actuel et la montée en puissance des cultures pérennes telles que l'anacarde qui domine le paysage, sont les principaux problèmes auxquels est confrontée la filière igname dans la région de Gontougo. Cette recherche vise à examiner les risques liés à la production d'igname et les méthodes d'adaptation mises en œuvre par les agriculteurs en utilisant différentes méthodes. Tout d'abord, nous avons calculé les changements d'occupation du sol et examiné la santé des végétations (NDVI) à l'aide d'images Landsat 8 et évalué leur effet sur la température de surface du sol. La corrélation de Pearson entre les deux paramètres indique que la température de surface des terres est élevée lorsque la végétation est basse (forte corrélation négative), aussi les classes d'occupation du sol forêt et cultures annuelles ont perdu respectivement 48,13 % et 65,14 % de leur superficie au profit des cultures pérennes entre 2015 et 2022. Par ailleurs, un total de huit échantillons composites de sol ont été prélevés entre 0 et 40 cm de profondeur sur la culture d'ignames dans les départements de Tanda et Bondoukou, qui sont respectivement des zones de forêt et de savane, et ont fait l'objet d'une analyse physico-chimique. Nous avons découvert que le sol sous savane est principalement sableux grossier (52,61%) et contient peu d'argile par opposition au sol sous forêt qui est moins sableux (41,63%) et contient plus d'argile et de limon. En calculant certains indices climatiques et en enquêtant auprès des communautés, nous avons découvert que les producteurs d'ignames sont principalement préoccupés par les incertitudes liées aux pluies, la diminution des terres propices à la culture d'igname et les températures de surface en raison du déclin de la végétation. Les effets sont plus ressentis dans le département de Bondoukou (92,48%) que dans le département de Tanda (61%). Enfin, les données des modèles historiques et futurs des scénarios de changement climatique du projet de comparaison des modèles couplés phase 6 (CMIP6), y compris ssp2-4.5 et ssp5-8.5, ont été utilisées dans le modèle statistique de régression linéaire multiple. Les résultats des simulations ont été effectués sur 30 ans (2025 - 2054) et indiquent que les deux scénarios climatiques (ssp2-4.5 ; ssp5-8.5) montrent que les rendements de l'igname seront inférieurs à ceux de la période de référence. Les variations de rendement pourraient varier entre -10% et -45% en fonction du scénario climatique. Des stratégies d'adaptation efficaces et solides, l'innovation agricole et des investissements substantiels seront essentiels pour atténuer ces impacts négatifs et soutenir la production d'ignames face à un changement climatique rapide.

Mots-Clés : production d'igname, Température de surface du sol, risques agro-climatologiques, prévision de rendement, sécurité alimentaire

LIST OF ABBREVIATIONS

ANOVA	: Analysis of variance
ANADER	: National Agency for Rural Development Support
AR5	: Fifth Assessment Report
AR6	: Sixth Assessment Report
C	: Carbon
c-Sand	: coarse Sand
c-Silt	: coarse Silt
CA	: Correspondence Analysis
CDD	: Consecutive Dry Days
CEC	: Cation Exchange Capacity
CGS or CS	: Cessation Of The Growing Seasons
CHIRPS	: Rainfall Estimates from Rain Gauge and Satellite Observations
CMIP6	: Coupled Model Intercomparison Project Phase 6
CNRA	: National Center for Agricultural Research
CUS	: Cumulative Rainfall Seasonal
CWD	: Consecutive Wet Days
ETCCDMI	: Expert Team on Climate Change Detection Monitoring and Indices
FAO	: Food and Agriculture Organization
f-Sand	: fine Sand
f-Silt	: fine Silt
GDD	: Growing Degree Days
GEE	: Google Earth Engine
GIS	: Geographic Information System
IPCC	: Intergovernmental Panel on Climate Change
JS	: JavaScript
LGS or LOS	: Lengths Of The Growing Season
LODS	: Length Of Intraseasonal Dry Sequence
LST	: Land Surface Temperature
LULC	: Land Use Land Cover
MINADER	: Ministry of Agriculture and Rural Development
ML	: Machine Learning
MLR	: Multiple Linear Regression
N	: Nitrogen
NDVI	: Normalized Difference Vegetation Index
OA	: Overall Accuracy
OGS	: Onset Of The Growing Seasons
OLI	: Operational Land Imager
ORSTOM	: Office of Scientific and Technical Research Overseas

P	Phosphorus
PA	: Producer Accuracy
PCA	: Principal Component Analysis
pH	: potential Hydrogen
PRCPTOT	: Total Precipitation index
RCP	: Representative Concentration Pathway
RF	: Random Forest
RFA	: Random Forest Algorithm
RGPH	: General Census of Population and Housing
SODEXAM	: Airport, Aeronautical and Meteorological Exploitation and Development Company
SPI	: Standardized Precipitation Index
SSA	: Sub-Saharan Africa
SSP	: Shared Socioeconomic Pathways
TIRS	: Thermal Infrared Sensor
Tmax	: Maximum temperature
Tmin	: Minimum temperature
UA	: User Accuracy
WA	: West Africa
WASCAL	: West African Science Service Centre on Climate Change and Adapted Land Use
WCRP	: World Climate Research Programme
WMO	: World Meteorological Organization

LIST OF FIGURES

LIST OF TABLES

GENERAL INTRODUCTION

Yam life cycle and its production worldwide

Yam (*Dioscorea spp*.) is an annual or perennial vine and a climbing plant with annual or perennial underground tubers. His life cycle includes the following stages: tuber, seedling, emerging seedling, mature plant, senescent plant and dormant tubers. Yam has an annual vegetative system consisting of a root system (**Figure 1**) extending into the upper layers of the soil, root hairs, a stem system, a leaf system and a reproductive system (Akoroda, 1993; Diby et al., 2011; Wumbei et al., 2022).

Figure 1: a-Yam plants growing in the field, b-Roots on tuber skin, c-Adventitious roots
Source: (Wumbei et al., 2022)

Yams are grown in mounds of soil between 30 and 50 cm high and are vegetatively multiplied using the basal nodal region of the tuber, as flowering is rare Additionally, yams can also be propagated through vine cuttings or by planting whole tubers (Adifon et al., 2019; Wumbei et al., 2022). The plant generally produces one or two tubers a year, up to 50 cm long and weighing between two and twelve kilograms, depending on the cultivar and growing conditions (Aighewi et al., 2015). The body may be elongated or spherical, with white, yellow or violet flesh (Adifon et al., 2019; Aighewi et al., 2021; Neina, 2021; Wumbei et al., 2022). Yams belong to the family *Dioscoreaceae*, with about 650 species produced around the world (Akoroda, 1993). To date, about 20 of these species are under production as principal food sources for the human diet in the tropics (World Bank Group, 2019; Wumbei et al., 2022). Almost all the world's yam production takes place in developing countries. According to the International Institute of Tropical Agriculture (IITA), the majority of this production (90%) takes place in Africa, the South Americas, the Caribbean, the South Pacific and Asia (**Figure 2**). Nigeria, Ghana, and Côte d'Ivoire dominate yam production in West Africa, accounting for around 94% of world yam output and serving as an important crop for food security and generating income (Danquah et al., 2022; Ema et al., 2023).

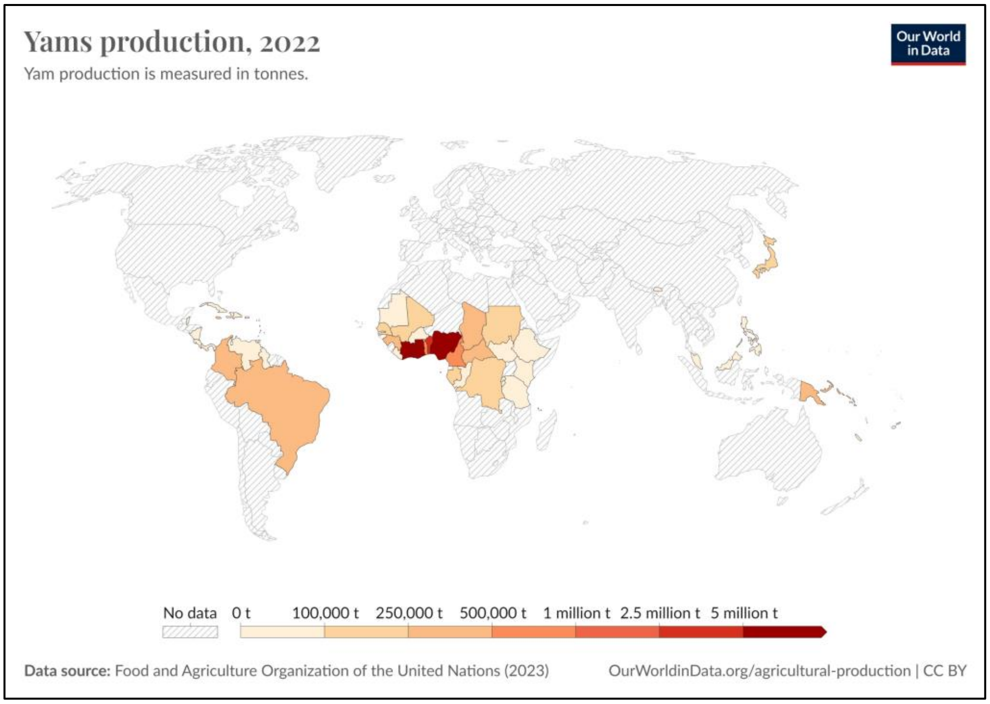

Figure 2: World yam production in 2022

White Guinea yam, "*D. rotundata"*, is the most important species, especially in the dominant yam production zone in West and Central Africa. It is indigenous to West Africa, as is the Yellow yam, "*D. cayenensis*". Water yam, "*D. alata*", the second most cultivated species, originated from Asia and is the most widely distributed species in the world (Ema et al., 2023; Frossard et al., 2017; Danquah et al., 2022; Lebot & Dulloo, 2021) Yam is the second most important root/tuber crop in Africa after cassava and is extremely important to food security in the world (Vincent Lebot & Ehsan Dulloo, 2021). It has excellent storage properties and can be stored for four to six months without refrigeration and provides an important food safety net between growing seasons (Adifon et al., 2019; Kouadio et al., 2022; Lebot & Dulloo, 2021). Yam tubers contain around 21% dietary fibre and are rich in carbohydrates (27-30g per 100g), crude fibre vitamin B, vitamin C and essential minerals which are small amounts. For consumption, yams are boiled, roasted, baked or fried. They are also mashed into a sticky paste after boiling (Akoroda, 1993; Kouakou et al., 2019; Kumar et al., 2017; Wumbei et al., 2022). In Africa, the yam is of particular traditional and cultural importance to many people. It is highly venerated and is at the heart of important festivities such as weddings, chiefs' ceremonies, yam festivals and sacrifices to the gods. On the other hand, resolutions of conflits and peace agreements are linked to it (Ema et al., 2023; Obidiegwu et al., 2020; Lebot & Dulloo, 2021).

Climate risks and adaptation strategies for yam farming in West Africa

Over the past 30 years, most countries have seen a rise in per capita food output. However, the opposite is happening in the Sub-Saharan Africa (SSA) region in West Africa (WA). The region faces food shortages almost every year due to crop failure or low crop yields (Diancoumba et al., 2023; Sultan et al., 2019; Waongo, 2015). As dominated by rainfed agriculture, SSA is one of the regions most affected by climate change. Furthermore, rainfed agriculture in SSA is dominated by smallholder farming systems with limited investment opportunities (e.g., fertilizers, pesticides, machinery) and irrigation, making it the most vulnerable agricultural system (Diancoumba et al., 2023; Roudier et al., 2011; Waongo et al., 2015). The region faces high seasonal variability in precipitation, rising temperatures and a lack of adaptive capacity. These constitute major barriers to rainfed agriculture in smallholder systems and can directly lower the yields of most food crops (IPCC, 2014; Langsdorf et al., 2022). However, rainfed agriculture is the main activity and source of income for the majority of SSA inhabitants, and so has a significant impact on regional food security (Diancoumba et al., 2023; Sultan et al., 2013). Climate being the most limiting factor to agricultural success in WA, several studies addressing yam production risks have tried to alleviate several problems in this sector. Most are based on the control of rainfall to establish a seasonal cultivation calendar because according to Waongo's planting date study, the growing season in WA lasts only a few months and therefore limits the time the crop should be planted for best results (Waongo, 2015). Indeed, there is a strong relationship between the growing season and the rainy season for any rainfed agriculture. Early sowing dates can lead to crop failure due to long dry spells that can occur soon after planting (Cheng et al., 2021; Missana et al., 2020). On the other hand, late sowing dates are likely to avoid bad harvests but they correspond to short growing seasons, which can reduce also crop productivity (Laux et al., 2008). The crops to be planted are the results of the length of the growing season and the farmer's ability to find labor (i.e., for farmland preparation and seeding) and seeds. Also, for a good harvest, there must not be a long period of drought after planting because this dries out the topsoil then reduces the availability of nutrients in the soil and has a negative impact on productivity (Danquah et al., 2022; Zougmoré et al., 2018). Other concerns, such as soil and vegetation type, were briefly discussed in the literature on yam cultivation. Yam is a nutrient-demanding crop that requires soils high in organic matter and critical nutrients such as nitrogen, phosphorus, and potassium. For Oka et al., (2021) the diversity of yam produced is determined by soil type, which has a considerable influence on yam growth and productivity. This has been echoed by several authors (Diby, Hgaza, et al., 2011; Diby, Tie, et al., 2011; N'guessan et al., 2009) who argue that soil fertility affects yam growth and therefore yield. The type of vegetation in a given location determines the microclimate, which in turn influences yam growth. Many yams are cultivated in the savannah zones (Adeleke Aturamu et al., 2021; Felix et al., 2020). However, depending on the type, wooded places may be ideal since they give shade and lessen the impact of high temperatures, which is advantageous to yam plants (Adeleke Aturamu et al., 2021). All of these are production risks that must be managed to maintain adequate yields. As a result, yam farmers have devised a variety of risk-management measures. Adaptation measures like planting date which is a cost-effective agricultural management strategy designed to reduce crop water stress and help improve agricultural decision-making, especially as a climate change adaptation strategy are urged to be implemented (Dobor et al., 2016; Laux et al., 2010; Olayiwola Eruola et al., 2012; Waongo et al., 2015). Besides, a wide range of crop management strategies minimizes production costs. Among these, we can mention improved endogenous knowledge, the stone bunds, micro-water harvesting (zaï technique) and demi-lune technique by water catchment, which have been largely uptaken by farmers (Bintou, 2010; FAO, 2015a; Mackio, 2022). Moreover, the introduction of early warning systems (EWS) for regular production monitoring is helping farmers cope with climatic hazards. It is a system designed to continually collect information on the food security situation in areas of concern. Monitoring helps generate zone-specific integrated food security analysis tools, as well as alerts on acute, emerging or expected food insecurity situations (Courault et al., 2021; Enten François, 2017). Several studies in this field have been carried out to predict future climate, monitor crops to prevent pest attacks or predict yield using dynamic or statistical agricultural models for decision-making (Adeleke et al., 2021; Cedric et al., 2022a; Egbebiyi et al., 2019; Kim et al., 2024; Leng & Hall, 2020; Rojas & Senay, 2021). However, the high level of poverty in WA leads farmers to abandon some crop management technologies and approaches, even though they are proven to be efficient (Waongo, 2015). Thereby, only those strategies which require little resources in terms of labor and money have a chance to engage a large number of farmers. Other agricultural adaption strategies may include agronomic practices that enhance soil water retention such as minimum tillage and increase in soil carbon and organic matter (FAO, 2015a). The use of adapted varieties or breeds, with different environmental optima and/or broader environmental tolerances, including currently neglected crops, also considering that increased diversification of varieties or crops is a way to hedge against risks of individual crop failure. Adaptive changes in crop management, especially planting dates, cultivar choice and sometimes increased irrigation have been studied to varying extents and are generally estimated to have the potential to increase yields by about 7–15% on average, though these results depend strongly on the region and crop being considered. Changes in post-harvest practices, for example, the extent to which grain may require drying and how products are stored after harvest (FAO, 2015a; Siddique et al., 2024).

Yam (*Dioscorea spp*) production and food security in Côte d'Ivoire

Yams belong to the family *Dioscoreaceae*, with about 650 species produced around the world (Akoroda, 1993). To date, about 20 of these species are under production as principal food sources for the human diet in the tropics (World Bank Group, 2019; Wumbei et al., 2022). Nigeria, Ghana, and Côte d'Ivoire dominate yam production in West Africa, accounting for around 94-98% of world yam output and serving as an important crop for food security and generating income (Danquah et al., 2022). Yam is produced throughout the Ivorian territory with different proportions depending on the agro-ecological zones. Its germination is optimal between 25 and 30°C and successful very well in areas where rainfall varies between 900 and 1800 mm (Adifon et al., 2019; Andres et al., 2016; Heller et al., 2022; Neina, 2021; Tchein et al., 2019). According to FAO statistics, yam's total production volume was around 7,853,083 tonnes in 2021 in Côte d'Ivoire (FAOSTAT, 2023). It accounts for over 45% of the rural population (MINADER, 2017) and is the first food crop produced in Côte d’Ivoire (Diarrassouba, 2019; Kouakou et al., 2019). However, its growing is costly and challenging. Planting and harvesting are labor-intensive. Some varieties have a long crop cycle and poor seed multiplication ratio. Nutritional value, yield, texture and postharvest durability vary significantly with soil quality and climactic factors. Due to its high soil nutrient demands, many farmers slash and burn directly before planting. Decreasing soil quality and soil pest pressures have pushed many traditional production zones to switch to other crops (World Bank Group, 2019). Innovations to improve productivity and reduce labor are needed in order to sustain this long-standing market. The northern, central and eastern regions are the biggest yam producers in Côte d’Ivoire. The landrace varieties *Kponan*, *Krengle*, *Djate*, are in high demand, as are the adapted varieties TDA, Mao and C20 (MINADER, 2017). These varieties have demonstrated good productivity, disease resistance and drought tolerance. Yam production is traditionally the work of men, while women are primarily involved in processing and marketing

(Doumbia et al., 2014; MINADER, 2017). But women now make up the vast majority in this sector. Men have shifted to cash crop agriculture, lowering both productivity and cultivation area. Several types of culinary uses of yams are made in Côte d'Ivoire because of its nutritional importance and its original familiarity with certain peoples especially from the eastern and northeastern parts. These uses are among others: "*foutou (pounded yam), Akpessi (boiled yam), yam stew, roasted yam and fries yam*". Six varieties of yams are generally found in markets in Ivory Coast. These are the early varieties *Kponan, Assawa and Lokpa* (*Dioscorea cayenensis-rotundata* with two harvests) and the late varieties *Krenglè* (*Dioscorea cayenensis-rotundata* with one harvest), *Bètè bètè* and *Florido*, (*Dioscorea alata*) (Doumbia et al., 2006; Kouakou, 2019; Kouakou et al., 2019) . The three species of yams mentioned take turns in time and the market is always characterized by the presence of at least two species including *kponan*. *Kponan* is the most popular yam variety in all culinary forms from its first harvest in the last decade of July to January. Extended storage until June lowers its culinary quality and it is *Bètè bètè* variety that is gaining consumer preference, after improving in quality at this time of year. *Krenglè* is especially appreciated during its harvest period in January. The other varieties, *Florido, Assawa* and *Lokpa* are the least appreciated in all culinary forms throughout the year (Anatole et al., 2017; Nindjin et al., 2009).

Problem statement

Gontougo region supplies 60% of the Ivorian economic capital's wholesale yam market, including *Kponan*, the most desired by Abidjan's people (Kouakou et al., 2019). This region therefore has a high potential for yam production which is also a staple food for its people. According to a traceability analysis of Bondoukou's *Kponan* yam, the Gontougo people have centuries of yam-producing experience. This extensive knowledge is evident in the unique farming procedures and traditional preservation techniques that have been passed down through generations to ensure sustainable production (Kouakou, 2019). Given the region's vast potential and farmer's skill in yam growing, what inspired our inquiry? Is there a specific issue affecting the crop and/or farmers in this region? The answers to these questions will help us grasp the goal of our research.

The first discovery that piqued our interest was that national yam yields have been dropping over time. This is borne out by FAO country statistics (FAOSTAT, 2023). **Figure 3** below shows that from 2000 to 2021 in Côte d'Ivoire, yams yield declined from 88,172 to 54,605 hg/ha while the production and area harvested increased gradually.

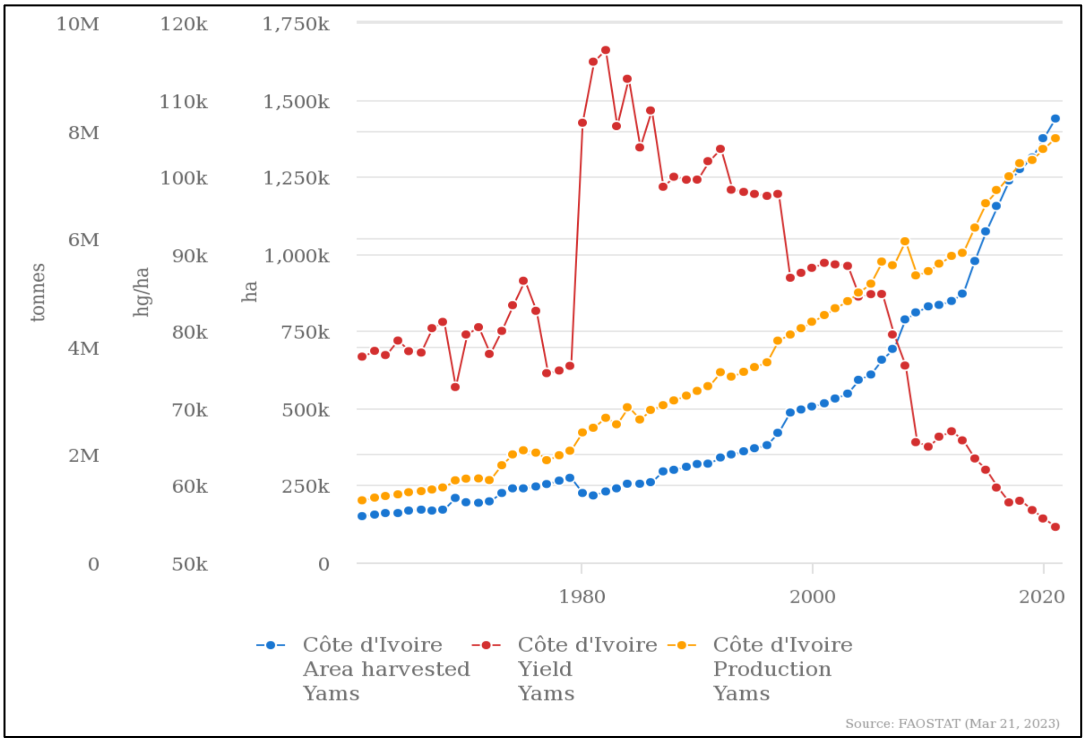

Figure 3: Annual variation in yam yield from 1961 to 2021 in Côte d'Ivoire

This national yield decreasing have an impact on the Gontougo region, which is a key local production area accordind to the National Rural Development Support Agencies (ANADER). Since we had no reliable yield data for each location, we carried out further investigations to find out more during our survey. Several studies also indicate that the region is an important cashew-growing area (Kambou et al., 2019; Konaté et al., 2021; Kouman et al., 2022). Cashew nut production requires a large amount of space, and fertile land is becoming increasingly rare as a result of overexploitation and plant cover deterioration. The spread of this cash crop is lowering the amount of space accessible for yam production, depletes the soil, changing the agricultural environment over time, and having a significant impact on land surface temperatures (Félicia et al., 2017; Gogoi et al., 2019; Yao et al., 2023) According to ANADER, perennial crops, particularly cashew nuts, are the most common LULC type in the Gontougo region. It takes up more than 60% of the study area. This is a real problem for subsistence crops such as yams, which are the most widely consumed crop in the households. In terms of climate, rainfall in the Zanzan district, of which the Gontougo region is a part, has ranged from 895.56 mm to 1327.2 mm between

2011 and 2020 (Kouman et al., 2022). These values are slightly higher than in previous decades, with false starts in rainfall and uncertainties over crop establishment (Brou et al., 2005; Kouman et al., 2022; Srivastava, et al., 2012). The growing seasons are therefore out of synchronization with the cropping calendars, making it difficult for yam farmers to reach maximum production. Finally, according to the secretary of the Permanent Inter-State Committee for Drought Control in the Sahel (CILSS), the Gontougo region is one of the areas with the highest prevalence of food insecurity (CILSS, 2021). All these raise multiple challenges in the study area including climate hazards manifested by rainfall uncertainties and dry spell frequencies, arable land availability and soil fertility issues. Thus, new farming methods or improved species must be implemented to boost yields. This is what we shall seek to comprehend and examine through this research, which we have the distinction of steering.

Objectives of the thesis

The general aim of this research project is to help achieve food and nutritional self-sufficiency in Côte d'Ivoire by addressing the risks of yam production in the Gontougo region.

To accomplish this goal, the following research questions will lead the investigation:

i. What is the prevailing state of vegetation cover dynamics and its implications for land surface temperature in yam production?

ii. What are the agro-pedological and agro-climatological risks that yam farmers experience, and what agricultural strategies do they implement to adapt?

iii. What will be the future trends in yam yields under IPCC climate scenarios conditions?

Answering these questions involves the following specific objectives:

i. Evaluate the effects of land use land cover change and NDVI on land surface temperatures

ii. Determine agro-pedological and agro-climatological threats to yam production and farmers' agronomic practices to mitigate them

iii. Analyze future trends in climate change and simulate yields

Innovations of the thesis

Yam production risk analysis is an approach intended to optimize agricultural output. It, therefore, helps to solve some problems of food insecurity. Very few studies conducted in Côte d'Ivoire address these different aspects around which we have developed methods. They feature the following innovations:

- ❖ Environmental risk assessment using remote sensing and GIS, pedological, climatic and socio-economic risks analyzed in a single study;
- ❖ Development of a statistical yield prediction model using SSP scenarios from the sixth IPCC report;
- ❖ This study is therefore timely to draw scientific world research attention and Ivorian decision-makers that the effects of climate change on agricultural resources must be anticipated now. At the end of COP15 on desertification which took place from 9 to 20 May 2022 in Abidjan, we are taking advantage of this research to implement climate-adaptive responses to the growing scarcity of rainfall and advancement of the desert.

Outline of the thesis

The thesis is split into five chapters excluding the general introductory section which addresses the context and problems, establishes the objectives and structure of the thesis and describes the study area and then the general conclusion section.

The first chapter is a literature review of the agro-climatological-related risks of yam production. Chapter two is devoted to addresses land use land cover changes and its effect on land surface temperature. Chapter three is dedicated to soil physicochemical properties under savannah and forest areas. Chapter four deals with agro-climatological risks and farmers' agronomic practices and their adaptive response. Chapter five concerns the last objective specifically the analyse of future trends under the IPCC Scenario and yield prediction.

The general conclusion which provides recommendations for farmers and technical support agencies and opens an outlook showing different avenues to be taken for future studies relating to the different aspects discussed, and the scientific, political and socio-economic implications of our study.

Study area description

The study was conducted in Gontougo region located in Eastearn part of Côte d'Ivoire. Since its creation in 2011, it has been one of the two regions in Zanzan District. The capital of the region is Bondoukou and the region's area is 16,100 km2, the population in the 2021 census was 917,828.

Gontougo is currently divided into five departments: Bondoukou, Koun-Fao, Sandégué, Tanda, and Transua (RGPH-CI, 2021) and located between 4°00’ and 2°50’ W longitudes. and 6°30’ and 8°50’ N latitudes. (**Figure 4**). Agriculture is mainly dominated by cashew nuts and yam, livestock production, trade (food crops, handicrafts, etc.) and services drive the region's economy (Kouakou, 2019; Kouman et al., 2022).

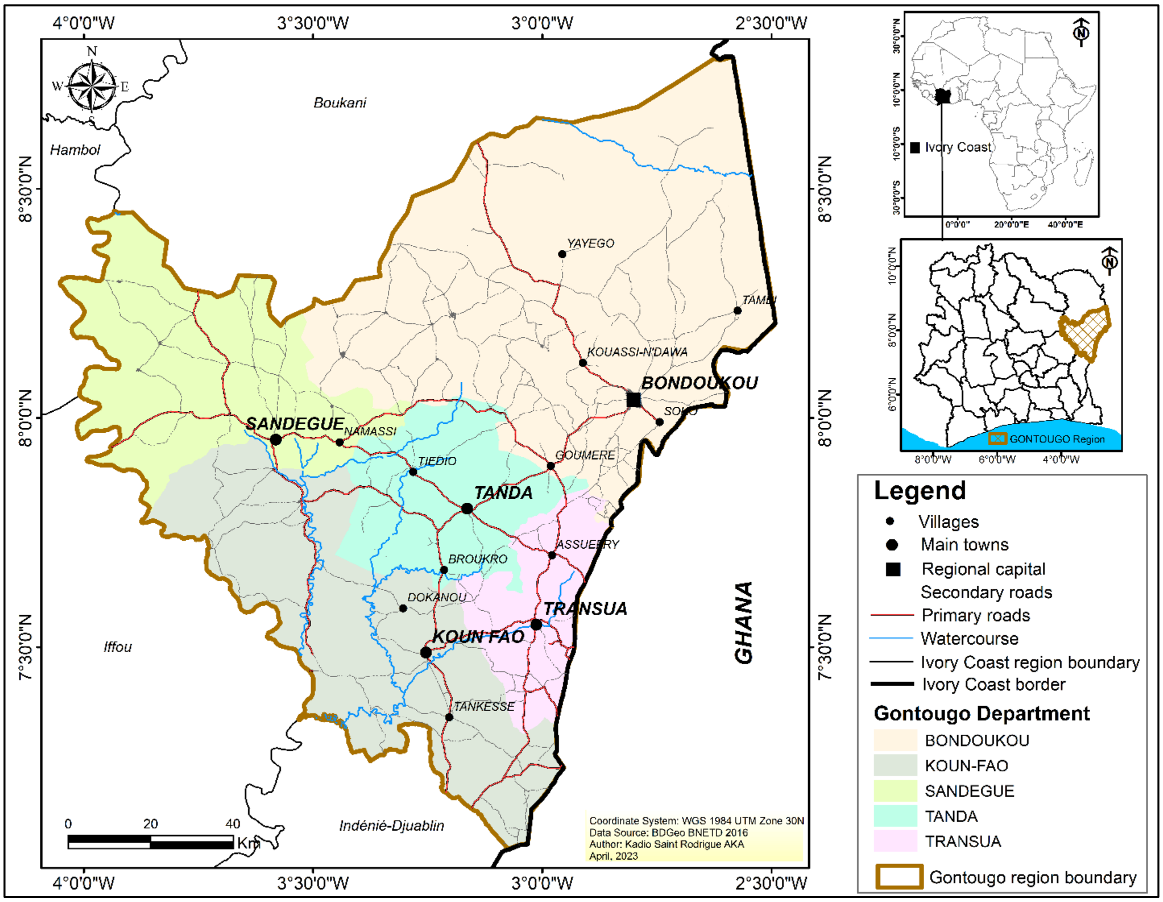

Figure 4: Geographic situation of the Gontougo region

The region's geological substratum is a type of granitoid, characterised by granodiorite intrusions around Bondoukou and in the Kihouo mountains. Elevations range from 114 meters in the southwest to 741 meters in the Bondoukou area, which contains elevated landscapes and mountains (**Figure 5**).

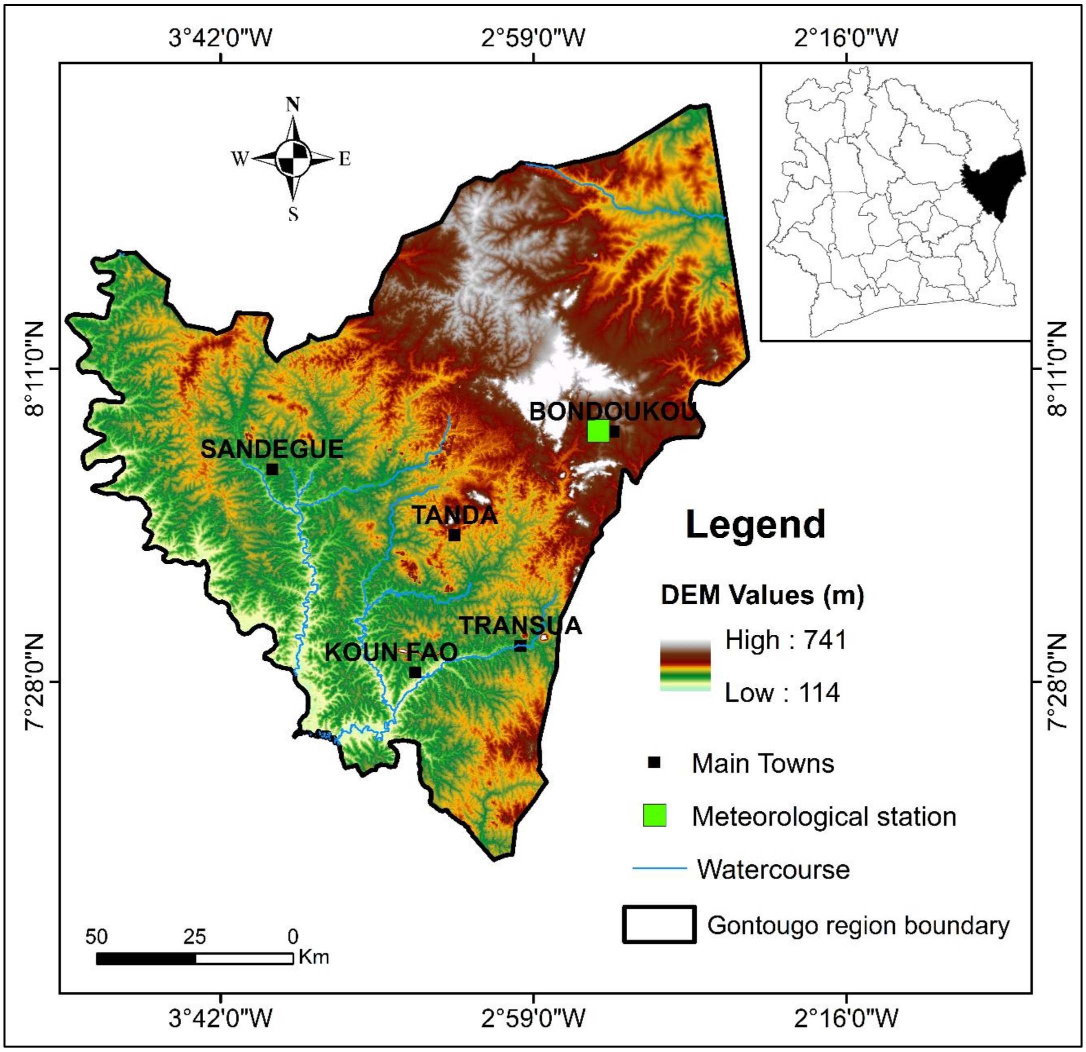

Figure 5: Topography of the Gontougo region

The region's soils are ferralitic, more or less desaturated, with deep sandy-clay soils that are highly suitable for cash crops (cashew, cocoa, coffee, rubber) and food crops such as yams (République de Côte d'Ivoire, 2019). Specifically, the region's soils are a mixture of Acrisols, Cambisols, Fluvisols and Luvisols as described by FAO Digital Soil Map of the World from the digitized version of the FAO-UNESCO Soil Map of the World produced in paper version at scale 1:5 million (Batjes, 1996) (**Figure 6**). The floristic density consists of a mixture of varied forest and savannah facies due to degradation caused by agricultural clearing and logging. The northern part is mainly dominated by savannah.

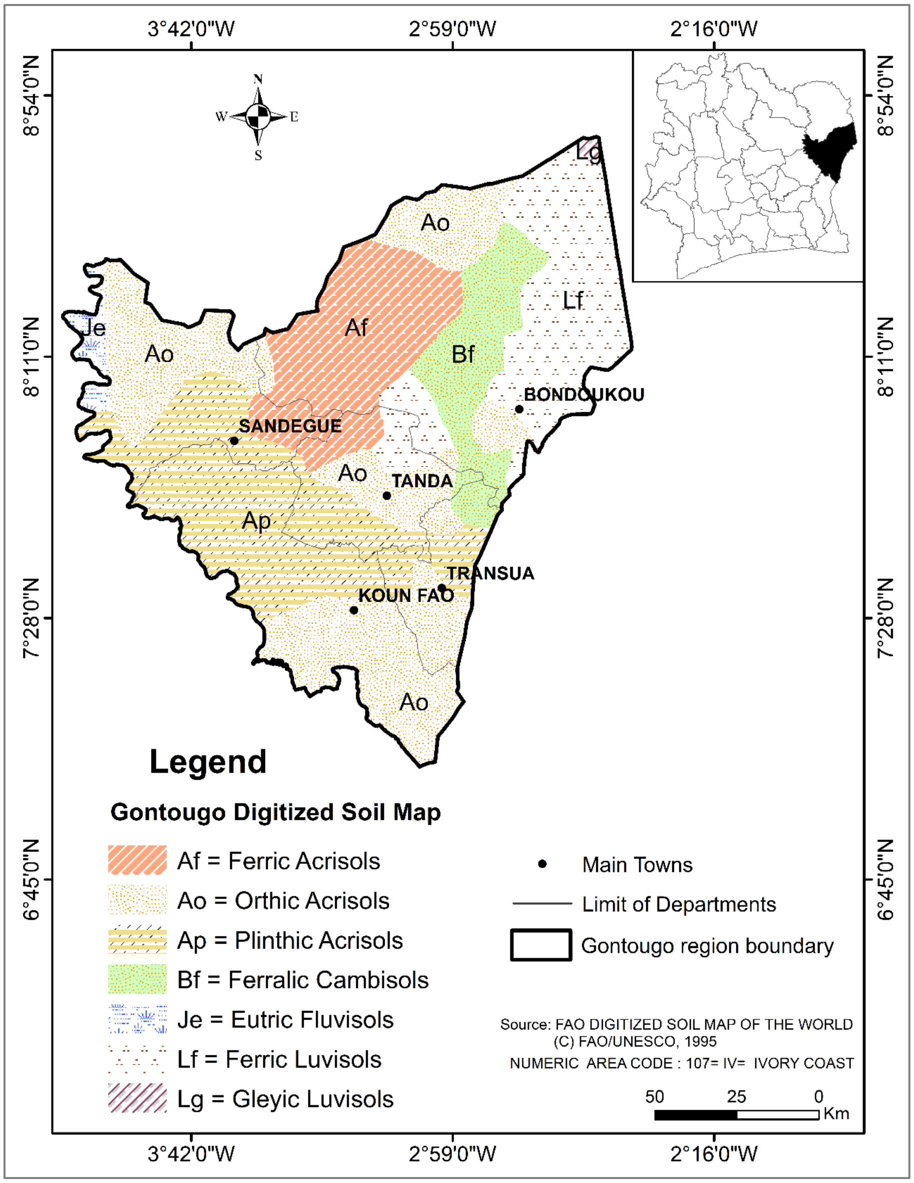

Figure 6: FAO Digitized Soil Map of the World (FAO DSMW) for the Gontougo region (source: https://www.fao.org/soils-portal/en/)

Gontougo region, along with the Boukani region, constitutes the Zanzan district. The major climate of this district includes four seasons. Two of which are wet, occurring from March to June and September to October. These rainy seasons alternate with two dry seasons, which last from November to February and July to August (**Figure 7**). The annual rainfall ranges from 800 to 1200 mm, with an average temperature of around 28 °C (Brou et al., 2005; Kouman et al., 2022).

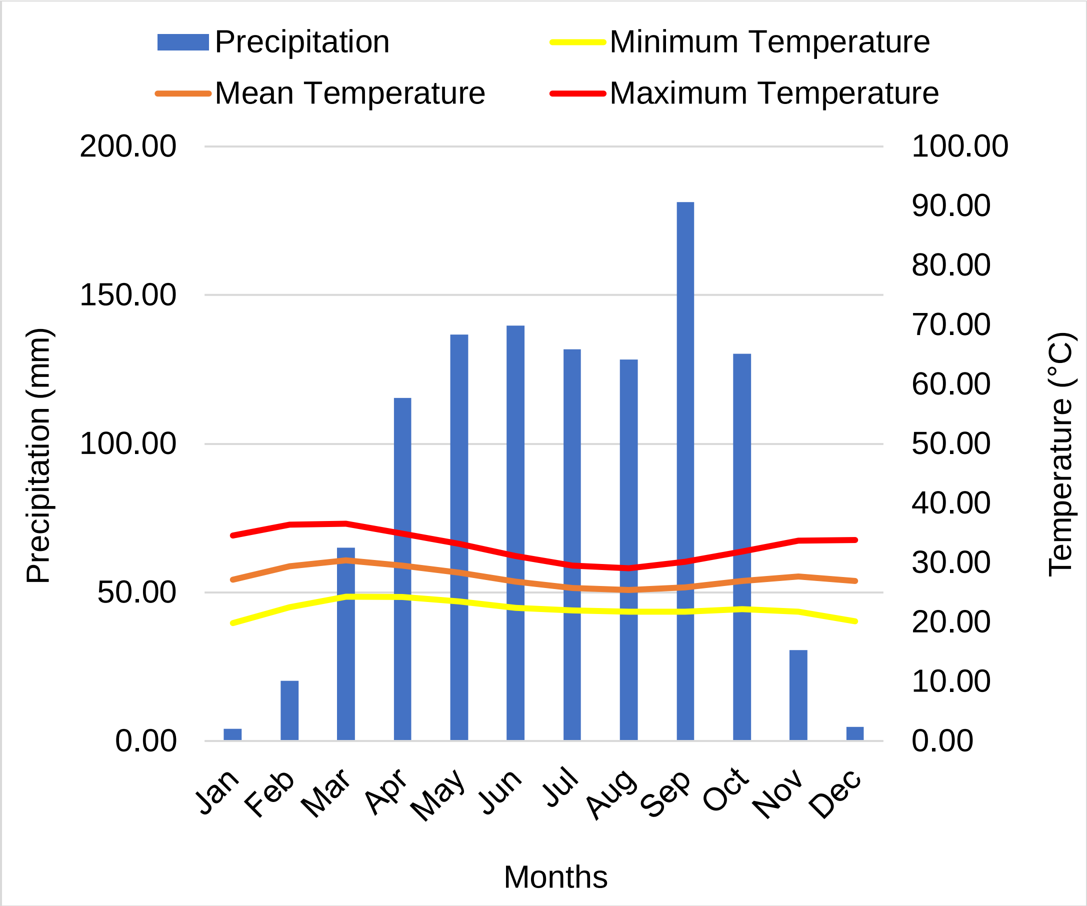

Figure 7: Monthly climatology of minimum, Mean & maximum temperature and precipitation from 1991 to 2022 in the Zanzan District
(Data source: World Bank Group, 2024).

To support yam farmers with scientifically sound information on yam risks production in the Gontougo region, attempts have been made to increase yield and satisfy the population with food security.

CHAPTER 1: YAM PRODUCTION-RELATED AGRO-CLIMATOLOGICAL RISKS AND YAM YIELD MODELING IN CÔTE D'IVOIRE: A REVIEW

1.1. Introduction

In the last two decades of the 20th century, the African continent has experienced longer and more intense heat waves (Engdaw et al., 2022). In addition, 50% of regional climate projections suggest that these heat waves, which are unusual in current climatic conditions, will be more regular by 2040 or even more severe under the RCP8.5 scenario (Faye et al., 2019). Regarding rainfall, many uncertainties remain: A decrease in rainfall is expected in the Western Sahel while the Eastern Sahel is expected to experience an increase in rainfall. It is worth noting that, under the worst-case climate change scenario, a reduction in mean yield of 13% is projected in West Africa (Sultan et al., 2015). Therefore, agriculture is one of the sectors which are most vulnerable to global weather and climate change. In Sub-Saharan Africa (SSA) it is the main occupation and source of income for most of the populations and, therefore, has a great influence on regional food security (Sultan et al., 2013; World Bank Group, 2019). However, the region faces food shortages almost every year due to crop failure or low crop yields (Cedric et al., 2022b; Waongo, 2015). According to FAO, (2015a, 2017) and Raes et al., (2018), the use of adapted varieties or breeds, with different environmental optima and/or broader environmental tolerances, including currently neglected crops, also considering that increased diversification of varieties or crops is a way to hedge against the risk of individual crop failure. Among the failures of these crops is yam which is the second most important root/tuber crop in Africa after cassava (Lebot & Dulloo, 2021). Yams (Dioscorea spp.) are extremely important to food security because of their excellent storage properties; they can be stored for four to six months without refrigeration and provide an important food safety net between growing seasons. They are a staple food for millions of people in tropical countries and provide pharmacologically active compounds for traditional medicine and the pharmaceutical industry (Andres et al., 2016; Adifon et al., 2019; Neina, 2021).

Yams are grown in about 50 tropical countries, not all of which provide their annual production statistics to the United Nations Food and Agriculture Organization. Annual world production is about 72 million tonnes of fresh tubers. More than 98% of this production is grown in Africa, mainly in four countries (Nigeria, Côte d'Ivoire, Ghana and Benin) accounting for 93% of this production (Lebot & Dulloo, 2021). Particularly, yams are widely grown in Côte d'Ivoire, and among food crops, yam is the most cultivated (MINADER, 2017; Diarrassouba, 2019). It is therefore a crop that plays a key role in the Ivorian economy and food and nutritional security. The landrace varieties Kponan, Krengle, and Djate, are in high demand, as are the adapted varieties

TDA, Mao and C20. The latter have demonstrated good productivity, disease resistance and drought tolerance. (Michel & Apata, 2017;Adifon et al., 2019; Kouakou et al., 2019). Despite all these assets, yam production is facing challenges due to several issues. Planting and harvesting are labour-intensive, yield and postharvest durability vary significantly with soil quality and climactic factors, decreasing soil quality and mounting pest pressures, rotting of seedlings in the mound due to high surface temperatures, the false start of the rainy season and the failure to update agricultural calendars according to rainfall variability are among the issues facing farmers and the yam sector in Côte d'Ivoire (Anogbro, 2015; Frossard et al., 2017; Kouakou et al., 2019; World Bank Group, 2019). So, it requires continuous monitoring to improve crop yields (Kosamkar & Kulkarni, 2019). Given the changing climate, predicting scenarios and crop yield based on models will help increase production, forecast the growing season, take adaptive measures and allow farmers to be more resilient (Kosamkar & Kulkarni, 2019; Fayaz et al., 2021; Malhi et al., 2021).

However, at national level, it should be noted that in the literature about yam cropping, almost all the studies done by researchers are in biology, genetics, physiology and the marketing of yam. Some climate variabilities highlighting the impacts have been also studied (Doumbia et al., 2006; Valerie, 2012; Anogbro, 2015; Kouakou et al., 2019;). For this reason, we present in this manuscript a review of the agro-climatological-related risk of yam production and models developed for yam yield prediction in Côte d'Ivoire. Crop models are an essential tool for studying the impact and potential adaptation options in root and tuber production. A crop model consists of mathematical equations that describe the development and growth of the crop over time, based on environmental factors (Raymundo et al., 2014; Fayaz et al., 2021; Cedric et al., 2022b). Crop models use crop characteristics, climate data and soil characteristics to simulate crop responses to management practices and various environmental conditions. Crop models can be used to anticipate the effects of climate change on root and tuber production (Raymundo et al., 2014; Degila et al., 2023). In this study, we will evaluate the existing models that have served as a study of yam in Côte d'Ivoire through scientific search engines, online documentary databases and national reports. The general differences, their structures, similarities, limitations and applications in the field of climate change and research gaps have been discussed.

1.2. Material and Methods

1.2.1 Presentation of Côte d'Ivoire

Côte d'Ivoire is located between Longitudes 2°30′ and 8°30′ W and Latitudes 4°30′ and 10°30′ N with an area of 322 462 km2, covering about 1% of the African continent. It is part of West African countries sharing borders with Liberia and Guinea to the West, Mali and Burkina-Faso to the North and Ghana to the East part **(Figure 1-1).** The Southern part of the country is covered by the Atlantic Ocean with a 550 km long coastline (Kouame et al., 2020). The central and coastal areas each have four seasons: April to mid-July: a long rainy season, with frequent rainfall and numerous thunderstorms; mid-July to September: a small dry season, the sky can remain overcast; September to November: a short rainy season, with some light rainfall; December to March: high dry season. The northern zone has two seasons: the period from June to September is the rainy season and the period from October to May corresponds to the dry season (Kouame, 2021; Kouame et al., 2020).

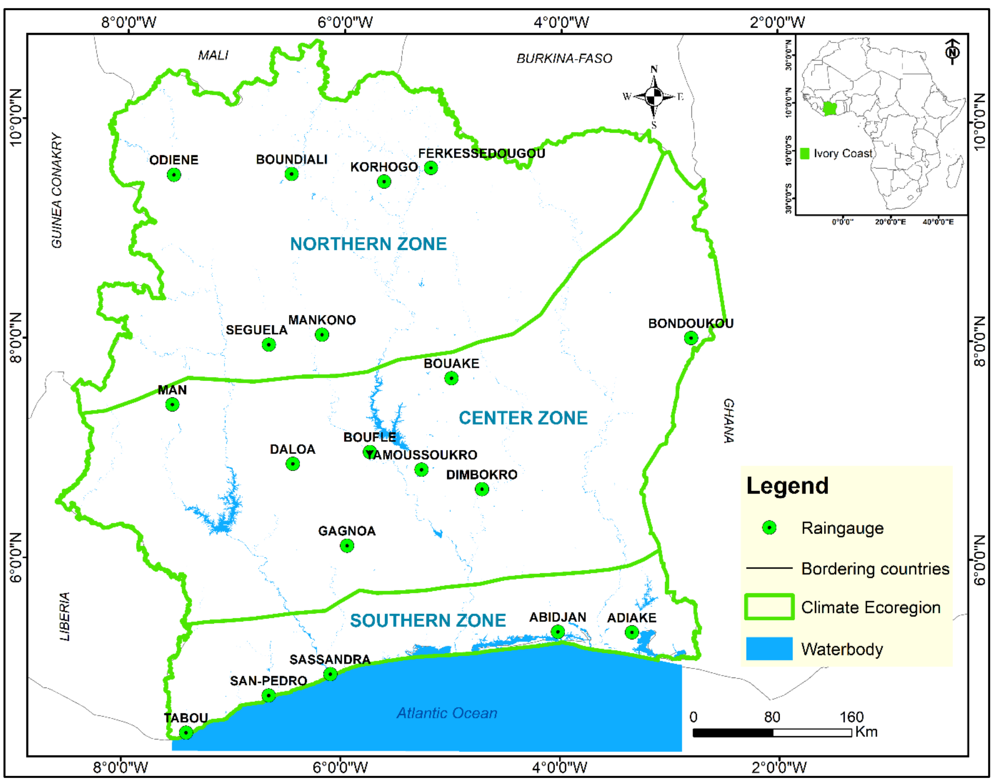

Figure 1- 1: Distribution of the rain gauges and climatic division depending on rainfall patterns in Côte d'Ivoire

Source: Kouame et al. (2020).

1.2.2 Research Methodology

This study was carried out in the framework of a literature review of existing studies, systematic reflection, and scientific journals/reports to highlight the approaches already done and available results relating to yam production-related risks and yam yield modelling in Côte d'Ivoire. We searched tools, methods, data used and results reported in the literature. Several documents, such as articles, national reports and peer reviews, were considered in this study. In order to achieve this, we referred to Boolean terms (Dahan & Kasei, 2022; Kohl et al., 2018; Ouattara et al., 2023; Tran et al., 2023). Boolean operators (sometimes called Boolean terms or commands) connect the keywords to create a logical phrase that the database can understand. This involves telling the database to look for multiple terms or concepts at once, which makes the search more precise (Kohl et al., 2018; Pušnik et al., 2022; Snyder, 2019). The Boolean operators used in this research are "AND", "OR" and "( )" **(Table 1-1)**.

Table 1- 1: Boolean operators: "AND", "OR" and "( )"

Boolean operators	**What does it do?**
AND	Find items that use BOTH keywords.
OR	Find items that use EITHER of the keywords.
Brackets ( )	GROUP multiple search strings and SET PRIORITIES

To exploit the boolean operators, and search for the necessary data to complete this study, four (4) official websites of Ivorian institutions in charge of agriculture for some and climate for others **(Table 1-2)** and six (6) scientific search engines for online documentation **(Table 1-3)** were defined and consulted individually. This makes a total of ten (10) information sources defined for this review.

Table 1- 2: Official websites of Ivorian institutions

	Institutions names	**Websites**
1	Ministry of Agriculture and Rural Development (MINADER)	https://www.agriculture.gouv.ci/
2	National Center for Agricultural Research (CNRA)	https://cnra.ci/
3	National Agency for Rural Development Support (ANADER)	http://www.anader.ci/
4	Airport, Aeronautical and Meteorological Exploitation and Development Company (SODEXAM)	https://www.sodexam.com/

Table 1- 3: Scientific search engines

	Platforms	Website*	Purpose and country	Launch year
1	Thesis search engines	https://www.theses.fr/	It is a search engine to find French doctoral theses. Located in French	Jul. 2011
2	African Journals Online	https://www.ajol.info/index.php/ajol	Provides access to African-published research, and increases worldwide knowledge of indigenous scholarship. Includes 38 African countries as well as Côte d'Ivoire	1998
3	Science Direct	https://www.sciencedirect.com/	Provides access to a large bibliographic database of scientific and medical publications of the Dutch publisher Elsevier. It hosts over 18 million pieces of content. Based in Netherlands	Mar. 1997
4	Google Scholars	https://scholar.google.com/	Google Scholar is a freely accessible web search engine that indexes the full text or metadata of scholarly literature across an array of publishing formats and disciplines. Based in USA	Nov. 2004
5	World Catalogue	https://www.worldcat.org/	WorldCat is a union catalogue that itemizes the collections of tens of thousands of institutions (mostly libraries), in many countries, that are current or past members of the OCLC (USA nonprofit cooperative organization) global cooperative. Based in USA	Jan. 1998
6	Semantic Scholar	https://www.semanticscholar.org/	Semantic Scholar is an artificial intelligence-powered research tool for scientific literature developed at the Allen Institute for Artificial Intelligence (AI). Based in USA	Nov. 2015

Note. *: These information sources can be found on the above websites.

1-2.3. Document Search

This phase consisted of a search strategy for the documentation. The search strategy allowed us to define an appropriate search string based on the relevant databases identified and defined in the

Tables 1-2 and 1-3. The number of articles included in the final analysis was influenced by the search criteria defined in **Table 1- 4**. Furthermore, the definition of the search string was based on the topic terminologies. The search string is listed focusing mainly on "Yam production-related agro-climatological risks" and "Yam yield modelling in Côte d'Ivoire" with the addition of Boolean operators (**Tables 1-5** and **1-6**). The search terms were performed separately or in limited combinations that took into account the requirements or limitations of the database used (Mengist et al., 2020). In these databases, publications that were not downloaded for further study were discarded. The articles were peer-reviewed journals from the seven data sources and the literature searches were finalized on 19 May 20023. The search was conducted in these different internationally recognized databases to collect relevant information from the publications (Gonçalves et al., 2018). These are all international databases of peer-reviewed publications from around the world (Gonçalves et al., 2018; Mengist et al., 2020). Besides, the size and types of databases used to search for publications helped determine the size of the sample drawn for examination. Note that the research on the national platforms was done both in English and French, the latter being the country's (Côte d'Ivoire) official language.

Table 1- 4: Selection of literature using inclusion and exclusion criteria

Criteria	**Decision**
When the predefined keywords exist as a whole or at least in the title, keywords or abstract section of the paper.	Inclusion
The paper was published in a scientific peer-reviewed journal.	Inclusion
The paper should be written in the English or French language.	Inclusion
Studies presenting evidence on crop modeling/climate impact studies on yam.	Inclusion
When the articles address at least one agro-climatological indicator.	Inclusion
Papers that are duplicated within the document search engines.	Exclusion
Papers that are not accessible, review papers and meta-data.	Exclusion
Papers that are not primary/original research.	Exclusion
Papers published before 1998.	Exclusion

Source: Adapted from Mengist et al. (2020).

Table 1- 5: The search terms used and the total number of publications from the country databases

Databases	Databases Searching string and searching terms		No. of papers	Date of acquisition
MINADER	Main searching terms	Yam production-related agro-climatological risks AND yam yield modeling in Côte d'Ivoire	00	5/19/2023
	Secondary searching terms	Yam production-related agro-climatological risks OR yam yield modeling in Côte d'Ivoire	00	5/19/2023
	Tertiary searching terms	Yam production-related agro-climatological risks (Côte d'Ivoire)	00	5/19/2023
	Fourth searching terms	yam yield modeling (Côte d'Ivoire)	00	5/19/2023
CNRA	Main searching terms	Yam production-related agro-climatological risks AND yam yield modeling in Côte d'Ivoire	00	5/19/2023
	Secondary searching terms	Yam production-related agro-climatological risks OR yam yield modeling in Côte d'Ivoire	00	5/19/2023
	Tertiary searching terms	Yam production-related agro-climatological risks (Côte d'Ivoire)	00	5/19/2023
	Fourth searching terms	yam yield modeling (in Côte d'Ivoire)	00	5/19/2023
ANADER	Main searching terms	Yam production-related agro-climatological risks AND yam yield modeling in Côte d'Ivoire	00	5/19/2023
	Secondary searching terms	Yam production-related agro-climatological risks OR yam yield modeling in Côte d'Ivoire	00	5/19/2023
	Tertiary searching terms	Yam production-related agro-climatological risks (Côte d'Ivoire)	00	5/19/2023
	Fourth searching terms	yam yield modeling (in Côte d'Ivoire)	00	5/19/2023
SODEXAM	Main searching terms	Yam production-related agro-climatological risks AND yam yield modeling in Côte d'Ivoire	00	5/19/2023
	Secondary searching terms	Yam production-related agro-climatological risks OR yam yield modeling in Côte d'Ivoire	00	5/19/2023
	Tertiary searching terms	Yam production-related agro-climatological risks (Côte d'Ivoire)	00	5/19/2023

	Fourth searching terms	yam yield modeling (in Côte d'Ivoire)	00	5/19/2023

Table 1- 6: The search terms used and the total number of publications from scientific search engines

Databases	Database searching string and searching terms		Searching matches	No. of papers	Date of acquisition
Thesis search engine	Main	Yam production-related agro-climatological risks AND yam yield modeling in Côte d'Ivoire		00	5/21/2023
	Secondary	Yam production-related agro-climatological risks OR yam yield modeling in Côte d'Ivoire		00	5/21/2023
	Tertiary	Yam production-related agro-climatological risks (Côte d'Ivoire)		00	5/21/2023
	Fourth	Yam yield modeling (in Côte d'Ivoire)	Searching terms don't match any title. Just one keyword	11	5/21/2023
African Journals Online	Main	Yam production-related agro-climatological risks AND yam yield modeling in Côte d'Ivoire	Searching terms don't match any title. Just some keywords	16	5/19/2023
	Secondary	Yam production-related agro-climatological risks OR yam yield modeling in Côte d'Ivoire	Searching terms don't match any title. Just some keywords	36	5/19/2023
	Tertiary	Yam production-related agro-climatological risks (Côte d'Ivoire)	Searching terms don't match any title. Just some keywords	42	5/19/2023
	Fourth	Yam yield modeling (in Côte d'Ivoire)	Searching terms don't match any title. Just	76	5/19/2023

			some keywords		
Science Direct	Main	Yam production-related agro-climatological risks AND yam yield modeling in Côte d'Ivoire		00	5/21/2023
	Secondary	Yam production-related agro-climatological risks OR yam yield modeling in Côte d'Ivoire	Searching terms don't match any title. Just some keywords	298	5/21/2023
	Tertiary	Yam production-related agro-climatological risks (Côte d'Ivoire)		00	5/21/2023
	Fourth	Yam yield modeling (in Côte d'Ivoire)	Searching terms don't match any title. Just some keywords	268	5/21/2023
Google Scholar	Main	Yam production-related agro-climatological risks AND yam yield modeling in Côte d'Ivoire		00	5/20/2023
	Secondary	Yam production-related agro-climatological risks OR yam yield modeling in Côte d'Ivoire		00	5/20/2023
	Tertiary	Yam production-related agro-climatological risks (Côte d'Ivoire)		00	5/20/2023
	Fourth	Yam yield modeling (in Côte d'Ivoire)	Searching terms don't match any title. Just some keywords	8,790	5/20/2023
World Catalogue	Main	Yam production-related agro-climatological risks AND yam yield modeling in Côte d'Ivoire		00	5/20/2023
	Secondary	Yam production-related agro-climatological risks OR yam yield modeling in Côte d'Ivoire	Searching terms don't match any title, any keyword	02	5/20/2023
	Tertiary	Yam production-related agro-climatological risks (Côte d'Ivoire)		00	5/20/2023

	Fourth	Yam yield modeling (in Côte d'Ivoire)	Searching terms don't match any title, any keyword	02	5/20/2023
Semantic Scholar	Main	Yam production-related agro-climatological risks AND yam yield modeling in Côte d'Ivoire		00	5/20/2023
	Secondary	Yam production-related agro-climatological risks OR yam yield modeling in Côte d'Ivoire		00	5/20/2023
	Tertiary	Yam production-related agro-climatological risks (Côte d'Ivoire)	Searching terms match only some keywords	05	5/20/2023
	Fourth	Yam yield modeling (in Côte d'Ivoire)	Searching terms don't match any title. Just some keywords	126	5/20/2023

1-3. Documents Analysis

The information extracted from the documents was analyzed qualitatively based on different criteria and categories **(Table 1-7)**. This objective analysis was done to ensure the viability and authenticity of the data source used in the papers collected (Dahan & Kasei, 2022; Gonçalves et al., 2018; Manikas et al., 2023; Mengist et al., 2020; Snyder, 2019). After a sufficiently thorough reading of the various documents, the information relevant to this study was extracted according to the criteria and categories captured in Table 1-7.

Table 1- 7: The criteria used for extracting information from the selected papers

No	Criteria	Categories considered	Justification
1	Document types	Official papers/articles/reports/thesis	from one of the ten (10) sources defined for this review is considered
2	Year of publication	Between 1998 and Mai 2023	The year in which the oldest journal goes online is considered
3	Study area	Country	-

4	Types of data sources	Primary data	Data derived from sampling in the field (e.g., field data, surveys, interviews or census data)
		Secondary data	Data not verified in the field (e.g., remote-sensed data, a bibliography, modeling, socioeconomic data)
		Mixed data	Mixed both above sources
5	Methods	Cultivar and soils types; Climate indices; statistics relationships; models used.	Incorporate existing knowledge to link with Yam models, climate models and Yam production-related agro-climatological risks.
6	Mode of assessment	Qualification, quantification, or both	Expressing climate and agriculture values with verbal terms or using numbers mathematics expressions or both
7	Difficulties mentioned	Methodological	Uncertainties on the result due to the application of the unclear or less developed method; Uncertainties linked with lack of conceptual clarity.
		Data analysis	Data analysis skills and the choice of suitable tools can challenge the work.
		Lack of model validation	Most crop modeling studies lack to verify the results using model validation.

1-4. Results and Discussion

1-4.1 Examination of research carried out

1-4.1.1 Search engines for national platforms

On the National platforms, none of the four (4) revealed a single trace of documents or research available. This could mean that no studies in this or a related field have been carried out and are available. It could also mean that the documents of the works are published elsewhere either than the platform or that the works are kept in hard copies in the libraries of these structures.

1-4.1.2 Theses.fr Search Engine

At the level of the Theses.fr platform: only eleven (11) documents were found in all the searches. It is the fourth searching term [yam yield modelling (Côte d'Ivoire)] that allowed us to have this result. The search was carried out by selecting all the possible search options available on the website, including 'defended theses only' and 'defended and online theses', and the year, which by default is defined as the broadest possible on the website 'before 2013 to 2023'. Thus, none of these 11 documents were selected according to the inclusion and exclusion criteria established beforehand. Indeed, the search terms do not appear at any level in the titles of the documents nor the keywords, but it should be noted that this French PhD platform provides a wide range of related fields in addition to what is requested.

1-4.1.3 AJOL Search Engine

On the AJOL databases, 181 papers were found across all four search terms. Among these documents, the most relevant ones deal with climate change for some and yam production for others, but in other countries. None of these papers addresses the issue of yam yield modelling in Côte d'Ivoire, or elsewhere. In fact, AJOL displays from its database the documents available according to the search terms used, including those that were not picked the topic. AJOL relies on the search terms found in the abstract of certain documents to suggest search results. This is why we had 170 documents and none of them were useful for our intended purpose.

1-4.1.4 Science Direct Search Engine

The research was successful in that we obtained five hundred and sixty-six (566) results from all four searches. With Science Direct, we were able to detect some documents that deal with our topic elsewhere in other countries. We have kept these documents for further analysis. It should be noted that synonyms for certain keywords such as 'modelling' were found in the form of 'simulation'. Moreover, we were able to find these words in the same document: 'Simulating', 'yield', 'yam' and also these words: 'Modeling', 'yam', and 'yield' in the same document. Some of these works whose association with these keywords were carried out in West African countries like Benin Republic and Ghana. In these documents, after analysis, it can be seen that some models have been used to effectively simulate yam yield. We note: the Environmental Policy Integrated

Climate (EPIC) model (Srivastava & Gaiser, 2010) and the Systematic Approach for Land Use Sustainability (SALUS) model (Liu et al., 2021).

1-4.1.5 Google Scholar Search Engine

On Google Scholar, no document was found after the three first search terms. In the last search terms, we got eight thousand seven hundred and ninety (8,790) results. All the key works were found but not in the same document. We applied three successive filters to select the most relevant ones using quotation marks (" "). The first was: [yam yield "modeling" (Côte d'Ivoire)], the second was: [yam "yield modeling" (Côte d'Ivoire)] and finally, the third was: ["yam yield modeling" (Côte d'Ivoire)]. Successively, the result went from 8,790 to 2,390 then to 08 and then to 00. One of the documents in which we can find keywords that Google Scholar provided is entitled: Simulating cocoa production: «A review of modeling approaches and gaps. But unfortunately, it does not address the subject of yam. It should be noted that Google Scholar is one of the most widely used scientific search engines worldwide and is accessible to all researchers for the promotion and enhancement of research. Therefore, the absence of a relevant document in Google Scholar implies If despite this fact, no relevant document has been found, there is reason to believe that the work has not yet been studied in Côte d'Ivoire.

1-4.1.6 WorldCat Search Engine

On WorldCat, the world's largest library catalogue, our searches yielded four (4) results in all especially two in the second and two in the fourth search terms. However, after analysis, there were the same two documents found in each search. These documents do not contain any of the keywords of our research, neither in the titles nor in the abstract keywords.

1-4.1.7 Semantic Scholar Search Engine

On Semantic Scholar, our searches yielded a hundred and thirty-one (131) results in all search terms. It includes all the keywords but all of them were found in the fourth search individually in different documents that do not necessarily deal with yams. An example of a topic: "Potential Impact of Climate Change on the Sediment Fluxes of a Watershed in West Africa". The other is: "Modeling greenhouse gas emissions of cocoa production in the Republic of Côte d'Ivoire". These are the most relevant of the 126 documents but are not useful because they do not address the cases we are looking for. However, Semantic Scholar is a powerful search engine with over 200 million papers from all fields of science. The best part is that it is free to access and all papers are open access to download with all possible metadata with redirections to other topics of interest depending on the papers downloaded.

Below is a screenshot of the search performed in each scientific search engine with the main search term which is: [Yam production-related agro-climatological risks AND yam yield modelling in Côte d'Ivoire] **(Figure 1-2).**

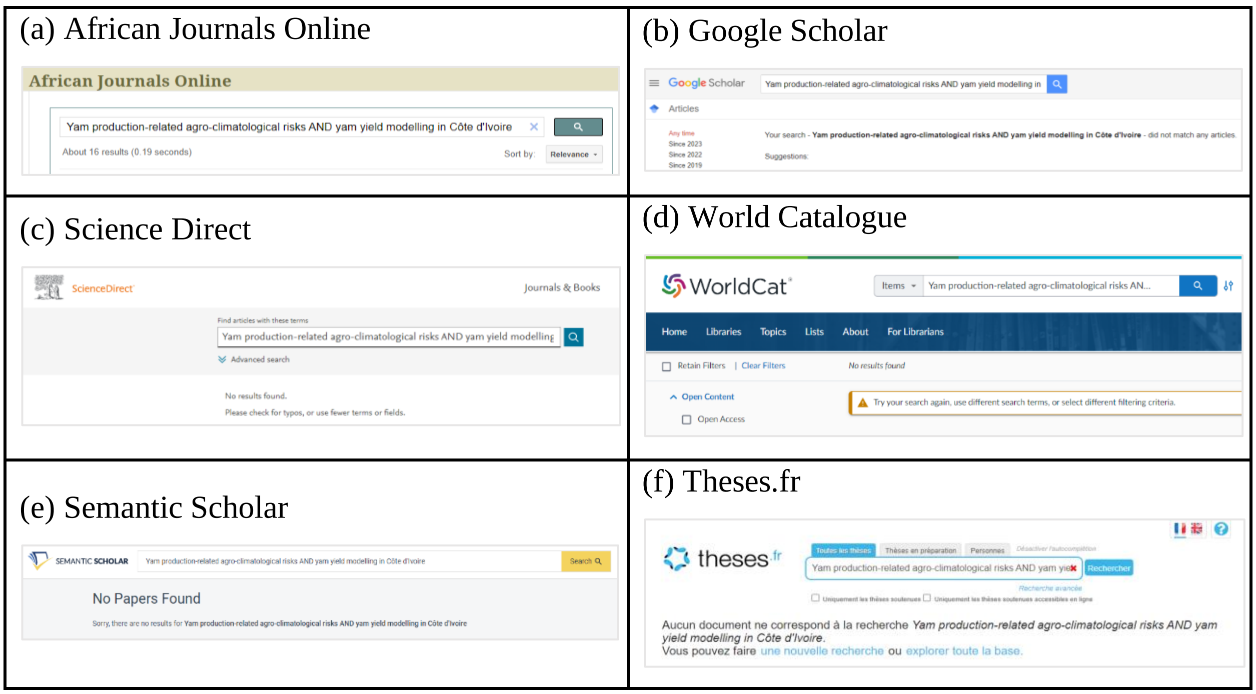

Figure 1- 2: An example of a screenshot of each research performed using the main search terms in scientific search engines

1-4.2 Outcomes Using Inclusion and Exclusion Criteria

By applying the inclusion and exclusion criteria, papers that fulfil the inclusion criteria were selected for further investigation and content assessments. Unfortunately, no papers dealing with the subject we are discussing have been selected for Côte d'Ivoire. The predefined literature inclusion and exclusion criteria to achieve this review work were presented in Table 1-4. It is important to add that papers like grey literature, extended abstracts, presentations, keynotes, and research work that are not original and duplications were omitted. Figure 1-3 shows the flowchart diagram of our research according to the exclusion and inclusion criteria.

1-4.3 Related Work

The related work section focuses on literature reviews involving the eligibility documents. As no studies in our field of research have been carried out in Côte d'Ivoire, we have turned to eligibility documents for further analysis to find out more about what is being done at this level in the West African sub-region or elsewhere. Indeed, related works have been done in Benin Republic, Nigeria and Ghana according to the eligibility papers (08 documents) in **Figure 1-3**. These countries are all Sub-Saharan West African coastal countries with the same hot and humid tropical climate. We have therefore used the results of this research to find out exactly what has been done and to explore the possibilities of transferring technology from these findings to the local level in Côte d'Ivoire following Table 1-7 categories and criteria for the analysis. Crop yield modelling is one of the most important elements of agricultural decision-making today. Crop system models are therefore valuable tools to inform agronomic decisions and advance research. The prediction accuracy of simulation models is one of the most vital components in yield modelling.

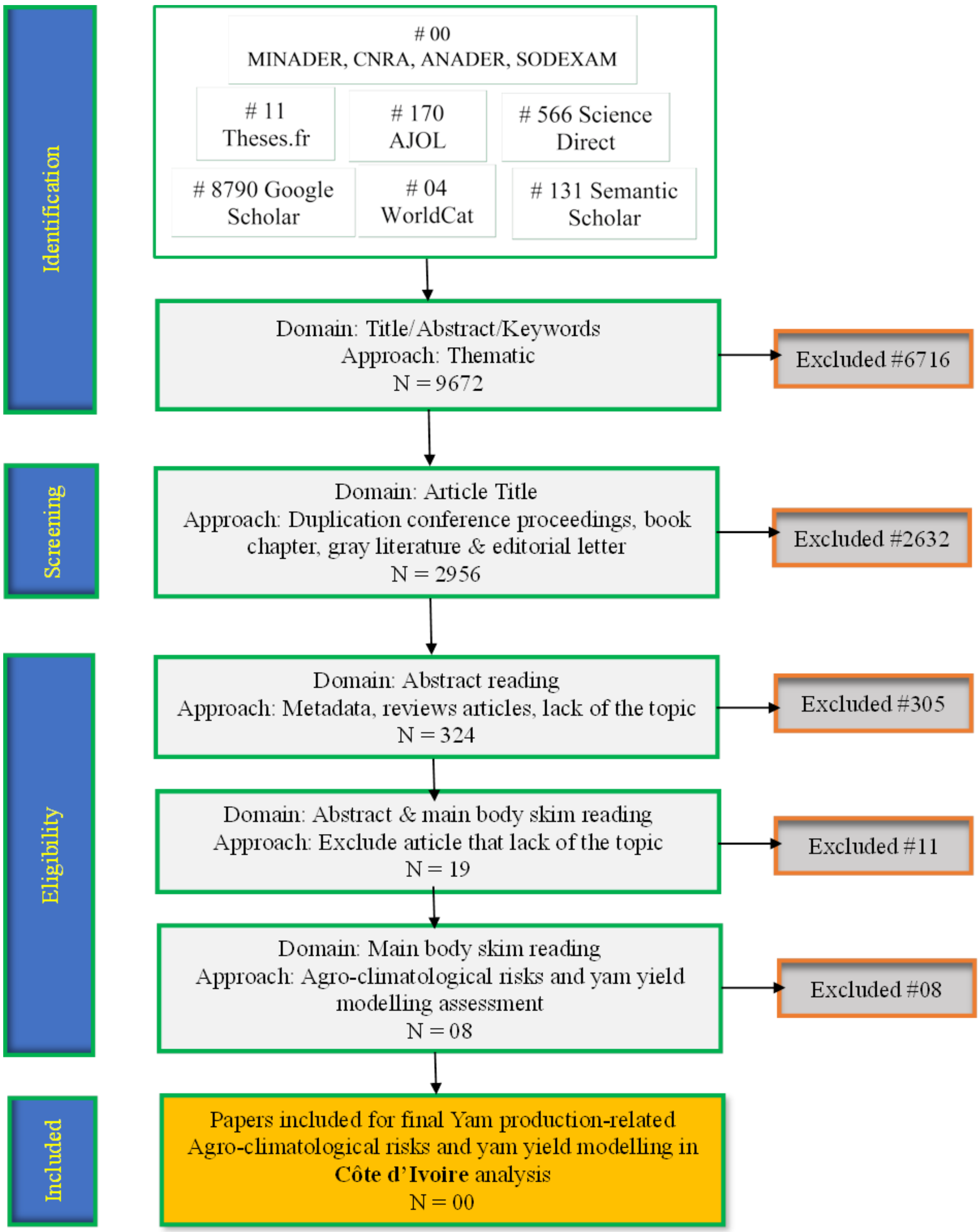

Figure 1- 3: Flowchart diagram for databases search of documentation for reviews and the results found

Source: Adapted from Mengist et al. (2020).

The basic operating mode of crop models requires input data such as soil, climate, plant and management which is used by crop simulation model for predicting the crop yield **(Figure 1-4)** and describe the process of growth and developmental stages of crops (Dzotsi et al., 2013; Kosamkar & Kulkarni, 2019; Srivastava et al., 2012).

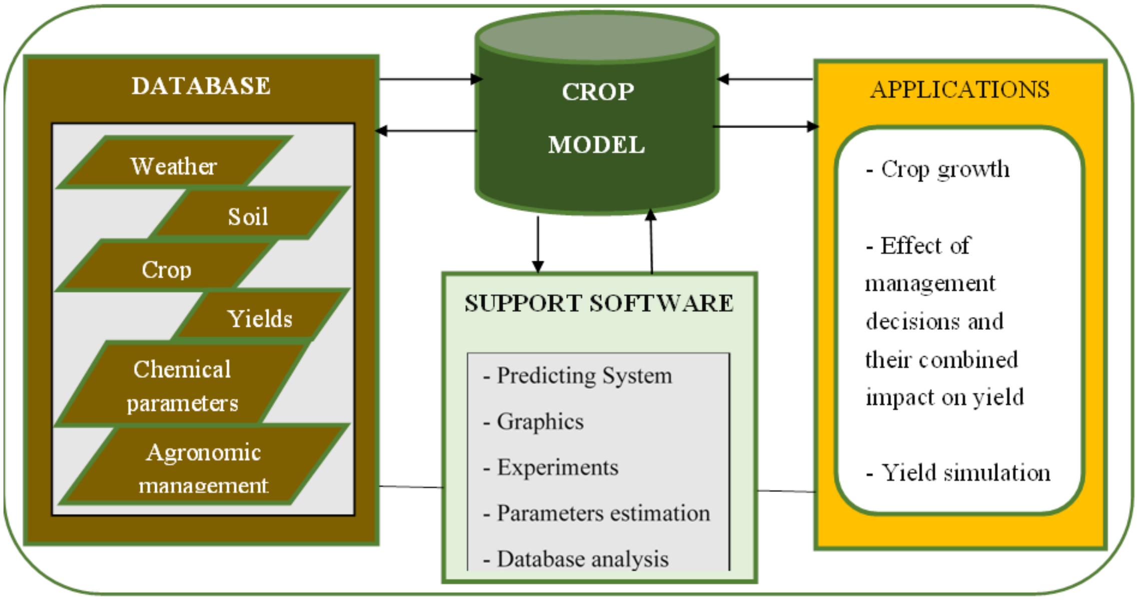

Figure 1- 4: Crop modeling operating system

Source: Adapted from (Dzotsi et al., 2013; Jones et al., 2003; Srivastava et al., 2012).

4.3.1 Yam Yield Modeling Approaches

In their work, these authors (Liu et al., 2021; Marcos et al., 2011; Srivastava et al., 2012; Srivastava & Gaiser, 2010) studied yam yield modelling, water yam (Dioscorea alata L.) growth and the prediction of yam productivity under different agronomic management. **Table 1-8** below summarizes the details of their modelling approaches. Several yam-adapted crop models and machine-learning techniques have been used for yam modelling across Africa and the Caribbean (French Antilles).

Table 1- 8: Summary of the approaches to yam yield modelling:

Study area/ Models used/ Authors and year	Inputs data	Parameterization/ Statistical analysis/ Model evaluation	Outputs modules
Ghana/ Approach for Land Use	- Yam parameters for the model were based on reported values in the	- Use of field observations and compare the simulated phenology	- Soil Organic Carbon (SOC) and yield response under the

Sustainability (SALUS) model/ (Liu et al., 2021)	literature and the calibration processes; - Crop coefficients and management (planting dates, fertilizer, irrigation water, and tillage); - Soil data (organic C, total N, bulk density, clay, and silt) derived from the Africa Soil Information Service (AfSIS) database includes soil layer parameters The gridded soil profile resolutions were 1 km and 250 m; - Weather data including min-max temperature, precipitation, and solar radiation from the gridded 0.5◦-resolution POWER dataset and also from stations at the two locations of the study.	and biomass (both tuber yield and aboveground biomass) to the field observations from two different locations to parameterize the SALUS-Yam model; - Root mean square of deviation (RMSD) and mean absolute percentage error (MAPE) used to evaluate SALUS-Yam model accuracy; - Outputs modules evaluations were based on comparisons between observed and simulated data applied to the crop model.	different agro-ecological zone soil types, and changes in nutrients and water; - Simulation of yam phenology and biomass response to N and P fertilizer; - Two major sources of uncertainty were observed: soil and weather inputs.
Benin Republic/ Environmental Policy Integrated Climate (EPIC) model/ (Srivastava et al., 2012; Srivastava & Gaiser, 2010)	- Data for the model calibration including rainfall distribution, crop characteristics (aboveground biomass, tuber yield, LAI, etc.) and soil properties (moisture retention properties, chemical composition, etc.) were obtained on-farm trials at Dogue village; - Crops parameters values were derived from four sources: experiments, cassava parameter file from EPIC (version 3060),	- The mean residual error (ME) and the mean absolute error (MR) were used to compare observed data and simulated values; - The EPIC model performance was evaluated by comparing the simulations of 2 years' worth of yam yields with an experiment from Dogue village and by determining the coefficient between the observed and simulated yield of yam.	- Simulation of yam growth and the effect of fertilizer on yam yield; - Yam (D. alata) growing conditions in sub-humid tropical savannah areas.

	literature and the adjusted value.		
Guadeloupe/ Cropping Systems Simulation (CropSyst) model/ (Marcos et al., 2011)	- Two independent data sets from field experiments under non-limiting conditions for water and nutrients and over a wide range of planting dates and photoperiods including Mean temperature (◦C), Mean global radiation (MJ m2 d-1), Mean photoperiod (h), Planting date and years of the experiment; - Rainfall data (annual rainfall for each year) from the Experimental Station of Duclos; Soil data, yam yield (variety Lupias); - 200g of fresh biomass was used for the yam planting.	- Calibration of the model and test of the model were based on comparisons between observed and simulated data from Experiment 1 and Experiment 2; - Determination coefficient ($R2$) and Root Mean Square Error (RMSE) were used to determine the best fit of parametrization of the model and to evaluate the two Experiments conducted.	- Change in the Radiation Use Efficiency (RUE) as a function of the planting date; - RUE effect on yam growth and yields; - Yam development and growth; - Vegetative and Tuberisation phase, Total biomass and Yam yield from the two Experiments (1 and 2) were compared.
West African countries/ Machine learning, models-based decision tree/ (Cedric et al., 2022b)	- Crop yield, annual rainfall, temperature, pesticides and chemical data from 1990 to 2020 from nine West African countries collected from the Food and Agriculture Organization for the United Nations and the Climate Knowledge Portal World Bank; - Analysis parameters: Yield (kg/ha), Temperature (K), Pesticide (t), Rainfall (mm), NO2 (1018 µg).	- Crops Multivariate Logistic Regression (CMLR), Decision tree, and k-Nearest neighbor algorithm as machine learning algorithms for modeling processing; - Pearson Correlation between features (NO2, Temperature, Rainfall, Pesticide, Yields, Years); - Use three metrics to evaluate the models: Determination coefficient (R2), Mean Absolute Error (MAE) and the Run-Time of each model.	- Illustrations of the main parameters influencing the six crop yields: rice, maize, cassava, cotton, yams, and bananas; - Prediction of each crop yield.

1-4.3.2 Impact of Climate Change on Yam Yield

Climate change has the potential to significantly impact yam production through soil degradation, increasing the incidence of pests, and diseases creating yam tuber beetles, and changes in rainfall patterns. As yam is a rainfed crop, hence, changes in rainfall patterns can significantly impact its production. According to a study by the World Bank Group (2019), these effects due to climate change lead to decreased yam yields in Côte d'Ivoire. Also, sorting out issues relating to yam production in Nigeria, the authors conducted a study forecasting the effect of climate variability on yam yield in the rainforest and guinea savannah agroecological zone of the country. They used secondary data sources including the climatic data variables, yam area cultivated and yam output in their study (Adeleke Aturamu et al., 2021). The results of the study showed that rainfall and temperature are changing over time and unpredictable. Using the Representative Concentration Pathway (RCP), yam yield for 2050 was predicted to be 0.34mmt/ha and 0.21 mmt/ha under RCP 4.5 and RCP 8.5 scenarios respectively. Over time (2030, 2040 and 2050) in the rainforest Agroecological zone (AEZ), yam yield is expected to be negative under both RCP scenarios (RCP 4.5 and RCP 8.5) **(Table 1-10)**. Furthermore, in the savannah zone of West Africa, Srivastava et al. (2012) addressed the global climate change impacts on tuber crops by using a simulation approach to assess the long-term regional-scale changes in yam production under A1B and B1 IPCC SRES scenarios. They did not stop only that, better, they were able to examine the vulnerability of yam to climate change in conjunction with the soil conditions. The methodology, data and approaches used are recorded in Table 1-8. Concerning their findings, they concluded that the impact of climate change under the A1B IPCC SERES scenario on yam production is significant and will be protuberant in the 2040s. Concerning the soil type, S1 (Ferruginous soils impoverished without concretions) seems to be the most sensitive to climate change followed by S2 (Ferralitic soils) and S3 (Raw mineral soils) (Srivastava et al., 2012). Still on the effects of climate variability on yam production, a study was conducted in the Nothern part of the Benin Republic by Adifon et al. (2020). Their study shows that the agro-climatic stress index (ASI) and the annual rainfall are the main climatic factors which determine the yield of yam in the various growing areas in Benin. He was also able, through a field survey among yam farmers, to gather their perceptions of yam production conditions and the challenges they face. The survey revealed that yam farmers are unanimous about the influence of the variability of climate parameters on the growth and production of yams (Adifon et al., 2020). The methodological approach he used is described in **Table 1-9**.

Table 1- 9: Summary of the approaches to climate change on yam production

Data description/sources	Methods/Approaches/Period of the study	Country/Area/ References
Data are from secondary sources: - Yam area cultivated; - Climate data: CRU, ECMWF, ERA-Interim; - Validation data: station-based observations; - Historic climate datasets (Daily data for 120 years); - Future climate data: RCP 4.5 and RCP 8.5.	- Surveys using multistage sampling and random techniques in the selection of communities. - Establishing empirical climate variability over time from 1900 to 2019 (118 years); - Analyze a historic climate data period (1901-2019) with thirty-year (30) subdivisions made to four (4) non-overlapping epochal climate periods; - Future climate data period (2020-2050); - Statistical methods: Probability Density Function (PDF), trend analysis and change points analysis for establishing climate variabilities over time.	Guinea/ Savannah and Agro-ecological zone of Nigeria/ (Adeleke Aturamu et al., 2021)
Data are from secondary sources: - Slope inclination and length, topographical information; - Regional climate model outputs (GCM ECHAM5 downscaled) with A1B scenario; - REMO model and the A1B scenario output of the GCM HADC3Q0 downscaled; - The RCMs SMHIRCA and HADRM3P with the A1B scenario output; - Regional soil database from the soil association map; - Regional cropland database with the EPIC crop growth simulation model.	- Comparison of EPIC output for baseline (1961-2000) and time horizon (2001-2050); - Combines the agro-ecosystem model EPIC with the hydrological model SWAT (Soil Water Assessment Tool); - Changes in temperature and precipitation and the response of soil types to these changes; - Subdivision of the catchment into agronomic response units of variable size which constitute the spatial simulation units (LUSAC = Land Use-Soil Association-Climate units); - The LUSAC represent an area with similar climate conditions, soil characteristics and a representative crop and soil management; - Yield of yam had been calculated within each LUSAC for the period of 40 years (1961-2000) and 50 years (2001-2050). - Validation of the model: A total of four climate scenarios based on A1B and B1 emission scenarios with different RCM output has been simulated: The baseline period with the simulated historical data (1961-2000) and the time horizon	Savanna zone of West Africa/ Particularly in the Upper Ouémé basin/ (Srivastava et al., 2012)

	(2001-2050) under IPCC SERES A1B and B1 scenario conditions. The CO2 concentration was set at 350 ppmv for the baseline simulations.	
Data are from primary sources: - Daily climate data: temperatures, precipitation, potential evapotranspiration, relative humidity and insolation collected from the METEO-Benin; - Field data (Survey); - Yam yield data.	- Daily climate data period (1981-2016); - Survey from 351 producers to collect their perceptions about climate variability on the yams production; - Descriptive statistics analysis of the field data; - Principal component analysis (PCA) to determine the local perceptions of the effect of climatic parameters on yam production; - Trend analyses, Lamb index calculations and the agro-climatic stress index (ASI) using the climate data to determine the climate variability; - Yam yields by zone were calculated based on data collected from farmers and the yam areas cultivated by year; - The econometric approach based on ordinary least squares (OLS) has been adopted in order to identify among the climatic parameters those that best explain the yield of fresh yam tubers.	Central and Northern Benin/ (Adifon et al., 2020)

In 2019, the World Bank Group conducted a study on “CLIMATE-SMART AGRICULTURE INVESTMENT PLAN” with the contribution of the Coat of Arms of Ivory Coast, Initiative for Adaptation of African Agriculture (Initiative AAA), International Center for Tropical Agriculture (CIAT), Climate Change, Agriculture and Food Security (CCAFS) which is provided an investment plan for climate-smart agriculture (CSA) in Côte d’Ivoire. Situation analysis indicates that climate change will impact the production of key agricultural products in the country, which will, in turn, impact each economic activity. Climate change will drastically alter what crops are suitable for a given place, reducing suitability across large areas but also creating pockets of increased suitability. Modelling using the International Model for Agricultural Commodity and Trade Policy Analysis (IMPACT) suggests that the landscape of economic incentives will change, offsetting the loss of ability for some crops while exacerbating it for others (World Bank Group, 2019). Concerning the yam cropping, their study shows that the percentage point difference in yield and area of production with different levels of climate change for yams will be reduced negatively in yield under Regional Climate Projection (RCP) respectively in 2030 and in 2050

(RCP4.5: -0.9%; -2.3% and RCP8.0: -1.0%; -2.4%) and increased in production in the same RCP for respectively 2030 and 2050 (RCP4.5: 0.2%; 0.5% and RCP8.0: 0.1%; 0.4%) **(Table 1-10).**

Table 1- 10: Percentage point difference in yield and area of yam production with different levels of climate change in Côte d'Ivoire

	Difference in yield (SSP3)				Difference in area of production (SSP3)			
	RCP 4.5		RCP 8.0		RCP 4.5		RCP 8.0	
	2030	2050	2030	2050	2030	2050	2030	2050
Yams	-0.9	-2.3	-1.0	-2.4	0.2	0.5	0.1	0.4

Note. SSP = Shared Socioeconomic Pathways; RCP = Representative Concentration Pathway.
Source: (World Bank Group, 2019)

1-5. Conclusion and Outlooks

Documentary research is a task to be carried out before embarking on a practical study. It enables gathering information from original papers about the work to be carried out. The objective of this study was, therefore, to review the state of the art on the topic entitled: «Yam production-related agro-climatological risks and yam yield modelling in Côte d'Ivoire». Four official national platforms (Ministry of Agriculture and Rural Development (MINADER), National Center for Agricultural Research (CNRA), National Agency for Rural Development Support (ANADER), Airport, Aeronautical and Meteorological Exploitation and Development Company (SODEXAM)) and six scientific search engines were investigated in this study including Theses.fr, African Journal Online, Science Direct, Google Scholar, WorldCat and Semantic Scholar. None of the results from these ten (10) search platforms found a study in Côte d'Ivoire according to the search terms. On the other hand, eight (8) related works in this field were retained and investigated. These documents deal with the climatic impact on yam and yam yield modelling in West Africa and the French Antilles (Guadeloupe). Regarding climate impact on yam cropping, the authors note the low annual yam yield rate caused by rainfall uncertainties, heat waves and soil infertility. As far as modelling, is concerned, three (3) models are the most widely used. These are the Approach for Land Use Sustainability (SALUS) model, the Environmental Policy Integrated Climate (EPIC) model and the Cropping Systems Simulation (CROPSYST) model. In addition to these models, artificial intelligence through machine learning models has been used by some authors for yield prediction for several crops including yams. These models, as good as they are, present uncertainties and limitations in modelling studies and climate change on yam production. Concerning the yield modelling-based machine learning tools, the proposed prediction models are generalizable to the West African region and support large-scale data sets which increase uncertainties and large estimates in the outputs. On the other side, the variability of crop yields and season length simulated by SALUS, EPIC and CROPSYST models are highly dependent on the uncertainty of crop parameters and model calibration. These models, therefore, use simple relationships to represent yam growth and production. The pattern and magnitude of relationships between crop parameters and model output in these studies were consistent with typical responses of crop physiological processes and to the environment. However, few modelling studies have taken into account the dynamic simulation of disease effects and the simulation of crop phenology at the same time. This could be an advantage and improve the accuracy of the model. By doing so, the calibrated model could be used to improve fertilizer management in yam production and will solve a major problem in this sector for the greater happiness of yam farmers. Finally, it should be noted that all the models and tools used in these studies have been developed for several crops, so using them needs to be accurately calibrated. In the case of yam, a specific model must be set up to fight against all kinds of environmental impact, as it is the main food crop in Côte d'Ivoire, with a production of 7853083.92 tonnes in 2021, the second most important in West Africa, and one of the most widely grown crops in Africa with 73493225.79 tonnes in 2021 according to Food and Agriculture Organization of the United Nations statistics.

CHAPTER 2: TOWARDS UNDERSTANDING LAND USE LAND COVER CHANGES AND THEIR EFFECTS ON LAND SURFACE TEMPERATURES IN YAM PRODUCTIONS AREA IN CÔTE D'IVOIRE, GONTOUGO REGION USING REMOTE SENSING AND MACHINE LEARNING TOOLS (GOOGLE EARTH ENGINE)

2.1. Introduction

Agriculture is the main occupation and source of income for most of Sub-Saharan Africa's (SSA) populations and, therefore, has a great influence on regional food security (Sultan et al., 2013; World Bank Group, 2019). However, due to climate change, many farmers are forsaking their favourite crops in favour of others. For example, in Nigeria, farmers in the northern region are increasingly planting more drought-resistant crops like groundnuts and maize instead of their usual crops like yam to adapt to changing weather patterns. Similarly, in Ghana, some farmers are transitioning from cocoa cultivation to cultivating crops like yam and plantain that are less vulnerable to erratic rainfall and temperature fluctuations caused by climate change (Danquah et al., 2022; Filho, 2021). These changes in cropping patterns alter land use land cover (LULC) and the landscape, acting as a climatic feedback mechanism on vegetation cover (Gogoi et al., 2019). Affected communities will thus need to discover methods to adapt by utilizing existing natural resources and making maximum use of the land (Asselin et al., 2022; Zougmoré et al., 2018). These natural feedback climate cycles influence land surface temperatures (LST), also linked to human activity (Benmecheta, 2016; Gogoi et al., 2019; Kafi et al., 2014; Moisa, Dejene, & Gemeda, 2022).

The most visible effect of anthropogenic activities at the regional and local level is the modification of LULC, which alters the energy balance of the surface, changes surface temperature, the microclimate of the region, and dwindling agricultural yields (Aighewi et al., 2015; Gogoi et al., 2019; Kosari et al., 2020; Moisa, Dejene, & Gemeda, 2022). In the Gontougo region in Côte d'Ivoire, there is an alarming regression of forest and annual crop areas, while cashew crops are increasing every year, which constitute the main landscape vegetation in this region (Koulibaly et al., 2016).

According to FAO statistics, from 2000 to 2021 in Côte d'Ivoire, harvested yams varied from 505,408 to 1,438,153 hectare and the yield values from 88,172 to 54,605 hectogram/hectare. That means land is increasing every year while yield is continuously decreasing (FAOSTAT, 2023). These statistics show high use of land. Fertile land will then certainly be in short supply due to overexploitation, canopy degradation and the expansion of cash crops which over time change the agricultural landscape (Ghaderizadeh et al., 2022; Sharifi et al., 2016; Sharifi & Amini, 2015). Several authors (Moisa, Dejene, & Gemeda, 2022; Phan et al., 2018; Syawalina et al., 2022) mention that these actions lead directly to changes in soil surface temperature. But, surface temperature warms up the soil in which the yam is grown. As a result, the yam seed could rot after sowing in such conditions. Moreover, we have not found a single study in the literature addressing this topic in this part of Côte d'Ivoire that analyzes the effects of LULC change and their effects on LST. Most of the studies in this region are about cashew nuts. This is the case of theses authors (Diulyale et al., 2019; Kambou Diulyale et al., 2019) who talked about cashew industry structuring, then the diversity of cashew uses by farmers and the evaluation of grafting techniques for the renewal of ageing cashew orchards. Some of them had focused on the inventory of insect pests of the cashew orchard (Félicia et al., 2017). Only Kouakou and colleagues, by addressing yam cropping system in Côte d'Ivoire (Kouakou et al., 2019), use to determine yam species and varieties cultivated in some regions in Côte d'Ivoire including Gontougo region. Thus, this novelty is important to maintain food security and will draw the attention of researchers as well as yam farmers to invest in these aspects which are also primordial in the success of yam cropping. It is therefore needed to investigate the effect of LULC changes but also of the real state of the vegetation through the Normalized Difference Vegetation Index (NDVI) on LST in the Gontougo region in Côte d'Ivoire. The LST is the brightness temperature of the ground and therefore determines the surface temperature (Rajendran & Mani, 2015). Increased land surface temperature is related to many factors, including changes in land use land cover, changes in NDVI and land surface parameters (Rajendran & Mani, 2015; Syawalina et al., 2022). According to some authors (Moisa et al., 2022; Phan et al., 2018; Syawalina et al., 2022), the LST is increased as a result of a decrease in NDVI. Thus, the NDVI has a strong negative association with LST. In the environmental monitoring of natural resources, more specifically, agricultural land monitoring, it is critical to examine the relationship between vegetation dynamics through NDVI, LULC and LST (Moisa et al., 2022; Wu et al., 2019).

Nowadays, with the evolution of technology and the advent of Artificial Intelligence (AI), many processes are automated. This is the case with Google Earth Engine (GEE), a Machine Learning tool that allows the automated processing of remote sensing data through algorithms such as Random Forest. GEE is a geospatial processing platform based on geo-information applications in the 'cloud'. This platform provides free access to huge volumes of satellite data for computing and offers support tools to monitor and analyse environmental features on a large scale (Ghosh et al., 2022; Pérez-Cutillas et al., 2023; Tamiminia et al., 2020).

In this project, through GEE, we used Random Forest (RF) which is a Machine Learning (ML) algorithm that is commonly used to improve classifications in remote sensing applications for land use land cover classification and change detection (Ashane & Senanayake, 2023; Phalke et al., 2020; Suryono et al., 2021; Tariq et al., 2022; Teluguntla et al., 2018; Yan et al., 2022; Zhao et al., 2023) to compute and run the LULC using JavaScript as a code.

2.2. Methodology

2.2.1. Material and data description

To be able to examine LULC change and assess the correlation between NDVI, LULC and LST, the present study has focused on satellite images and field training reference data collected between November and December 2022 in the Gontougo region. Satellite images include Landsat-8 Oli/Tirs and Sentinel-2 Msi.

2.2.1.1. Satellite images description

2.2.1.1.1. Landsat-8

The Landsat data used are from United States Geological Surveys (USGS) and consist of Landsat 8 Collection 2 Tier 1 Top Of Atmosphere (TOA) Reflectance. This dataset's availability at the time of use is from March 2013 to April 2023 (**Table 2-1**). We used them through GEE to calculate NDVI and LST. We used 8 images at a rate of one image per year, from 2015 to 2022 from the same collection.
(https://developers.google.com/earth-engine/datasets/catalog/LANDSAT_LC08_C02_T1_TOA)

Table 2- 1: Landsat 8 TOA Reflectance images description

Name (Bands)	Pixel Size	Wavelength	Description
B1	30 meters	0.43 - 0.45 µm	Coastal aerosol
B2	30 meters	0.45 - 0.51 µm	Blue
B3	30 meters	0.53 - 0.59 µm	Green
B4	30 meters	0.64 - 0.67 µm	Red
B5	30 meters	0.85 - 0.88 µm	Near-infrared
B6	30 meters	1.57 - 1.65 µm	Shortwave infrared 1
B7	30 meters	2.11 - 2.29 µm	Shortwave infrared 2
B8	15 meters	0.52 - 0.90 µm	Band 8 Panchromatic

B9	30 meters	1.36 - 1.38 µm	Cirrus
B10	30 meters	10.60 - 11.19 µm	Thermal infrared 1, resampled from 100m to 30m
B11	30 meters	11.50 - 12.51 µm	Thermal infrared 2, resampled from 100m to 30m
QA_PIXEL	30 meters		Landsat Collection 2 QA Bitmask

2.2.1.1.2. Sentinel-2

The Sentinel-2 data used are from Copernicus and consist of Harmonized Sentinel-2 MSI: Multi-Spectral Instrument, Level-1C. This dataset's availability at the time of use is from 23 June 2015 to April 2023 (**Table 2-2**). We used them through GEE to do the classification and compute the LULC and its changes (change detection). We used 2 of these images. One in 2015 and the other in 2022.
(https://developers.google.com/earth-engine/datasets/catalog/COPERNICUS_S2_HARMONIZED)

Table 2- 2: Harmonized Sentinel-2 MSI image description

Name (Bands)	Pixel Size	Wavelength	Description
B1	60 meters	443.9nm (S2A) / 442.3nm (S2B)	Aerosols
B2	10 meters	496.6nm (S2A) / 492.1nm (S2B)	Blue
B3	10 meters	560nm (S2A) / 559nm (S2B)	Green
B4	10 meters	664.5nm (S2A) / 665nm (S2B)	Red
B5	20 meters	703.9nm (S2A) / 703.8nm (S2B)	Red Edge 1
B6	20 meters	740.2nm (S2A) / 739.1nm (S2B)	Red Edge 2
B7	20 meters	782.5nm (S2A) / 779.7nm (S2B)	Red Edge 3
B8	10 meters	835.1nm (S2A) / 833nm (S2B)	NIR
B8A	20 meters	864.8nm (S2A) / 864nm (S2B)	Red Edge 4
B9	60 meters	945nm (S2A) / 943.2nm (S2B)	Water vapor
B10	60 meters	1373.5nm (S2A) / 1376.9nm (S2B)	Cirrus
B11	20 meters	1613.7nm (S2A) / 1610.4nm (S2B)	SWIR 1
B12	20 meters	2202.4nm (S2A) / 2185.7nm (S2B)	SWIR 2
QA60	60 meters		Cloud mask

2.2.1.2. Google Earth Engine description

Google Earth Engine (GEE) is a geospatial cloud platform for data analysis and geo-information applications processing. This platform provides free access to huge volumes of satellite data for computing and offers support tools to monitor and analyse environmental features on a large scale. Such facilities have been widely used in numerous studies about land management and planning

(Amani et al., 2020; Ghosh et al., 2022; Pérez-Cutillas et al., 2023; Tamiminia et al., 2020). Several programming languages are used for data processing on GEE including JavaScript (JS) coding. So, through the GEE-integrated code editor, we computed and ran our data with JS Application Programming Interface (API).

2.2.2 Computing of the NDVI and LST using Landsat 8 OLI/TIRS images from 2015 to 2022

According to America's space agency (NASA Earth Observation (https://earthobservatory.nasa.gov/), LST is how hot the "surface" of the Earth would feel to the touch in a particular location and NDVI is used to quantify vegetation greenness and vegetation density and is useful in understanding plant health (**Figure 2-1**).

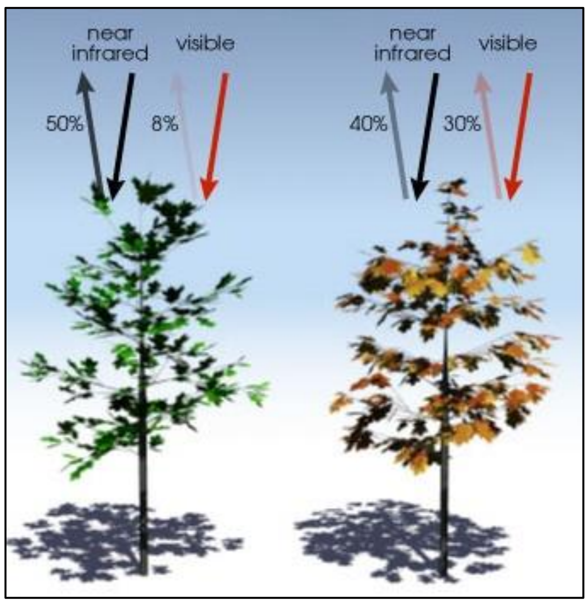

Figure 2- 1: Illustration of vegetation functioning from NDVI.

Source:https://earthobservatory.nasa.gov/features/MeasuringVegetation/measuring_vegetation_2.php

Calculations of NDVI for a given pixel always result in a number that ranges from minus one (-1) to plus one (+1); however, no green leaves give a value close to zero. A zero means no vegetation and close to +1 (0.8 - 0.9) indicates the highest possible density of green leaves.

2.2.2.1. Retrieval of LST

The thermal bands of Landsat images from OLI/TIRS were used to calculate the LST. Single-channel Landsat 8 images were utilized to derive LST (band 10 for each year). For determining

LST, it employs the brightness temperature of one band of thermal infrared (TIR), as well as the mean and differential in land surface emissivity (Abulibdeh, 2021; Benmecheta, 2016; Moisa, Gabissa, et al., 2022; Schmugge et al., 2020).

2.2.2.2. Conversion of digital number into radiance

The first step in calculating LST from metadata of Landsat image files was to convert the digital number to radiance for Landsat OLI/TIRS before calculating brightness temperature (Moisa, Dejene, & Gemeda, 2022; Moisa, Gabissa, et al., 2022; Schmugge et al., 2020). The Landsat 8 OLI's digital numbers (DNs) of band 10 were first converted to spectral radiance (**Eq. 1**).

$$L\lambda = (ML \times QCal) + AL \quad (1)$$

where:

$L\lambda$ is the top of atmosphere (TOA) spectral radiance in watts/ (meter squared ster µm).

ML is a band-specific multiplicative rescaling factor from the metadata (RADIANCE_MULT_BAND_x, where x is the band number).

AL is the band-specific additive rescaling factor from the metadata (RADIANCE_ADD_BAND_x, where x is the band number).

QCal corresponds to band 10. Is quantized and calibrated standard product pixel values (DN).

TOA = 0.0003342 * "Band 10" + 0.1

2.2.2.3. TOA to brightness temperature conversion

Based on land surface emissivity, atmospheric trans-emissivity, brightness temperature, and average atmospheric temperature, the mono-window algorithm is used to determine LST (**Eq. 2**). (Benmecheta, 2016; HUANG et al., 2020; Moisa, Dejene, & Gemeda, 2022).

$$BT = \frac{K2}{\ln\left(\frac{K1}{L\lambda}\right) + 1} - 273{,}5 \quad (2)$$

where:

BT is an effective at-sensor brightness temperature (K).

K1 = Band-specific thermal conversion constant from the metadata (K1_CONSTANT_BAND_x, where x is the thermal band number). (W/(m2 sr µm)).

K2 = Band-specific thermal conversion constant from the metadata (K2_CONSTANT_BAND_x, where x is the thermal band number). (K)

Lλ is spectral radiance at the sensor's aperture (W/(m2 sr μm)). Lλ = TOA.

Therefore, to obtain the results in Celsius, the radiant temperature is adjusted by adding the absolute zero (approx. -273.15°C).

BT = (1321.0789 / Ln ((774.8853 / "%TOA%") + 1)) – 273.15

2.2.2.4. Calculate the NDVI

The NDVI formula is written according to (Aka et al., 2022; Dibi et al., 2008; Sharifi, 2018) as follows (**Eq. 3**):

$$\mathrm{NDVI} = \frac{\mathrm{NIR-R}}{\mathrm{NIR+R}} \tag{3}$$

Where:

NIR = Near-Infrared; Corresponds to the band B5

R = Red; Corresponds to the band B4

Note that the calculation of the NDVI is important because, subsequently, the proportion of vegetation (PV), which is highly related to the NDVI, and emissivity (ε), which is related to the Pv, must be calculated.

2.2.2.5. Calculate the proportion of vegetation Pv

PV is the vegetation proportion acquired according to the formula of (Carlson & Riziley, 1997) as indicated in the following (**Eq. 4**)

$$\mathrm{PV} = \left[\frac{\mathrm{NDVI - NDVImin}}{\mathrm{NDVImax - NDVImin}}\right]^2 \tag{4}$$

2.2.2.6. Calculate Emissivity ε

According to (Gogoi et al., 2019; Sobrino et al., 2004), the land surface emissivity is computed using (**Eq.5**)

$$\varepsilon = 0.004 * \mathrm{PV} + 0.986 \tag{5}$$

The value of 0.986 corresponds to a correction value of the equation.

2.2.2.7. Calculate the Land Surface Temperature

Finally, apply the LST equation to obtain the surface temperature maps. The calculated radiant surface temperatures were corrected for emissivity using the following equation (Moisa, Dejene, & Gemeda, 2022) (**Eq. 6**)

$$\mathrm{LST} = \frac{\mathrm{BT}}{1 + \lambda\left(\frac{\mathrm{BT}}{\rho}\right)\ln\varepsilon} - 273{,}5 \tag{6}$$

LST = [BT / ((1 + (0.00115 * BT / 1.4388) * Ln(ε) – 273,5)]

where:

LST: land surface temperature (in Kelvin).

BT: Brightness surface Temperature (in Kelvin).

λ: the wavelength of emitted radiance (10.8 μm).

ρ: h × c/σ (1.438 × 10−2 mK): h is Planck's constant (6.26× 10−34 J s); c is the velocity of light (2.998× 108 m/s);

σ is Stefan Boltzmann's constant (1.38× 10−23 J/K), and ε is land surface emissivity.

2.2.3. Computing of LULC using Sentinel-2 Multi-Spectral Instrument (MSI) of 2015 and 2022

2.2.3.1. Collection of field training data and adoption of the legend

A three (3) week field mission in the Gontougo region collected three hundred and ninety (390) samples of training points distributed over each land use unit. These data were used to classify the two (2) Sentinel-2 images by training the Random Forest (RF) algorithm on 60% of these data and 40% for testing. Below is a spatial distribution of the data collected on the ground on the 2022 Sentinel-2 image (**Figure 2-2**).

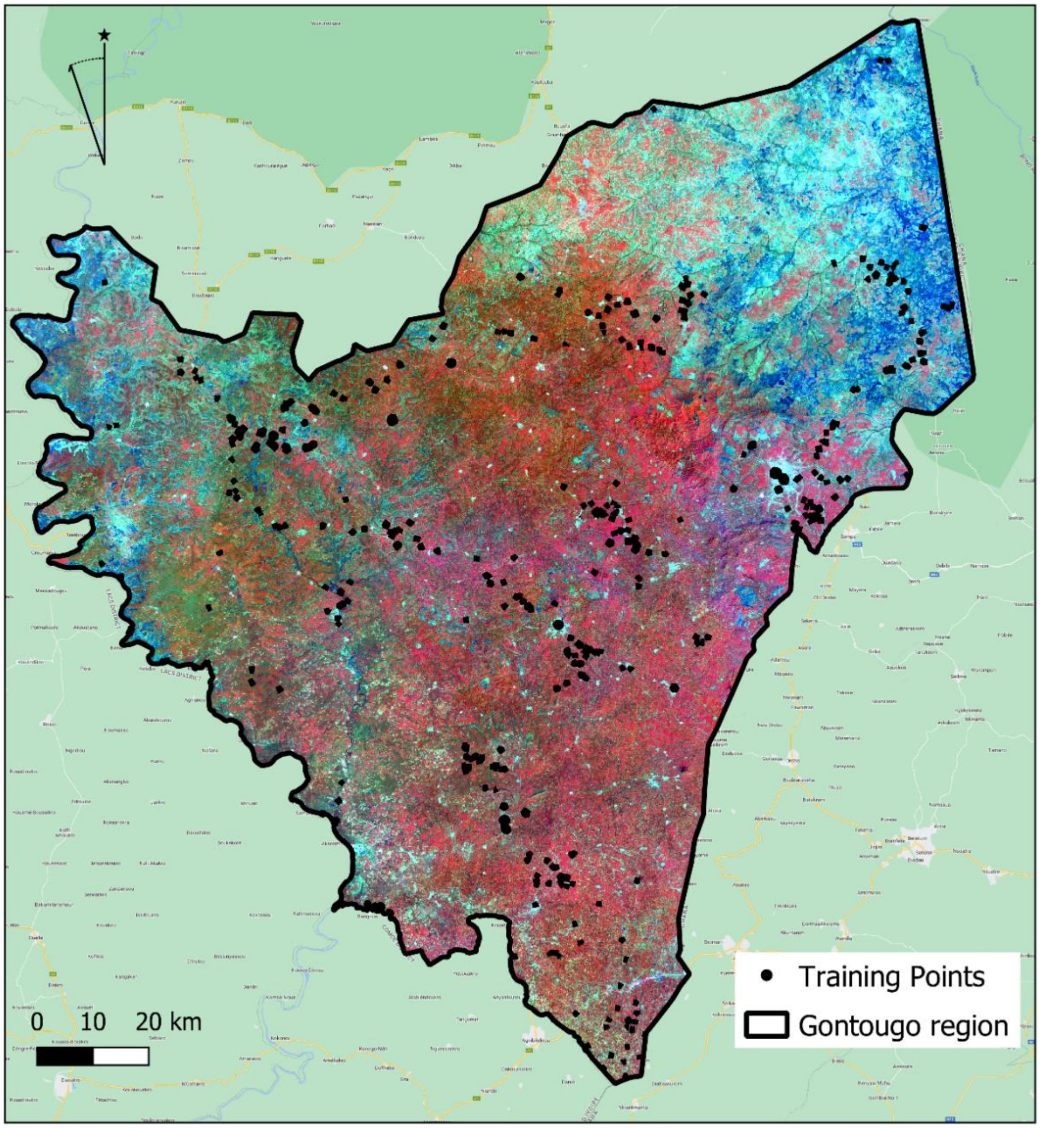

Figure 2- 2: Distribution of point samples collected for the classifications

This step led us to define and adopt the legend according to the major LULC units found in the field. Thus, six (6) classes were retained. They are described in the table below (**Table 2-3**)

Table 2- 3: Description of land occupation units according to the field

Code	LULC classes	Description of the classes	LULC units reflectance
0	Annual crops	This class includes cultivated land, as well as fallow land, sparsely wooded land and clearings with some wood which serve as stakes for yam growth	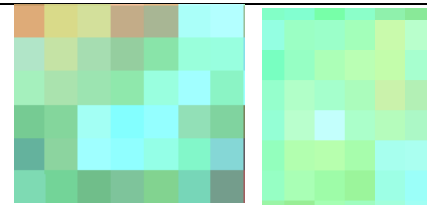
1	Perennial crops	They are essentially cash crops with a very strong presence of cashew nuts, and very low representations of hevea and cocoa.	
2	Savannah	These are continuous grassland formations over large areas with the presence of shrubs and savannah trees	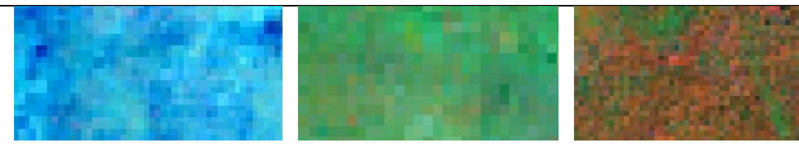
3	Forest	There are mostly gallery and islets forests, which are more or less sacred and protected by the populations, there are also degraded forests and the presence of teak wood.	
4	Bareland & Settlement	These are mainly dwellings or human constructions, urban patches, roads, denuded soils and rock slabs	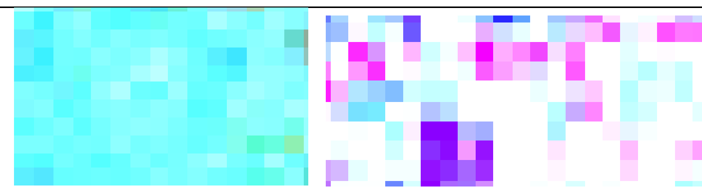
5	Waterbody	Waterbody includes the form of streams, puddles, watercourses, rivers and swamp	

2.2.3.2. Loading of Sentinel-2 images

We loaded the Sentinel-2 image collection and applied the filters to them to select the images of the study area, then applied the mask, the mosaic and made the clip. The filters are filter date, filter bounds, cloud cover, cloud pixel and the select bands.

2.2.3.3. Index computation and create image composite

Before moving on to the classification, it is important to calculate the biophysical indices in order to highlight the spectral characteristics of the LULC units according to their reflectance (Aka et al., 2022; Dibi et al., 2008; Kadio et al., 2022). Therefore, we automatically calculated four indices: Soil index (SI), Normalized Difference Vegetation Index (NDVI), Enhanced Vegetation Index (EVI), Soil Adjusted Vegetation Index (SAVI) (Barriguinha et al., 2022; Morawitz et al., 2006; Zheng et al., 2014). Then, we combined them with the clipped images of the study area to create new channels, stacked them together to enhance the reflectance of the units; and achieved less confusion, better classification and good accuracy. They were calculated according to the following scripts:

```
// Soil index (SI)
  var SI= image.expression('((65536-Green)*(65536-Blue)*(65536-Red))',
{ 'Red':image.select(['B4']),  'Green':image.select(['B3']),   'Blue':image.select(['B2'])  }
// Normalized Difference Vegetation Index (NDVI)
var NDVI= image.normalizedDifference(['B8', 'B4']).rename('NDVI');
// Enhanced Vegetation Index (EVI)
var EVI = S2.expression( '2.5 * ((NIR -RED) / (NIR + 6 * RED -7.5 * BLUE + 1))',
//Soil Adjusted Vegetation Index (SAVI)
var SAVI = S2.expression ('float (((NIR - RED) / (NIR + RED + L))* (1+L))',{ 'L': 0.5}
//Compilation of Sentinel-2 bands and calculated indices
var compositeS2SS= S2.addBands(si).addBands(ndvi).addBands(evi).addBands(savi)
Map.addLayer (compositeS2 , viparams, "compositeSS");
```

2.2.3.4. Setting up of input parameters for classification using Random Forest Algorithm (RFA)

Random Forest (RF) is one of the machine learning algorithms used for satellite image classification and geo-information processing. RF is a powerful algorithm for feature selection, as it ranks the importance of each input variable based on how much it contributes to the overall accuracy of the classification (Ashane & Senanayake, 2023; Suryono et al., 2021; Teluguntla et al., 2018; Yan et al., 2022; Zhao et al., 2023).

2.2.3.4.1. Classification features set up

We define the code of each class and we give it the name of the LULC units. Then the points of the LULC samples collected are distributed. 60% were used for training and 40% for testing.

//Classification functions

Class code = [0, 1, 2, 3, 4, 5]

Class code rename = OCS = ["Annual crops", "Perennial crops", "Savannah", "Forest", "Bareland and Settlement", "Waterbody"];

//Distribution of training and testing points

// Training 60%

var training_22 = RedRegions_S2SS.filter(ee.Filter.lt('random', 0.6));

// Testing 40%

var testing_22 = RedRegions_S2SS.filter(ee.Filter.gte('random', 0.4));

2.2.3.4.2. Define Random Forest function for classification

The RFA (*smileRandomForest*) is applied to the set of stacker images for 2022 and for 2015, and then the algorithm is executed.

var Classification= function(training, label, bands, image, testing) {}

var trainedRF= ee.Classifier.smileRandomForest(100).train({ features: training, classProperty: label, inputProperties: bands, });

var classifiedRF = S2.select(bands).classify(trainedRF)

2.2.3.5. Computing of the LULC changes: Change Detection

The analysis of the changes that occurred over the entire study period was conducted using the two Sentinel-2 images. It produces a change detection matrix from the comparison between the maps of the two dates. So, once the two LULC have been obtained, we identified the difference between the two dates (Aniah et al., 2023; Gou et al., 2022; Kafi et al., 2014) and then obtain the change according to the following script:

```
// Define a function to compute change detection using the LULC maps
function compute_change(lulc1, lulc2) {
  var change = lulc2.subtract(lulc1);
  // Mask out areas where the LULC did not change
  var mask = change.neq(0);
  change = change.updateMask(mask);
  // Return the change map
  return change;}
// Compute change maps for 2015 and 2022
var change_2015_2022 = compute_change(lulc_2015, lulc_2022);
```

Notably, the LULC results obtained from GEE have been geo-processed using ArcGIS software to give the best possible representation of the different land uses and land cover that the Gontougo Region reflects. This is one of the limitations of this study.

2.2.3.6. Define and generate the Accuracies assessment

The classification details and accuracy are generated using the RFA functions, The function that displays them on GEE is "print" (Aniah et al., 2023; Ghayour et al., 2021). There are: Error Matrix, Kappa, Overall accuracy (OA), Producer's accuracy, User's accuracy and the classification Score for each LULC classes

```
print('Training Results RF',TrainingResults_RF);
print('RF Matrice Confusion: ', cmRF);
print('RF Produceers accuracy: ', paRF);
print('RF Users/Cons accuracy: ', caRF);
print('Validation Results RF',results_RF);
```

2.2.4. Analysis of LULC changes rate

The Overall Change Rate (Tg) is used to estimate the overall progress (the proportion of gain or loss) of the areas of LULC units (Aka et al., 2022; Dahan et al., 2021). The overall rate of change is obtained from the following mathematical formula (**Eq. 7**).:

Tg = [(S2 – S1)/ S1] *100 (**Eq. 7**).

where:

Tg = Overall rate of change (%);

S1 = Area of the class on date t_1 (initial date);

S2 = Area of the class on the date t_2 (final date), and $t_2>t_1$.

2.2.5 Correlations Analysis between NDVI and LST

We used Pearson correlation coefficient (also known as Pearson R statistical test) to measure the strength between the different variables and their relationships (**Eq. 8**). Here we measure a statistical test between two variables (NDVI and LST) Therefore, according to authors such as Peng et al., (2020; Zheng et al., (2014), the calculation of the correlation coefficient value allows to know the strength of the relationship between two variables. Pearson's correlation coefficient can range from +1 to -1, where +1 indicates the perfect positive relationship between the variables considered, -1 indicates the perfect negative relationship between the variables considered, and 0 value indicates that no relationship exists between the variables considered (Njoku & Tenenbaum, 2022; Zheng et al., 2014).

$$r_{xy} = \frac{n\sum x_i y_i - \sum x_i \sum y_i}{\sqrt{n\sum x_i^2 - (\sum x_i)^2}\ \sqrt{n\sum y_i^2 - (\sum y_i)^2}} \quad (8)$$

Where:

r_{xy} = Pearson r correlation coefficient between x and y

n = number of observations

x_i = value of x (for ith observation)

y_i = value of y (for ith observation)

2.2.6 Correlations Analysis between LULC and LST

Through qualitative and quantitative comparison of the change, the LULC types were compared with the LST values over the classification years based on their respective changes (Moisa, Dejene, & Gemeda, 2022).

2.3. Results

2.3.1. NDVI Analysis

Over the study period, between 2015 and 2022, the NDVI of the Gontougo region was determined according to the NIR and Red multispectral bands of the Landsat images. We noticed that the year 2021 presents the highest NDVI mean value with 0.246 and the year 2016 presents the lowest with 0.205 (**Table 2-4**). Each of the NDVI values per year of study is statistically presented in a histogram. These histograms show the distribution of vegetation cover according to the channel in which the NDVI value is high, medium or low (**Figure 2-3**). It can be seen that the distribution of NDVI revolves around the mean values where the highest peaks are observed.

Table 2- 4: NDVI variation from 2015 to 2022

Year	**2015**	**2016**	**2017**	**2018**	**2019**	**2020**	**2021**	**2022**	**NDVI change (2015 - 2022)**
Minimum NDVI	-0.046	-0.030	-0.108	-0.064	-0.081	-0.040	-0.105	-0.090	-0.044
Maximum NDVI	0.567	0.415	0.416	0.431	0.482	0.454	0.557	0.414	-0.153
Mean NDVI	0.215	0.205	0.214	0.221	0.240	0.244	0.246	0.243	0.029

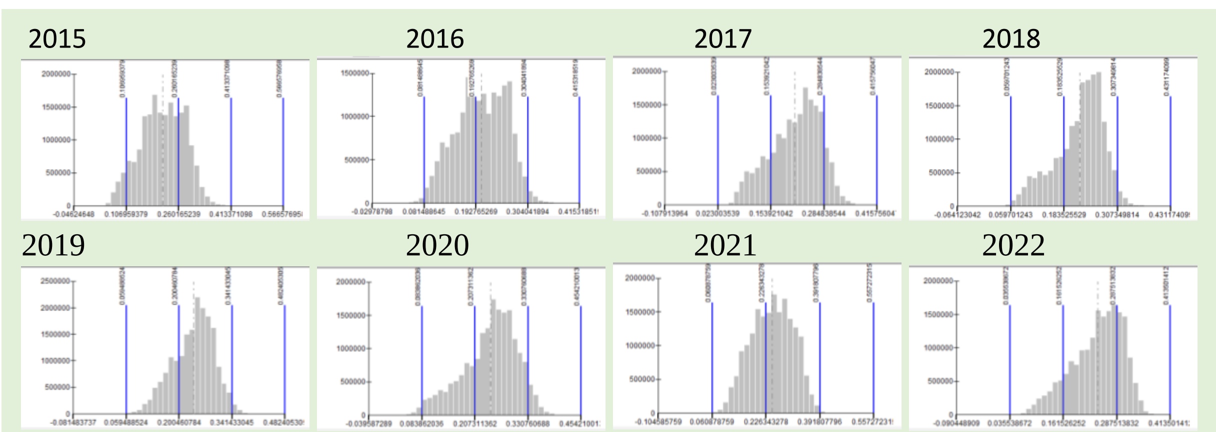

Figure 2- 3: NDVI histograms per year

Qualitatively, the results show that the North-East, North-West and West parts are much more devoid of vegetation than the other parts of the study area. The central and southern areas have some greenery. It should also be noted that overall, the values vary from -0.108 to 0.566 (**Figure 2-4**). The mean values of each NDVI were extracted to appreciate the trend of the vegetation

(**Figure 2-5**) and it was found that the years 2019 to 2022 show higher average vegetation than the years 2015 to 2018 where the trend is lower.

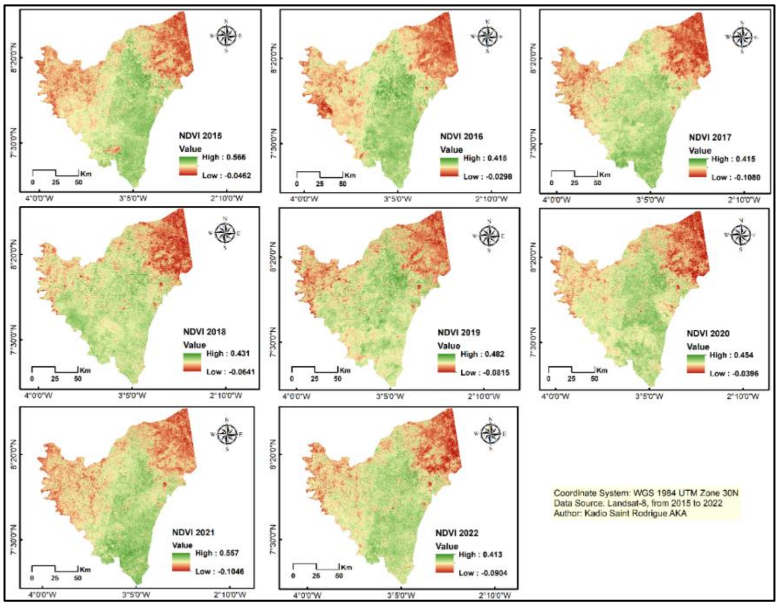

Figure 2- 4:NDVI maps from 2015 to 2022

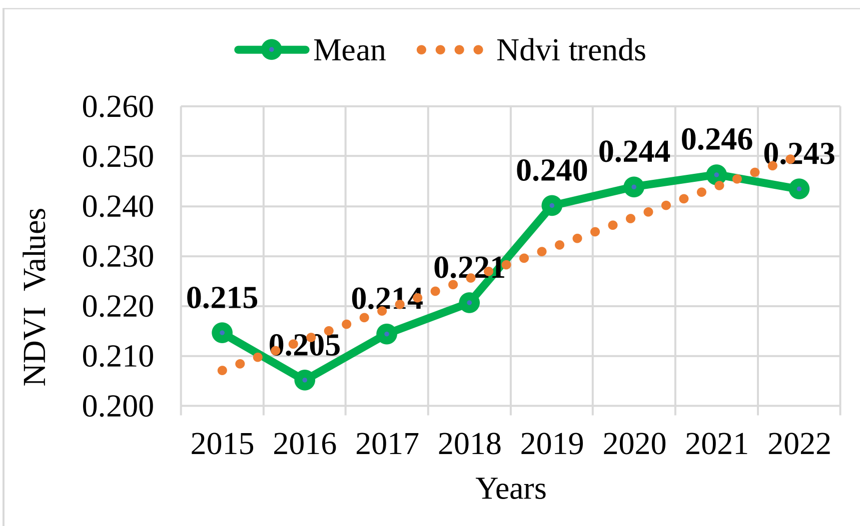

Figure 2- 5: Gontougo Ndvi mean over time

2.3.2. LST Analysis

The LST is used in monitoring the temperature and surface processing of land features. In the present study, LST is calculated using thermal bands from Landsat images from 2015 to 2022. Table 5 reveals that the maximum temperature peaked at 50.11°C in the year 2021, while the minimum temperature recorded 9.21°C in 2019. Overall, LSTs are around 31°C when considering mean values. Similarly, at the mean level, there has been a temperature decrease of 0.19°C over the years from 2015 to 2022 (**Table 2-5**).

Table 2- 5: LST variation from 2015 to 2022

Year	**2015**	**2016**	**2017**	**2018**	**2019**	**2020**	**2021**	**2022**	**LST change (2015 - 2022)**
Minimum LST (°C)	17.33	12.48	12.47	8.71	9.21	16.69	9.71	16.53	-0.79
Maximum LST (°C)	45.22	46.35	44.95	46.37	46.27	49.32	50.11	45.81	0.58
Mean LST (°C)	31.05	32.73	30.47	31.01	31.98	32.52	32.15	30.86	-0.19

To appreciate these values, we generated histograms for each year of LST. These histograms show the distribution of LST values. The horizontal axis shows the minimum values at the beginning, the middle, the mean value and the maximum value at the end. On the vertical axis, we can see the evolution especially the concentration of the LST values from the diagonal line (**Figure 2-6**). For all years, the distribution of LST is more or less concentrated on the mean where the highest peaks are observed.

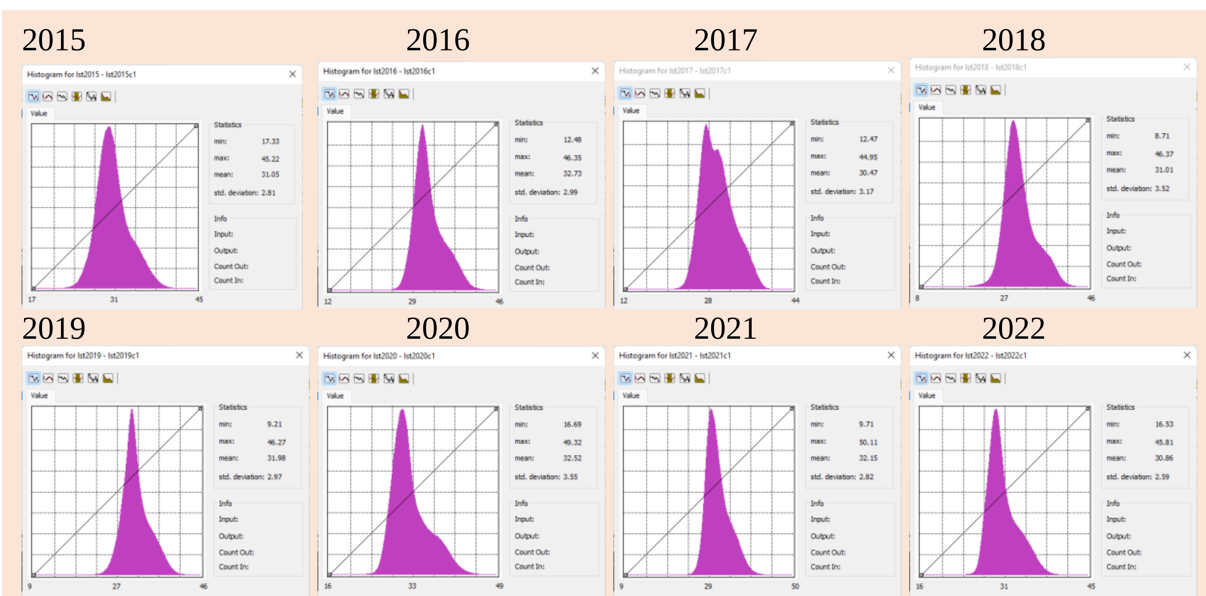

Figure 2- 6: LST histograms per year

The findings of the study revealed that the Northeastern and some few Western parts of the study area had high LST except in the year 2019 where the western part is not high, whereas the southern and Centre-eastern parts had low LST (**Figure 2-7**).

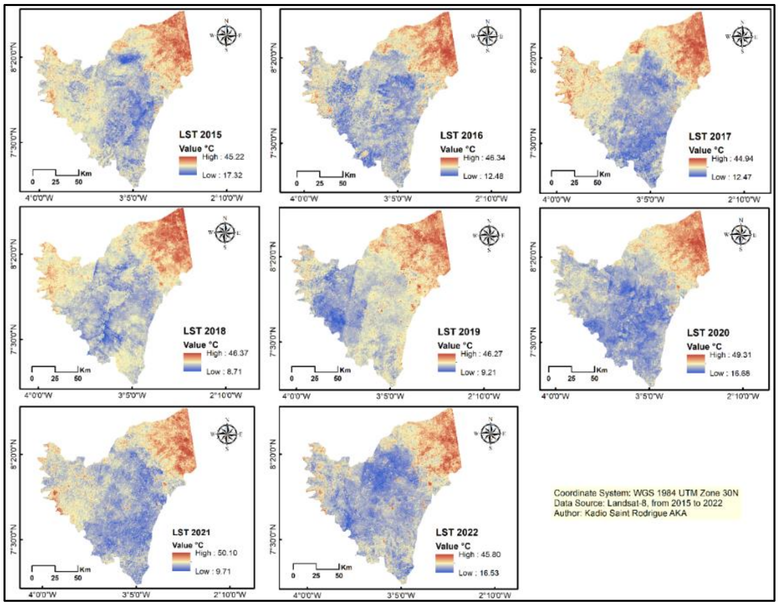

Figure 2- 7: LST maps from 2015 to 2022

Based on the mean values, we have represented the trend of the LST. The year 2017 recorded the lowest temperature at 30.47°C and the year 2016 had the highest temperature at 32.73°C The overall trend shows a constant and slight evolution along the LST trend line (**Figure 2-8**)

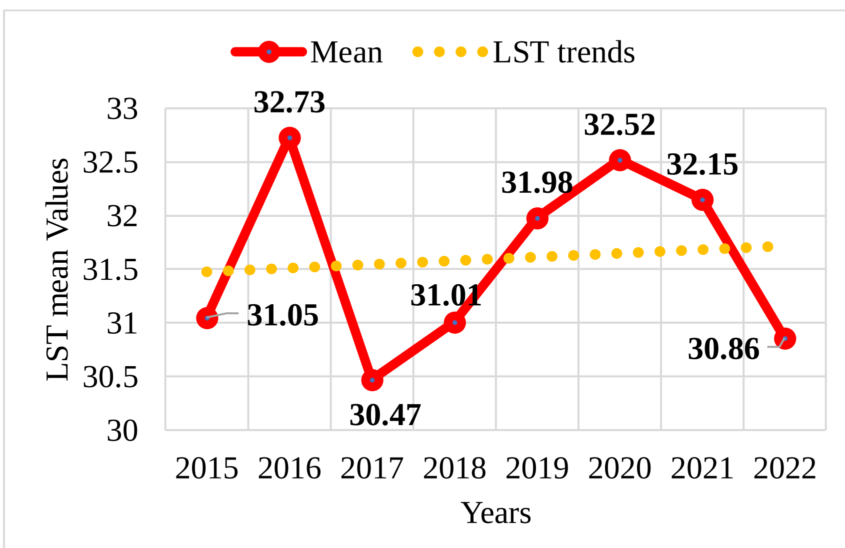

Figure 2- 8: Gontougo LST mean over time

2.3.3. Land use land cover changes

All the results obtained in this section are from the classification of Sentinel-2 images via GEE, therefore, we have used the following abbreviations: UA: User Accuracy; PA: Producer Accuracy;

OA: Overall Accuracy Acrops: Annual crops; Pcrops: Perennial crops; Sav: Savannah; Forest: Forest; BarSet: Bareland and Settlement; Wb: Waterbody.

2.3.3.1. Accuracy assessment

Accuracy assessment is a process of evaluating the accuracy of a land use land cover (LULC) classification map (the classified data) by comparing it to reference data (Aniah et al., 2023; Olofsson et al., 2013). The field sample of LULC units serves as our reference data. Accuracy assessment provides a quantitative measure of the classification's overall accuracy and identifies the LULC classes where errors are more prevalent. Thus, we were able to determine for each classification the following precision statistics: F1 score, PA and UA (**Table 2-6**). The F1 score takes into account both precision (PA and UA) and recall so that the two reach the highest at the same time and take a balance (Zhang et al., 2023) In this case, the BarSet class has the greatest score for the year 2015 (0.98), while Acrops has the lowest (0.70). For the year 2022, the highest score is the Wb class (1.00) and the lowest is Acrops (0.83). The percentage of pixels in each class that were correctly classified to all of the pixels in that class in the reference data is what determines the producer's accuracy in table 2-6. It evaluates how accurately a classification can identify a given class. And then, the user's accuracy is the proportion of correctly classified pixels in each class to the total number of pixels in that class in the classification map. It measures the accuracy of classification in correctly assigning pixels to a particular class (Aniah et al., 2023; Congalton, 1991; Jensen, 1986; Olofsson et al., 2013; Rwanga & Ndambuki, 2017; S. Zhang et al., 2023). In our situation, we had low values of PA and UA in 2015 of 0.73 and 0.67, respectively, which belonged to the classes Acrops and Sav. Also, as high values, 0.96 and 1.00 belong to the classes of Pcrops and Wb respectively. Following the year 2022, the trend was better and we had as low values of PA and UA 0.80 and 0.81 belonging respectively to the Savannah and Acrops classes. And as a high value, 1.00 of each side belonging to the classes Wb and BarSet for PA and Wb for UA. **Figure 2-9** shows graphically these precisions with all the different values in the vertical axis.

Table 2- 6: Samples training data classifications precisions by LULC class

LULC classes	2015			2022		
	F1 score (%)	**Producer Accuracy (%)**	**User Accuracy (%)**	**F1 score (%)**	**Producer Accuracy (%)**	**User Accuracy (%)**
Acrops	0.70	0.73	0.67	0.83	0.85	0.81

Pcrops	0.97	0.96	0.98	0.98	0.99	0.97
Sav	0.75	0.86	0.67	0.86	0.80	0.94
Forest	0.85	0.85	0.85	0.92	0.85	1.00
BarSet	0.98	1.00	0.96	0.98	1.00	0.96
Wb	0.89	0.80	1.00	1.00	1.00	1.00

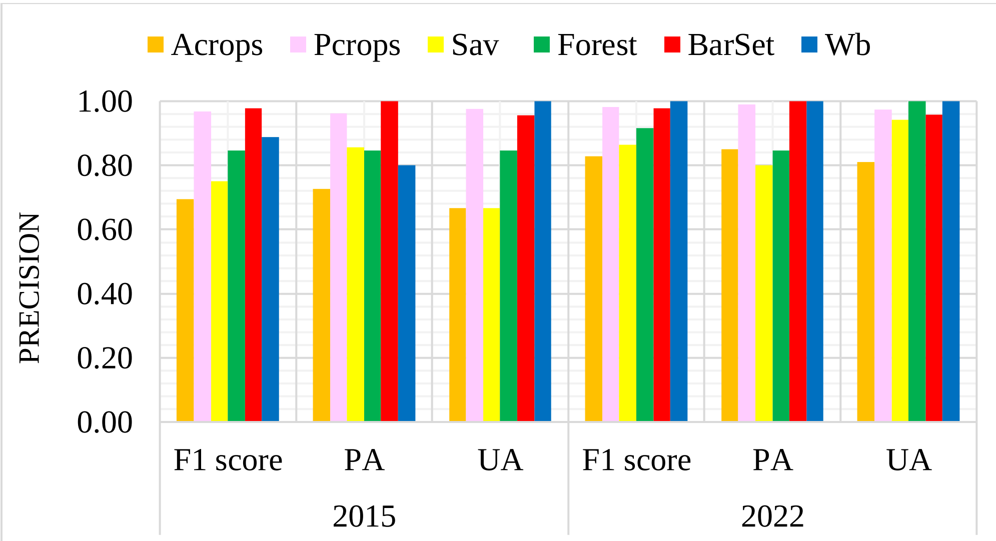

Figure 2- 9: Samples precisions of the LULC mapping for the two years

The overall cartographic accuracy and kappa coefficient of the classification process on the two Sentinel-2 images are presented in **table 2-7 and table 2-8** (**error matrices).** Bold values in these tables represent row or column totals**.** For each year's classification, we calculated Overall Accuracy (OA) and Kappa to evaluate the accuracy of the classification results. Overall accuracy is the proportion of correctly classified pixels to the total number of pixels in the image. It provides a measure of the classification's overall accuracy. The kappa coefficient is a measure of agreement between the classification map and the reference data that takes into account the possibility of chance agreement. It ranges from -1 to 1, with 1 indicating perfect agreement and 0 indicating no agreement beyond chance. (Aka et al., 2022; Banko, 1998; Congalton, 1991; Rwanga & Ndambuki, 2017; Zhang et al., 2023). In the 2015 LULC classification, the OA was 0.94% and the kappa 0.87. However, in the year 2022, the OA was 0.96% and the kappa 0.92. The diagonal values in grey font represent the well-classified pixels between the UA and the PA and the other values represent the commission and omission errors. Both errors occur during these LULC mapping. Indeed, an error of omission refers to when a feature that should have been mapped was missed, while an error of commission occurs when a feature is mapped that should not have been included in the LULC classification (Akomolafe & Rosazlina, 2022; Banko, 1998; Congalton, 1991).

Table 2- 7: LULC error matrix 2015

Overall accuracy = 93.77% **Kappa = 0.87**							
Data Classified 2015	**Acrops**	**Pcrops**	**Sav**	**Forest**	**BarSet**	**Wb**	**Row Total**
Acrops	66.67	1.25	0.00	0.00	4.35	0.00	**72**
Pcrops	25.00	97.50	22.22	7.69	0.00	0.00	**152**
Sav	0.00	0.63	66.67	0.00	0.00	0.00	**67**
Forest	8.33	0.00	11.11	84.62	0.00	0.00	**104**
BarSet	0.00	0.00	0.00	0.00	95.65	0.00	**96**
Wb	0.00	0.63	0.00	7.69	0.00	100.00	**108**
Column Total	**100**	**100**	**100**	**100**	**100**	**100**	**600**

Table 2- 8: LULC error matrix 2022

Overall accuracy = 96.01% **Kappa = 0.92**							
Data Classified 2022	**Acrops**	**Pcrops**	**Sav**	**Forest**	**BarSet**	**Wb**	**Row Total**
Acrops	80.95	0.53	5.88	0.00	4.17	0.00	**92**
Pcrops	9.52	97.37	0.00	0.00	0.00	0.00	**107**
Sav	9.52	1.05	94.12	0.00	0.00	0.00	**105**
Forest	0.00	1.05	0.00	100.00	0.00	0.00	**101**
BarSet	0.00	0.00	0.00	0.00	95.83	0.00	**96**
Wb	0.00	0.00	0.00	0.00	0.00	100.00	**100**
Column Total	**100**	**100**	**100**	**100**	**100**	**100**	**600**

2.3.3.2. LULC mapping

The LULC mapping of the study area led to two maps, each showing the following six classes: Annual crops, Bareland and Settlement, Forest, Perennial crops, Savannah, and Waterbody (**Figure 2-10**). At first glance, we can see the regression of forest and annual crop classes between the two dates. The savannah class is more present in the northeast and in the extreme west, and little represented in the central region where the forest is dominant. The Waterbody class is very thin and is almost invisible. However, it can be observed on the western side in the year 2015, where a river flows, of which the study area is the limit. Generally, water in the research region is mostly in the form of puddles, ponds, and wetlands, which dries up during the dry season leaving bare soil. The Bareland and Settlement class is disseminated and more present in the northwest on both images and accentuated in 2022. Finally, the Perennial crops class, the most obvious and visible in both images, occupies the largest area (63% in 2015 and 67% in 2022) of all LULC classes (**Table 2-9** and **Figure 2-11**).

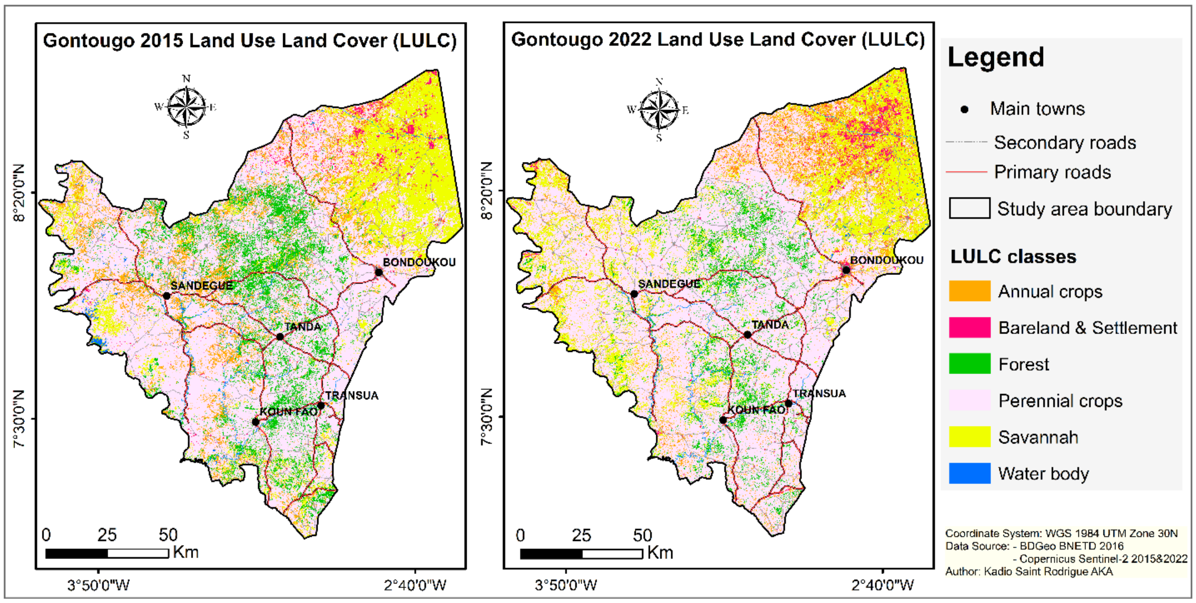

Figure 2- 10: Gontougo LULC map of 2015 and 2022

Table 2- 9: LULC area in hectares and percentage

LULC classes	**2015**		**2022**	
	Area (Ha)	**Area (%)**	**Area (Ha)**	**Area (%)**
BarSet	32958.91	2.03	44745.25	2.76
Forest	158052.47	9.74	89220.32	5.50
Wb	10396.58	0.64	5455.90	0.34
Sav	236322.41	14.56	271900.00	16.75
Acrops	155524.34	9.58	123500.00	7.61
Pcrops	1029566.75	63.44	1088000	67.04
Total	**1622821.48**	**100.00**	**1622821.48**	**100.00**

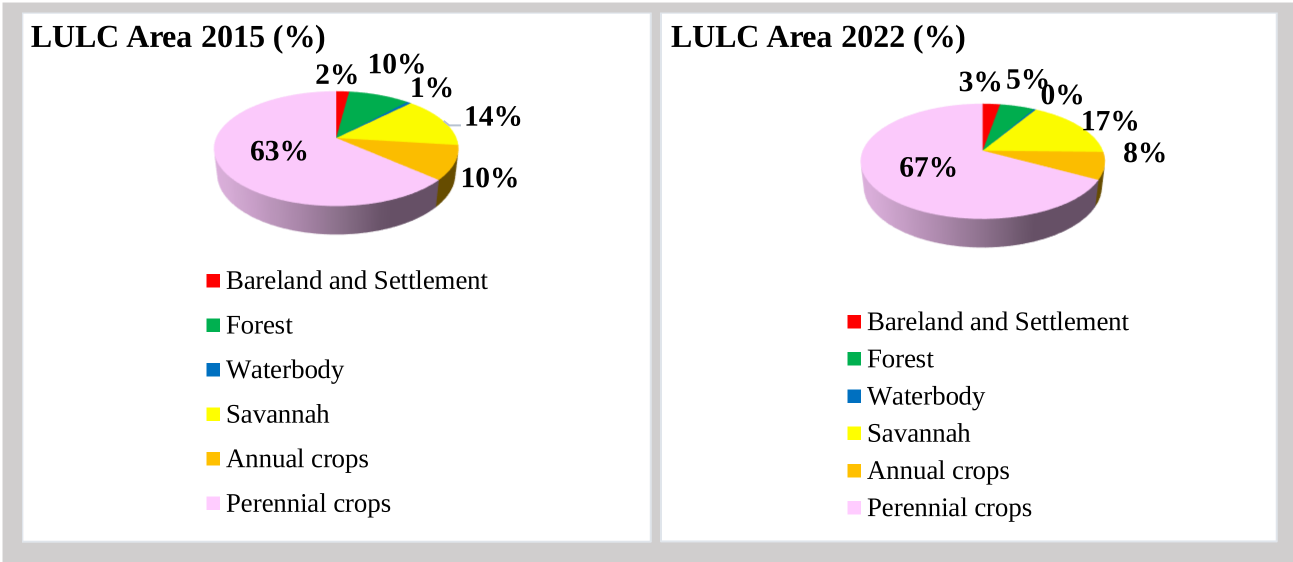

Figure 2- 11: Spatial-temporal evolution in LULC areas (%) from 2015 to 2022

2.3.3.3. Assessment of the LULC changes

The overall rate of LULC changes made it possible to estimate the overall increase in gains and losses proportion of LULC areas (Aka et al., 2022). Analysis of the rate of change shows that BareSet, Sav and Pcrops have positive values then indicate a “gain or progression in the area” and Forest, Wb and Acrops have negative values thus indicating a “loss or regression in the area” (**Figure 2-12**). The critical loss is Wb (-47.52%) and the most gain is for the BarSet (35.76%) class.

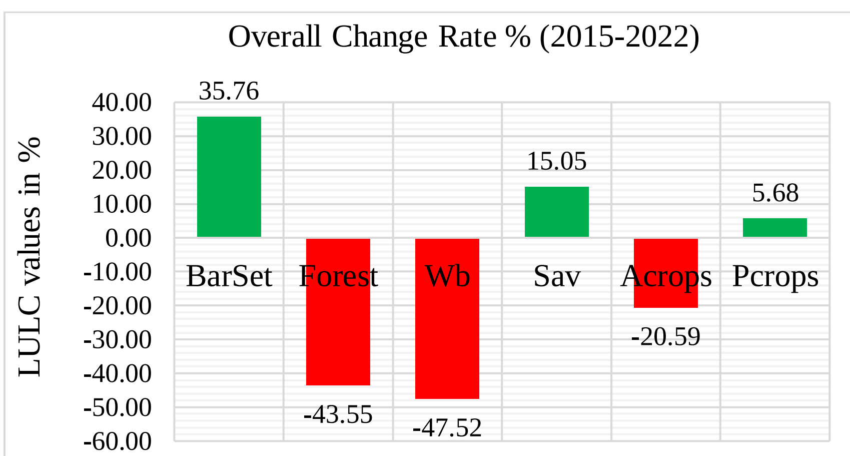

Figure 2- 12: Overall rate of LULC changes in the study area between 2015 and 2022

The assessment of the LULC Overall change rate led us to set up and calculate the LULC change matrix, also called the transition matrix. The LULC change matrix is used to quantify changes in the distribution of LULC types over time. We used it to monitor and analyze changes between the 2015 and 2022 LULC maps. The matrix rows represent the LULC types in the earlier period, whereas the columns represent the LULC types in the later time. The matrix cells show the areas converted from one LULC type to another. However, the diagonal values in grey colour represent the percentages of LULC classes that remained stable. Only 13.40% of the Acrops areas have remained stable and 65.14% have been converted into Pcrops, which is alarming (**Table 2-10**). These statistics can be seen in detail with the overall area in hectares, the percentage of each LULC type and the changes it has experienced from 2015 to 2022 in **Table 2-11.** As shown in the area column (in percentage), the values in grey colour stand for LULC classes that remained stable and the other values have undergone mutations by moving from one class to another.

Table 2- 10: LULC changes matrix in percentage between 2015 and 2022

LULC classes		**2015**					
		Acrops	**BarSet**	**Forest**	**Pcrops**	**Sav**	**Wb**
2022	**Acrops**	13.40	26.04	0.87	5.93	12.94	9.80
	BarSet	2.26	43.22	0.05	0.57	8.78	2.40
	Forest	0.10	0.00	37.81	2.39	1.06	2.25
	Pcrops	65.14	12.30	48.13	83.23	19.99	20.68
	Sav	18.79	18.32	13.02	7.79	56.16	51.51
	Wb	0.31	0.12	0.12	0.08	1.06	13.36

Table 2- 11: LULC changes matrix details between 2015 and 2022

LULC change (2015 - 2022)	Area (Ha)	LULC classes change (Ha)	Area (%)
BarSet - Forest	1.258	32958.91	0.00
BarSet - BarSet	14246.437		43.22
BarSet - Pcrops	4052.67		12.30
BarSet - Acrops	8583.481		26.04
BarSet - Sav	6036.728		18.32
BarSet - Wb	38.336		0.12
Forest - Forest	59761.825	158052.474	37.81
Forest - BarSet	74.705		0.05
Forest - Pcrops	76077.739		48.13
Forest - Acrops	1376.897		0.87
Forest - Sav	20575.849		13.02
Forest - Wb	185.459		0.12
Wb - Forest	233.771	10396.586	2.25
Wb - BarSet	249.596		2.40
Wb - Pcrops	2149.912		20.68
Wb - Acrops	1018.358		9.80
Wb - Sav	5355.618		51.51
Wb - Wb	1389.331		13.36
Sav - Forest	2507.408	236322.412	1.06
Sav - BarSet	20760.611		8.78
Sav - Pcrops	47252.3		19.99
Sav - Acrops	30580.906		12.94
Sav - Sav	132720.742		56.16
Sav - Wb	2500.445		1.06
Acrops - Forest	162.239	155524.344	0.10
Acrops - BarSet	3515.856		2.26
Acrops - Pcrops	101314.754		65.14
Acrops - Acrops	20834.644		13.40
Acrops - Sav	29216.859		18.79
Acrops - Wb	479.992		0.31
Pcrops - Forest	24590.075	1029566.746	2.39
Pcrops - BarSet	5900.056		0.57
Pcrops - Pcrops	856922.474		83.23
Pcrops - Acrops	61093.983		5.93
Pcrops - Sav	80197.774		7.79
Pcrops - Wb	862.384		0.08
TOTAL	**1622821.47**	**1622821.47**	**600**

2.3.4. Correlation between NDVI and LST

The relationship between LST and NDVI index was examined using Pearson Correlation analysis. We performed this statistical analysis by comparing the LST and NDVI values after a reclassification where both variables have the same number of classes. We had eight images on each side, so eight matches were made per pair (LST and NDV together).LST values were discovered to range from maximum temperature (50.11 °C) to minimum temperature (9.21 °C), whereas NDVI values are found to range from 0.567 to −0.108 maximum to minimum. The results show that LST and NDVI have a significant (strong negative) correlation each year (**Table 2-12**). Following table 2-12, which shows the type of correlation between NDVI and LST, we looked at the plots generated by these tables, which show how the regression line declines at each correlation (**Figure 2-13**). This means a negative correlation between NDVI and LST. Pearson's correlation coefficient (r) recorded at each correlation thus indicates negative values from 2015 to 2022. Respectively these values are (from 2015 to 2022): r= -0.992, r= -0.982, r= -0.975, r= -0.977, r= -0.966, r= -0.994, r= -0.990, r= -0.978.

Table 2- 12: Pearson's correlation coefficient (r) between NDVI and LST

Pearson's Correlations

	Pearson's r		p
NDVI 2015 - LST 2015	-0.992	***	< .001

*; **; ***

Pearson's Correlations

	Pearson's r		p
NDVI 2016 - LST 2016	-0.982	**	0.003

*; **; ***

Pearson's Correlations

	Pearson's r		p
NDVI 2017 - LST 2017	-0.975	**	0.005

*; **; ***

Pearson's Correlations

	Pearson's r		p
NDVI 2018 - LST 2018	-0.977	**	0.004

*; **; ***

Pearson's Correlations

	Pearson's r		p
NDVI 2019 - LST 2019	-0.966	**	0.007

*; **; ***

Pearson's Correlations

	Pearson's r		p
NDVI 2020 - LST 2020	-0.994	***	< .001

*; **; ***

Pearson's Correlations

	Pearson's r		p
NDVI 2021 - LST 2021	-0.990	**	0.001

*; **; ***

Pearson's Correlations

	Pearson's r		p
NDVI 2022 - LST 2022	-0.978	**	0.004

*; **; ***

Note: * = p < 0.5; ** = p < 0.1; *** = p < 0.01

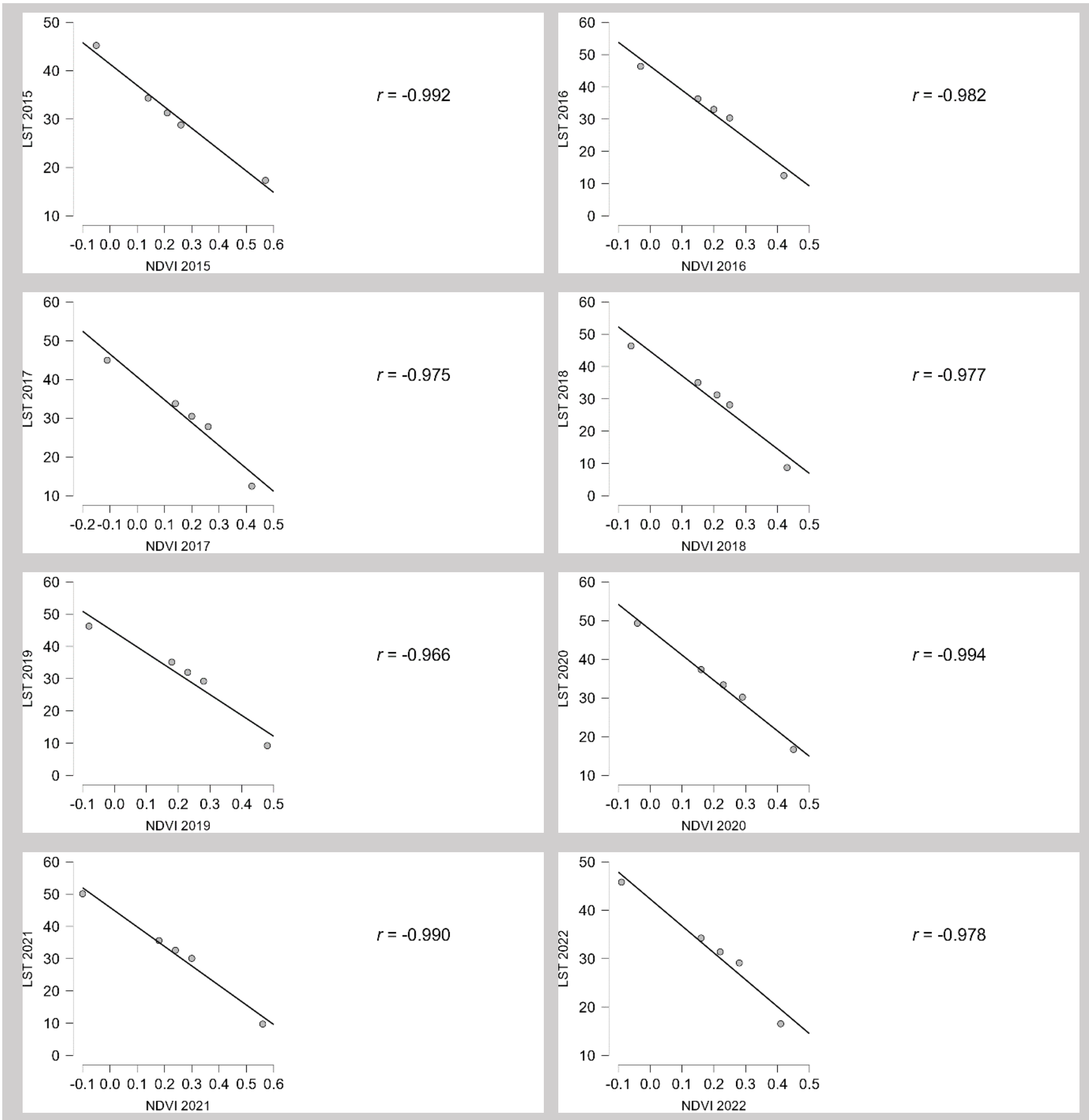

Figure 2- 13: Pearson’s correlation (Scatter plots) between NDVI and LST

2.3.5 Correlation between LULC and LST

The spatial LST values distributions for the different LULC classes were reclassified and mapped for each of the two LULC years 2015 and 2022. This was done to depict temperature differences on the maps and thus shows the LULC areas which are more or less heated (**Figure 2-14**). These LST values reclassify maps to show that the hottest areas are the savannah and the bareland and settlement areas. Similarly for the low-temperature areas which are more or less forest areas. In addition, there is a lot of spread of LULC classes as well as temperatures that vary immensely over the whole area on both maps. Furthermore, the surface temperatures varied between 17.33°C and 45.22°C for 2015 and 16.53°C and 45.81°C for 2022. These values can be observed on the map through the legend as in the following table (**Table 2-13**).

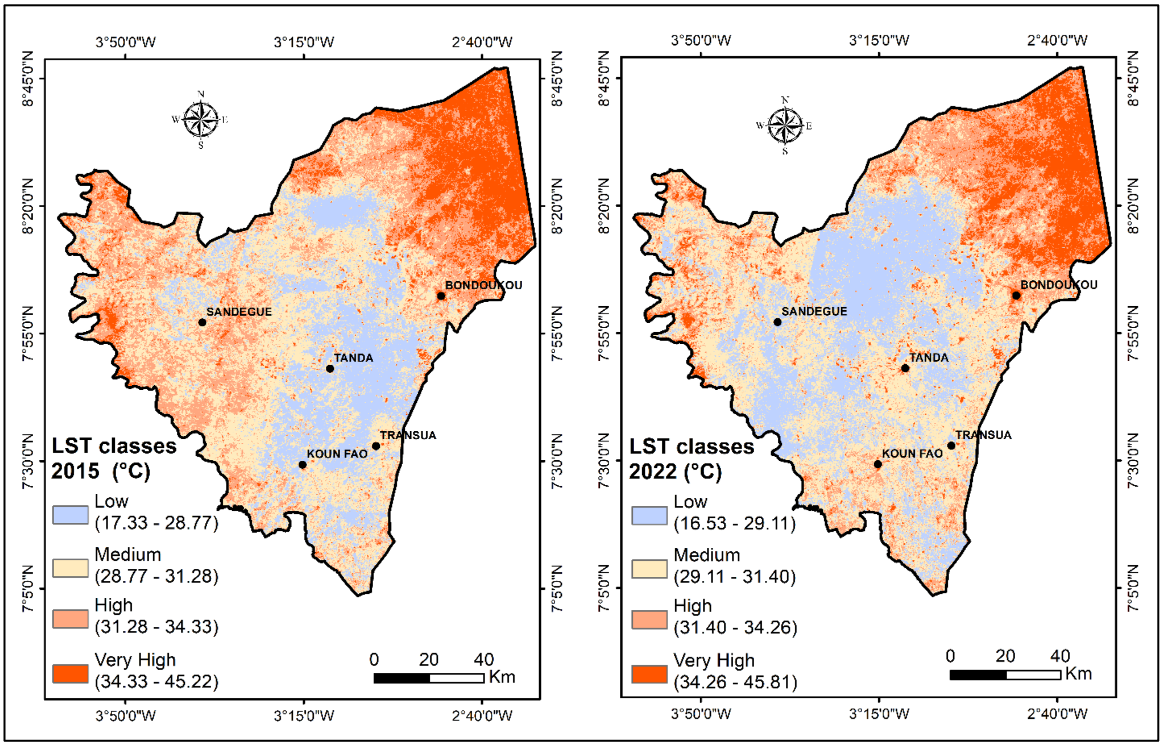

Figure 2- 14: LST reclassification.

Table 2- 13: LST 2015 and 2022 levels reclassification

LST reclassification	LST degree 2015			LST degree 2022		
Low	17.33	-	28.77	16.53	-	29.11
Medium	28.77	-	31.28	29.11	-	31.40
High	31.28	-	34.33	31.40	-	34.26
Very High	34.33	-	45.22	34.26	-	45.81

Then, the mean LST values were matched to the LULC classes and it was found that in 2015 the Bareland and Settlement class recorded the highest surface temperature (35.18°C), followed by the Savannah class (34.60°C). The forest class recorded the lowest temperature (28.69°C) (**Table 2-14**). In 2022, still with the mean LST values, the correlation shows again that the Bareland and Settlement class recorded the highest LST at 35.41°C and the lowest LST was recorded by the forest class (28.46°C). The differences in mean temperature are a decrease in LST of 0.23 for the forest class and an increase for the Bareland and Waterbody classes.

Table 2- 14: Correlation between LULC and LST

	2015		2022		(2015-2022)
LULC classes	**LST Mean (°C)**	**LST Level**	**LST Mean (°C)**	**LST Level**	**Change in LST Mean (°C)**
Bareland and Settlement	35.18	Very High	35.41	Very High	0.23
Forest	28.69	Low	28.46	Low	-0.23
Waterbody	33.74	High	34.54	Very High	0.80
Savannah	34.60	Very High	33.44	High	-1.17
Annual crops	31.67	High	32.93	High	1.26
Perennial crops	30.35	Medium	29.98	Medium	-0.37

2.4. Discussion

2.4.1. Mutation and change in LULC in the Gontougo region

The spatio-temporal analysis of Gontougo LULC change made it possible to categorize 6 LULC classes for each year. There are: annual crops; perennial crops; savannah; forest, bareland and settlement; and waterbody The overall accuracy obtained is 93.77% with a kappa coefficient of 0.87 for the year 2015 map, and 96.01% overall accuracy and 0.92 kappa coefficient for the year 2022 map. These results are close to those obtained by Kadio. *et al*., (2022) who mapped Sentinel-2 image and compared it with Landsat-8 Oli in the Azagny site Ramsar in Côte d'Ivoire. The Overall Accuracy was 90,63% and the Kappa 0,94. Also, Zhang (2023) used GEE and Random Forest with three Sentinel-2 images in the crop mapping type, agronomic purposes to quantify cultivated areas and determine yields in China and obtained respectively 95.72%, 97.21%, and 98.13% as overall accuracy and 0.94, 0.96 and 0.98 as kappa for the year 2017, 2018 and 2020. This latter study is somewhat similar to ours, in the sense that it discusses the use of machine learning, the RF algorithm and highlights all the cartographic precisions that we were able to obtain in this study. In remote sensing, a classification is deemed acceptable when the value of the Kappa coefficient is greater than 75% (Congalton, 1991; Jensen, 1986; Zhang et al., 2023). It confirms that the results of this analysis are statistically acceptable. Regarding RF algorithm, it's nowadays widely used in satellite image classification because it gives better results (Phalke et al., 2020;

Teluguntla et al., 2018; Yan et al., 2022; Zhao et al., 2023). We are increasingly turning to machine learning technology like GEE for the implementation of LULC change. These authors have also done the same in their LULC study using Landsat collection images.(Ashane & Senanayake, 2023; Phalke et al., 2020; Suryono et al., 2021; Teluguntla et al., 2018; Yan et al., 2022; Zhao et al., 2023). The particularity of our study here is to use Sentinel-2 which is one of the studies that has so far mapped the LULC change of the entire Gontougo region and assessed the land surface temperature using machine learning technology (GEE) and RF algorithm. However, it should be noted that Sentinel-2A was launched in June 2015 and the first images were available on 23 June 2015. These early images of the Sentinel-2 mission over our study area show quite a bit of artefact and constitute bits of images with continuous haze. The mosaicking and speckle cleaning allowed us to have a homogeneous image from which the 2015 classification was made. This is what justifies the low precision obtained compared to 2022 where the filter interval search was on a full year.

The other striking aspect of our research is the drastic loss of forest and the dramatic decrease in annual crop areas. Indeed, from 2015 to 2022, forests lost 62.19% of their area and annual crops lost 86.6% of their area. These various losses are to benefit perennial crops up to 48.13% for the forest and 65.14% for annual crops. Indeed, according to a study carried out in the region on the re-profiling of roads by the State of Cote d'Ivoire, and according to the latest census of the population and habitat, Gontougo region's potential economy is based primarily on agriculture, and the reputation of this region in this area is based on the famous variety of yam called "Kponan (République de Côte d’Ivoire, 2019; RGPH-CI, 2021). The current situation shows a landscape that is strongly dominated by perennial crops, with cashew nuts in the lead. The region is one the most cashew producer in Côte d’Ivoire with 65,018 tons in 2022 according to the Cashew Cotton Council (CCA). In detail, at the level of each Gontougo department, it is 49,735t in Bondoukou 3315t for Koun Fao, 7725 t for Sandégué, 4094 t for Tanda, and 194t forTransua. These statistics are given by the Agenice Ivoirienne de Presse (AIP) in an article published on 3 February 2023 at 8:01 GMT entitled: «Côte d'Ivoire - AIP/ Noix de cajou : L'Indénié-djuablin et le Gontougo ont réalisé une production annuelle de 68 697 tonnes en 2022» Edited by Memel Franck Niagnely[1] This necessitates the availability of a large production area. This explains why the vegetation cover and yearly crop area have been drastically reduced. As for the yam crop, in most cases, it is used to prepare or lay out the soil for the next cashew season. According to the yam farmers themselves, they transplant small cashew seedlings into their producing yam fields. And after the yam harvest, the cashew field takes over completely, and new annual crop areas are sought for the following year. : This is one of the factors contributing to the annual decline in the area planted for annual crops. The fact that annual crops are not grown in isolation and that it is important to leave trees in the fields of annual crops, particularly yam, in order to encourage the growth of yam buds, also serves to justify technically the low precision of mapping and discriminating of the annual crops class.

1: https://www.aip.ci/cote-divoire-aip-noix-de-cajou-lindenie-djuablin-et-le-gontougo-ont-realise-une-production-annuelle-de-68-697-tonnes-en-2022/ .

2.4.2. Effect of the LULC changes and NDVI on LST

Land surface heating is the cumulative effect of LULC change and global atmospheric warming (Moisa, Dejene, Merga, et al., 2022; Moisa, Gabissa, et al., 2022). The decline of vegetation cover driven by agricultural expansion in the study area substantially increases the LST. Indeed, the results show that the lowest observed temperatures are in areas where forests are present. Respectively, the LULC forest areas of 2015 and 2022 recorded the lowest mean LST of 28.69°C and 28.46°C. This translates into a slight decrease in temperature over the year. This trend is verified within NDVI calculations. According to some authors (Carlson & Rizileý, 1997; Davi et al., 2006; Du et al., 2017; Morawitz et al., 2006; Syawalina et al., 2022; Z. Wu et al., 2019), healthy vegetation absorbs most of the visible light that hits it and reflects a large portion of the near-infrared light. Unhealthy or sparse vegetation reflects more visible light and less near-infrared light. (Davi et al., 2006; Dibi et al., 2008; M. R. Khan et al., 2010; P. Phan et al., 2021). Therefore, the NDVI has a huge influence in LST calculation and the surface temperature content. This is why we used it to correlate with the LST. Similarly, like the LST, the NDVI was reclassified into four classes and was also well-corrected with the LST (**Table 2-15**). This NDVI classification corresponds to the vegetation standards from Sub-Saharan humid tropical countries since a definition of the forest depends on the forestry code of each country (Dibi et al., 2008; RCI-Code Forestier, 2019b, 2019a). Accordingly, the negative NDVI values corresponding to the description "Non-vegetation land" recorded the highest temperatures. This can be also perceived with Pearson's correlation coefficient (r) for each year (**Figure 2-13**) and confirms that the absence of vegetation induces a high surface temperature compared to the vegetated land which records a low temperature (Zheng et al., 2014) Yet, the negative Pearson correlations coefficient values found in the relationship between the LST and NDVI are indicating the presence of the green areas mitigates the surface temperature effect. This is because the vegetation is wet and contains water almost over most months of the year through the leaves compared to other types of LULC and therefore moistens the surface, absorbs more, and reflects less solar radiation (Davi et al., 2006; Morawitz et al., 2006).

Table 2- 15: NDVI classification in correlation with LST

NDVI Values	NDVI Description	LST Correspondence
- 1 <NDVI< 0.00	Non-vegetation land	Very High
0.00 <NDVI< 0.20	Low vegetation land	High
0.20 <NDVI< 0.40	Medium vegetation land	Medium
0.40 <NDVI< 1	High vegetation land	Low

In contrast, the water surfaces have often recorded high temperatures (33.74°C in 2015 and 34.54°C in 2022 for the mean temperature). In fact, the waterbody class is not a large river or big stream. It is made up of puddles, backwaters, small lakes, ponds, and swamps. As you have noticed it is the class with the smallest extent and represents less than 1% of the total area of the classes in 2015 and exactly 0.34% in 2022. This means that the waters dry up, especially in the dry season and become bareland. As a result, the temperatures will be very high like in the bareand and savannah areas. Indeed, our study has shown that the hottest surfaces with the highest temperatures are the bareland/settlement and savannah. The means temperature of these LULC classes are 35.18°C and 35.41°C for bareland/settlement respectively in 2015 and 2022 and 34.60°C and 33.44°C for savannah respectively in 2015 and 2022. The bareland/settlements are devoid of vegetation and the savannah is dominated by grasses and shrubs, which cannot strongly absorb the sun's rays, so the reflections are strong, which justifies the high temperatures recorded at these LULC classes. A recent study by these authors: (Moisa, Dejene, & Gemeda, 2022; Moisa, Dejene, Merga, et al., 2022; Moisa, Gabissa, et al., 2022) in the wettest parts of Ethiopia, which covers the present study confirmed the increasing trend of temperature is driven by weak NDVI values and land use land cover conversion. One of their outputs is about the great variation between daytime and nighttime temperature which can influence the land surface temperature. As highlighted by these same authors, the LST increases during the daytime than at night. Akomolafe & Rosazlina, (2022) found a moderate negative relationship between NDVI and LST in Penang Island, Peninsular Malaysia. This shows that higher LSTs correspond to lower vegetation cover and vice versa, as our results also show. Through the urban heat island characteristics and mitigation strategy analysis for eight arid and semi-arid gulf region cities, Abulibdeh, (2021), stated that vegetation, particularly trees, can prevent direct surface heat as a result of solar radiation by providing shade, cooling the air through generating cool island effects, by evapotranspiration and emissivity processes, and by reducing the wind speed under the canopies. In the Pearson correlation coefficient analysis, the same author (Abulibdeh, 2021) stated that the LST has a significant relationship with NDVI but in different directions. The relationship between the LST and NDVI is negative indicating that the presence of green areas mitigates the LST preponderance effect. All these claims by different authors confirm our results and demonstrate once again the importance of land use land cover changes and their effects on the LST modification.

2.5. Conclusion

This study examined LULC change analysis and its effects on LST using ML through GEE in the Gontougo Region. Regarding LULC, we could discriminate six classes: annual crops; perennial crops; savannah; forest, bareland/settlement; and waterbody. From 2015 to 2022, the OA values for each LULC map were 93.77% and 96.01% respectively. Similarly the kappa was 0.87 in 2015 and. 0.92 in 2022. The prevailing LULC class is perennial crops. It occupies more than 60% of the area of each LULC map. LULC change found that the forest and annual crops classes lost respectively 48.13% and 65.14% of their areas for the benefit of perennial crops from 2015 to 2022. The NDVI and LST reclassifications correspondence have shown that Non-vegetation land corresponds to very high temperature, Low vegetation land corresponds to high temperature, Medium vegetation land corresponds to medium temperature and High vegetation land corresponds to low temperature. Similarly, their correlation using Pearson coefficient (r) gave a significant relationship and we obtained negative coefficients at each correlation. In terms of the LST/LULC correlation, the forest class has recorded the lowest temperatures each year. In 2015, the mean temperatures recorded were: 28.69°C and 28.46°C in 2022. On the other hand, the highest temperatures are recorded by the bareland/settlement class. In 2015 it recorded a mean of 35.18°C and 35.41°C in 2022. The existence of vegetation coverage is therefore indispensable to decreasing the amount of surface temperature. It is recommended that natural resources managers and environmental experts should create awareness and environmental conservation to minimize LST in the study area. Furthermore, the decline in annual crop area each year to perennial crops should aware all decision-makers and even all farmers in the region that this will lead to a real food security issue. We must now raise the alarm so that the crops that feed us directly are brought to the forefront in our choice of crops in order to be food self-sufficient. This study has benefits for monitoring and evaluating food security in Côte d'Ivoire, adding to the evidence base of other studies on the use of remote sensing to identify crop types and cropping patterns in other countries. However, it should be noted that one of the limitations of this study is that it wasn't possible to map the yam crop specifically. This would have enabled us to assess the impact of LSTs on yams directly. This aspect will be addressed in future work using very high spatial-resolution images. The results of this work are a response to the food security challenges related to land use in the area. Based on these study results, we plan to conduct a socio-economic study in the future, in which we will gather yam farmers' perceptions of climate change, the difficulties they face in yam production and available solutions. In addition, a soil sampling and analysis study is planned in an attempt to solve the soil fertility problems faced by people in the Gontougo region.

CHAPTER 3: EVALUATING SOIL PHYSICOCHEMICAL PROPERTIES IN YAM-PRODUCING FOREST AND SAVANNAH AREAS.

3.1. Introduction

Yams are widely grown in Côte d'Ivoire, particularly in northern, central and eastern regions and it's the most cultivated among food crops. Yams are especially vital to food security in the country, accounting for 63% of all daily caloric intake from roots and tubers, and 63% of all root and tuber cultivation, (BCEAO, 2017; Diarrassouba, 2019; Dibi et al., 2021; MINADER, 2017; World Bank Group, 2019). The landrace varieties *Kponan, Krengle, Djate,* are in high demand, as are the adapted varieties *TDA*, *Mao* and *C20*. The latter have demonstrated good productivity, disease resistance and drought tolerance (R. Michel and G. Apata, 2017; World Bank Group, 2019). Its production requires fertile soils (Diby, Hgaza, et al., 2011; Heller et al., 2022; N'guessan et al., 2009). That's why some suggest that the absence of specific arbuscular mycorrhizal fungi could lead to impaired yam growth due to lower phosphate uptake (Diby, Hgaza, et al., 2011; FAO, 2015b). For some authors, the drastic drop in yam yields and the increase in cultivated area in Côte d'Ivoire can be linked to several factors, including overexploitation of the land use land cover and its dynamics leading to high land surface temperatures (Aka et al., 2023), the scarcity and variability of rainfall patterns (Adifon et al., 2020; Heller et al., 2022), and soil fertility issue (Dibi et al., 2021; Frossard et al., 2017; N'guessan et al., 2009).This last factor pushes yam farmers to make large farms or to spend excessively on fertilizers (Dibi et al., 2021; Hgaza, 2010; Pouya et al., 2022). These fertilizers are frequently chemical, organic or organo-mineral (Dibi et al., 2021). A study by the Office of Scientific and Technical Research Overseas (ORSTOM) showed that in the north-eastern of Côte d'Ivoire, especially in the Gontougo region, beyond Bondoukou, we have leached tropical ferruginous soils with concretions, most of which have formed on amphibolic schists (B. DABIN, 1960). As important as those soils are for yam production, they are still degraded by perennial crops such as cashew nuts, which predominate in this region (Aka et al., 2023). So, knowing their state and determining their fertilisation indicators will enable farmers to meet their yam-growing needs. Apart from this ORSTOM soil study dating from 1960, there has not yet been any study to quantify the physicochemical properties in the Gontougo region, even though it is one of the largest yam-producing regions in Côte d'Ivoire (Kouakou et al., 2019; Nindjin et al., 2009). However, a study on the status of soil fertility in cotton-based cropping systems in Côte d'Ivoire underlined and analysed the various soil fertility indicators. The author inspected cotton yields by analyzing different soil sample dates: the year 2013 and the year 2021 (Koné et al., 2022). Several authors have also addressed the physicochemical characterisation of soil properties through the literature. In their study on Pigeonpea (*Cajanus cajan*) and white yam

(*Dioscorea rotundata*) cropping systems in Ghana, Owusu Danquah et al., (2022) took nine (9) composite soil samples and conducted soil analysis for total nitrogen (N), pH, organic carbon, phosphorus, and potassium measured at 0–20 and 20–40 cm on the ridges. Total N was determined using the Kjeldahl method, the ammonium acetate method determined exchangeable cations and Cation Exchange Capacity (CEC) and the Walkley-Black method for the carbon. These various physicochemical analyses have been replicated worldwide in multiple investigations with some differences in the techniques utilized. This is the case with these authors (BARI et al., 2022; Geng et al., 2024; Madeira et al., 2003; Mustapha et al., 2023; N'doufou et al., 2022; Pedersen et al., 2023; Shi et al., 2017; Steinfurth et al., 2021) who use several comparative methods to determine the physical and chemical properties of the soil. The statistical aspect is not forgotten in all these cases. Many statistical analyses are also applied after laboratory analysis. The most commonly used are ANOVA, correlation analysis, linear regression, principal component analysis (PCA) and correspondence analysis (CA) (Koné et al., 2022; N'doufou et al., 2022; Owusu Danquah et al., 2022; Sufardi et al., 2023; Zro et al., 2016). In this study, we will assess the physicochemical properties based on land use land cover type (Liu et al., 2021; Mustapha et al., 2023; Neina, 2021; Ostrowska & Porębska, 2015; Zro et al., 2016). This is what prompted us to conduct this study, where we had previously shown that the region's vegetation is predominantly savannah in the department of Bondoukou and predominantly forest in the department of Tanda (Aka et al., 2023) This study is a new research contribution for drawing politics interest, researchers and funders to devote to this research field which is imperative to maintaining food security. In this manuscript, we aim to quantify and evaluate the difference between physicochemical soil properties in forest and savannah areas under yam farms harvested and not yet cultivated. Indicators such as pH, Carbon (C) total nitrogen (N), available phosphorus (P) potassium (K^{+}), calcium (Ca^{2+}), magnesium (Mg^{2+}), sodium (Na^{+}), cation exchange capacity (CEC), and Particle size distribution were all quantified and assess.

3.2. Methodology

3.2.1. Material and data description

This study is based on two types of data: satellite data with which we identified the vegetation and the locations where the soil samples were collected based on this vegetation.

3.2.1.1. Satellite image

We used two Sentinel-2 images, one from the year 2015 and the other from the year 2022. These images are from the Copernicus platform and are available in the Google Earth Engine (GEE) data catalogue (https://developers.google.com/earth-engine/datasets/catalog/COPERNICUS_S2_HARMONIZED).

3.2.1.2. Soil sample

Sampling was carried out in July 2023 in two localities. These are *Amanvi* in Tanda's department and *Djikparedouo in* Bondoukou's department (**Figure 3-1**).

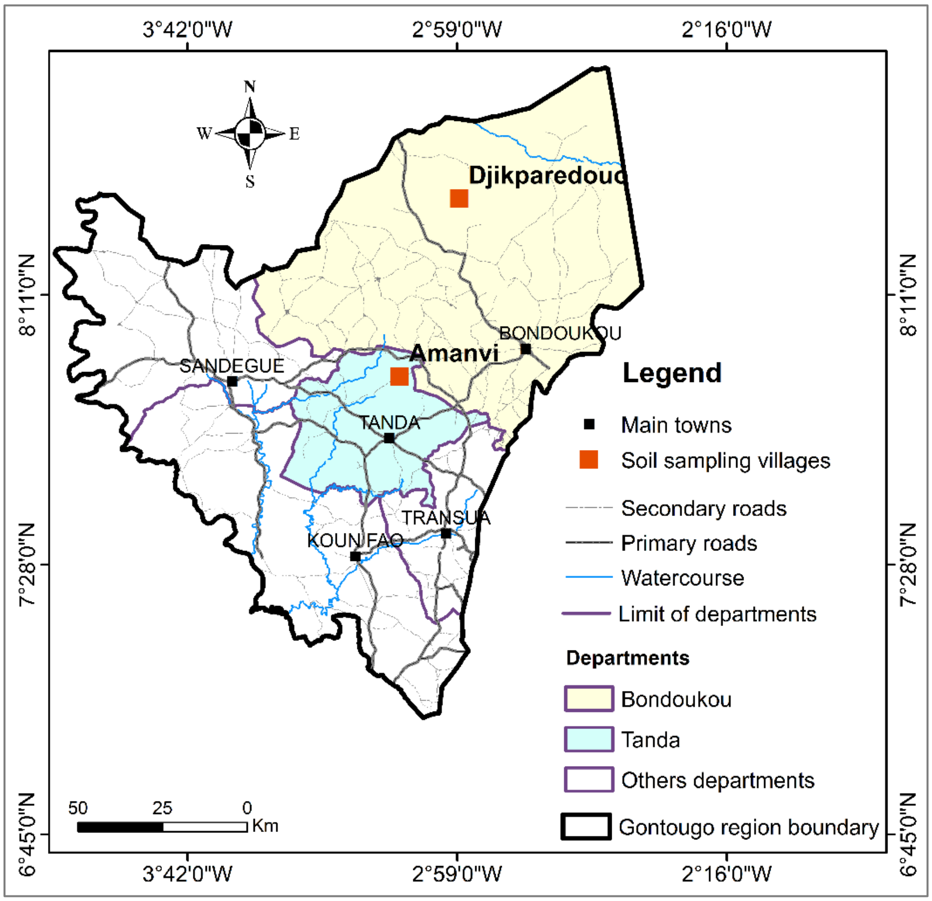

Figure 3- 1: Soil sampling locations

In each of these villages, we investigated two fields based on local and endogenous knowledge. This meant four fields were visited. We named them Field_1, Field_2, Field_3 and Field_4. Then, in each field, the sample was taken in two different sites: a control site, i.e., a virgin plot that had not yet been cultivated, and the other that had already been cultivated and harvested lately (**Table 3-1**). At each sampling site, as described in table 1, samples were taken in three subsamples along the topographical gradient of the field in order to obtain a composite sample representative of the entire area (**Figure 3-2**).

Table 3- 1: Description of soil samples in the field

Department	Locality	Field	Sampling sites	Samples
Tanda	Amanvi	Field_1	Control site_1	Cs1
			Harvested site_1	Hs1
		Field_2	Control site_2	Cs2
			Harvested site_2	Hs2
Bondoukou	Djikparedouo	Field_3	Control site_3	Cs3
			Harvested site_3	Hs3
		Field_4	Control site_4	Cs4
			Harvested site_4	Hs4

Overall, Height (8) composite soil samples of which 4 from the control site and 4 from the harvested site are made up of twenty-four (24) subsamples from each plot. They have been combined based on the site's characteristics. They were thus built in such a way as to represent the entire landscape before starting any of the laboratory measures.

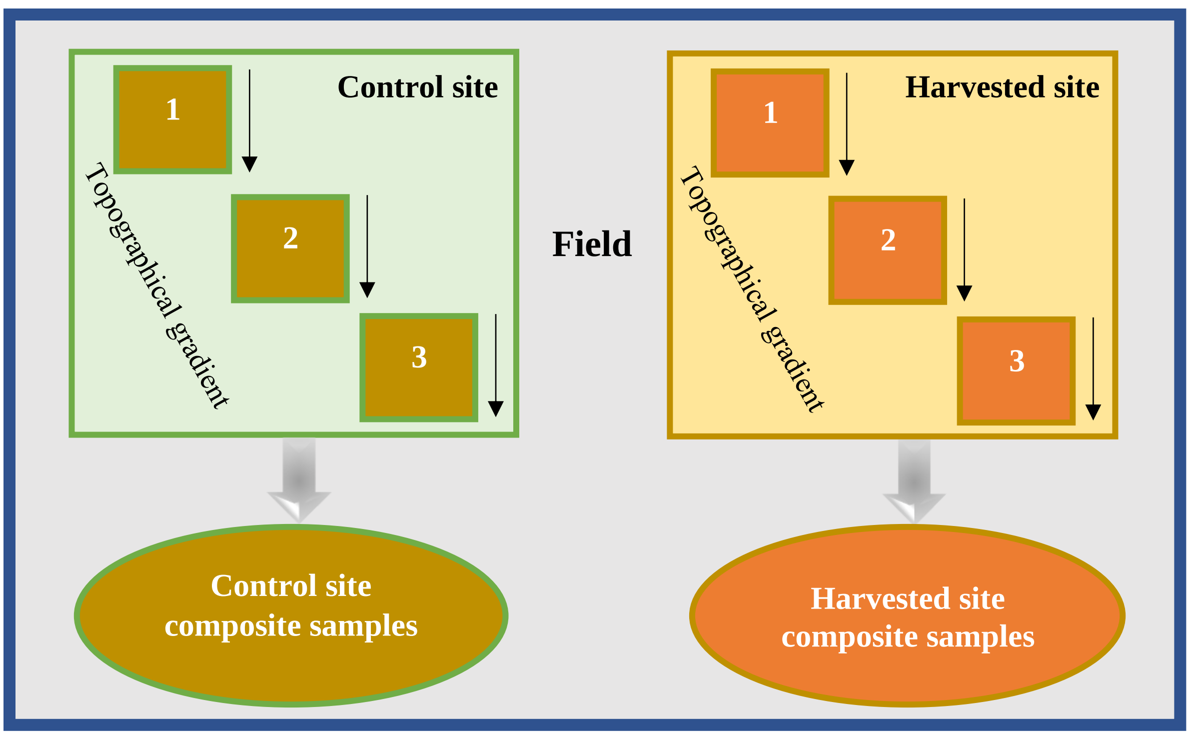

Legend

1 = First subsample taking

2= Second subsample taking

3 = Third subsample taking

↓ = Depth: 0 - 40 cm

Auger hole's Control site

Auger hole's Harvested site

Figure 3- 2: Composite soil sample collection design: an example for one field

We explored each of the twenty-four (24) subsampling areas (control and harvested site) and using suitable tools, dug holes no deeper than 40 centimetres (0-40 cm) into the ground to collect soil samples. Each of these images is an example of the pit we dug to collect the samples (**Figure 3-3**). For each auger, sampling was carried out at the level of the humus horizon, at mid-distance and then at the bottom of the hole.

A: Auger sampling in Tanda B: Auger sampling in Bondoukou

Figure 3- 3: Soil sampling by auger in the forest (A) and savannah (B) zones

3.2.2. Data processing

3.2.2.1. Sentinel-2 images

We processed the year 2015 and 2022 sentinel-2 images using Google Earth Engine (GEE) to map the land use land cover (LULC) types from which we extracted vegetation classes[1]. Next, we identified the unchanging forest and savannah over the years on the 2022 LULC map to set the soil sampling location. The cartographic rendering was possible using ArcGIS Desktop 10.8 software.

3.2.2.2. Sampling and soil analysis

3.2.2.2.1. Sorting and husking of samples

In the field, the samples taken were placed in plastic bags marked with a ribbon to distinguish them. Once back from the field, we composed samples by sampling site to make them composite and then dried them. Using a 2.0 mm mesh sieve, they were sieved and labelled again before being sent to the laboratory for physical and chemical analysis. Each sample was labelled using the following code: Cs1; Hs1; Cs2; Hs2; Cs3; Hs3; Cs4; Hs4

3.2.2.2.2. Laboratory analysis of samples

In the laboratory, the chemical analysis involved the following indicators: potential hydrogen (pH), total nitrogen (N), carbon (C), available phosphorus (P), cation exchange capacity (CEC), and calcium (Ca2+), magnesium (Mg2+), potassium (K+) and sodium (Na+) ions. The physical indicators focused on particle size particularly: Clay, fine silt (f-silt), coarse silt (c-silt), fine sand (f-sand) and coarse sand (c-sand).

3.2.2.2.2.1. Potential Hydrogen

pH was defined by Sorensen (1909) as the negative logarithm to base 10 of the hydrogen ion concentration but is now defined in terms of hydrogen ion activity.

$$pH = \frac{1}{\log[H+]} \qquad [1]$$

Thus, the pH of pure water would be: -Log of 1_x10^{-7} or 7. As defined, any solution with a pH below seven is considered acidic, and one with a pH greater than seven is defined as basic (Thomas, 1996).

There are many ways of soil pH measuring. Some use a saturated paste extract, others a 1:5 soil/water dilution and then measure the pH of the resulting solution using a laboratory meter. Others use the 1:5 dilution, but instead of water, they use a dilute solution of calcium chloride ($CaCl_2$) (He et al., 2012; Kargas et al., 2022; Miller & Kissel, 2010; Šimek & Cooper, 2002). In our case for this work, we used the method of suspending 20g of dried soil sample in 50 ml of distilled water. To do this, we used a standard pH meter with a display, a pH electrode, a bar stirrer, a beaker and distilled water. This consisted of adding 20 ml of distilled water to each beaker containing the samples and homogenizing them well using the bar stirrer for 5 minutes until a very homogenous solution was obtained. Then leave to stand for 30 minutes before measuring the values. A dual input electrode (anode and cathode), connected to the pH meter, is plugged in and immersed in the solution, where the graphical deviations can be seen on the pH meter screen indicating the pH value.

3.2.2.2.2.2. Carbon test: Walkley-Black method

The Walkley-Black (WB) method is widely used in most soil-testing laboratories across the world (De Vos et al., 2007; Matus et al., 2009; Skjemstad & Taylor, 1999). It uses concentrated sulfuric acid and dichromate solution, which are added to soil samples. The chromic ions produced are proportional to the oxidised organic carbon and measured colourimetrically. The heat of the acid-based reaction is used to induce the oxidation of organic matter (Walkley, A. & Black, 1934). The procedure in the laboratory was to grind and measure 1g of each sample and then place them in the Hellenes (test tubes) into which we poured 10 ml of potassium dichromate ($K_2Cr_2O_7$) and 20 ml of sulphuric acid (H_2SO_4) to heat the dilution and potentiometric or colorimetric titration. The same solution was prepared in another Hellene without the soil sample used as a control solution to determine soil carbon. After this step, we left the Hellenes to stand in the open air for 30 minutes and then added 200 ml of tap water and 10 ml of orthophosphoric acid (H_3PO_4) to the solutions in all the Hellenes. Now, to speed up the reaction, a few drops of a catalyst (barium) are added gradually into the solutions. They are placed gradually on a magnetic stirrer where a bar magnet is immersed in the solution. During stirring, the iron (II) sulphate ($FeSO_4$), also known as the "death salt", is gradually poured into the solution. When the solution turned bluish, we closed the shut-off valve and stopped adding the iron (II) sulphate to the solution, then read off the value at which the iron (II) sulphate stopped after being added. The percentage of WB carbon is given by the equation 2 (De Vos et al., 2007; FAO, 2019):

$$WBC = \text{M x} \frac{(\text{V1}-\text{V2})}{\text{W}} \text{ x } 0{,}30 \text{ x } CF \quad [2]$$

Where:

WBC is the Walkley-Black Carbon; M is the molarity of the $FeSO_4$ solution; V1 is the volume (mL) of $FeSO_4$ required in blank titration; V2 is the volume (mL) of $FeSO_4$ required in actual titration; W is the weight (g) of the oven-dried soil sample and CF is the correction factor. The CF is a compensation for the incomplete oxidation and is the inverse of the recovery. This CF was set by WB to 1.32 (recovery of 76%).

3.2.2.2.2.3. Determination of exchangeable cations and cation exchange capacity

In the literature, it is stated that CEC is not easy to obtain and each CEC determination would require unique reagents. This is the case of these authors who used different reagents and methods depending on the objectives sought, the quality and the source or provenance of the sample to determine the CEC (Aprile & Lorandi, 2012; Ciesielski, Sterckeman, Santerne, & Willery, 1997; Ciesielski, Sterckeman, Santerne, Willery, et al., 1997; Dohrmann, 2006; X. Zhao et al., 2020). In our case, we determined the CEC of each soil sample using the ammonium acetate method followed by washing the samples with alcohol in the laboratory. This method measures the soil's capacity to adsorb cations from an aqueous solution with the same pH, ionic strength, dielectric constant and composition as that encountered in the field since the CEC varies according to these parameters (Ciesielski, Sterckeman, Santerne, & Willery, 1997; Madeira et al., 2003; X. Zhao et al., 2020). Determining the exchangeable cations, which include Ca^{2+}, Mg^{2+}, Na^{+} and K^{+} ions, is a step in determining the CEC. This involved weighing 5g of dried soil sample and storing it in an Erlenmeyer flask. Then prepare the ammonium acetate ($NH_4CH_3CO_2$.) solution using 77.8 g of it and dilute it in 1 L of distilled water. Measure out 100 ml of this solution and pour it into each Erlenmeyer flask containing the samples. Close them tightly and place them on an electric shaker for 2 hours of agitation. They are then removed and stand to decant for approximately 10 minutes before being filtered to collect the submerged liquid which was used to determine the cations (Ca^{2+}, Mg^{2+}, Na^{+}, K^{+}). The rest of the solution remaining in the Erlenmeyer flask was washed with alcohol to remove all the ammonium acetate. To do this, 25 ml of alcohol (C_2H_5OH) was spilt into each Erlenmeyer flask containing the remaining solutions and shaken for 30 minutes before sieving. This washing process was carried out 4 times and required 100 ml of alcohol for 2 hours of agitation before proceeding to determine the CEC. A linear regression curve was prepared between pH_{mis} and $H^{+}+Al^{3+}$. With the values of $H^{+}+Al^{3+}$ obtained by equation 3 and the sum of bases extracted with 0.05 N HNO_3, these were used to calculate the values of CEC by equations 4 and 5 (Aprile & Lorandi, 2012; Ciesielski, Sterckeman, Santerne, & Willery, 1997; Ross & Ketterings, 2011):

$$\log(H + A) = 3.76 - 0.53pHmis \quad [3]$$

Where: pH_{mis} is the pH of the relation soil-water-buffer

$$(H + Al) - (NH4OAc) = 1.126(H + Al) - 0.764 \quad [4]$$

Where: NH4OAc is the volume of ammonium acetate (ml).

$$CEC - (NH40Ac) = 1.155CEC - 1.253 \quad [5]$$

3.2.2.2.2.4. Phosphorus test: Olsen's method

The method estimates the relative bioavailability of inorganic ortho-phosphate (PO_4-P) in soils with neutral to alkaline pH. It is based on the extraction of phosphate from 0.5 g of soil by sodium bicarbonate solution adjusted to pH 8.5 (Olsen, S. R. and Sommers, 1982; Recena et al., 2022; Steinfurth et al., 2021). In the process of extraction, we weighed 0.5 g of dried soil samples, placed them in flasks called Godé, then poured 25 ml of sodium hydrogen carbonate ($NaHCO_3$) into them and shook them for 1 hour on an electric shaker. Then leave them to stand for a while and decant the submergent from each flask into beakers. To each, 50 ml of sodium hydrogen carbonate and 0.75 ml of sulphuric acid (H_2SO_4) are added. In another empty beaker (without soil sample), we prepared the same solution with 1.5 ml of sulphuric acid. Then, all the solutions were allowed to settle for 24 hours for the chemical reaction to take place with colour stabilization, maximum absorption of the soil sample and development of the maximum intensity of phosphorus. The results are then read off using electrodes connected to a monitoring device.

3.2.2.2.2.5. Total nitrogen test: Kjeldahl method

Two methods have gained widespread acceptance for the determination of total-N: the Kjeldahl method, which is essentially a wet-oxidation procedure, and the Dumas method, which is fundamentally a dry oxidation (i.e. combustion) technique (Bremner, 1965; Pontes et al., 2009; Sáez-Plaza et al., 2013). In our case, we used the Kjeldahl method to determine total nitrogen. The

Kjeldahl method determines total nitrogen content and protein as the nitrogen content of the sample multiplied by a conversion factor. The sample is digested in sulfuric acid, using $CuSO_4/TiO_2$ as catalysts, converting N to NH_3, which is distilled and titrated (Thiex et al., 2002) We could also convert the nitrogen (N) in the sample to ammonium ($NH4^+$) by digestion with concentrated H_2S0_4 containing substances that favour this conversion, and the $NH4^+$ is determined from the quantity of NH^3 released by distillation of the digestion product with alkali (Bremner, 1965; Khee C. Rhee, 2001; Sufardi et al., 2023). This is exactly what we did, using 1g of grinded soil per sample and 10 ml of concentrated sulphuric acid (H_2SO_4), all of which were placed in the elongated tubes at a temperature of 350°C for 180min. The caustic acid (NaOH) was then prepared and left to stand for 72 hours. 25ml was then taken and poured into the tubes and placed in the Kjeldahl machine for 5min 45s of simmering. The bromothymol indicator was used for the final dosage. The percentage of N is given by the equation 6:

$$\text{Kjeldahl nitrogen} = \frac{(\text{Vs.Vb})\text{xMx}14\text{x}14.01}{W.10} \qquad [6]$$

Where:

VS = volume (ml) of caustic acid; VB = volume (ml) of sulphuric acid; M = molarity of standard HCl; 14.01 = atomic weight of N; W = weight (g) of soil sample; 10 = factor to convert mg/g to percent.

3.2.2.2.2.6. Particle size: Robinson's method (or Pipette method)

The granulometric fraction (clay, silt and sand) is an important characteristic that influences several soil functions. One of the most important properties is pores distribution, water retention, thermal and resorption properties, and indirectly affects soil nitrification (de Santana et al., 2023; Polakowski et al., 2023). Currently, there are many methods of particle dimension measurement available that are based on different physical principles. Robinson's method (or Pipette method) based on the different sedimentation velocities of particles with different diameters is considered to be one of the worldwide standard methods for determining individual grain size fraction distribution (Delaune et al., 1991; QIU et al., 2021; Šinkovičová et al., 2017; Svensson et al., 2022). In practice, we needed 5g of sieved soil using a 0.05 and 0.2mm sieve, an Erlenmeyer flask and 50 ml of oxygenated water to destroy the organic matter. The mixture was placed in an oven at 60°C for 24 hours. After removal from the oven, 200 ml of tap water and 20 ml of tetrasodium pyrophosphate ($Na_4P_2O_7$) were added to each Erlenmeyer flask before shaking for 1 hour and transferring into a sedimentation tube. The next day, the clay + silt are extracted together and 6 hours later, another clay is extracted using a Robinson pipette by dipping the pipette into the solution up to the surface. After these two extractions, each sedimentation tube is emptied by siphoning until the sandy bottom of the sample is obtained. They are taken and dried in an oven and sieved at 3 levels with different sieves to determine the coarse elements. However, particle sedimentation is the result of two opposing forces: gravity and friction causing movement in a fluid environment. A sample is pipetted at different times and different depths from the sample suspension into a test tube. Time and depth are determined using Stokes' law. The pipetted suspension is condensed and dried, and the mass ratio of the pipetted fraction is determined by weighing. Stokes' law and the sedimentation rate of particles suspended in a liquid are given by equations 7 and 8 (Feller & Christian, 1993; Kargas et al., 2022; Svensson et al., 2022; Zhang et al., 2013) :

$$F = 6\pi r \eta v \quad [7]$$

Where:

F = drag force; π = pi; r = sphere radius; η = fluid viscosity; v = velocity of the sphere.

$$V = Kr^2 \quad [8]$$

Where:

V = Velocity; K = Constant; R = Radius of the particle

3.2.3. Statistical soil analysis

Correspondence Analysis (CA), Pearson correlation and analysis of variance (ANOVA), were done as statistical processes using R software at a 5% significant level ($P \leq 0.05$) to assess whether the soil characteristics (physicochemical properties) recorded under savannah and forest areas differ significantly from one another. CA analysis was applied to describe the relationships between the physicochemical properties of the samples and the vegetation from which they were gathered. Then, Pearson's correlation coefficient gives information about the magnitude of the correlation between organic matter and pH variables. As a result, the value ranges between -1 and +1 measures the strength and direction of the relationship between two variables (Inamdar et al., 2018; P. Phan et al., 2021; QIU et al., 2021). A simple linear regression model was executed to estimate the relationship between variables (C/N ratio – samples and available P – samples). The ANOVA test was performed to determine the physical and chemical properties abundances before and after yam growing in the soil sample under forest and savannah zones. Shapiro Wilk normality (homogeneity) tests are performed prior to the ANOVA test. (Owusu Danquah et al., 2022; Zro et al., 2016). If the assumptions for ANOVA weren't met i.e., the null hypothesis (H_0) of the normality test was rejected, we use the non-parametric Kruskal Wallis test (H statistic test). The calcul for ANOVA, H statistic test and Pearson's correlation coefficient are given by following equations 9, 10 and 11 (Heumann et al., 2016):

$$\boldsymbol{F} = \frac{\boldsymbol{MSB}}{\boldsymbol{MSE}} \qquad [9]$$

With:

MSB= SST/p-1; MSE= SSE/N-p; and SSE = $\sum$ (n−1)

where:

F= ANOVA coefficient; MSB= Mean sum of squares between the groups; MSE= Mean sum of squares due to error within groups; SST= total Sum of squares; SSE= Sum of squares due to error; p= Total number of populations; n= Total number of samples in a population; N= Total number of observations.

$$H = \left[\frac{12}{n(n+1)} \sum_{j=1}^{c} \frac{T_j^2}{n_j} \right] - 3(n+1) \qquad [10]$$

Where:

H = Kruskal Wallis test; n = sum of sample sizes for all samples; c = number of samples; Tj = sum of ranks in the jth sample; nj = size of the jth sample.

$$r_{xy} = \frac{n \sum x_i y_i - \sum x_i \sum y_i}{\sqrt{n \sum x_i^2 - \left(\sum x_i\right)^2} \sqrt{n \sum y_i^2 - \left(\sum y_i\right)^2}}. \qquad [11]$$

where r_{xy} is Pearson *r* correlation coefficient between *x* and *y*; *n* represents the number of observations, *xi* means the value of *x* (for *i*th observation), and *yi* indicates the value of *y* (for *i*th observation).

NB: In the remainder of this work, the symbols ∗, ∗∗, ∗∗∗ denote significance at the 0.05, 0.01, and 0.001 probability (P) levels, respectively of statistical outcomes.

3.3 Results

3.3.1. Vegetation analysis and mapping of soil sampling location

The results in this section were obtained from the classification of Sentinel-2 year 2015 and 2022 images. Six classes were determined at the end of this land use land cover (LULC) classification. These are bareland & settlement, forest, waterbody, savannah, annual crops, and perennial crops. To better assess the two types of vegetation in the study area and employ them as a foundation for collecting soil samples, we sorted these LULCs into three classes: Forest, Savannah, and Other LULC which includes the bareland & settlement, waterbody, annual crops, and perennial crops classes. The training points were collected for classification, whereas the control points were utilized for validation, both gathered from the field. A second validation was possible thanks to the accuracy assessment.

3.3.1.1. Accuracy assessment

Accuracy assessment is a process of determining the accuracy of a LULC classification map. The table below (**Table 3-2**) shows the area values obtained for the LULC, the accuracies and the rate of change. The overall accuracy (OA) was 93,77%, in the year 2015 LULC map and the kappa was 0.87. However, in the year 2022, the OA was 96.01% and the kappa 0.92. Analysis of the change rate shows that the Forest class has gone from 158052.47 hectares in the year 2015 to 89,220.32 hectares in 2022, which means a loss of 4.24% of its surface area. The Savannah class increased by 2.19% in an area between the year 2015 and 2022.

Table 3- 2: LULC change rate and accuracy assessment values

	2015		**2022**		**LULC change rate**	
	Area (Ha)	Area (%)	Area (Ha)	Area (%)	Area (Ha)	Area (%)
Forest	158052.47	9.74	89,220.32	5.5	-68832.15	-4.24
Savannah	236322.41	14.56	271900.00	16.75	35577.59	2.19
Other LULC	1228446.60	75.7	1261701.16	77.75	33254.56	2.05
Overall accuracy (%)	93.77		96.01		2.24	
Kappa	0.87		0.92		0.05	

3.3.1.2. LULC mapping and soil sampling location

The LULC mapping of the study area resulted in two maps. Each shows the three classes: forest, savannah, and other LULC. An analysis of the forest and savannah stability zones on the LULC map enabled us to select two localities for sampling soils in the year 2022 LULC map: these are the localities of *Amanvi* in Tanda's department where there is more forest and *Djikparedouo* in Bondoukou's department where there is a higher concentration of savannah. (**Figure 3-4**). These LULC types are designed to give a better idea of the trend over the two years using their area values in hectares (**Figure 3-5**).

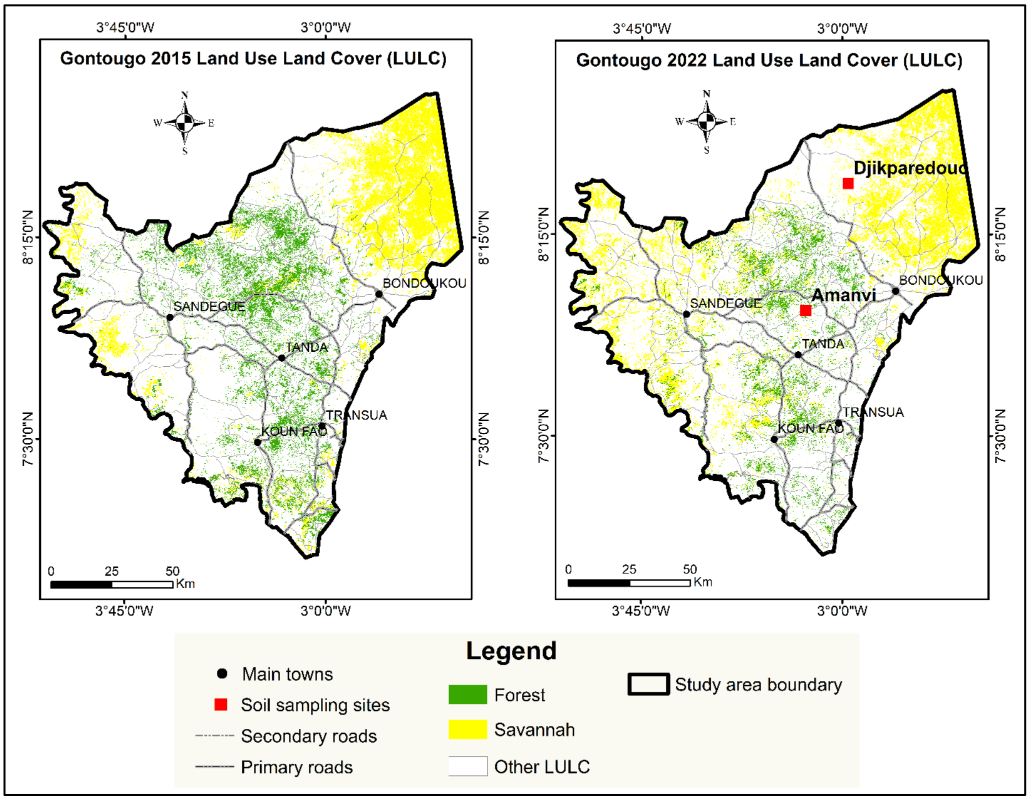

Figure 3- 4: Gontougo vegetation map of 2015 and 2022

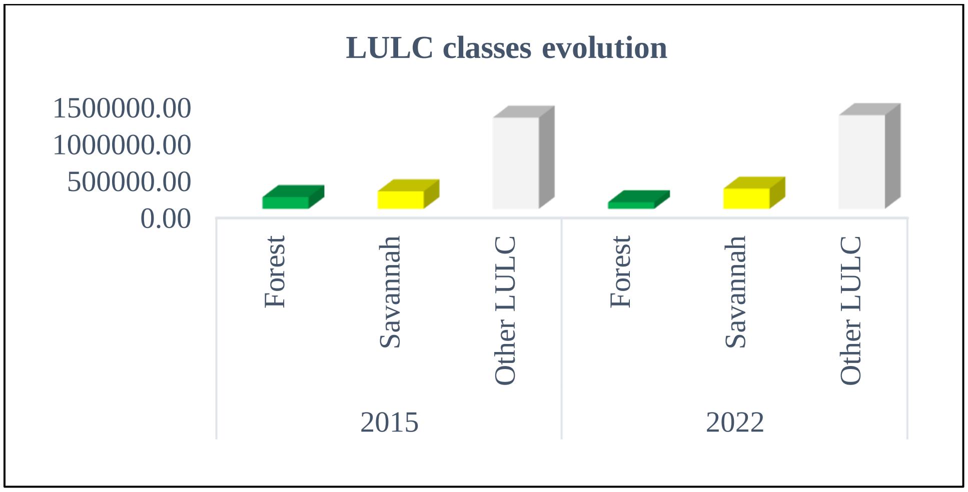

Figure 3- 5: Changing in the Gontougo vegetation trend

3.3.2. Laboratory analyses carried out

The laboratory tests included chemical and physical analyses. It should be noted that samples were derived from these sampling site characteristics: Cs1= Control site_1; Hs1= Harvested site_1; Cs2= Control site_2; Hs2= Harvested site_2; Cs3= Control site_3; Hs3= Harvested site_3; Cs4= Control site_4; Hs4= Harvested site_4. Terminologies ending in 1 and 2 are from the forest area (Tanda's department) while terminologies ending in 3 and 4 are from the savannah area (Bondoukou's department) (see table 1 above).

3.3.2.1. Chemical analysis

Chemical analysis involved: pH water, carbon (C) total nitrogen (N), available phosphorus (P) potassium (K^+), calcium (Ca^{2+}), magnesium (Mg^{2+}), sodium (Na^+), cation exchange capacity (CEC).

3.3.2.1.1. pH water

pH is a measure of how acidic/basic water is. The range goes from 0 to 14, with 7 being neutral. pHs of less than 7 indicate acidity, whereas a pH of greater than 7 indicates a base The pH was measured on the soil samples ranging from 5.4 to 5.7, as shown in the chart (**Figure 3-6**). Hs1, Hs2, and Cs3 recorded the highest pH which is 5.7 while Cs1 the lowest 5.4.

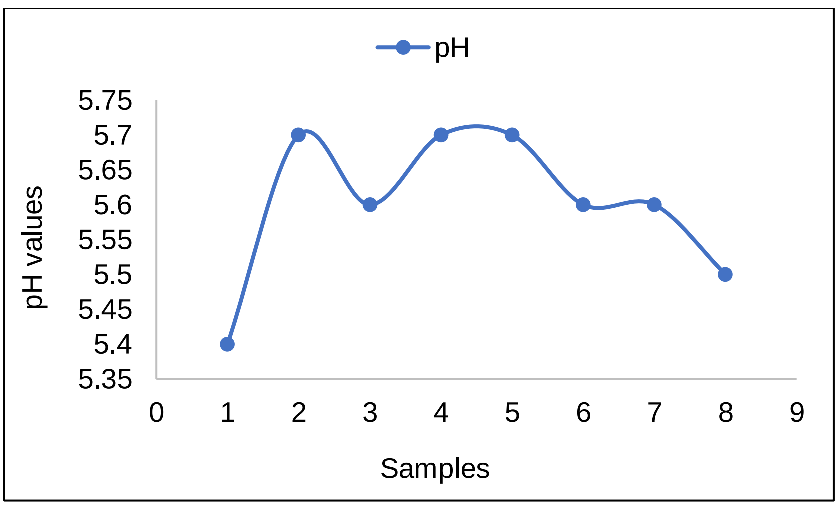

Figure 3- 6: pH measurements on soil samples

3.3.2.1.2. Organic matter

Soil organic matter is a collection of all the organic constituents of plant, animal, or microbiological origin, transformed or not, that are present in the soil. These components include carbon and nitrogen, of which we have measured. Firstly, it can be seen that the carbon content is higher than the total nitrogen content in the eight samples. These same values are higher at the four first samples, which recorded 1.17, 1.26, 1.28 and 1.11% carbon and 0.12, 0.16, 0.13 and 0.14% nitrogen respectively than the four last sites. These last (Cs3, Hs3, Cs4, Hs4) have respectively 0.40, 0.27, 0.50, and 0.27%, of carbon content and 0.11, 0.08, 0.12, and 0.07%.of total nitrogen content (**Figure 3-7**)

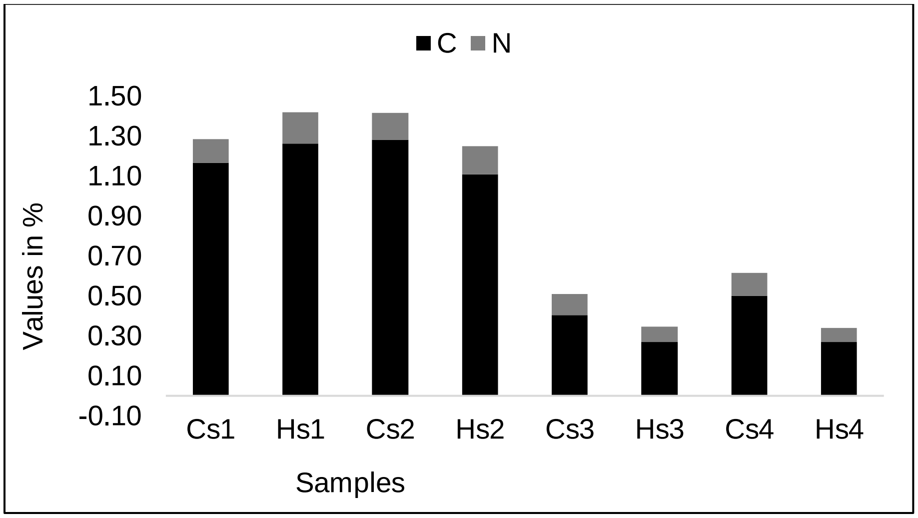

Figure 3- 7: Carbon and total Nitrogen soil sample content distributions

3.3.2.1.3. Available phosphorus

Assimilable phosphorus levels in Gontougo's region soils (**Figure 3-8**) reveal an abundance in Cs1 and Cs2 soils, with 119 and 94 ppm, respectively. Cs3 and Hs4 soils contain the lowest quantities of assimilable P, with 24 and 33 ppm, respectively.

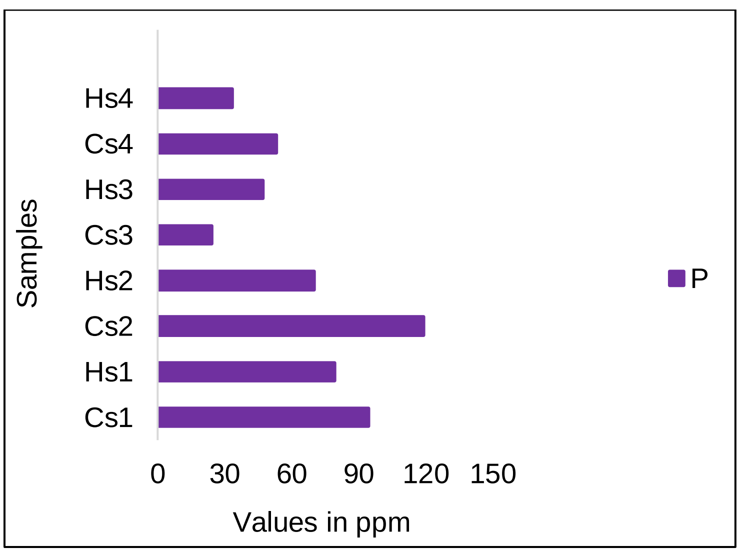

Figure 3- 8: Available phosphorus distribution in the soil samples

3.3.2.1.4. Complexe absorbent

Complexe absorbent includes CEC and exchangeable cations**.** CEC is a measure of the negatively charged sites on the surface, that help hold positively charged ions and nutrients such as sodium (Na), potassium (K), calcium (K) and magnesium (Mg) (A. Kumar et al., 2016). As with previous remarks, the observation is the same. CEC values and exchangeable cations decrease from the first four soil samples to the last four, with a peak at Cs2, which has the highest CEC value (15 Cmol.kg-1), while Hs4 has the lowest (2 Cmol.kg-1). Ca^{2+} is the most abundant cation in all eight samples ranging respectively (from Cs1 to Hs4) from 1.131 to 0.623 Cmol.kg-1 (**Figure 3-9**).

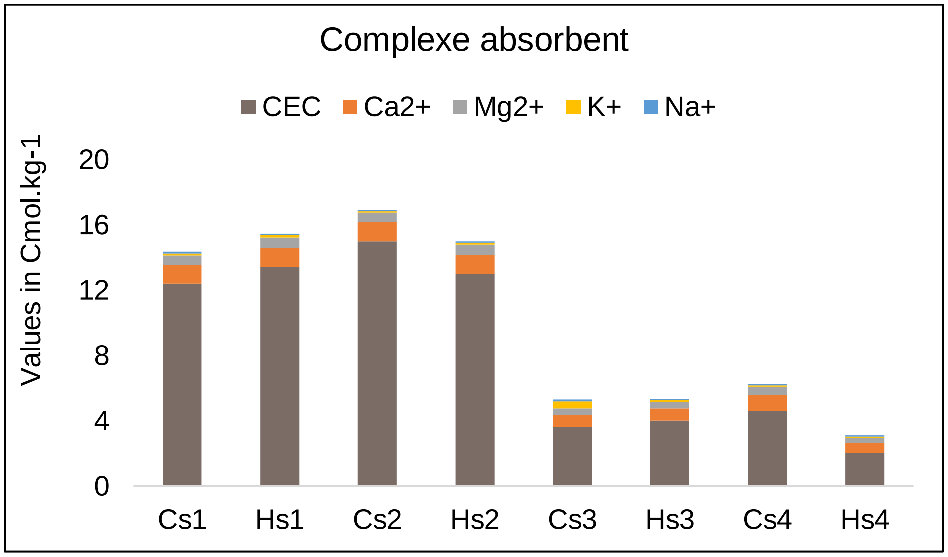

Figure 3- 9: CEC and exchangeable cations breakdown

3.3.2.2. Physical analysis

The physical analysis has taken into account particle size distribution. They constitute the inorganic portion of soil and are 2 mm or less in diameter(de Santana et al., 2023; Polakowski et al., 2023). On each side, coarse sand is more plentiful, with a distribution of more than 40% throughout, followed by coarse silt, which ranges from 12 to 26%. Clay is the least abundant in the samples, with concentrations ranging from 6 to 10% (**Figure 3-10**). NB: f-silt = fine silt; c-silt = coarse silt; f-sand= fine sand and c-sand= coarse sand.

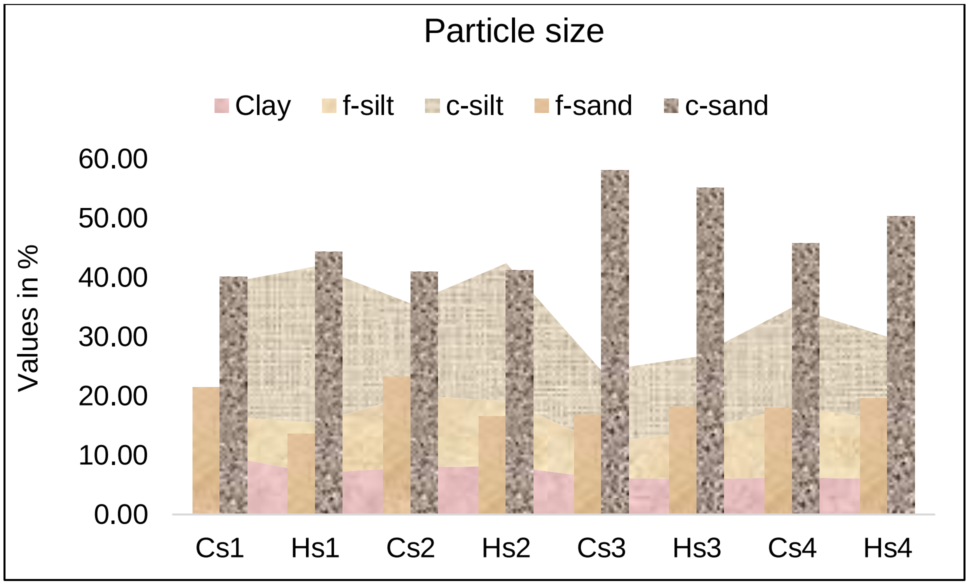

Figure 3- 10: Particle size distribution

3.3.3. Statistical analysis conducted

The sample codes will be used throughout the outcomes as follows: 1, 2, 3, 4, 5, 6, 7, and 8 respectively correspond to Cs1, Hs1, Cs2, Hs2, Cs3, Hs3, Cs4 and Hs4. This mean: Cs1= Control site_1; Hs1= Harvested site_1; Cs2= Control site_2; Hs2= Harvested site_2; Cs3= Control site_3; Hs3= Harvested site_3; Cs4= Control site_4; Hs4= Harvested site_4. They also represent the sampling sites. The symbols ∗, ∗∗, ∗∗∗ denote respectively significance at the 0.05, 0.01, and 0.001 probability(P) levels, respectively.

3.3.3.1. Correspondence Analysis (CA)

All Physicochemical properties were subjected to correspondence analysis to find out and display the relationship between categories. This was a link between the content of the chemical and physical composition and the samples. At the point of chemical components, the dataset has 8 rows and 10 columns. Rows belong to numbers and columns to chemical elements as described in this R software script: *Dataset.CA<-Dataset[c("1", "2", "3", "4", "5", "6", "7", "8"), c("CEC", "Ca2.", "Mg2.", "K.", "Na.", "C", "N", "C.N", "P", "pH")]*. (**Figure 3-11**). The chi-square of independence between the two variables is equal to 21.16038 (p-value = 0.9999998). Therefore we can observe, that the Chi-square statistic is greater than the critical value (χ^2> p-value). Also, the test recorded 7 dimensions in the eigenvalues table, each dimension has its variance values less than 0,05. The two first dimensions have the highest % of variance and their cumulative is 94.722% (**Table 3-3**).

Table 3- 3: CA eigenvalues in relation to chemical composition and samples

Eigenvalues							
	Dim.1	Dim.2	Dim.3	Dim.4	Dim.5	Dim.6	Dim.7
Variance	0.021	0.007	0.001	0.001	0.00	0.00	0.00
% of var.	69.971	24.751	2.59	2.203	0.401	0.074	0.011
Cumulative % of var.	69.971	94.722	97.312	99.515	99.915	99.989	100.00

At the level of physical sample components, the dataset has 8 rows and 5 columns. Rows belong to numbers and columns to physical properties as described in this R software script: *Dataset.CA<-Dataset[c("1", "2", "3", "4", "5", "6", "7", "8"), c("Clay", "f.silt", "c.silt", "f.sand", "c.sand")]* (**Figure 3-12**). The chi-square of independence between the two variables is equal to 27.78246 (p-value = 0.4760193). We notice that χ^2> p-value. About the eigenvalues, the test registers 4 dimensions. Each of them has variance values less than 0,05. The two first dimensions have the highest % of variance. Their cumulative variance is 86.701% (**Table 3-4**).

Table 3- 4: CA eigenvalues in relation to physical composition and samples

Eigenvalues				
	Dim.1	Dim.2	Dim.3	Dim.4
Variance	0.022	0.009	0.004	0.00
% of var.	61.975	24.726	12.907	0.393
Cumulative % of var.	61.975	86.701	99.607	100.00

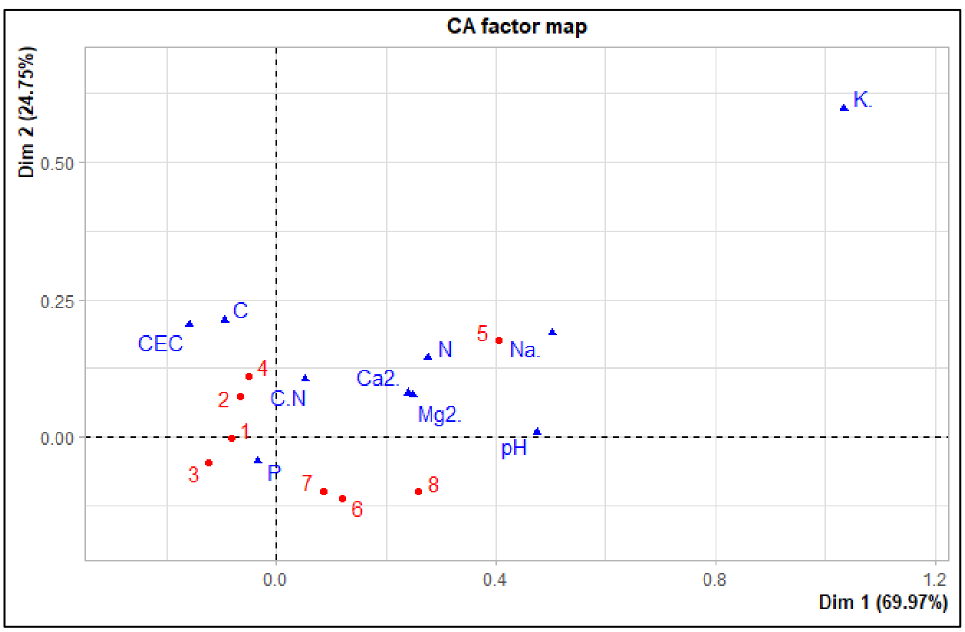

Figure 3- 11: CA factor map between chemical characteristics and samples

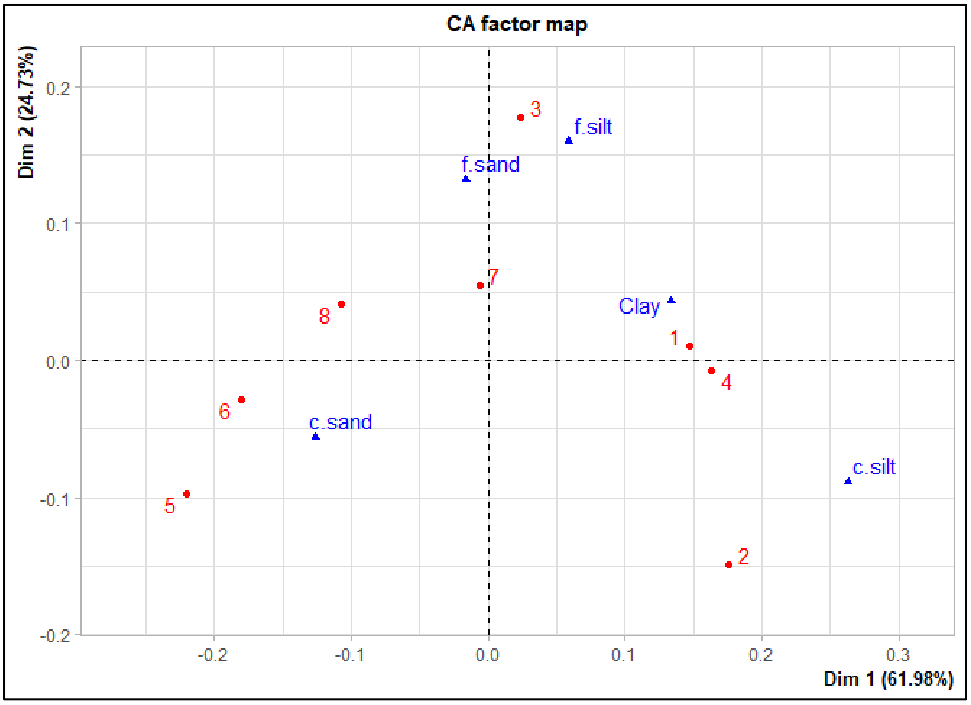

Figure 3- 12: CA factor map between physical characteristics and samples

On these two CA factor maps (figures 12 & 13), the soil components are better correlated on the dimension 1 axis than on the dimension 2 axis. The physical and chemical properties are represented by blue colors whereas the samples (or sampling sites) represent red colors. It can be seen that sample 1 is well correlated to clay, sample 3 to fine sand, and fine silt, sample 5&6 for coarse sand and sample 2&4 for coarse silt. On the other side, pH, CEC, C, Na, Ca, Mg and the C/N ratio are very abundant in the samples 2 and 4. Na, pH and K are high in sample 5. The latest is quite far away and hardly present in the remaining samples. The samples 1, 2, 3 and 4 have a high P content.

3.3.3.2. Pearson's correlation

Pearson correlation coefficient (r) measures the strength of the linear relationship between two variables. It has a scale of -1 to 1. -1 represents a perfectly negative correlation, 1 represents a perfectly positive correlation and 0 represents no correlation means that the variables studied are linearly independent. In this test between organic matter and pH, the stronger correlation is between C and C/N ratio, then between P – C, between P – C/N and between C – N. The variables pH and C are practically linearly independent and pH – P are negatively correlated (**Table 3-5 and Figure 3-13**).

Table 3- 5: Pearson correlation coefficient (r) between organic matter and pH

Pearson's Correlations

Variable		pH	P	C	N	C/N
1. pH	Pearson's r	—				
2. P	Pearson's r	-0.201	—			
3. C	Pearson's r	0.046	0.884 **	—		
4. N	Pearson's r	0.449	0.590	0.841 **	—	
5. C/N	Pearson's r	-0.190	0.917 **	0.965 ***	0.688	—

* p < .05, ** p < .01, *** p < .001

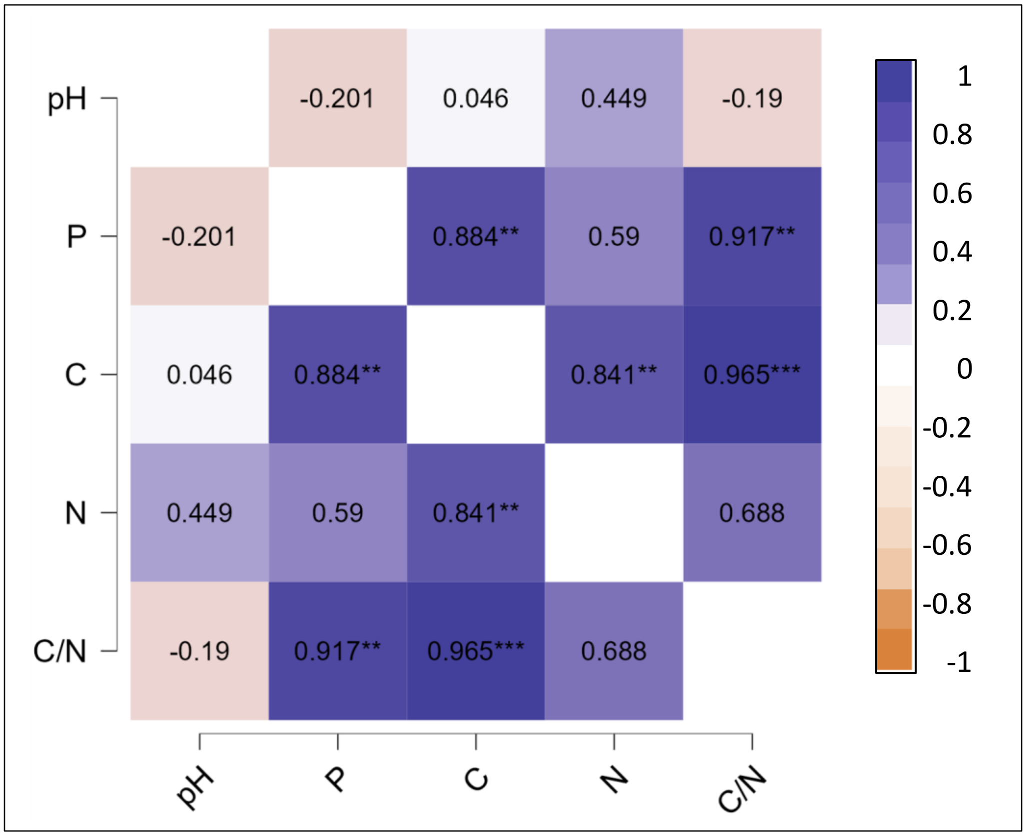

Figure 3- 13: Pearson's r Heatmap between organic matter and pH

Given the relationships between organic matter and pH, we applied the simple linear regression test between these same chemical components to assess the accuracy of the coefficient of determination (R^2) and forecast their content in the soil. It is thus advised statistically to perform correlation analysis to establish if a linear relationship exists between variables before modelling the relationship between pairs of quantities (Hastie et al., 2017).

3.3.3.3. Simple linear regression.

Simple linear regression (SLR) is a statistical tool which models the relationship between a single independent variable (*x*) and a single dependent variable (*y*). The slope of the regression line indicates the direction and strength of the relationship between variables. A positive slope indicates a positive relationship, meaning that as *x* increases, *y* is also expected to increase. A negative slope indicates a negative relationship, meaning that as *x* increases, *y* is expected to decrease (Heumann et al., 2016). SLR produces the R^2 and explains how much the variance of one variable explains the variance of the second variable. This coefficient ranges between 0 and 1 and increases with the regression's fit to the model: If R^2 is close to zero, the regression line fits 0% of the given points. If the model's R^2 is 0.50, the points can explain half of the variation found in the estimated model. If R^2 is 1, the regression determines 100% of the point distribution. In practice, obtaining an R2 of 1 from empirical data is impossible. An R^2 is considered high when it is between 0.85 and 1. Thus, we have two linear regressions with decreasing slopes, and the R-squared is 0.7761 and 0.56 respectively (**Figures 3-14 & 3-15**). The cloud of points graphically illustrates a better regression with the C/N ratio than the one with the assimilable phosphorus whose points are far from the linear regression line. The greatest C/N ratio value is 9.93% (Cs1), and the lowest is 3.43% (Hs3). As a result, we obtained C/N values ranging between 3 and 10 (10>C/N>3). As a consequence, they are less than 25%, which is the threshold for determining the quality of the carbon-to-nitrogen ratio (Francou, 2003; Moctar, 2019). The biggest result for assimilable phosphorus is 119ppm (Cs2) and the lowest is 24ppm (Cs3). These values are higher in the forest zone than in the savannah zone, and they generally decrease from the control sites to the harvested site.

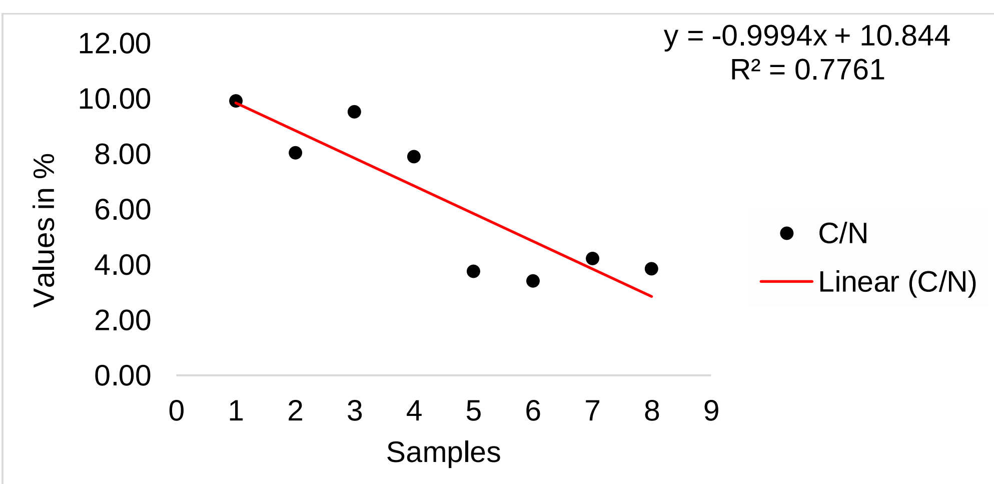

Figure 3- 14: Linear regression relation between C/N ratio and samples

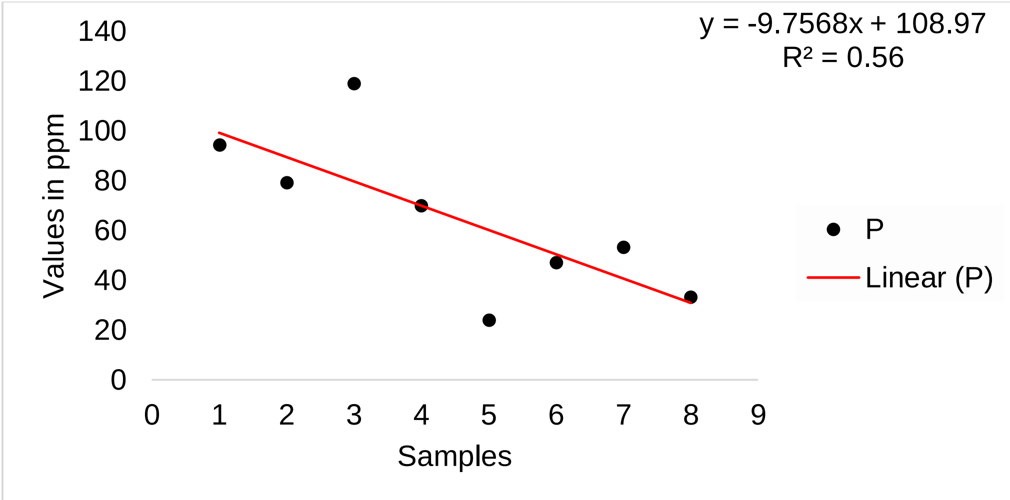

Figure 3- 15: Linear regression relation between available P and samples

3.3.3.4. Analysis of variance (ANOVA)

ANOVA stands for Analysis of Variance. It is a statistical method used to analyze the differences between the means of two or more groups or treatments. It is often used to determine whether there are any statistically significant differences between the means of different groups (Heumann et al., 2016). In this work, we used one-way ANOVA because it is part of ANOVA for testing differences in the means of three or more groups. It's also the parametric test used for comparing more than 2 independent samples. We employed it when the populations considered are normally distributed with the same variance. Before carrying out the ANOVA, Shapiro-Wilk normality was tested to determine if the variables were normally distributed. So, after running this test, if p-value ≤ 0.05, the null hypothesis is rejected (i.e. the variable is not normally distributed). If p-value > 0.05, the null hypothesis cannot be rejected (i.e. the variable is normally distributed) (Hastie et al., 2017).

3.3.4.1. ANOVA test on the particle size distribution

The particle size distribution includes fine silt; coarse silt; fine sand and coarse sand (**Table 3-6**).

Table 3- 6: Shapiro-Wilk test on the particle size distribution

Variables	W	p-value
c.sand	0.88844	0.2263
c.silt	0.89863	0.2808
clay	0.83516	0.06716
f.sand	0.9788	0.9567
f.silt	0.91967	0.4272

W is a decision variable

The p-value observed on each variable is superior to the null hypothesis (H0) (p-value>0.05). That means the variables are normally distributed. Thus we can apply the ANOVA because variables in the table 3-6 meet the assumption. This one-way ANOVA test yields the mean of each variable as an average of the values obtained for each sample in the control site and harvested site. The highest average in all samples is coarse sand (46.64%), followed by coarse silt (28.78%). Clay has the lowest average (2.077%). (**Table 3-7**).

Table 3- 7: Anova table for particle size distribution

Variables		**c.sand**	**c.silt**	**clay**	**f.sand**	**f.silt**
Indicators	Samples			Values		
Mean	Cs1	40.15	22.24	10.00	21.50	6.60
	Cs2	40.95	15.60	8.00	23.20	12.00
	Cs3	58.11	12.20	6.10	16.80	6.00
	Cs4	45.74	16.80	6.20	18.00	12.00
	Hs1	44.35	26.40	7.00	13.60	8.48
	Hs2	41.20	23.20	8.20	16.60	11.08
	Hs3	55.14	12.60	6.03	18.20	8.08
	Hs4	50.34	14.00	6.00	19.60	10.08
Df		7	7	7	7	7
Sum Sq		326.50	201.50	14.54	63.12	38.49
Mean Sq		46.64	28.78	2.077	9.017	5.499

Df= degree of freedom; Sum Sq= sum-of-squares; Mean Sq= mean square.

3.3.3.4.2. ANOVA test on the Absorbent Complex

Absorbent Complex includes CEC, and exchangeable cations (Ca^{2+}, Mg^{2+}, K^{+}, Na^{+}). Let's apply the Shapiro-Wilk normality test to determine the distribution of the variables first. All the p-values observed don't meet the assumptions of the Shapiro-Wilk test because p-values are inferior to the null hypothesis (H0) (p-value<0.05) in K^{+} and Mg^{2+} (**Table 3-8**). That means the variables are not normally distributed, so we cannot apply the ANOVA. Thus, we handled the non-parametric test which is the Kruskal Wallis (H statistic test). This test determines whether the medians of two or more groups are different.

The Kruskal-Wallis test was applied to the data following this script *(kruskal.test(variable ~ factor, data=StackedDataCplexAbs) Kruskal-Wallis rank sum test. data: variable by factor*). As a result, we got: Kruskal-Wallis chi-squared = 35.944, df = 4, p-value = 0.0000002971.

Table 3- 8: Shapiro-Wilk test on the absorbent complex

Variables	**W**	**p-value**
Ca2+	0.86281	0.128
CEC	0.82843	0.05717
K+	0.59476	0.0001381
Mg2+	0.59476	0.0001381
Na+	0.8363	0.8363

W is a decision variable

The Kruskal-Wallis test p-value (0.0000002971) < p-theoretical (0.05), therefore the null hypothesis is rejected. Not all the population medians are equal. The medians by group find out are distributed as follows: Ca^{2+}= 1.0535; CEC= 8.5000; K^{+}= 0.1215; Mg^{2+}= 0.5385 and Na^{+}= 0.0835

3.3.3.4.3. ANOVA test on the organic matter and pH

Firstly, we have applied the Shapiro-Wilk normality test to determine the distribution of the variables. Data in table don't meet the assumption of the Shapiro-Wilk test because the p-value for the variable C is inferior to the null hypothesis (p-value<0.05) (**Table 3-9**). We performed the non-parametric test (Kruskal Wallis) to assess whether the medians of two or more groups differed.

Table 3- 9: Shapiro-Wilk test on the organic matter and pH

Variables	**W**	**p-value**
C	0.80692	0.03393
C/N	0.82792	0.05648
N	0.95433	0.7547
P	0.97147	0.9093
pH	0.85995	0.1199

The Kruskal-Wallis test was applied to the data following this script *(kruskal.test(variable ~ factor, data=StackedData OrgMat)   Kruskal-Wallis rank sum test. data: variable by factor*). As a result, we got: Kruskal-Wallis chi-squared = 35.624, df = 4, p-value = 0.0000003458. The H statistic test p-value (0.0000003458) < p-theoretical (0.05), hence, the null hypothesis is rejected. Not all the population medians are equal. The medians by group observed are broken down as follows: C= 0.804180; C/N= 6.083204; N= 0.117600; P= 61.620795; pH= 5.600000

3.4 Discussion

3.4.1. Yams growth, land use land cover (LULC) and soil sampling

Gontougo region is one of the biggest yam-producing area in Côte d'Ivoire. The sector (yam) is managed by ANADER (National Rural Development Support Agencies). This agency has two autonomous offices in the region due to the expanse of the territory, the high number of farmers, and the diversity of products farmed. One is based in Tanda's department (forest zone) and covers three other departments: Koun-Fao, Transua, and Sandegue. The other is in Bondoukou's department (the savannah zone) and handles the area where it is based. We met them in the region during our research for this project and they claimed that yam growing is one of their most significant prerogatives. According to Tanda ANADER, yam production employs 95% of the farming community, covering the departments of Tanda, Sandegue, Transua and Koun-Fao, with more than 2,000 hectares of land cultivated each year. As for ANADER which covers Bondoukou's department, they registered more than 1,856 yam farmers and recorded a production of 47,840 tonnes of yams in 2022. These data demonstrate how much the residents of this region rely on yams for their livelihood. These facts have been scientifically validated by these authors (Kouakou, 2019; Kouakou et al., 2019; Miège, 1952; MINADER, 2017; World Bank Group, 2019) who have also established the Gontougo region's socioeconomic, cultural, food and nutritional relevance of yams. Yam cropping belongs to the group of annual crops. This LULC class accounted for 9.58% in 2015 and 7.61% in 2022 (Aka et al., 2023). It has lost about 2% of its total acreage to cashew nuts, the region's principal perennial crop. Vegetation consists primarily of forest and savannah. Gallery and islets forests, holy woodland, and degraded forests are all examples of forests. Savannas can alternatively be classified as tree savannas and shrub savannas. On the one hand, these many traits were discovered in the field and then studies by CUNY et al., (2023) and the Ivorian forestry laws (RCI-Code Forestier, 2019a) support these claims. In summary, we obtained three (3) LULC classes: forest, savannah and other LULC. The obtained overall accuracy (OA) is 93.77% with a kappa coefficient of 0.87 for the year 2015 map and 96.01% with a kappa coefficient of 0.92 for the year 2022 map. These findings are consistent with those of Aka et al., (2022), who mapped the Sentinel-2 picture and compared it to Landsat-8 Oli data at the Azagny site Ramsar in Côte d'Ivoire. The OA was 90.63%, with a kappa of 0.94. Indeed, classification is considered satisfactory in remote sensing when the kappa coefficient value is greater than 75% (Congalton, 1991; Jensen J. R., 1986; Zhang et al., 2023). It confirms that the findings of this investigation are statistically sound. Based on this classification joined with yam-producing areas, the location of Amanvi, situated in the forest zone in the department of Tanda, and Djikparedou, located in the department of Bondoukou, were chosen for soil sampling. This method has also been employed by several authors to examine and characterize soil based on vegetation types. This was the situation for Mustapha et al., (2023) who evaluated different methods to determine soil organic carbon and soil physical and chemical properties in the four Nigerian agro-ecological savannah zones. Ditto for Owusu Danquah et al., (2022) in Ghana who improved Pigeonpea (*Cajanus cajan*) and white yam's (*Dioscorea rotundata*) resource use and productivity by sampling nine (9) composites sample in the forest and forest-savannah transition zones of Ghana. He was able to determine soil fertility and measure the physicochemical characteristics of the soil such as total nitrogen (N), pH, organic carbon, phosphorus, and potassium at 0–20 and 20–40 cm on the ridges under these two types of vegetation. As for the sampling, the auger method was utilized to collect soil samples in the field. Auger sampling is a widely used method of collecting soil samples for a variety of environmental and agricultural applications. It is a relatively simple and inexpensive method that can be used to collect samples from a variety of soil types and depths (Fernández-Ugalde et al., 2020; Walworth, 2023). The holes we dug in the field ranged from 0 to 40 cm in some sites because the yam's root system in the mound (which is already raised more than 50 cm above ground) does not reach this depth during maturation (10 months later varieties). Adifon et al., (2019) have addressed this point in their writings on ecology, cropping systems, and food uses of yams in tropical Africa, providing more details on yam growing conditions. Several authors in soil physicochemical properties and soil fertility assessment for yam production have also employed the same method and the hole was dug nearly to the same depth (Diby, Hgaza, et al., 2011; Diby, Tie, et al., 2011; N'guessan et al., 2009; Owusu Danquah et al., 2022). In the following discussion, we will look at the interpretation of the physicochemical and statistical outcomes.

3.4.2. Sample's physicochemical parameters assessment under vegetation

Soil physicochemical properties are the physical and chemical characteristics of soil to assess the overall health and quality of the soil, as well as its suitability for different uses, such as agriculture. Physicochemical properties which were the subject of this research are pH, carbon (C) total nitrogen (N), available phosphorus (P) potassium (K^+), calcium (Ca^{2+}), magnesium (Mg^{2+}), sodium (Na^+), cation exchange capacity (CEC) and particle size distribution. These components are crucial in determining soil fertility for agricultural purposes. According to Thomas, (1996), the pH of a soil is a measure of its acidity or alkalinity. Most plants prefer slightly acidic soils. Next, organic matter (C, N, P) is a major component of soil performance. It provides energy for micro-organisms and nutrients for plants, regulates pH variations, improves soil porosity, resistance to compaction and erosion, and water storage capacity. (Suraj Poudel, 2020). Then, CEC is a measure of the soil's ability to hold and exchange positively charged ions, such as calcium, potassium, and magnesium. Soils with high CEC are more fertile and can retain nutrients more effectively (X. Zhao et al., 2020). Particle size determines texture and soil structure by proportions of sand, silt, and clay (de Santana et al., 2023) The different methods for determining them have been thoroughly tested on soil samples and are widely utilized in the scientific community. These authors (BARI et al., 2022; Bremner, 1960; De Vos et al., 2007; Khee C. Rhee, 2001; Koné et al., 2022; N'doufou et al., 2022; Steinfurth et al., 2021; X. Zhao et al., 2020) have also used the Walkley-Black method to quantify soil carbon, the Olsen method to determine assimilable phosphorus, the Kjeldahl method for total nitrogen and the ammonium acetate method to determine CEC and echengeable cations in their respective research work on the physical and chemical state of the soil. As a result, the pH observed in both forest and savannah environments is acidic, ranging from 5.4 to 5.7. The difference between these numbers is not large, but the pattern indicates that the values decline a bit in the savannah area. Our pH results are confirmed by N'doufou et al., (2022) who also found an acid pH value varying from 5 to 6 by measuring the soil's pH in northern Côte D'Ivoire (Sinematiali and Niakaramadougou). In terms of organic matter, samples Cs1, Hs1, Cs2, Hs2 (forest region) had substantially greater C, N, and P contents than samples Cs3, Hs3, Cs4, Hs4 (savannah area). C/N ratio values in the forest varied from 7.93 to 9.93%, whereas in the savannah area they ranged from 3.43 to 4.24%. Assimilable phosphorus was very high in the forest (70 ppm for the lowest value recorded in sample Hs2) and very low in the savannah zone (53 ppm for the highest value obtained in sample Cs4). The same is true for the absorbent complex. The first four samples (forest zone) have higher CEC and exchangeable cations than the last four (savannah zone). At the particle size level, where the elements are quite stable on either side, the balance is pretty even, with a strong presence of coarse sand in the savannah zone and a strong presence of coarse clay in the forest zone. The most significant finding is the increased concentration of these physicochemical characteristics in samples from control sites compared to samples from yam-harvested sites. This can be seen in the C/N ratio, available P and CEC which are respectively 19.47%, 213 ppm, and 27.4 $Cmol.kg^{-1}$ in the forest zone control sites, compared to 8.03%, 77 ppm, and 8.2 Cmol.kg-1 in the savannah zone control sites. The same holds true for yam-harvested sites in both the forest and savannah zones. The C/N ratio, available P, and CEC in the forest zone are respectively 15.98%, 149ppm, and 26.4 $Cmol.kg^{-1}$, compared to 7.3%, 80ppm, and 6.0 Cmol.kg-1 in the savannah zone. The findings clearly show that the savannah zone is deficient in organic matter compared to the forest zone. Related to other studies, an evaluation to compare the amount of organic carbon determined by diverse methods within the Nigerian savannah ecological zone, Mustapha et al., (2023), observed that the use of the WB method determined the highest organic carbon of 5.82 g kg^{-1} and 9.04 g kg^{-1} in the Derived savannah (DS) and Southern Guinea Savanah (SGS) respectively against 4.75 g kg^{-1} and 3.69 g kg^{-1} in the Northern Guinea (NGS) Savanna and Sudan Savannah (SS) respectively. In its study on the edaphic drivers of yam production in the West African agroecological zone (Neina, 2021) discovered that cultural practices, climatic change, and the unpredictability of ecological factors are crucial in soil fertility. Tillage, soil type, texture, and fertility are edaphic elements. Soil fertility, the most essential of these components, includes the biological and chemical elements that allow nutrients to be released, as well as soil physical fertility, which enhances bulk density, porosity, and water retention for the free expansion of yam tubers. According to some authors (Dahan et al., 2021, 2023; Dahan & Kasei, 2022), savannas are more prone to fires than forests, and these fires can consume organic matter and reduce their accumulation in the soil. Frequent fires can also disrupt the establishment of vegetation, further limiting the input of organic matter. Also, Sandy soils tend to have lower organic matter content because they are less able to retain organic matter particles. This is what we observed in our case where samples from the savannah area have a higher proportion of sand (103.85% coarse sand, from the control site) and a lower proportion of clay (12.30% from the control site) compared to forest soil samples (81.10% coarse sand and 18.00% of clay from the control site).

These findings were statistically analyzed, and various tests, including correspondence analysis (CA), Pearson's r correlation, a simple linear regression and analysis of variance (ANOVA) were

performed. These approaches have also been the focus of world-renowned soil investigations. This was the case for (Koné et al., 2022), which employed ANOVA to measure soil fertility in cotton-growing areas in Côte d'Ivoire. In their research in Côte d'Ivoire, several authors (Diby, Hgaza, et al., 2011; Moctar, 2019; N'doufou et al., 2022; N'guessan et al., 2009; Zro et al., 2016) used correlation and correspondence analysis as well as linear regression as statistical tests to compare the values of physicochemical soil parameters. Other authors from throughout the world have utilized comparable approaches for other goals (He et al., 2012; Madeira et al., 2003; Mekbib et al., 2020; Mustapha et al., 2023; N'guessan et al., 2009; Owusu Danquah et al., 2022; Zhang et al., 2013). All of these support the statistical approaches and procedures used in this investigation. The CA test on the physical and chemical properties revealed that the Chi-square statistic is greater than the critical value, which means that the row and the column variables are not independent of each other. Also, all the dimensions have variance values less than 0.05, which confirms that variables are not independent. Only the two first dimensions are signficative because their cumulative variance is greater than 75%. By exploring the relationships between the two sets of variables (samples and physicochemical properties), we identified clusters of samples that are most matched with soil properties. Soils in clusters 5, 6, 7, and 8 mainly consist of coarse sand, whereas clay is more abundant in clusters 1, 2, 3, and 4 (forest zone). Silt is spread among several sites. This means that the savannah zone's soil is silty-sandy, whereas the forest zone's soil is clay-loam. When it comes to chemical components, clusters 1,2,3, and 4 (forest zone) dominate in CEC, C, P, and C/N. Clusters 5,6,7, and 8 (savannah zone) have varying levels of Na, N and K. Indeed, silty-sandy soils have low water-holding ability. This means that organic matter is more likely to decompose and be lost from the soil (Moctar, 2019). A clay and silt-based soil, on the other hand, keeps more water in the soil, allowing organic matter to degrade and microorganisms to function more efficiently. This explains why samples 1 – 4 have a higher concentration of organic materials than samples 5 – 8 (Feller & Christian, 1993; Nacro et al., 1996; Ostrowska & Porębska, 2015)
For additional testing, Pearson's correlation coefficient (r) revealed a positive relationship between the independent variables C, N, P, and C/N connected each other labelled at $p < 0.05$. according to Zro et al., (2016), positive significant correlations between organic matter components reflect the adsorption on the surface of the clay-humus complex major cations of soils (Ca2+, Mg2+, K+, Na+). When soil can hold onto essential nutrients and minerals, they are more available to plant roots that need them for survival. Cations can be held and stored in the soil by negatively charged colloids (Dpt Geographie, 2021).

Then, the linear regression used to model the relationship between the C/N ratio – samples and available P – samples displayed respectively a positive coefficient of determination ($R^2 = 0.7761$ and $R^2 = 0.56$). Variables are dispersed in a cloud of points, some far from and others near the regression line. Regarding the R-square values, the linear regression does not precisely match the data. So, the strength of the independent variable (soil samples) explains respectively 77.61% and 56% of the variation in the dependent variables (C/N ratio and available P). Thus, the goodness of fit measured is more accurate for the C/N ratio than the available P. This implies that the samples have a higher C/N concentration ratio than accessible P. It is worth noting that the C/N ratio is a measure of organic matter's evolution, or its ability to dissolve more or less fast in soil. An imbalance in the amount of carbon and nitrogen in agricultural soil disrupts these cycles severely. The C/N ratio informs us about carbon and nitrogen balance in an ecosystem and allows us to forecast the evolution of organic matter (Batjes, 1996; Sahoo et al., 2023; Xu et al., 2013). At this level, the linear regression line matches to the point clouds fits the point clouds more or less well because the C/N ratio is distributed fairly in each soil sample. A low C/N ratio (<15) indicates that there is a lot of nitrogen in the soil (or not enough carbon), so microorganisms can mineralize organic materials quickly. This supports our claim because we achieved 10>C/N>03. Then, A high C/N ratio (>25) indicates that there is insufficient nitrogen (or too much carbon) and, as a result, carbon mineralization is slow (Francou, 2003). Mineral nitrogen is only restored to the soil in trace amounts. The humus formed under these conditions, on the other hand, is quite stable (Sahoo et al., 2023). Assimilable Phosphorus plays an essential role in the establishment of the root system, photosynthesis and fruiting of the plant. It is essential because it is part of the composition of all the cells of living organisms. Knowing the soil's assimilable phosphorus level is critical for optimizing additional fertilization from an agronomic and economic standpoint, based on the needs of the soil and the crops. But also, to sustain long-term phosphate fertility. In this investigation, available phosphorus is unequally distributed and lower in some parts of the soil sample because, like organic stuff, available phosphorus migrates slowly or not at all at depth. So, deep tillage, however, can dilute it.(Hgaza, 2010; M. Kumar, 2021; N'guessan et al., 2009).

On the other side, the ANOVA test on the soil samples showed that p-value>0.05 for particle size. This indicates that there is a statistically significant difference between the soil samples and the particle size groups means. As you notice, the means of each particle size are different. Soil quality (texture, structure) is thus determined by particle size distribution. This was previously observed upstream, where our data revealed that soil samples from the savannah zone had a sandy-loam soil type, but soil samples from the forest zone had a clayey-loam soil type. some scholars have also confirmed similar claims in their writings on Côte d'Ivoire soils (B. DABIN, 1960; KEITA Djibril Sékou, 2014; Koné et al., 2022; N'doufou et al., 2022). The ANOVA test on the absorbent complex (CEC and exchangeable cations) and organic matter and pH showed no statistically significant difference because the Shapiro-Wilk normality test on these data did not meet the assumptions (p-values<0.05). Thus, we dealt with the Kruskal Wallis (H statistic test), a non-parametric test to examine whether two or more groups' medians differ. The p-values between the groups were less than 0.05, so we rejected the null hypothesis. There is thus a statistically significant difference between the group medians in terms of reaction. Indeed, the medians by group (concerning CEC and exchangeable cations) find out are distributed as follows: Ca^{2+}= 1.0535; CEC= 8.5000; K^{+}= 0.1215; Mg^{2+}= 0.5385 and Na^{+}= 0.0835. On the other side (organic matter and pH), The medians by group observed are broken down as follows: C= 0.804180; C/N= 6.083204; N= 0.117600; P= 61.620795; pH= 5.60. ANOVA and Kruskal Wallis tests were both statistically significant on the soil data. We concluded that the soil properties within the samples from both sides (Tanda's and Bondoukou's departments) are different. Using the same statistical procedures, these studies (Koné et al., 2022; N'doufou et al., 2022; Owusu Danquah et al., 2022; Zro et al., 2016) reported statistically significant values for soil fertility.

3.5. Conclusion and outlooks

The study aimed to evaluate the physicochemical properties of huit (8) composite soil samples of which four (4) were taken in forest zone (Tanda's department) and four (4) in savannah zone (Bondoukou's department). They were collected from control sites (where yams had not yet been grown) and harvested sites (where yams had recently been removed from the mound). The laboratory analyses revealed an acid pH of between 5.4 and 5.7 in all samples, and the organic matter values indicate that the C/N ratio in the forest varies from 7.93 to 9.93%, while in the savannah zone it varies from 3.43 to 4.24%. The same goes for assimilable P, CEC and exchangeable cations (K^{+}, Ca^{2+}, Mg^{2+}, Na^{+}), which are respectively 362.69 ppm, 53.80 $Cmol.kg^{-1}$, and 7.92 $Cmol.kg^{-1}$ in forest area from samples Cs1, Hs1, Cs2, and Hs2 compared to the samples from savannah area (Cs3, Hs3, Cs4, and Hs4) where the same characteristics are respectively 157.80 ppm, 14.20 $Cmol.kg^{-1}$, and 5.80 $Cmol.kg^{-1}$. The Bondoukou's soil is mainly sandy with coarse sand (209.32%) and a low clay percentage (24.33) as opposed to the Tanda's soil which is less sandy (166.65%) and has a high clay concentration (33.20%). Silt and fine sand are spread proportionally in both soil types. This led us to conclude that the soil in the savannah zone is silty-sandy, whereas it is silty-clay in the forest zone. Starting with CA, the numerous statistical tests revealed that the variables are not independent of one another. Pearson's correlation coefficient (r) found a positive link between the independent variables C, N, P, and C/N, with $p<0.05$ indicating significance. The simple linear regression test revealed a strength of variation of 77.61% and 56%, respectively for the C/N ratio and available P in the samples distributed in the scatter plot. Then, ANOVA analysis indicates that there is a statistically significant difference between the soil samples and the particle size groups means. This was not the case for the absorbent complex or with the organic matter and pH because the Shapiro-Wilk normality test on these data did not meet the assumptions (p-values were less than 0.05). The Kruskal Wallis test performed then on these data showed a statistically significant difference between the group medians in terms of reaction and confirmed that the soil properties within the samples from Tanda's and Bondoukou's departments are different. This study revealed that the presence of trees increases the physicochemical properties content in the soil. In the case stand, soils under forest are richer in physicochemical elements than savannah soils for a variety of reasons discussed in this article, including climate, edaphic conditions, ecology with or without fire, and so on. It should be pointed out, however, that the conclusions of this study are based solely on two localities in the region. Sampling did not cover the entire study area, and this is a limitation of our investigation that must be taken into account. Nevertheless, in the case of yam farming, may this under forest soil be the most suitable? Aren't agronomic and growing practices the most important factors? Aren't rainfall and temperature in the savannah zone best suited to the production of the yam varieties most widely grown in the Gontougo region? These are the questions we will be trying to answer in our upcoming research in the study area. This study has benefits for monitoring and evaluating food security in Côte d'Ivoire adding to the evidence database further studies on yam production conditions based on the varieties' ecological, edaphic, climatic, and physiological environment.

CHAPTER 4: CHARACTERISATION OF KEY AGRO-CLIMATOLOGICAL HAZARDS AND ASSESSMENT OF YAM FARMERS' AGRONOMIC PRACTICES AND ADAPTIVE RESPONSES

4.1. Introduction

The recent and future global climate projections in the sixth report of the Intergovernmental Panel on Climate Change (IPCC) predict an intensification of warming in addition to precipitation variability, as well as an increase in the frequency and intensification of extreme events (IPCC, 2022). The impacts of this climate variability vary from one region of the world to another, with particularly significant socio-economic consequences in developing countries (Sultan et al., 2015). In Sub-Sahelian West Africa, the false start and the early end of the rainy season, the intensification of the frequency of daily showers, the increase in the number of warm nights and days, and the upward trend in daily temperature variation threaten food security in the region (Alhassane et al., 2013; Cedric et al., 2022b; IPCC, 2022; Srivastava, Gaiser, Paeth, et al., 2012). Furthermore, West Africa is currently under multiple stress from recent military and socio-economic events, making it highly vulnerable to the effects of climate change. The influence of these multiple stress factors, such as environmental disasters, economic turbulence due to globalisation, privatisation of resources and civil conflict, combined with a lack of resources, make serious problems for African communities striving to adapt to climate change (Sanogo et al., 2023). Indeed, according to FAO statistics on food security in Côte d'Ivoire (https://www.fao.org/faostat/en/#data/FS), the country recorded a prevalence of undernourishment of 7.7% and 12.1 million people in a situation of moderate or severe food insecurity between years 2020 and 2022. All the reasons mentioned above could be the source of such a situation, with a more pronounced emphasis on climate variability. In Côte d'Ivoire, the climatic context is characterised in comparison with observations prior to the 1960s, by a reduction in rainfall and a shortening of the seasons. The isohyet curves recorded at national stations vary between 800 mm, 1,000 mm, 1,400 mm and 2,400 mm (Télesphore Brou, 2009). This study was repeated at the local level by Kouman et al., (2022) in the Zanzan district, which includes the Gontougo region. Their study showed that: From years 2011 to 2020, total precipitation was between 895.56 and 1327.2 mm, corresponding to an increase of 181.9 mm compared with the last two decades when precipitation amounts varied respectively between 852.14 and 1145.3 mm for the decade 2001-2010 and between 837.69 and 1276.9 mm for the decade 1991 to 2000. Then, in an attempt to mitigate the effects of climate variability and achieve food self-sufficiency, Côte d'Ivoire has opted to produce certain adapted crops, including yams. Indeed, Yam (*Dioscorea spp*.) is a staple food crop and tropical plant with a large food reserve in their under-ground tubers and comprises various species that originated from Southeast Asia, West Africa, East Africa, Brazil, and Guyana (Dibi et al., 2021; Gweyi-Onyango et al., 2021; A. M.

Kouakou et al., 2019; Neina, 2021). Its production requires a rainfall of between 1000–1500 mm for a Forest-Savannah transition zone; 1000–1400 mm for Guinea Savannah; and 900–1200 mm for Derived Savannah (Aighewi et al., 2021; Diby, Tie, et al., 2011; Heller et al., 2022; Neina, 2021; N'guessan et al., 2009). It's widely grown in Côte d'Ivoire, and among food crops, it's the most cultivated.(BCEAO, 2017; Diarrassouba, 2019; Kouakou, 2019). It is therefore a crop that has a choice place in the Ivorian economy and food and nutritional security. The landrace varieties *Kponan, Krengle,* and *Djate*, are in high demand, as are the adapted varieties *TDA*, *Mao* and *C20*. The latter have demonstrated good productivity, disease resistance and drought tolerance (Adifon et al., 2020; Kouakou et al., 2019; R. Michel and G. Apata, 2017). Gontougo region is one of the largest yam-producing regions in Côte d'Ivoire. According to the Census of Farmers and Agricultural Holdings (REEA), it accounts for 71,283 farming households with 5.6% of Côte d'Ivoire's farming population (MINADER, 2017). During our survey in July 2022 about farmer's perceptions in the field, National Rural Development Support Agencies (ANADER) told us that yam production counts for 95% of the farming population covering the departments of Tanda, Sandegue, Transua and Koun-Fao. Bondoukou's department registered more than 1,856 yam farmers and recorded production of 47,840 tonnes of yams in 2022. Despite all the advantages that yam represents for the country and Gontougo's population, it has not yet been formalized, less discovered and less studied in terms of scientific research. Some authors have carried out several studies on yam at the national level, but very few in this region (ANOGBRO PASCAL, 2015; Dibi et al., 2021; Hgaza, 2010; Kouadio et al., 2022; Kouakou et al., 2019; KOUAME Hgaza Kouassi Valerie, 2012; Miège, 1952). This study aims to analyze the agro-climatological risks that threaten yam production through the indices generated by the World Meteorological Organization (WMO) Expert Team on Climate Change Detection Monitoring and Indices (ETCCDMI), gather farmers' perceptions and determine the strategies adopted and adaptive response to increase yield.

4.2. Methodology

4.2.1. Climate data

The data used to characterize the main agro-climatological trends of the seasons in the study's area mainly consist of those relating to rainfall and temperature from the CHIRPS database (Rainfall Estimates from Rain Gauge and Satellite Observations). By definition, CHIRPS data are gridded data with a high spatial resolution (0.05°*0.05°, i.e. approximately 5km) obtained by combining satellite data and in situ observation data. These data are available for the period from 1981 to the present day and are defined worldwide with variable timescales (daily, pentad, decadal, monthly and yearly); they can be accessed via the following link: https://www.chc.ucsb.edu/data/chirps. The use of these data is justified by the data's quality, horizontal resolution, and, most importantly, the fact that the observation data from the area's meteorological stations contain a considerable number of gaps, restricting their use. Funk et al., (2015) highlighted the quality of these data as well as the many scientific approaches to their generation. Again, CHIRPS data have been frequently used in scientific studies by various authors (Georganos et al., 2017; Harrison et al., 2022; Kpanou et al., 2021; Laux et al., 2021; Pervez et al., 2021). For this study, these gridded data were extracted at daily time intervals over 32 years (1991-2022), taking into account the most recent World Meteorological Organization (WMO) standard climatic normal, which corresponds to the last three decades (1991-2020).

4.2.2. Survey data

Before surveying a population, it is essential to determine the sample size required. According to the general census of the Ivorian population in 2021, the Gontougo region's population is estimated at 917,828 inhabitants (RGPH-CI, 2021). As a predominantly agricultural region, agriculture is practised by 90% of the population. Among them, 95% are yam farmers (Individual surveys, July 2023). Therefore, we can estimate the yam farmer's population to be **784,742**. To determine the sample size (S) for the survey, we used the formula developed by Krejcie and Morgan in 1970 and taken up by Penyelidikan, (2006), which is presented as follows in **equation 1:**

$$s = \frac{X^2NP(1-P)}{d^2(N-1)+X^2P(1-P)} \qquad [1]$$

S= Necessary sample size

X^2= chi-square value for 1 degree of freedom at a confidence level of 95%

N = population size

P = proportion of the population (estimated as .50 for maximum sample size)

d = degree of accuracy expressed as a proportion (.05)

The application of this formula yielded a sample size of **384** yam farmers, with whom we conducted our surveys. To cover the entire study area in conducting our surveys, we visited 11 villages (**Figure 4-1**) out of the 14 planned. We ran into many issues, including localities that were inaccessible due to the impracticability of roads and tracks; appointments that were not made by traditional chiefs due to their unavailability; invalid returns of access requests from several villages; insecurity in some areas due to conflicts between livestock breeders and farmers; and so on. As a result, 03 communities, including two in the Sandegue department, were not visited. In total, we surveyed **492** yam farmers from 4 departments in the region.

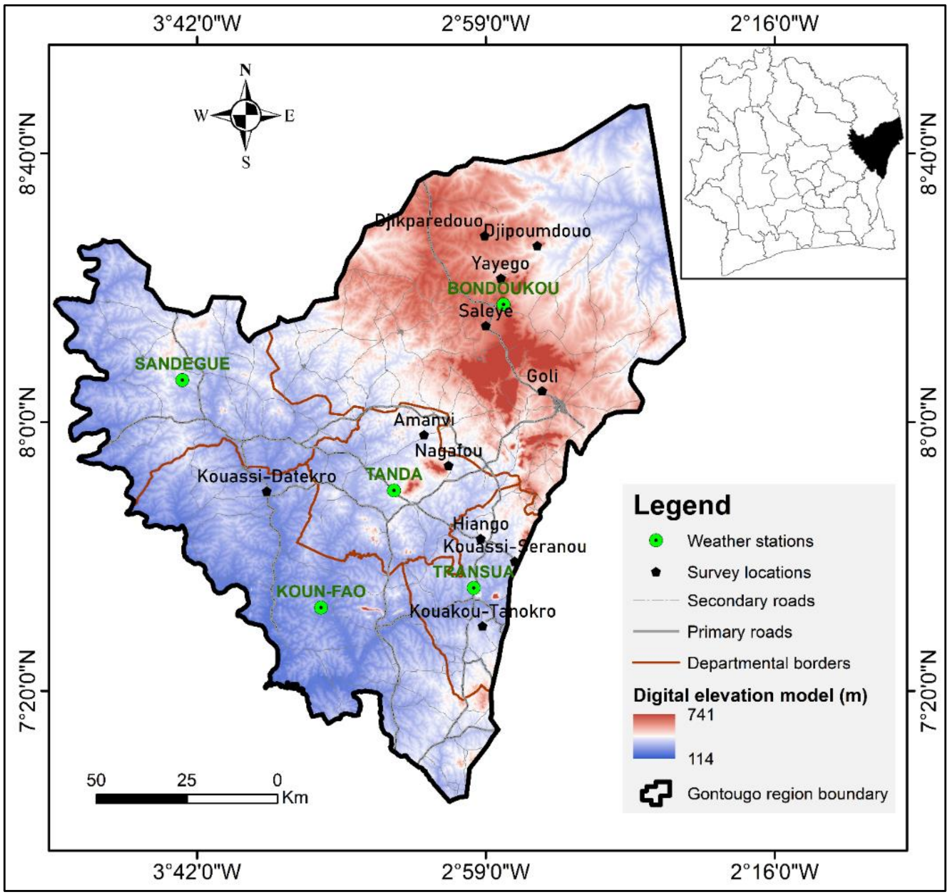

Figure 4- 1: Survey locations visited

4.2.3. Data analysis

4.2.3.1. Climate data

R software version 4.2.2 was used to manipulate and analyse the data. R is also a programming language and environment for statistical computing and graphics. It was used to process the climatic data files acquired in NetCDF format, by extracting them from the grid points, calculating agroclimatic characteristics using a developed algorithm, carrying out statistical tests and producing maps and graphs. All of these tasks were made possible by the scripts we developed for this purpose.

4.2.3.1.1. Data extraction

The various precipitation and temperature data for the study period (1991-2022) were extracted for the five administrative departments in the study area (**Table 4-1**) using the K-nearest neighbor method (K-NN). The K-NN is a method that identifies and extracts the grid or mesh point closest to the station coordinate (X, Y), representing the station in the study area, based on Euclidean distance (Javari, 2018; S. Kim et al., 2016; Yates et al., 2003). This approach differs from the bilinear extraction method, which assigns to the extraction point the average of the data from the various grid points around the extraction point (ud din et al., 2008). Once the data had been extracted and formatted, the various agro-climatological characteristics were calculated for each station following current scientific approaches and the main climate patterns in the region

Table 4- 1: Weather station coordinates generated for data extraction

No	Stations Name	Longitude	Latitude
1	KOUN-FAO	-3.392	7.540
2	TANDA	-3.211	7.830
3	SANDEGUE	-3.737	8.104
4	TRANSUA	-3.014	7.588
5	BONDOUKOU	-2.940	8.292

4.2.3.1.2. Precipitation analysis

Total seasonal precipitation (PRCPTOT) was estimated using the accumulated precipitation between the start and end dates of the seasons. The length of the seasons is the gap between the seasons' end and start dates (in Julian days) and the cumulative seasonal rainfall is the total amount of rain collected during a rainy season. We then calculated the consecutive wet days (CWD) and the consecutive dry days (CDD). CWD is a maximum consecutive number of rainy days during which rainfall is above a threshold of 1 mm (P>1mm). As for dry spells, it can be beneficial for rainfed agriculture (farmers can use dry spells to do field operations such as sowing, weeding, applying fertilizer, and harvesting). According to the WMO standard, a dry spell is a succession of consecutive days during which rainfall is below a threshold of 1 mm (P<1mm) (WMO, 2012). In this study, we considered only the so-called extreme dry sequences defined by Salack (Salack et al., 2012). These are intra-seasonal dry spells frequency lasting between 10 and 30 days. The occurrences and maximum lengths of these dry sequences were extracted for each station.

4.2.3.1.3. Temperature analysis

The temperature indices calculated express the minimum and maximum temperatures over the two growing seasons from 1991 to 2022 for each station. The most striking index is Growing Degree Days (GDD). The GDD or heat units, is used to estimate the growth and development of crops during the growing season.

The accumulation of average daily temperatures during yam development has a strong influence on their growth. If this temperature is too high for the tubers, the yam will not grow large enough. This is because it dries out the water that the yam contains. The accumulation of average daily temperatures is calculated as "growing degree days" and also includes a minimum development threshold that must be reached for growth to take place from the time the seedlings are planted until they mature. The GDD formula is given by the **equation 2** (Mcmaster & Wilhelm, 1997).

$$GDD = [(Tmax + Tmin) / 2] - Tbase \qquad [2]$$

Where:

Tmax and *Tmin* are respectively daily maximum and minimum air temperature, and *Tbase* is the yam base temperature. Typically ranging between 10°C to 15°C (Ufoegbune et al., 2014).

4.2.3.2. Statistical trends analysis

A statistical technique based on the Mann-Kendall test was used to analyze trends in a series of different agroclimatic variables in each department of the research area. The Mann-Kendall (MK) test is a popular non-parametric statistical test for detecting patterns in environmental data and allows to characterize trends. (New et al., 2006; Perez Melo, 2014). Due to its robustness and insensitivity to outliers in the time series, it is possible to analyze the statistical significance of trends and precisely quantify the magnitude of trends in climatic extremes indices (Croitoru et al., 2013; Kouman et al., 2022). The non-parametric Mann-Kendall test has been used in various of research studies since it makes no assumptions about data distribution or trend linearity (Davis et al., 2016). In contrast to parametric trend tests which require both regularly distributed and independent data, MK test trend tests simply require independent data (Kpanou et al., 2021). It is used to assess whether the trend is regressive or progressive over time through a form of monotonic regression trend analysis. In the calculation of this test, the null hypothesis (H0) argues that there is no trend in climate extremes over time, whereas the alternative hypothesis (H1) suggests a monotonic decreasing or increasing trend. The Mann-Kendall coefficient (S) and the Mann-Kendall trend tau (T) are calculated using the following mathematical **equations 3 and 4:**

$$S = \sum_{k=1}^{n-1} \sum_{j=k+1}^{n} sgn(Xj - Xk) \quad [3]$$

$$T = \frac{2S}{n-(n-1)} \quad [4]$$

Where:

T is the Mann-Kendall tau*; S* is the Mann-Kendall correlation coefficient and *n* is the length of the data series studied.

sgn is defined by: *sgn(Xj-Xk) = 1 if Xj > Xk;*

= 0 if Xj = Xk;

= −1 if Xj < Xk.

For this study, the test was applied to the series of annual mean data for the different agroclimatic variables, based on the base period 1991-2022. The test was carried out under the null hypothesis H0 that "there is no trend". The significance of the value of the Mann-Kendall tau was determined at the 5% threshold.

4.2.3.3. Characteristics of the growing season

For agricultural planning and implementation in a given geographic area, it is important to have reliable estimates of rainfall amounts. The probabilities of rain give an idea of the date that can start the agricultural season. In Gontougo region, farmers are sometimes replanting yams in mounds because the first yam seeds rot due to the high temperature. In order to mitigate the risk of seed loss, and to promote the conditions for germination and growth of the yam, rainfall-based methods define the onset of the growing season (OGS) as the date when accumulated rainfall exceeds a specific amount, provided that there was no long dry spell after this date. The rainfall threshold and the length of dry spells are the main parameters of rainfall-based methods for determining the true start and end dates of rainfall. For each department in the study area, growing season calculations were carried out for both the long and short rainy seasons. Various definitions of the onset of the rains exist in the literature. Three potential approaches are currently in use in the West African sub-region:

1. The date after 1st May, when rainfall accumulated over 3 consecutive days is at least 20 mm and when no dry spell of more than 10 days occurs within the next 30 days (Diallo, 2001).

According to Waongo, (2015), this approach is currently used at AGRHYMET Regional Center in Niamey (Niger).

2. The first day of a spell of 5 days in which at least 25 mm of rain falls, on the condition that no dry period of more than 7 days occurs in the following 30 days (Dodd & Jolliffe, 2001). According to Waongo, (2015), this approach is currently in operation as an agricultural decision support tool at the Directorate-General for Meteorology in Burkina Faso.

3. The onset of rains (X) started when we received a quantity of 20 mm of rain collected in 3 consecutive days, after 1 May (for the Sahelian zone) without a dry period of more than 7 days being observed within 30 days. The date of rain cessation (Y) is defined as the date after 1 September on which no rain occurs over a 20-day period. The length of the growing season (Z) is taken as the difference (Y-X). (Sivakumar, 1988).

So, based on probabilities of precipitations and dry spells for growing season lengths of varying durations for a given date of onset of rains, Sivakumar's method is best designed to be adapted to the specific case in our study area. It should also be emphasized that this approach is considered both West Africa's Sahelian and Sudanese zones. As a result, the dates of the growing season in any country may shift depending on the wet season. As such, the study's goal was to forecast the potential of the rainy season based on the start of rainfall in each climatic zone. His research was conducted in five countries: Burkina Faso, Niger, Mali, Senegal, and Chad. Also, Sivakumar's method (Sivakumar, 1988). is currently used in Côte d'Ivoire by several authors in agro-climatological studies (Anogbro Pascal, 2015; Dekoula et al., 2018; Kouamé et al., 2018; Noufé et al., 2011).

Then, an adapted from Sivakumar's method was applied to rainfall to determine the onset, cessation and length of the growing season in the study area for the period 1991-2022.

- The Onset and Cessation of the growing season are therefore defined for the **long rainy** season as: The long rainy season begins on 01 February when there is at least 20 mm of rain on 1, 2, or 3 consecutive days without a dry spell of more than 7 days in the 30 days following this date. The long rainy season ends on July 1 when there has been no rain for at least 20 consecutive days.
- The Onset and Cessation of the growing season are therefore defined for the **short rainy** season as: The short rainy season is considered to be effective when, from 1st August, the amount of rainfall collected on 1, 2 or 3 consecutive days is at least equal to 20 mm without

a dry spell of more than 7 days in the 30 days following this date. It ends when, from 1st November, there is no rain for at least 20 consecutive days.

- The Lengths of the growing season (LGS): The length of the rainy seasons (long and short rainy seasons) results from the difference between the cessation and the onset growing season dates. These two dates are expressed in Julian days.

The cessation date of the growing season (CGS) is used in combination with the OGS to compute the length of the growing season. At the farm level, it corresponds to the period of harvest. Therefore, information on the CGS is useful for harvest planning activities.

4.2.3.4. Analysis of extremes precipitation indices

Extreme annual precipitation was calculated according to the frequency indices based on percentile thresholds: 95^{th} (R95p) and 99^{th} (R99p) percentile. These heavy precipitations correspond to the events at the tail of the distribution. Percentile thresholds are calculated for a given time period, and the ensuing analysis focuses on the frequency with which these thresholds are exceeded. This technique is following the World Climate Research Program's (WCRP) and World Meteorological Organization's (WMO) standards (Schär et al., 2016; WMO, 2020).

4.2.3.5. Standardized Precipitation Index

The Standardized Precipitation Index (SPI) is a widely used index to characterize meteorological drought on a range of timescales. It's an index based on the probability of precipitation for any time scale (Guttman, 1999; Koudahe et al., 2017; H. Wu et al., 2001). Annual SPIs were derived using the arithmetic mean and standard deviation of the precipitation record to characterize wet, normal, and drought years, which have an impact on seasons and crops. Negative values produced from the model suggest precipitation shortfalls (drought events), whereas positive values indicate normal or excess precipitation (wet events). To compute the SPI, we followed the method provided by McKee Thomas B. et al., (1993). It is computed using the following equation 5:

$$\mathrm{SPI} = \frac{\mathrm{RRi} - \mu}{\mathrm{sd}} \qquad [5]$$

SPI is the index value; RRi is the precipitation for a year i; μ is the average precipitation over the period 1991-2022; and sd, is the standard deviation of precipitation over the base period.

The indices calculated in this work can be summarized in **Table 4-2** according to the WMO Expert Team on Climate Change Detection Monitoring and Indices (ETCCDMI).

Table 4- 2: ETCCDMI precipitation and temperature-related indices used for this study

Indices	Definitions	Descriptions	units
Precipitations			
PRCPTOT	Annual total precipitation	Annual total amount of precipitation cumulated in wet days	mm
CDD	Consecutive dry days	Maximum number of consecutive days with PR<1mm	days
CWD	Consecutive wet days	Annual maximum number of consecutive days with RR≥1 mm	days
OGS	Onset of the growing seasons	Start of the crop growing rainy season	days
CGS	Cessation of the growing seasons	End of the crop-growing rainy season	days
LGS	Lengths of the growing season	Difference between the end and the start of growing season dates	days
R95p	Very rain days	Sum of daily precipitation when PR>95th percentile	mm/days
R99p	Extremely rain days	Sum of daily precipitation when PR>99th percentile	mm/days
SPI	Standard Precipitation Index	Drought periods over the years	mm
Temperatures			
Tx	Maximum temperature	Extreme temperatures on consecutive days	°C
Tn	Minimum temperature	Low-temperatures consecutive days	°C
GDD	Growing Degree days	Daily high and daily low temperature	°C

4.2.3.6. Survey data

During the investigation, a partially pre-coded questionnaire on KoboToolbox was distributed via smartphones and tablets to smallholder yam farmers in the eleven selected areas (see Figure 1). The overall sample size at the end of the survey was 492, all qualitative data. These surveys focused on the causes of rising land surface temperatures, the agronomic and environmental methods and practices used to cultivate yams, farmer vulnerability, and the resilience techniques adopted to cope with climate change. Then, to acquire a better knowledge of all the varied occurrences in this area, an in-depth interview was conducted with ANADER agents. These socioeconomic data were entered and analyzed using Excel 2021 in two ways. The first was descriptive statistical analysis, which allowed us to detect trends reflected in numbers and percentages, and the second was a cross-tabulation of replies based on the breadth of the questions and the goals sought. This method proved useful for describing one or more variables, in particular, the distribution of the attributes they include (Lemessa et al., 2019; Odame Appiah et al., 2018; Sanogo et al., 2023).

4.3. Results

4.3.1 Agro-climatological characteristics of the yam growing season

4.3.1.1 Onset of growing season

The onset growing season dates, for both long and short seasons, vary greatly from one year to the next in the Gontougo region. **Figure 4-2** depicts the interannual variability of season start dates in the region's 5 departments over the study period 1991-2022. The equation lines $Y=ax+b$ represent the average evolution of onset dates over years for the long and short rainy seasons.

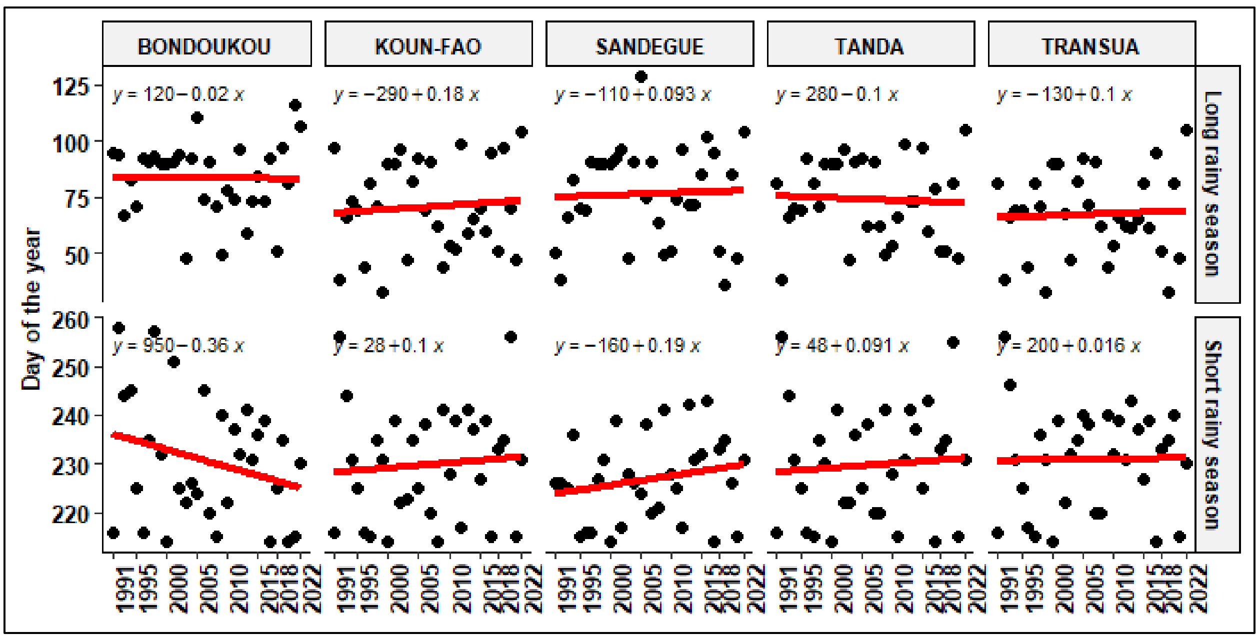

Figure 4- 2: Onset of the growing seasons in the Gontougo region

The lengthy rainy season begins on March 25 for Bondoukou, March 12 for Koun-Fao, March 18 for Sandegue, March 15 for Tanda, and March 9 for Transua. The brief rainy season began on 19 August, 18 August, 15 August, 18 August, and 19 August for Bondoukou, Koun-Fao, Sandegue, Tanda, and Transua, respectively. **Table 4-3** shows these various trends as well as the standard deviation and the Man-Kendall tau.

Table 4- 3: A summary average of the onset season

	BONDOUKOU	KOUN-FAO	SANDEGUE	TANDA	TRANSUA
			Long rainy season		
Mean	25-Mar	12-Mar	18-Mar	15-Mar	9-Mar
StDev (Days)	17	20	22	18	19
M-K tau	-0.002	0.06	0.09	-0.004	-0.006
p-value	1	0.61	0.47	0.98	0.97
			Short rainy season		
Mean	19-Aug	18-Aug	15-Aug	18-Aug	19-Aug
StDev (Days)	13	12	9	12	11
M-K tau	-0.17	0.05	0.16	0.05	0.04
p-value	0.16	0.6	0.2	0.6	0.7

StDev = Standard deviation; **M-K tau** = Mann-Kendall tau

In terms of rainfall probabilities, a frequency analysis of onset dates reveals that in nearly 25% of cases (early years), the seasons began on the 50th day of the year, i.e. around February 20 for the long rainy season, as opposed to the 220th day of the year (around the end of the first dekad of August) for the short rainy season. In contrast, three out of four (75% probability) years in the study region had seasons that began in early April (125th day) for the long rainy seasons and around the third dekad of August (260th day) for the short rainy seasons. **Figure 4-3** illustrates the frequencies of probable onset of rainy seasons over the period 1991-2022.

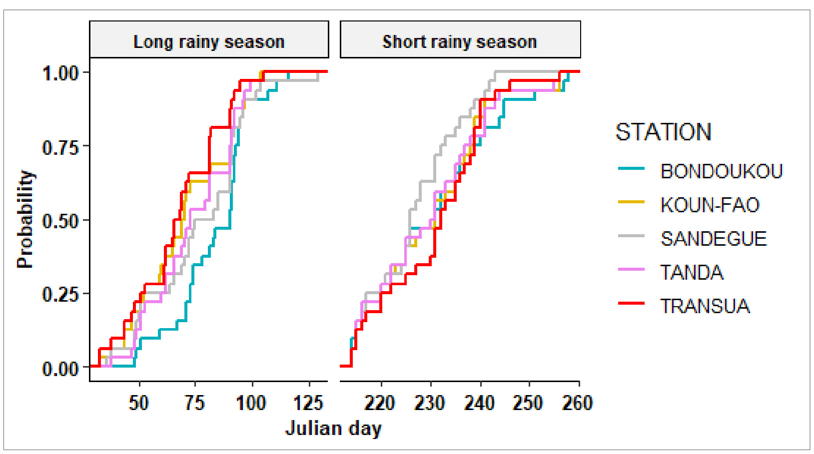

Figure 4- 3: Probability of onset season dates

4.3.1.2. Cessation dates of growing seasons

The average cessation growing season dates for the long rainy season are July 22 to 24 with standard deviations ranging from 8 to 28 days, and between November 20 and 26 for the short rainy season with standard deviations ranging from 10 to 13 days. Besides, a positive Mann-Kendall Tau was observed over the long rainy season in all 5 departments and was more or less negative, tending towards zero for the short rainy season. **Table 4-4** presents the average cessation season dates for the five departments.

Table 4- 4: Average cessation dates of the growing season

	BONDOUKOU	KOUN-FAO	SANDEGUE	TANDA	TRANSUA
			Long rainy season		
Mean	22-Jul	22-Jul	24-Jul	23-Jul	22-Jul
StDev (Days)	8	28	11	6	12
M-K tau	0.6	0.24	0.06	0.29	0.24
p-value	0	0.06	0.6	0.02	0.05
			Short rainy season		
Mean	20-Nov	26-Nov	22-Nov	24-Nov	26-Nov
StDev (Days)	13	11	13	10	11
M-K tau	-0.07	0.05	-0.04	0	-0.12
p-value	0.5	0.65	0.7	1	0.3

StDev = Standard deviation; **M-K tau** = Mann-Kendall tau

Furthermore, an analysis of trends frequency in season-end dates over the last three decades (study period 1991-2022) shows that the end of the long and short rainy seasons most often occurs respectively around the 200th and 340th day (**figure 4-4**).

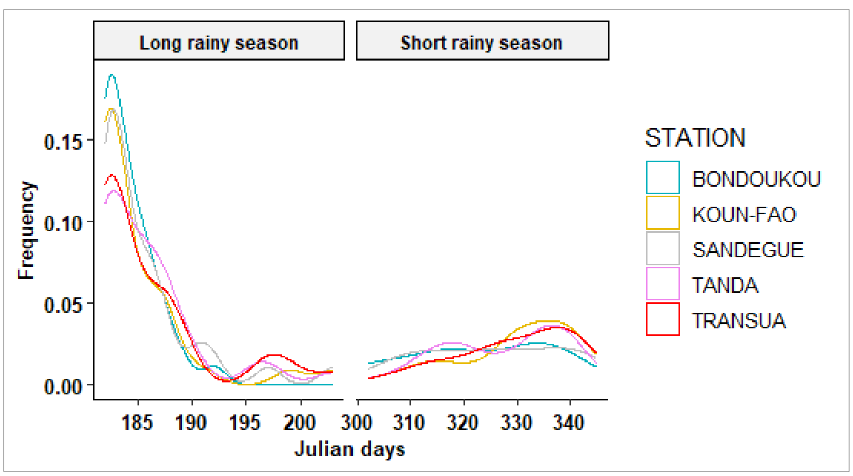

Figure 4- 4: Frequency of cessation dates of the season

4.3.1.3. Length of the growing seasons

Analysis of these outcomes reveals that the length of the growing seasons in the study area varies between 70 and 150 days for the long rainy season, and between 61 and 125 for the short rainy season (**figure 4-5**). In this sequence, there is an average trend with standard deviation variations in the growing season length and M-K tau values that specify different patterns, either reverting or lengthening in **Table 5**.

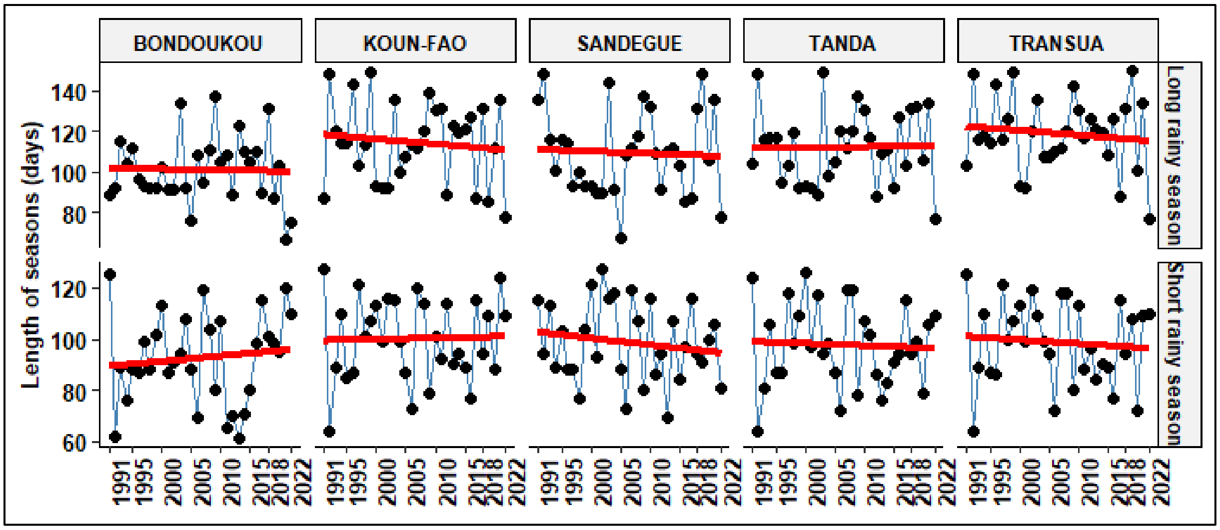

Figure 4- 5: Length dynamics of the growing season

For the long rainy season, the average length of rainfall was between 120 and 135 days, and between 93 and 100 days for the short season, depending on the station (**Table 4-5**). However, trend analysis shows that, except for a few stations, the seasons tend to lengthen (positive M-K tau).

Table 4- 5: Length trends of the growing seasons

	BONDOUKOU	KOUN-FAO	SANDEGUE	TANDA	TRANSUA
			Long rainy season		
Mean (days)	120	132	128	130	135
StDev	19	32	26	20	25
M-K tau	0.22	0	0.004	0.09	0.12
p-value	0.07	1	0.98	0.44	0.32
			Short rainy season		
Mean (days)	93	100	98	97	99
StDev	18	16	15	16	16
M-K tau	0.11	0	-0.1	-0.02	-0.08
p-value	0.3	1	0.4	0.8	0.4

StDev = Standard deviation; **M-K tau** = Mann-Kendall tau

4.3.2. Total seasonal precipitation

Total seasonal precipitation refers to the cumulative amount of precipitation that falls within a specific season over a defined period. It is expressed in millimetres (mm) It can be seen that in the Gontougo region, average seasonal total rainfall varies between 457.4 and 574.3 mm, depending on the station, over the long rainy season. In the same way, the observed M-K tau is negative for all stations with a p-value > 0.05. Over the short rainy season, total seasonal precipitation varied between 386.1 and 441.8 mm, depending on the station. Here, the observed M-K tau is positive at all stations with a p-value > 0.05 (**Table 4-6**). Standard deviations for the two different seasons vary significantly, with up to 100 mm of rainfall depending on the station.

Table 4- 6: Total seasonal precipitation

	BONDOUKOU	KOUN-FAO	SANDEGUE	TANDA	TRANSUA
	Long rainy season				
Mean (mm)	519.9	549.5	457.4	550.3	574.3
StDev	85.8	115.8	114.1	102.5	116.9
M-K tau	-0.06	-0.1	-0.12	-0.12	-0.18
p-value	0.63	0.42	0.34	0.33	0.14
	Short rainy season				
Mean (mm)	386.1	420.6	413.6	437.2	441.8
StDev	100.1	100.6	94.3	108.12	99.5
M-K tau	0.16	0.22	0.18	0.2	0.25
p-value	0.18	0.07	0.6	0.1	0.04

StDev = Standard deviation; **M-K tau** = Mann-Kendall tau

4.3.3. Standard Precipitation Index

The total seasonal precipitation anomaly has been highlighted by the Standardized Precipitation Index (SPI). SPI is a valuable tool for interpreting seasonal precipitation anomalies. It helps quantify and classify the intensity and duration of droughts or wet periods (Guttman, 1999). Positive SPI values indicate above-average precipitation (wet conditions) and negative SPI values indicate below-average precipitation (dry conditions). Over the period 1991-2022, both long and short rainy seasons faced anomalies in rainfall. **Figure 4-6** depicts the trends shown by two colours, red and blue. The red ar the dry period and the blues are the wet period. We can notice that from the year 2010 to the year 2016, SPI < -1.5 over the long and short rainy seasons which corresponds to severely dry. Then, from 2005 to 2010, we observed an SPI > 1.5 in all stations which corresponds to moderately to very wet. Especially, in 2022, the SPI for the short rainy season was negative at all stations, with values ranging from -1.5 to -1.0, indicating relatively dry conditions. In contrast to the long rainy season, where values are relatively positive (-0.5 ≤ SPI ≤ 1.0) at 4 stations Bondoukou, Koun-Fao, Sandegue and Tanda. At the 5th station, Transua, the SPI is negative (-1 ≤ SPI ≤ 0).

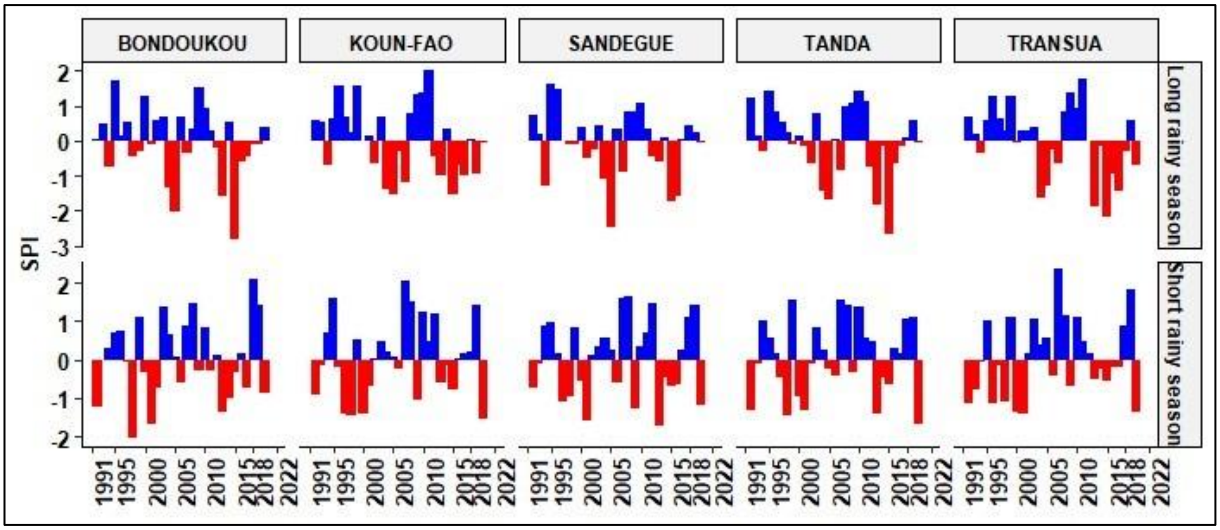

Figure 4- 6: Trends in SPI over the period 1991-2022

4.3.4. Occurrence of rainy days

The occurrence of rainy days was computed to determine the frequency of consecutive rainy days with measurable precipitation from 1991 to 2022. Measurable precipitation typically means any amount of rainfall that can be detected and quantified using standard meteorological instruments, usually defined as at least 0.01 inches (0.25 mm) of rain according to ETCCDMI standards (Klein Tank et al., 2009). This occurrence of rainy days graph (**Figure 4-7**) shows a consistent seasonal rainfall pattern in the short rainy season than in the long rainy season. We can see that the peaks are observed in approximately 5% frequency over the Bondoukou, Koun-Fao and Tanda stations during the short rainy season over two consecutive decades. Whereas during the long rainy season, only around 4% rainfall frequencies are observed over a decade for the Bondoudoukou and Transua stations.

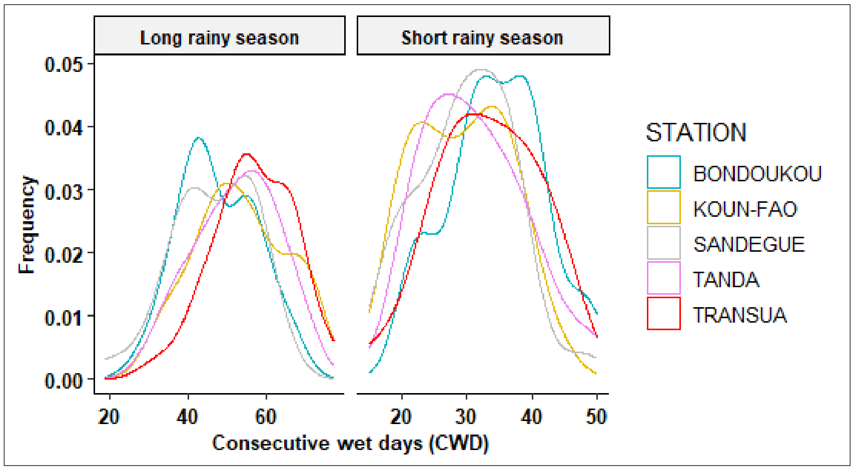

Figure 4- 7: Occurrence of rainy days

4.3.5. Extreme rainfall events (R95p, R99p)

The frequency and intensity of precipitation days relative to the ETCCDMI climatological norm represented by indices R95p and R99p were computed to determine extreme rainfall events in the study area from 1991 to 2022 (**Figure 4-8**). At the 95th and 99th percentile, precipitation ranges respectively from 20 to 35 mm, and from 30 to 50 mm, with an evolving frequency up to 1 for both percentiles. Extreme rainfall on either side occurs at a frequency ranging from 0.75 to 1 throughout long and short rainy seasons. Extreme rainfall was reported in the Koun-Fao, Tanda, and Transua stations in the 95th percentile, whereas the most extreme occurred at each of the five stations that recorded more than 50 mm of rain in one day, with a frequency of 1 in the 99th percentile.

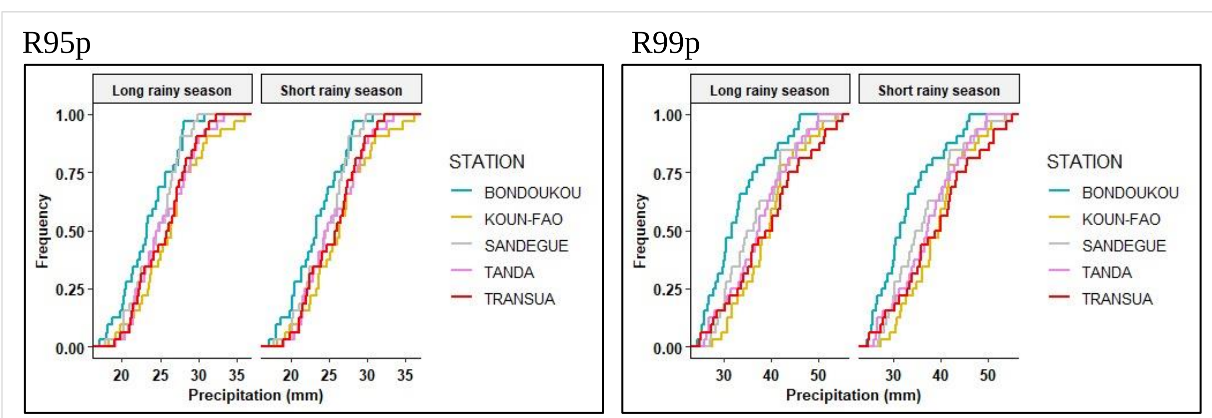

Figure 4- 8: Distribution of percentile R95p and R99p

4.3.6. Occurrence of intraseasonal dry periods

Dry spells during the rainy season are mentioned in numerous studies (Agbazo et al., 2021; Ibrahim et al., 2022; Kouamé et al., 2018) as a key factor hindering crop growth. The impact of dry spells on crops depends on their period of occurrence during the growing season, as well as their duration and frequency. In the growing season, drought frequency is most intense in the first 10 days, reaching 0.15 at the Bondoukou station and around 0.10 at the Koun-Fao and Sandegue stations in the long rainy season. In the short rainy season, the first two weeks of the growing season are considered critical, with drought frequency reaching 0.05 at each of the 5 stations. In terms of the occurrence of dry spells, Bondoukou station recorded the highest peak corresponding to a frequency of 1 over the long rainy season. This occurred on the second consecutive dry day. Similarly, the Sandegue and Koun-Fao stations recorded peaks on the second consecutive dry day, with 0.50 dry intensity. Over the short rainy season, peaks corresponding to the Tanda and Sandegue stations were observed only between the second and fourth consecutive dry days, with a 0.50 intensity (**Figure 4-9**).

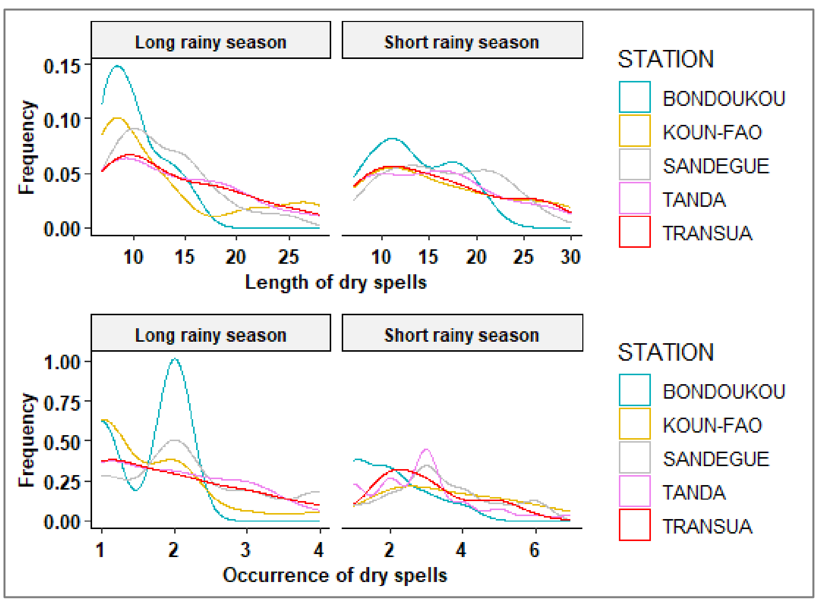

Figure 4- 9: Distribution of dry spell frequency

Analysis of the key agro-climatological parameters affecting yam cultivation led us to investigate yam farmers' perceptions of growing conditions and the adaptive methods they adopt to deal with various climatic issues they face.

4.3.7. Profile of respondents

The survey was conducted in the Gontougou region, mainly in the departments of Bondoukou, Koun-Fao, Tanda and Transua (**Table 4-7**). A total of 492 respondents were surveyed, including 100 women and 392 men. Note that the percentage of people surveyed was 54.07% in Bondoukou.

Table 4- 7: Profile of people surveyed

Departments	**Female**	**Male**	**Total population**	**Percentage**
Bondoukou	40	226	266	54.07
Koun-Fao	10	26	36	7.32
Tanda	7	52	59	11.99
Transua	43	88	131	26.63
Total respondents	**100**	**392**	**492**	**100**

3.8. Agronomic practices and yam growing circumstances

The Gontougo region in Côte d'Ivoire is known for its agricultural activities, particularly yam cultivation as a staple food. Climatic uncertainties and local environmental conditions hinder its production. The population facing these difficulties were surveyed to find out how they adapt. Here is an overview of the agronomic practices and yam growing circumstances in the region.

4.3.8.1. Yam harvest cycle per variety

In the Gontougou region, several species of yam are grown, depending on soil type and, above all, on the crop cycle. Species produced in the region include: "Bètè bètè, Florido, Kponan, Krenglè, Assawa, Lokpa, Païté, Azaguié and others including Kokoasse, Anader, Kokomssené, Afassiè and Kamgba" (**Figure 4-10**). From planting to harvest lasts between 6 and 12 months, depending on the species. Unanimously, over 40% of the region's population grows '*Païté*'. Its growing cycle lasts 8 months. After Païté, *'Florido'*, *'Bètè bètè*' and '*Kponan*' are the most widely produced, each accounting for more than 10%.

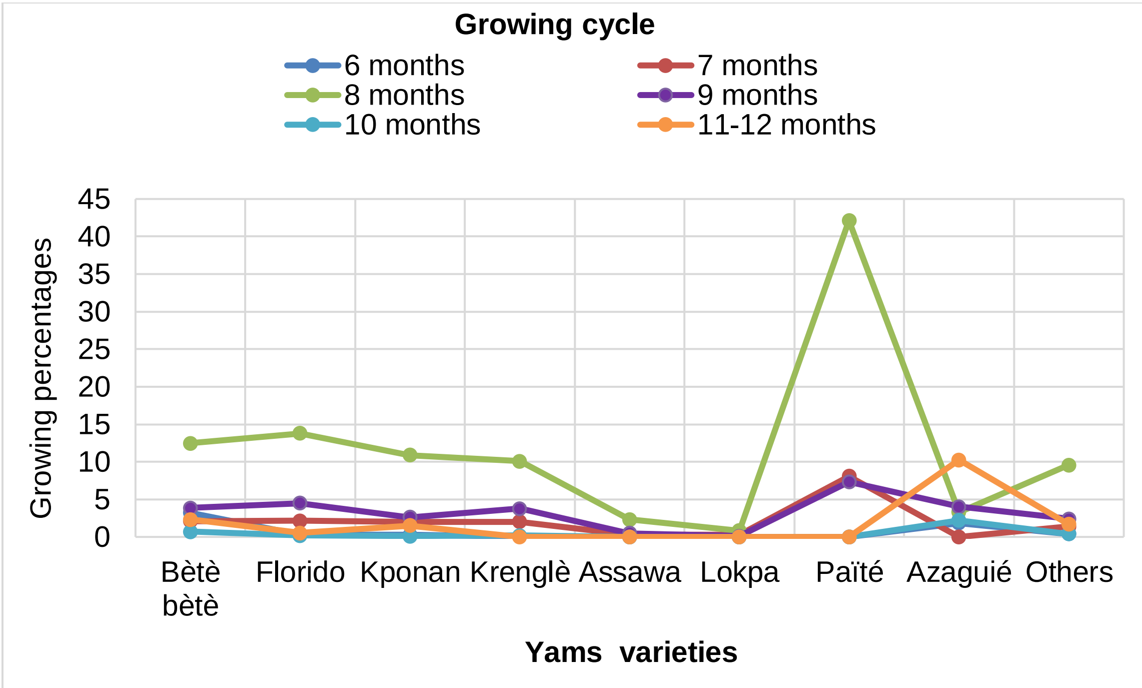

Figure 4- 10: Length of the yam growing cycle according to the varieties grown

NB: Other species include *"Kokoasse, Anader, Kokomssené, Afassiè and Kamgba"*

4.3.8.2. Yam growing method

Yam cultivation methods are traditional techniques inherited from the local population. According to our surveys, populations adopt either slash-and-burn, intensive, extensive or rotational cultivation. Most people who practise rotational cropping or fallowing let the previously cultivated plots rest for a year before planting the new crop. In short, slash-and-burn cultivation is dominant in Transua, with over 95%. In Bondoukou and Tanda, extensive cultivation accounts for over 85% and 70% respectively. In Koun-Fao, rotational cropping is dominant at 50%, followed by intensive cropping at over 30% (**Figure 4-11**).

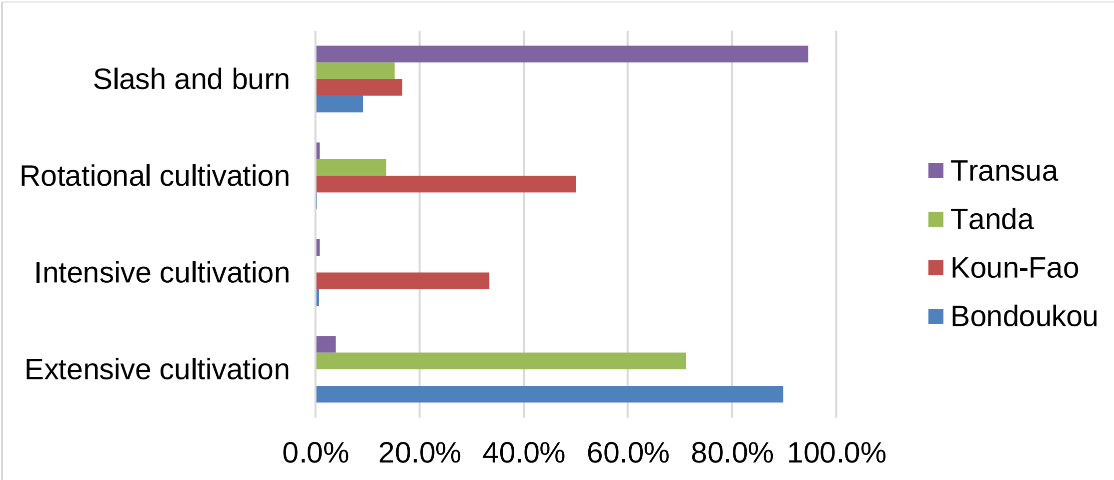

Figure 4- 11: Farming methods by department

4.3.8.3. Mounding and yam planting moment

Good crop yields depend on the production period. By production, we mean the preparation of the soil, the mounds, the moment when the yam is put into the mounds, and the harvest. In the Gontougo region, mounds are made between November and May. Specifically, Bondoukou farmers do for them in November and December. Those in Tanda prefer March, April and especially May when more than 50% of them do so. Farmers in Transua and Koun-Fao make their mounds in March and April. Then, very few yam farmers make their mounds in January and February. Of these, 50% put the yam in the mound a month or more after mounding. Among those who make the mounds in March, April and May, most of them put the yam in the mound on the same day. For those who do it in November and December, more than 40% of farmers prefer to wait for heavy dews caused by the harmattan, and around 60% prefer to wait a month before putting the yam in the mound (**Figure 4-12**). The reasons for these different practices are motivated by personal experiences that have been collected and represented in **Figure 4-13**. According to this figure, 37% of yam farmers adopt the practice of mounding the yam seed to prevent it from rotting and 24% do so to reduce the temperature in the mound before planting the yam seed.

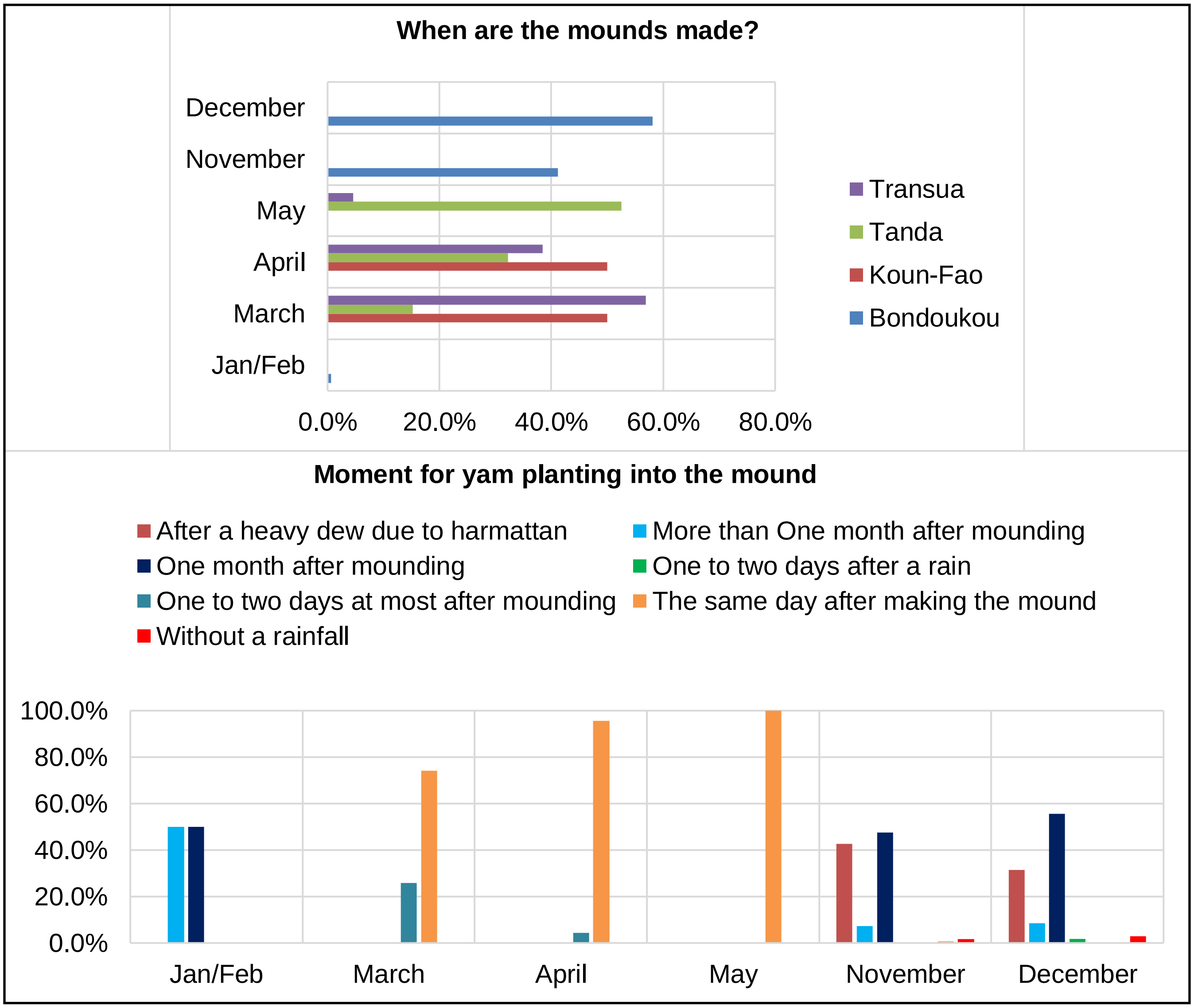

Figure 4- 12: Time of yam planting according to the month in which the mounds are made

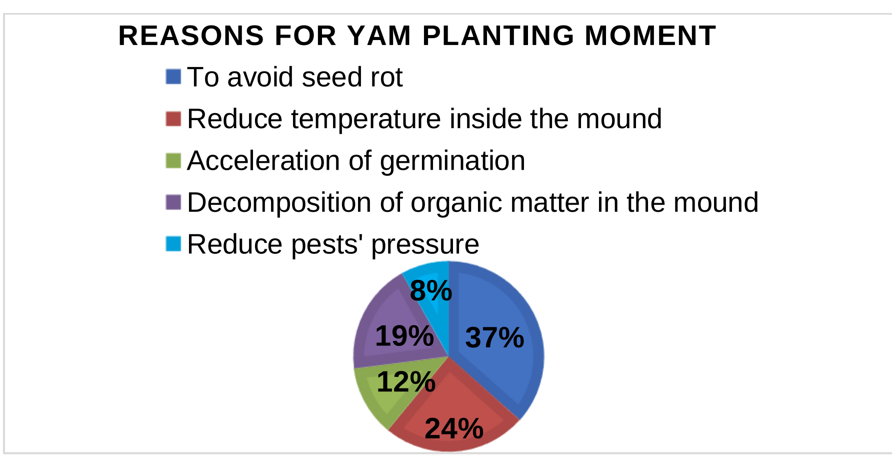

Figure 4- 13: Reasons for mounding yam seeds

4.3.8.4. Yam farming environment

The type of environment in which the yam is grown is very important for its success. In the Gontougo region, 90% of the Bondoukou population grows yam in association with cashews, and around 60% under shrub savannah zones. In Koun-Fao, more than 80% of the population prefers shallow areas, with a few in forest land. In Tanda, yam farmers mainly opt for wooded or tree savannah (75%). Finally, in Transua, fallow dominates at 60% (**Figure 4-14**).

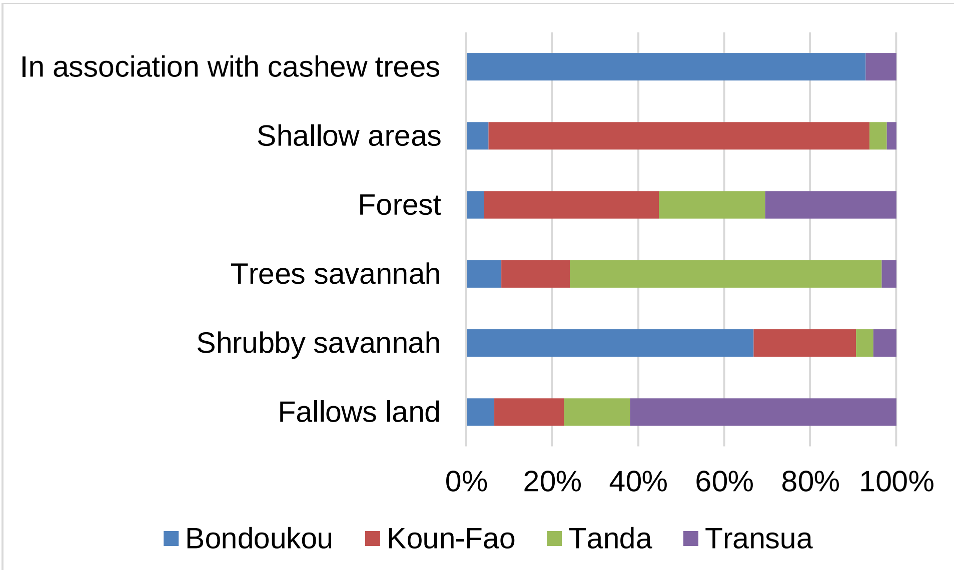

Figure 4- 14: Yam growing environment by department

4.3.9. Understanding the increasing causes of vegetation loss in yam-producing area

Agriculture is a source of deforestation and leads to land surface temperatures (LST). We demonstrated this in one of our investigations in the Gontougo region: “The decline in vegetation cover driven by agricultural expansion in the study area substantially increases the LST” (Aka et al., 2023). As a result of this study, we found that forests lost 62.19% of their area in 2022. It’s to find out more about this phenomenon, we have conducted this study to discover the real causes of deforestation. It can be seen in **Figure 4-15** that in the Bondoukou department, cashew nut production (25%) and logging (over 15%) are at the root of deforestation. In Transua, it is the drying up of vegetation at over 25%, in Tanda, also logging at 10% and around 5% for the expansion of the savannah at Koun-Fao.

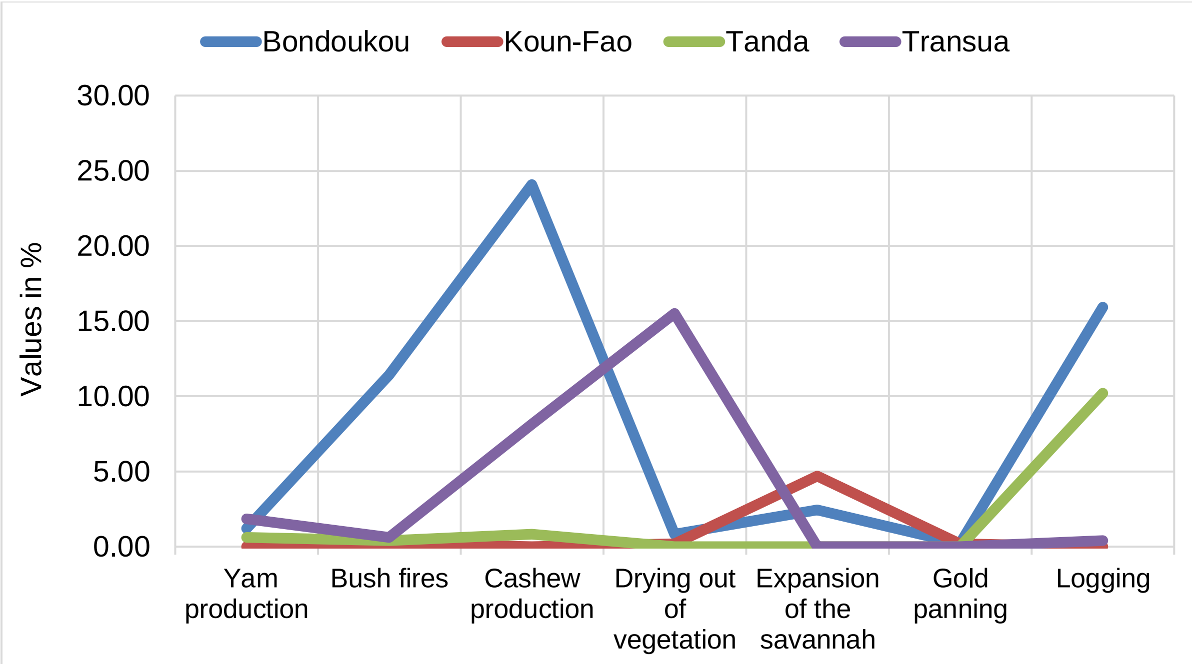

Figure 4- 15: Causes of vegetation loss per department

4.3.10. Impact of Land Surface Temperature and climate variability on yam growing

Land surface temperature is the cumulative effect of land use land cover (LULC) change and global atmospheric warming (Aka et al., 2023). Its impact on yam cultivation is many. According to our survey, it delays bud growth (25.50%), rots the yam seed (24.69%), slims down tubers (20.23%), compacts and reduces soil porosity (12.06%), inhibits microorganism's actions in the soil (9.42%) and increases pests in the mound (8.10%). According to the surveyed people, high surface temperatures are harming yam production throughout the region. The effects are felt most in Bondoukou, with a percentage of 92.48%. Only in Tanda were the effects felt less with 61% (**Figure 4-16**).

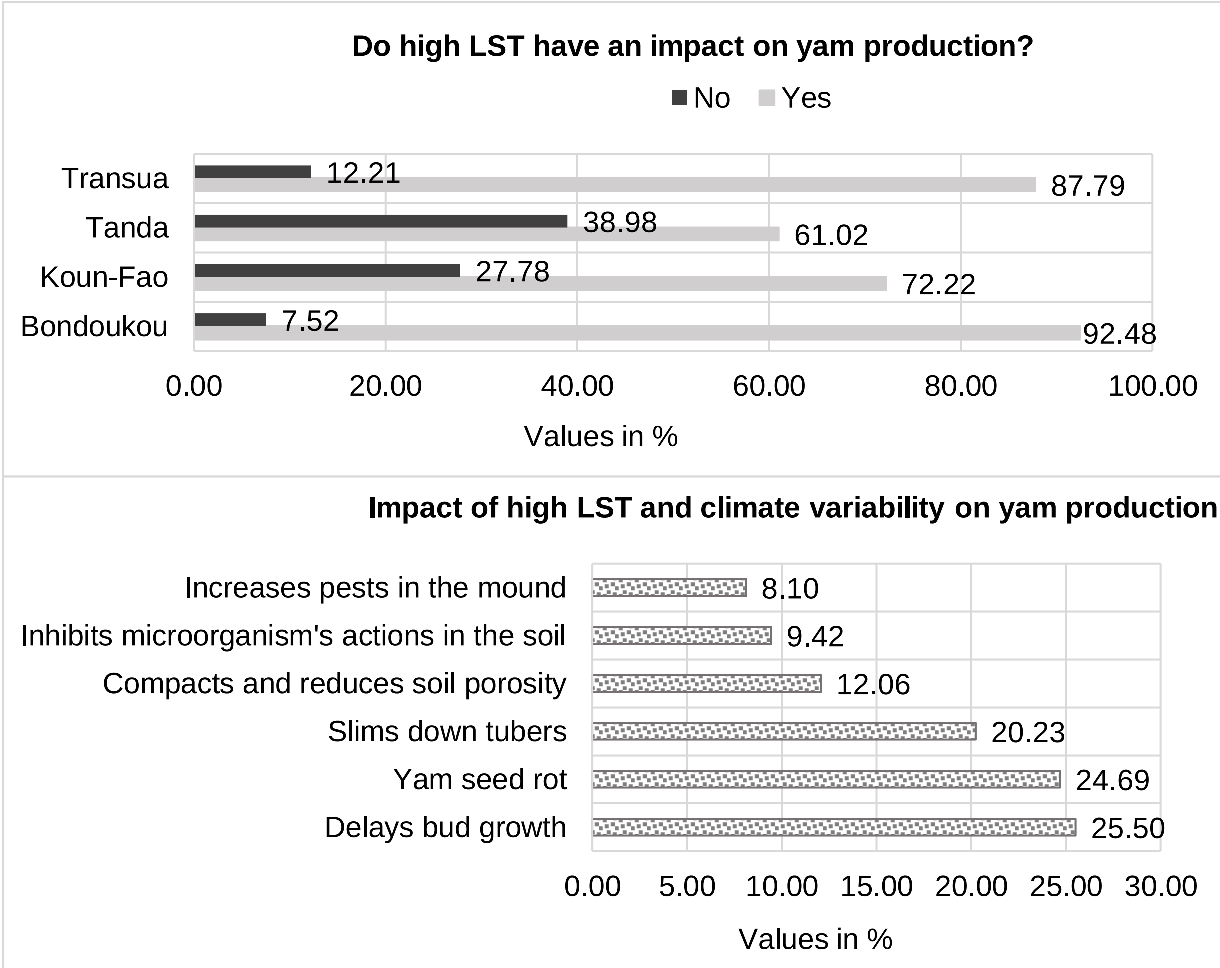

Figure 4- 16: Impact of land surface temperature and climate variability on yam growing

4.3.11. Yam farmer's adaptative responses

Several adaptive solutions enabling people in the Gontougo region to be climate resilient were highlighted. The people interviewed revealed that they adopt specific agricultural practices associated with expert agronomic techniques in response to climate hazards and to prevent crop failure (**Figure 4-17**). These techniques are mainly related to SODEXAM weather forecasts (1.63%), CNRA agricultural advice (2.44%), ANADER farming practices (46.54%), and endogenous knowledge combined with traditional habits (49.39%). The greatest concern of the population, which is adopted as a solution to avoid high land surface temperatures and their impact is to master the rainy season (24.39%) and also to control the growing season of yam species to be cultivated (20.33%). Similarly, most of the respondents felt that diversification of agro-economic activities (20.73%) was the best way to prevent crop failure. For others, it is important to diversify the yam species to be grown to avoid any nasty annual yield (17.89%).

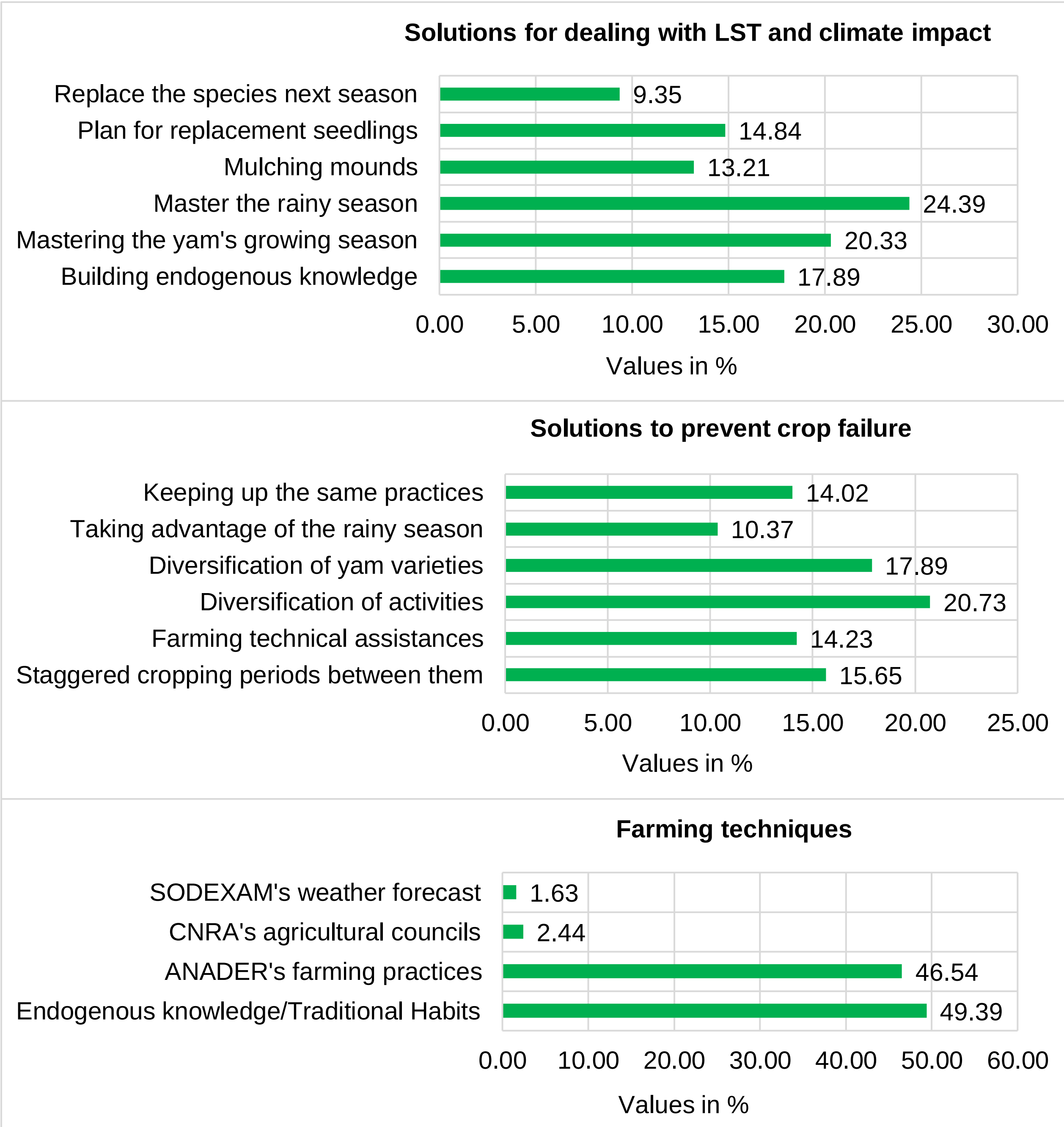

Figure 4- 17: Yam farmer's adaptative response to climate hazards

4.4. Discussion

4.4.1. Analysis of agro-climatological characteristics related to yam growing

Agricultural activities in Côte d'Ivoire are heavily reliant on the rainfall pattern. As a result, irregular rainfall has undeniable repercussions on crop production. The Gontougo region in eastern Côte d'Ivoire, which is a mixed (forest-savannah) and bimodal zone with two rainy seasons (one long and one short), is naturally impacted by the North's unimodal regime due to its geographical proximity. This shifting rainfall pattern makes executing the region's numerous agricultural campaigns difficult. The start date of the rains and the length of the growing season are two critical elements for agricultural operation planning because they govern, on the one hand, when to make mounds or sow seeds, and on the other, how long crops can benefit from consistent rainfall (Kouamé et al., 2018; Waongo, 2015; Y. Wu et al., 2023). Analyzing the onset and cessation of the growing season in the five departments from 1991 to 2022 allowed us to establish the average dates of rainy periods and identify rainfall irregularities in the region. On average in the 5 départements, the onset dates of the long rainy season were observed between the first and last decade of March, precisely between March 09 and March 25. As for the short rainy season, the average start dates were mainly around the second decade of August, between August 15 and 19. Respectively, the cessation dates for the long rainy season are July 22 to 24 and 20 to 26 November for the short rainy. Other studies in Côte d'Ivoire, particularly on the impact of rainfall variability on the growing season in the cotton production area (Dekoula et al., 2018) and on the characterisation of the key agroclimatic parameters of the growing season in forest-savannah contact zones (Kouamé et al., 2018) have found similar results for onset and cessation dates of the growing seasons in their research for bimodal zones. This supports our findings. However, a series of rainfall abnormalities throughout the growing season caused early starts and late endings in the Bondoukou, Tanda and Transua departments, as well as late starts and late ends in the Koun-Fao and Sandegue departments for the long rainy season, between 1991 and 2022. This explains the Mann-Kendall Tau values, which were either positive or negative within the same time period. Several scholars believe that rainfall's start and end dates are essential elements in the tropical agricultural cycle. This is especially important given that climatic variability is predicted to cause significant changes in many parts of the planet. These changes are expected to have an impact on the onset and cessation of the rainy season (and consequently the length of crop's growing seasons), which has been increasingly unpredictable in recent years (Danquah et al., 2022; Mosunmola et al., 2020; Noufé et al., 2011). By studying total seasonal precipitation, extreme rainfall events

(R95p, R99p) and the occurrence of intraseasonal dry spells in the Gontougo region, we have identified the main factors of climate variability likely to harm agricultural production, particularly yam crops. A recent study by the Intergovernmental Panel on Climate Change (IPCC) highlights these impacts in its sixth assessment report (IPCC, 2022). According to the IPCC, "climate change, including increases in the frequency and intensity of extreme events harmed food security and terrestrial ecosystems, and has contributed to desertification and land degradation in many regions". The UN Food and Agriculture Organisation (FAO) also notes that climate variability and extreme events are among the main causes of serious food crises. The FAO report "The State of Food Security and Nutrition in the World 2022" (FAO et al., 2022) explains how climate-related disasters are exacerbating food insecurity and malnutrition around the world. In the Gontougo region, our research shows that total seasonal precipitation varies between 457.4 and 574.3 mm over the long rainy season and between 386.1 and 441.8 mm over the short rainy season, depending on the stations. This gives an annual total cumulative rainfall of around 1016.1 mm over the long rainy season. Studies by Kouamé et al., (2018) show that the cumulative seasonal rainfall for regions above the 7th parallel in Côte d'Ivoire with four seasons, i.e. two dry seasons and two wet seasons, taking Bouake and Beoumi as examples, which are also major yam-producing areas, varies between 445 and 499 mm for the long season and between 359 and 401 mm for the short season. These findings corroborate our investigations. Furthermore, yam cultivation, depending on the species, is more successful in agroclimatic zones where rainfall is between 900 and 1500 mm per year (Adifon et al., 2019, 2020; Neina, 2021). This is why it is widely produced specifically in the central, northern and eastern regions of Côte d'Ivoire.

In addition to all these factors, it should be noted that the Gontougo region experiences both dry and wet rainfall fluctuations. This is highlighted by the SPI calculation, which shows that from 2010 to 2016, there was a severe drought. Then, from 2005 to 2010, we observed a moderate to wet season. In particular, in 2022, relatively dry conditions were reported over the short rainy season at all stations. According to several agricultural studies on households, the SPI highlight the impact of climate variability on agricultural productivity over time, contributing to the development of resilient agricultural practices (Giannini et al., 2021; Sultan et al., 2015, 2019; Yimam & Holvoet, 2023). Then By identifying periods of water scarcity, SPI aids in managing water resources more efficiently, ensuring adequate supply for crops and livestock (Sanogo et al., 2023). It provides insights into seasonal precipitation patterns, aiding in the selection of suitable crops and planting dates to match expected moisture conditions (Ibrahim et al., 2022; Waongo, 2015). As for the dry spell frequency, it’s a key factor hindering crop growth. In the region, Bondoukou station had the highest peak, equal to a frequency of one, during the long rainy season. This happened on the second successive dry day of the growing season. According to Waongo’s optimizing planting date study (Waongo, 2015; Waongo et al., 2015) Dry periods occurring after crop planting time are critical meteorological indicators for agricultural management. Dry spells may be both beneficial and detrimental to rainfed agriculture. Farmers can use them to execute field activities including mounding, planting, weeding, fertilizer application, and harvesting. Concerning Extrem rainfall events, days with moderate extreme rainfall (above the 95th percentile) are becoming increasingly frequent at Koun-Fao, Tanda, and Transua stations, suggesting changes in weather conditions that may lead to increased risks of flooding. Research has also shown that occasional peaks (99th percentile) may indicate sporadic but extremely intense rainfall in the region. A steady increase could indicate a move towards more severe weather conditions. Understanding and interpreting these indices helps to assess the impacts of climate change, plan flood management and prepare for the potential socio-economic impacts of extreme weather events (Ibrahim et al., 2022; Schär et al., 2016).

4.4.2. Yam production conditions and farmers' adaptation response analysis

Climate variability is one of the leading natural threats and a root cause of food insecurity in developing countries. In Côte d'Ivoire, we assist a loss of yam yield every year whereas it’s the most widely grown food crop. According to FAO statistics, yam's total production volume was around 7,600,000 tonnes in 2022 in Côte d'Ivoire (https://www.fao.org/faostat/en/#data). The Gontougo region is one of the major producing areas, with around 90,000 tonnes/year in 2022, according to Bondoukou’s and Tanda’s ANADER service. So, to find out and address production conditions, cropping methods, production-related challenges and adaptive measures, a survey of yam farmers in the region as mentioned above has been conducted. The survey revealed that the species called '*Païté*' is widely grown in the region and lasts eight months to be harvested. The mounding periods vary per department, ranging from November to May. Everyone starts planting based on their own meteorological and traditional knowledge. The most common reason reported for this (37%) is to avoid the rotting of the yam seed to be planted. Most yam farmers slash and burn before cultivation, but it is extensive cultivation that is dominant in the region. Indeed, every year, farmers transplant cashew nurseries while the yam is growing. As a result, even rotational cropping, where they leave the fallow land to rest and return to it at least a year later, is starting to drop because of the widespread cultivation of cashew nuts. According to Aka et al.'s, (2023) research on land use land cover (LULC), perennial crops, particularly cashew plantations, are the most common LULC type in the Gontougo region. It takes up more than 60% of the study area. Furthermore, it states that from 2015 to 2022, the LULC shift resulted in the loss of 48.13% and 65.14% of forest and annual crop areas, respectively, in favour of cashew plantations. Surveyed populations and ANADER both told us that in locations where long-term fallows are no longer practicable owing to land pressure, yam production has dropped dramatically or mutated into something more rustic and unsuitable for pounded yam, maybe leading to crop abandonment. This production has also been firmly incorporated into the market economy, transitioning from a food crop to a cash crop, with some exports to neighbouring countries. As a result, abandonment or fall in production in specific locations of Cote d'Ivoire causes food insecurity and economic loss for farmers.Yam farmers have discovered that to adapt, they must plant yams in a variety of environments, particularly in conjunction with cashew trees, in lowlands, and, of course, in the savannahs and woodlands that are still available. These same concerns have led to the implementation of improved fallows in Benin and Ghana, which utilize shrub and herbaceous legumes (*Aeschynomene histrix*, *Mucuna pruriens var utilis,et Gliricidia sepium*), and the use of NPK fertilizers, and fallow rotations with a combination of plant species (*Andropogon gayanus-yam*, *Mucuna pruriens var utilis/ maize*, *Aeschynomene histrix/ maize*) to address the issue of reducing surface areas allotted for yam farming (Adifon et al., 2019, 2020; Felix et al., 2020; Owusu Danquah et al., 2022). Later on, the land surface temperatures (LST) and climate uncertainties were the two main issues mentioned by the yam farmers when discussing production losses. The impacts of LST, climate uncertainties and seasonal variability on yam production in the Gontougo region are multiple. These include the delays of bud growth, rots of the yam seed, slims down tubers, compacts and reduces soil porosity, inhibits microorganisms' actions in the soil and increases pests in the mound. Many studies (Adeleke Aturamu et al., 2021; Adifon et al., 2020; Owusu Danquah, Danquah, et al., 2022; Srivastava et al., 2012) state that agroclimatic factors whose management and control are essential to optimum agricultural production for rainfed crops like yam include the characteristics of the growing season, the distribution of rainfall during the vegetative cycle, the air temperature and the consecutive dry periods throughout the production cycle especially after the planted tuber seedlings emerge from their mounds. On this point, we discussed with many different organizations of yam farmers, and they expressed their perceptions to us. All these yam “farmer's organizations in the Gontougo region recognise the impacts of climate variability on their yam crops, particularly the challenges posed by irregular rainfall, prolonged dry spells and rising temperatures. However, there is often a gap between this awareness and the adoption of adaptive practices. Limited access to information, resources and agricultural extension services hampers the widespread implementation of modern, climate-resilient techniques. Despite these difficulties, they continue to value yams for their cultural significance economic importance and nutritional values”. Besides this viewpoint, other solutions were also highlighted during the survey. In terms of responses to LST and climate variability, they agreed that mastering the rainy season linked to the yam growth cycle and the strengthening and practising of endogenous knowledge are the primary ways to mitigate their effects. Second, most yam farmers stagger their planting periods, vary the varieties of yams they grow, and diversify their socio-economic activities to prevent crop failure. Finally, ANADER trains them in endogenous knowledge-based adaptive farming techniques. A study similar to ours has come to reinforce our statements and declares that farmers are also adopting behavioural and infrastructural strategies to deal with hazards that threaten their food security (Njoya et al., 2022). This is correspondingly in line with other results found in the academic literature (Ema et al., 2023; FAO, 2015; Faye et al., 2023) indicating that endogenous and technical and/or infrastructural responses are mostly common to cope with farmers' vulnerability to climate. The use of measures such as improved seeds, crop diversification, improved fallow lands, optimization of planting date and early warning systems are also reported in many studies in Sub-Saharan Africa (Abubakar et al., 2021; Adifon et al., 2019; Giannini et al., 2021; Harouna et al., 2019; Waongo et al., 2015; Zeleke et al., 2023) as farmers’ adaptive responses.

4.5. Conclusion

The study introduces an integrated framework that evaluates key agro-climatological characteristics, agronomic practices and adaptive responses of smallholder yam farmers in the Gontougo region in Côte d’Ivoire. By incorporating both climate analysis and local knowledge through a survey, the study sheds light on key findings about yam production that have important implications for future research and practical applications for yam farmers. The findings underline the importance of understanding and using weather information while cultivating yam crops and farmers' adaptive reactions to the threats they meet. It should be noted that yam is a rainfed crop, and we demonstrated that in the Gontougo region, almost 25% of the time (early years), the growing season began around the 50th day of the year, i.e. around 20 February under the long rainy season, compared to the 220th day of the year (around the end of the first decade of August) under the short rainy season. Furthermore, the typical cessation of the growing season is July 22 to 24 during the long rainy season, and November 20 to 26 during the short rainy season. Regarding perceptions, surveyed people stated that high land surface temperatures due to the decline of vegetation and climate uncertainties are harming yam production. The effects are felt most in Bondoukou, with a percentage of 92.48%. Only in Tanda were the effects felt less with 61%. In terms of growing methods, the most dominant is extensive cultivation, practised more than 90% in Bondoukou. As a result of this practice, farmers used to cultivate perennial crops, particularly cashew nuts, which replace yams on the same plot after harvesting. From then on, fallowing is unusual, and crop rotation on the same plot is rapidly reducing. The end effect is a reduction of natural plant resources, local biodiversity, and depletion of soil fertility. Besides, ANADER's technical services train farmers in agricultural techniques that are resilient to climate hazards and adaptive to different types of production environments, based on endogenous and experimental knowledge to improve yields. In brief, farmers in the Gontougo region mainly use traditional farming methods to grow yams. These practices include manual soil preparation, the use of organic matter (such as farmyard manure) to improve soil fertility, and planting yams in mounds or ridges to improve drainage and aeration. Crop rotation and fallowing are also commonly used to maintain soil health and reduce the incidence of pests and diseases. However, increasing pressure on land due to population growth has led to shorter fallow periods, which, combined with limited access to modern inputs such as fertilisers and improved seed varieties, has resulted in lower yam yields over time. Moreover, it is worth noting that farmers' perceptions of yam production and climate change are crucial in shaping their farming practices. Despite these difficulties, farmers continue to value yams for their cultural significance, economic importance and nutritional values and express a strong desire to be supported in accessing improved technologies and knowledge that could help them mitigate the effects of climate change on their production. Through this study, we are drawing the attention of decision-makers, researchers and politicians to the need to prioritize yam farming, which is a significant pillar in the fight against food insecurity.

CHAPTER 5: ANALYZING FUTURE TRENDS IN CLIMATE CHANGE ON YAM YIELDS

5.1. Introduction

Considering climate change-induced risks that make farmers highly vulnerable and reduce yield, simulating scenarios and crop yields using models can help farmers enhance productivity, forecast the growing season, adopt adaptive measures, and be more resilient (Fayaz et al., 2021; Malhi et al., 2021). Very few studies exist aiming to understand the future of yam growing in Côte d'Ivoire by predicting yields. One of the extant investigations on the issue in the literature is the World Bank's (World Bank Group, 2019) using the International Model for Policy Analysis of Agricultural Commodities and Trade (IMPACT model), discovered in Côte d'Ivoire that the percentage point difference in yield and the area harvested with different levels of climate change for yams will be lowered negatively in yield under RCP4.5 and RCP8.0 respectively, and increased in area harvested in the same RCP for 2030 and 2050. Thus, it would be interesting to examine the dynamic of yam yields using an agronomic model. Crop models are collections of mathematical equations that depict activities inside a specific plant system and interactions between crops and their surroundings (Adeleke Aturamu et al., 2021; Khan et al., 2023; Leng & Hall, 2020; Liu et al., 2021; C. Müller et al., 2024). Despite these models still simplified approximations of reality, the complexity of agricultural systems and the remaining knowledge gaps make it hard to explain complete crop system operations in mathematical terms (Cedric et al., 2022; Jones et al., 2017; Khan et al., 2023; Wallach et al., 2014). In this study, we applied the statistical model of Multiple Linear Regression (MLR) to model yam yields. MLR is a statistical prediction test used to estimate the value of one dependent variable using multiple (at least two) independent variables (Khan et al., 2023). This is the fundamental principle of regression, which allows us to identify the relationship between several independent variables and a dependent variable. MLR involves establishing a linear relationship between the dependent and independent variables (Hastie et al., 2017; Heumann et al., 2016; Khan et al., 2023). The MLR technique involves prior identification of the variables required by the model, which we carefully determined using Sivakumar's method (Sivakumar, 1988). Its approach is based on agro-climatological characteristics and was deemed the best designed to be adapted to the specific case in our study area. The method was developed for forecasting rainy seasons in five different West African countries, namely Burkina Faso, Niger, Mali, Senegal, and Chad, and was also applied in different agro-climatological studies on Côte d'Ivoire (Anogbro Pascal, 2015; Dekoula et al., 2018; Kouamé et al., 2018; Noufé et al., 2011). Unlike our approach, previous research, like the World Bank study cited above, employed a dynamic agricultural model (IMPACT model), which required various sources and types of data to be obtained in situ through experimentation and used for model calibration, training, and validation. Employed in many prediction studies, the MLR is more suitable when field observation data are sometimes lacking. It requires less data than the dynamic agricultural model and enables future modelling using current trends and outcomes (Mosunmola et al., 2020; Pokona et al., 2021; Setiya et al., 2023). These are the reasons why we used it, as there is a lack of genuine field and observation data in the region, which is one of our investigation's shortcomings. This is where our work differs from earlier studies employing the IMPACT model, which were conducted at the national level and used a variety of crops, including yam. Our research is local (Gontougo region) and focuses on a particular crop, yam. Furthermore, for future prediction, we use updated scenario data known as Socio-Economic Shared Pathways (SSP) from the sixth report of the Intergovernmental Panel on Climate Change (IPCC AR6), as opposed to the previous study's Representative Concentration Pathway (RCP) from the fifth report of the IPCC (IPCC AR5). The SSP scenarios are part of the international Coupled Model Intercomparison Project 6 (CMIP6) of the World Climate Research Programme (WCRP) that comprises a new set of scenario runs for the 21st century. They represent different socio-economic developments as well as different pathways of atmospheric greenhouse gas concentrations (IPCC, 2023a; Mackallah et al., 2022; Weijer et al., 2020). The SSP scenarios are based on five narratives that depict various societal development paths: SSP 1, SSP 2, SSP 3, SSP 4, and SSP 5 (IPCC, 2023a; Zhou et al., 2023). SSP1 titles the sustainable and "green" pathway describes an increasingly sustainable world; SSP2: The "Middle of the road" or medium pathway extrapolates the past and current global development into the future; SSP3: Regional rivalry; SSP4: Inequality; and SSP5: Fossil-fueled Development (IPCC, 2022). Using the SSP 2 and SSP5 and agro-climatological characteristics, this study assesses the interactions between the different parameters and agricultural seasons on yam yields in the Gontougo region in Côte d'Ivoire in order to identify the agroclimatic factors that have the greatest negative impact on yields in the area. This will then be followed by predicting future yam yield trends under climate change scenarios.

5.2. Methodology

5.2.1. Data descriptions

5.2.1.1. Climate observations data

The meteorological observation data comprises precipitation and temperature variables (maximum and minimum temperature) and were extracted over the historical study period 1981-2010. These data were used to assess agro-climatological hazards and provide support for climate projections data in the research area. These are Rainfall Estimates from Rain Gauge and Satellite Observations (CHIRPS) data (https://www.chc.ucsb.edu/data/chirps), which are gridded data with high spatial resolution (0.25°*0.25°, i.e. approximately 25 km) obtained by a combination of satellite data and in situ observation data (Funk et al., 2015; Georganos et al., 2017). Then NASA Power temperature data (Tmax & Tmin) (https://power.larc.nasa.gov/data-access-viewer/), which are horizontal resolution gridded data, were re-sampled to 0.25°*0.25° (25 km). These data are used by several authors (Kouman et al., 2022; Laux et al., 2021; Salack et al., 2015) as part of studies in the absence of observational data. The choice of these data is justified by the lack of continually updated information over a long period from the meteorological station in the study area.

5.2.1.2. Climatic models and scenarios

To analyze future trends in climate change on yam yields, data from 10 climate models from the Coupled Model Intercomparison Project Phase 6 (CMIP6) were used. **Table 1** lists the various climate models considered in the study. These data were obtained from NASA Earth Exchange Global Daily Downscaled Data Projections (NEX-GDDP-CMIP6). The NEX-GDDP-CMIP6 data set includes global climate scenarios at a reduced scale derived from simulations of the general circulation model (GCM) conducted during the sixth phase of the coupled model comparison project (CMIP6), as well as four scenarios of greenhouse gas emissions at "level 1" known as "Shared Socioeconomic Pathways" (SSPs) (Adeyeri et al., 2022; Akinsanola et al., 2021; Peng et al., 2023). The latter, in particular, ssp2-4.5 and ssp5-8.5 scenarios were used in this study. The SSP2 scenario (SSP2-4.5), entitled "Middle of the Road (Medium Mitigation and Adaptation Challenges)", presents a situation in which the world's social, economic, and technical tendencies vary slightly from the past patterns. In this scenario, the trajectory of emissions will induce a radiative forcing of +4.5W/m^2 in the long term (by 2100), with a warming level of around 2.7°C compared with the pre-industrial period. In practice, this scenario will result in CO_2 emissions remaining close to current levels until the middle of the century (around 40GtCO_2/year) before declining to around 10 40GtCO_2/year in 2100 (IPCC, 2022). The second scenario (SSP5-8.5), entitled "Fossil Energy Driven Development - Taking the High Road (High Mitigation Challenges, Low Adaptation Challenges)", defines a society that increasingly relies on competitive markets, innovation, and participatory communities to drive rapid technology advancement and human capital development as a means of achieving sustainable development period. (IPCC, 2022). We analyzed them using the R statistical software. The simulations were run for 30 years (from 2025 to 2054) based on historical data (Weijer et al., 2020).

Table 5- 1: List of different CMIP6 climate models used

Climatic models	Institution/Country	Spatial resolution	Sources
ACCESS-CM2	Commonwealth Scientific and Industrial Research Organization/ Australia	1.88*1.25	(Bi et al., 2020; Mackallah et al., 2022; Rashid et al., 2022)
EC-Earth3	EC-EARTH Consortium/ Europe	0.7*0.7	(Döscher et al., 2021, 2022; Van Noije et al., 2021)
EC-Earth3-Veg	EC-EARTH Consortium/ Europe	0.7*0.7	(IPCC, 2023a; Weijer et al., 2020)
FGOALS-g3	Chinese Academy of Sciences Flexible Global Ocean-Atmosphere- Land System Model/ China	2.0*2.0	(Li et al., 2020; Pu et al., 2020)
GFDL-ESM4	Geophysical Fluid Dynamics Laboratory (GFDL)/ USA	1.25*1.0	(Dunne et al., 2020; Zhao et al., 2018)
INM-CM4-8	Institute of Numerical Mathematics	2.0*1.5	(E. M. Volodin et al., 2018; Weijer et al., 2020)
INM-CM5-0	Institute of Numerical Mathematics	2.0*1.5	(IPCC, 2023b; E. Volodin & Gritsun, 2018)
IPSL-CM6A-LR	Institute Pierre Simon Laplace(IPSL)/ France	2.5*1.26	(Boucher et al., 2020; Wang et al., 2019)
MPI-ESM1-2-HR	Max Planck Institute/ Germany	1.88*1.88	(Gutjahr et al., 2019; Mauritsen et al., 2019; W. A. Müller et al., 2018)
NorESM2-MM	Norwegian Climate Centre ESM Climate ModelingConsortium/ Norway	0.9*1.3	(IPCC, 2023c; Seland et al., 2020)

5.2.1.3. Yield data

Yam yield data utilized in this study were obtained from FAO's database (FAOSTAT, 2023). We obtained the national average yields for the study's reference period (1981-2010). These data were used to develop the Yam yield prediction model.

5.2.1.4. Time horizon

The baseline for the study was set to be between 1981 and 2010. This baseline is the basis for the future horizon forecast of which a medium-term period was chosen (2025-2054). This prospective 30-year timeframe was selected to allow for the assessment of climatic trends in yam yields in the study area to guide future production decisions.

5.2.2. Computing of agro-climatological characteristics

The long rainy season is considered in this study. The criteria are those of modified Sivakumar's agroclimatology method (Sivakumar, 1988). The criterion states that the onset of the growing season (OGS) begins when there is at least 20 mm of rain on 1, 2, or 3 consecutive days after February 1st, without a dry period of more than 7 days being observed within 30 days. The cessation of the growing season (CGS or CS) is defined as the date after July 1st on which no rain occurs over 20 consecutive days or when a daily evapotranspiration loss of 4 mm is depleted in soil capable of retaining 70 mm of available water. In other words, when the water balance reaches zero. The length of the growing season (LGS or LOS) results from the difference between the cessation and the onset growing season dates (CS-OGS). These two dates are expressed in Julian days (Dekoula et al., 2018; Ibrahim et al., 2022; Sivakumar, 1988). The other agroclimatic variables computed are seasonal cumulative (CUS) (sum of rainfall between OGS and CS); occurrence of rainy days or wet days (WD); length of maximum intraseasonal dry sequence (LODS); growing degree-days (GDD), its sum of the difference between the average daily temperatures and the base temperature of the yam (15°C). The GDD formula is given by **equation 1** (Mcmaster & Wilhelm, 1997):

$$\mathbf{GDD = [(Tmax + Tmin)/2] - Tbase} \qquad \mathbf{[1]}$$

Where: Tmax and Tmin are respectively daily maximum and minimum air temperature, and Tbase is the yam base temperature, typically ranging between 10°C to 15°C (Ufoegbune et al., 2014). This calculation was made over the period defined between OGS and CS. The indices calculated in this work can be summarized in **Table 5-2.**

Table 5- 2: Risks agro-climatological-related indices computed for this study

Indices	Definitions	Descriptions	units
Precipitations			
WD	Occurrence wet days	Occurrence of rainy days	mm
OGS	Onset of the growing seasons	Start of the crop growing rainy season	Julian days
CS	Cessation of the growing seasons	End of the crop-growing rainy season	Julian days
LOS	Lengths of the growing season	Difference between the end and the start of growing season dates	Julian days
LODS	Length of intraseasonal dry sequence	Length of maximum intraseasonal dry sequence days	days
CUS	Cumulative seasonal rainfall	Sum of rainfall between OGS and CS	Julian days
Temperatures			
Tmax	Maximum temperature	Extreme temperatures on consecutive days	C
Tmin	Minimum temperature	Low-temperatures consecutive days	C
GDD	Growing Degree days	Daily high and daily low temperature	C

5.2.3. Yield modelling

5.2.3.1. Development of the model

We applied a Multiple linear regression (MLR) statistical model to estimate yield using multiple independent variables. MLR is a mathematical regression method that establishes the relationship between several variables and an outcome variable, assuming a linear association between the variable categories (Perez Melo, 2014; Setiya et al., 2023). The mathematical formula for MLR is expressed using **equation 2**:

$$\mathbf{Y = a0 + a1X1 + a2X2 + \ldots + anXni + \varepsilon} \qquad \textbf{[2]}$$

Where **Y** is the dependent variable (yam yield in our case); **a0** is the **Y**-intercept (the value dependent variable when all the independent variables are zero); **i = n** observations and represents the regression coefficient of independent variable **xi** while **ε** is the model error.

5.2.3.2. Statistical test requirements

To ensure the reliability of the model for estimating yield, we established some statistical assumptions required for MLR models. We used the Shapiro-Wilk test to determine the normality of model residuals. The criterion is that the model's residuals follow a normal distribution. Shapiro-Wilk test is expressed as follows (**Equation 3**):

$$\mathbf{W} = \frac{(\sum_{i=1}^{n} a_i x_{(i)})^2}{\sum_{i=1}^{n} (x_i - \bar{x})^2} \quad [3]$$

Where $\bar{x} = \frac{1}{n} \sum_{i=1}^{n} x_i$ and the random variables $x_{(1)} < \cdot \cdot \cdot < x_{(n)}$ denote the orderstatistics corresponding to $x_1, ..., x_n$. The vector $(a_1, ..., a_n)'$ is a function of the expectation and covariance matrix of the order statistics vector for a standard normal random sample of size **n**.

Then, the Variance Inflation Factor (VIF) test was applied to determine collinearity between variables. Here, the model must prove that the variables are not collinear. Otherwise, the variables must not be linked in such a way as to influence the model. Moreover, we used the homoscedasticity test to determine the equality of variance in the residuals. To do it, the Golfeld-Quandt test was run to evaluate if the variances were equivalent. Finally, The Durbin-Watson test was applied to assess whether or not there is autocorrelation among the residuals. The Durbin-Watson test statistic, DW, is (**Equation 4**):

$$\mathbf{DW} = \frac{\sum_{i=1}^{n-1} (r_{i+1} - r_i)^2}{\sum_{i=n}^{n} r_i^2} \quad [3]$$

where r_i is the **ith** raw residual, and **n** is the number of observations.

All tests performed are summarized in **Table 5-3** at a 5% (α =0,05)significant level.

Table 5- 3: Conditionalities of statistical tests carried out for model validation requirements

Type of test	Characteristics	Interpretations
Shapiro-Wilk	Determine the normality of model residuals	If p-value < α, no normality If p-value > α, normality
Variance inflation factor (VIF)	Determining the existence of collinearity between variables.	If VIF < 5: No colinearity If VIF > 5: Existence of colinearity
Golfeld-Quandt (Homoscedasticity test)	Determination of the homoscedasticity of the variance of residuals.	If p-value < α: Heteroscedasticity of residues; If p-value > α: Homoscedasticity of residuals.
Durbin Watson (DW)	Determination of autocorrelation of residuals in a linear regression model.	No autocorrelation of errors when the DW value is close to two (2) or generally between 1.5 and 2.5

5.2.4. Identifying relevant variables for the model

A backward elimination approach using statistical conditionalities was run to identify relevant variables for the final model. In backward elimination, the model starts with all possible predictors and successively removes non-significant predictors until it reaches the stopping criterion. The stepwise regression method combines these two approaches, adding and eliminating predictors as it builds the model (Hastie et al., 2017). As we employed a multiple linear regression model, statistically non-significant variables can be subjected to conformity tests to determine whether or not they should be used in the final model. The idea is to look for variables that provide important information in explaining our response variables. Thus, the variables retained are those that, from the point of view of the backward approach, appear to be quite important in explaining the model and the yield prediction (Heumann et al., 2016; Wickham & Grolemund, 2017).

5.2.5. Model validation

We drew up the data into two series based on the 30-year yield from 1981 to 2010. Sample 1 – the training sample – comprised 67% of the data, which corresponds to 20 years used to create the prediction model, and Sample 2 – the testing sample – had 33% of the data, corresponding to 10 years used for model validation. Four statistical metrics (RMSE: Root Mean Squared Error, MAE: Mean absolute error, PBIAS: Percent Bias, and ME: Mean Error) were computed to determine the difference between observed and projected data for the 2010 timeframe, as shown by **equations 4, 5, 6, 7** below.

$$\mathrm{RMSE} = \sqrt{\frac{\mathrm{W}_{i=1}^{N} (x_i - \hat{x}_i)^2}{N}} \qquad \textbf{[4]}$$

i = variable

N = number of non-missing data points

$\mathbf{x_i}$ = actual observations time series

$\hat{\mathbf{x}}$ = estimated time series

$$\mathrm{MAE} = \frac{\sum_{i=1}^{n} |y_i - x_i|}{n} \qquad \textbf{[5]}$$

$\mathbf{y_i}$ = prediction

$\mathbf{x_i}$ = true value

n = total number of data points

$$\mathrm{PBIAS} = \frac{\sum_{i=1}^{n} ({Y_i}^{obs} - {Y_i}^{sim})}{\sum_{i=1}^{n} ({Y_i}^{obs})} \qquad \textbf{[6]}$$

$\mathbf{Y^{obs}}$ = observed records

$\mathbf{Y^{sim}}$ = corrected records

n = data records.

$$\mathrm{ME} = \frac{\sum_{i=1}^{n}(\varepsilon i)}{n} \qquad \textbf{[7]}$$

$\boldsymbol{\varepsilon_i}$ = sum of all error values

n = data records or number of records

Subsequently, a graphical analysis was performed to assess the model's capacity to reflect the interannual variability in yam yields throughout the same period (2001-2010). After the model had been validated, a future simulation was performed using climatic scenario data (ssp2-4.5 and ssp5-8.5), accounting for the promising variables and the model parameters.

5.2.6. Trend analysis

The Mann-Kendall test is a non-parametric statistical test commonly used to identify patterns in environmental data (Faour et al., 2016; Kpanou et al., 2021; New et al., 2006; Perez Melo, 2014; Yin et al., 2021). We performed it to judge whether the trend in a series is regressive over time (decreasing trend), progressive (increasing trend) or neutral over time (stable trend). The test **equations (8 and 9)** are defined as follows:

$$\mathbf{S} = \sum_{i=1}^{n-1} \sum_{j=i+1}^{n} \mathbf{sgn}(\mathbf{Yi} - \mathbf{Yj}) \qquad [8]$$

$$\mathbf{sgn}(\mathbf{Yi} - \mathbf{Yj}) = -\mathbf{1}\ \mathbf{si}\ (\mathbf{yi} - \mathbf{yj}) < \mathbf{0}\ ;$$

$$\mathbf{sgn}(\mathbf{Yi} - \mathbf{Yj}) = \mathbf{1}\ \mathbf{si}\ (\mathbf{yi} - \mathbf{yj}) > \mathbf{0}\ ;$$

$$\mathbf{sgn}(\mathbf{Yi} - \mathbf{Yj}) = \mathbf{0}\ \mathbf{si}\ (\mathbf{yi} - \mathbf{yj}) = \mathbf{0}\ ;$$

$$\mathbf{T} = \frac{\mathbf{2S}}{\mathbf{n} - (\mathbf{n} - \mathbf{1})} \qquad [9]$$

Where **T** is the tau; **S** is the Mann-Kendall correlation coefficient; **n** is the length of the data series studied (2025-2054) and the series **Yi** to **Yn** corresponds to the average yield data. The test has been carried out under the null hypothesis H_0 according to which: "there is no trend in the yield series". The $\boldsymbol{\alpha}$ threshold corresponds to the error of the first kind and has been set at 5%.

5.2.7. Determining the relative yield gap

The impacts of climate change on yam production were studied using ssp2-4.5 and ssp5-8.5 climatic scenarios for the period 2025 and 2054. In this approach, the changes for each climatic scenario throughout the specified time horizon were estimated about the reference period (1981–2010). The formula for estimating the gap is as follows (**equation 10**):

$$\mathbf{Gap}\ (\%) = \frac{\mathbf{yf-yh}}{\mathbf{yh}} * \mathbf{100} \qquad \textbf{[10]}$$

The **"Gap (%)"** depicts the relative percentage change, with **"yf"** and **"yh"** being yam yields for the future and historical periods, respectively.

5.3. RESULTS

5.3.1. Interannual variation in yam yields from 1981 to 2010

We conducted a trend analysis to determine yield trends for the baseline period. The yield trend reveals the trend across the 30 historical years studied (from 1981 to 2010). The results show a significant decline in average yam yield from 11.6 t/ha to 6.5 t/ha (**Figure 5-1**). The Mann-Kendall tau statistic is negative (-0.8), and significant (p-value < 0.01) pointing to a yield decline trend.

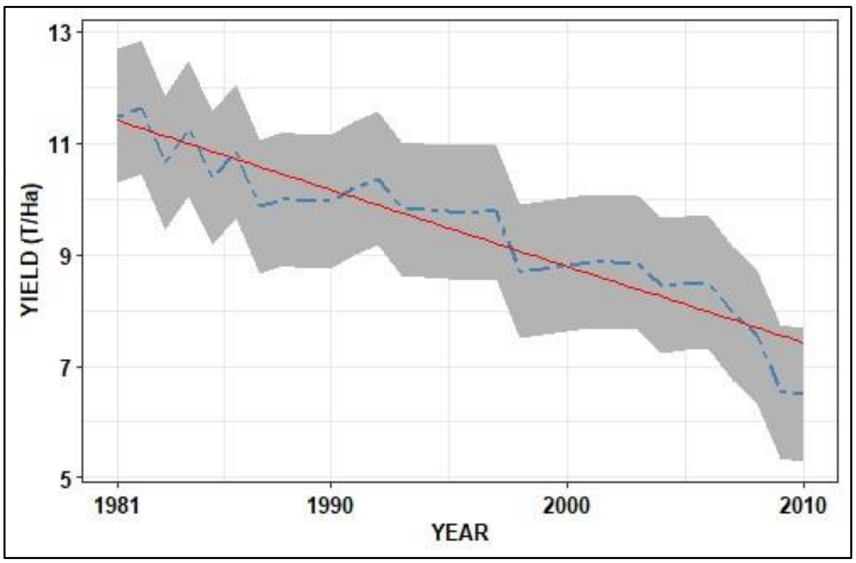

Figure 5- 1: Average yam yield trend for the baseline period

5.3.2. Correlations analysis between agroclimatic parameters and yam yields

Agro-climatological characteristics have a substantial impact on agricultural production, including crop growth, development, and productivity. This study takes into account key agroclimatic parameters from precipitation and temperature. Using correlation analysis, we can see how each parameter impacts yam yield. The variables having the highest correlation with yield are those whose values tend to be -1 or +1. The correlations range from -0.6 to 0.2. One of the most notable observations is the positive correlation between yield and the variables CUS (r=0.14), and LODS (r=0.21), while the other predictors have a negative correlation. The general trend of correlations remains weak and insignificant (p-value> 0.05), except for the correlation of Tmin (r = -0.62) that is significant with yam yield (**Fig.5-2**).

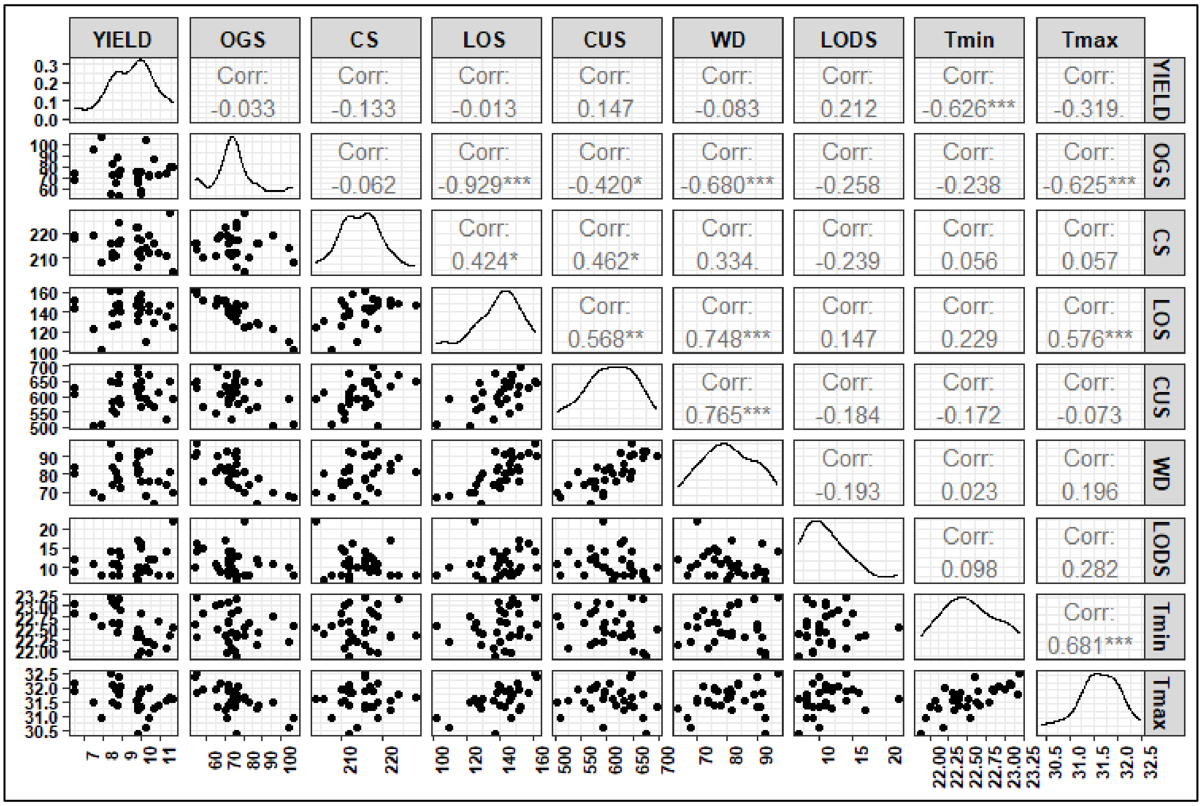

Figure 5- 2: Table correlations between agroclimatic parameters and yam yields
Note: *p < 0.5; **p < 0.1; ***p < 0.01.

5.3.3. Model building

The dependent variable is yam yield and the independent variables are (OGS; CS; LOS; CUS; WD; LODS; Tmin; Tmax) the agroclimatic parameters. Implementing multiple linear regression (MLR) to assess the trend of a model with all explanatory variables yields the following findings **(Table 5-4)**. At the 5% level, none of the agroclimatic variables are statistically significant. However, the minimum temperature is significant at the 10% level. Therefore, we used backward elimination with all possible predictors through statistical validation approaches and successively removed non-significant variables until they reached the stopping criterion.

Table 5- 4: Trend of a model with all explanatory variables

Coefficients	Estimate	Std. Error	t value	Pr(>|t|)
(Intercept)	57.546328	28.740483	2.002	0.0705 *
OGS	-0.368996	0.422331	-0.874	0.4009
CS	0.305922	0.400937	0.763	0.4615
LOS	-0.327373	0.426167	-0.768	0.4586
CUS	0.010329	0.009089	1.136	0.2799
WD	-0.100409	0.057858	-1.735	0.1106
LODS	0.016264	0.064099	0.254	0.8044
Tmin	-1.807584	0.955904	-1.891	0.0852 *
Tmax	0.070817	0.736145	0.096	0.9251

Signif. codes: 0 '***' 0.001 '**' 0.01 '*' 0.05 '.' 0.1 ' ' 1
Residual standard error: 0.8205 on 11 degrees of freedom Multiple R-squared: 0.419; Adjusted R-squared: -0.00359
F-statistic: 0.9915 on 8 and 11 DF, p-value: 0.4911

5.3.4. Model validation

5.3.4.1. Shapiro-Wilk and Goldfeld-Quandt test

We determine the normality of data residuals and the homoscedasticity of the variance respectively through the Shapiro-Wilk and Goldfeld-Quandt test to validate the model. We obtain a p-value=0.1494 > 0.05 for the Shapiro-Wilk test and a p-value=0.7069> 0.05 (**Table 5-5**).

Table 5- 5: Evaluation of the residual normality and homoscedasticity

Shapiro-Wilk	Goldfeld-Quandt
W = 0.92926	GQ = 0.55831
p-value = 0.1494	p-value = 0.7069
	df1 = 4; df2 = 4
YM01= data Residuals:	

NB: The data residuals YM01 are all the variables; df= degrees of freedom

The Shapiro-Wilk test demonstrates a normality between the residuals while the Goldfeld-Quint test shows equality of variance or homoscedasticity of the residuals.

5.3.4.2. Variance inflation factor (VIF) and residuals autocorrelation

The variance inflation factor (VIF) test was performed to categorize the variables (residuals YM01) into different levels of correlation: low and high. The variables CUS, WD, LODS, Tmin and Tmax show a VIF value of less than 5% (1.27<VIF<2.86), thus indicating no collinearity between variables. On the other hand, the variables OGS, CS and LOS have very high collinearity with a very high VIF percentage. Also, it should be noted that the low-correlation variables have no autocorrelation of error. Their Durbin Watson (DW) values range between 1.13 <DW< 1.69. The variables OGS, CS and LOS have very large autocorrelation of error (DW > 11) (**Table 5-6**). These variables were excluded from the model.

Table 5- 6: Model validation by statistical inclusion and exclusion of variables

Term	VIF (%)	VIF 95% CI	Increased SE (DW)	Tolerance	Tolerance 95% CI
Low-Correlation					
CUS	2.86	[1.95, 4.65]	1.69	0.35	[0.22, 0.51]
WD	2.43	[1.70, 3.93]	1.56	0.41	[0.25, 0.59]
LODS	1.27	[1.06, 2.23]	1.13	0.79	[0.45, 0.95]
Tmin	1.77	[1.32, 2.85]	1.33	0.57	[0.35, 0.76]
Tmax	2.28	[1.61, 3.68]	1.51	0.44	[0.27, 0.62]
High-Correlation					
OGS	567.82	[377.34, 854.71]	23.83	1.76e-03	[0.00, 0.00]
CS	142.08	[94.57, 213.71]	11.92	7.04e-03	[0.00, 0.01]
LOS	673.15	[447.30, 1013.30]	25.95	1.49e-03	[0.00, 0.00]

NB: CI= Confidence Interval ; SE= standard error

With the four statistical test requirements (normality, homoscedasticity or homogeneity, multicollinearity, and autocorrelation) of variables validated, we can assess the performance or robustness of the model using yield data for the period 2001-2010.

5.3.5. Evaluating the performance of the predictive model

We evaluated the model's performance by comparing the interannual variability of the observed yield to the predicted yield over the same timeframe (2001-2010). The data is standardized to the reference period, eliminating the influence of the unit, in order to see patterns on the graph generated throughout time. The goal is to determine the model's capacity to detect trends in comparison to the normal, which is 0. The graph on the right depicts both the observed (blue) and expected returns (red). The negative slice denotes a downward trend, whereas the positive slice reflects an upward trend. (**Fig. 5-3**). The model indicates a performance of 90% in detecting the interannual variability of observed yields. The average difference between simulated yields (9.3 T/Ha) and observed yields (8.5 T/Ha) is 0.8 T/Ha. Despite the tendency to fairly overestimate predicted yields, we obtained some statistically acceptable model parameter values: RMSE (root mean square error): 1.34 t/ha; MAE (Mean Absolute Error): 1.04 t/ha; PBIAS (Percentage bias): 11.2%; and ME (Mean error): 0.92.

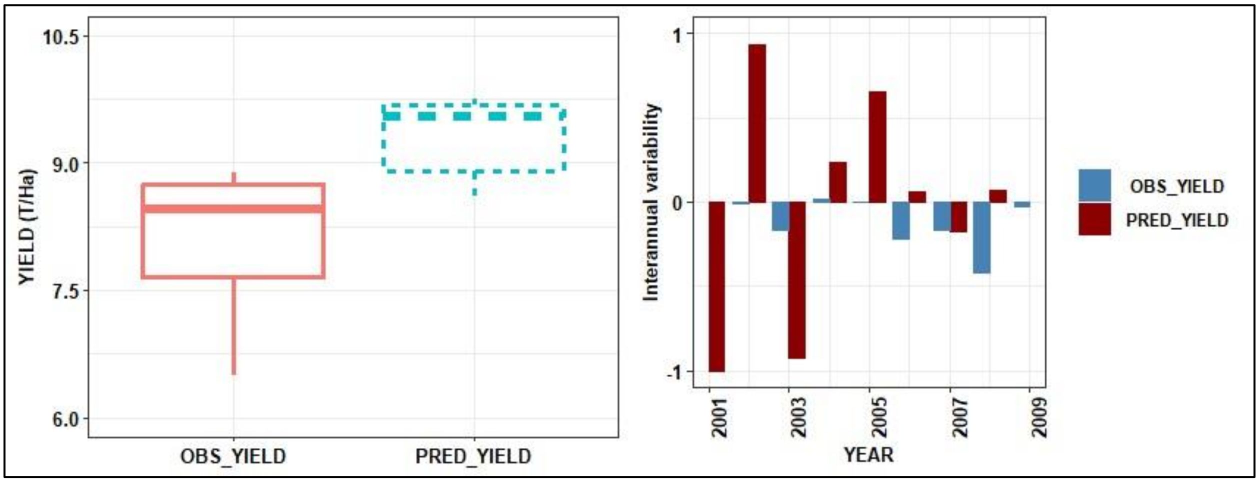

Figure 5- 3: Observed interannual yield variability compared to the prediction by the model

Despite its shortcomings – a propensity to overstate – the model works rather well in simulating yam yields. We then establish the ultimate model with all 30 years of historical data with the most significant and uncorrelated variables based on equation 11 (**Eq 11**).

Y= 0.007*CUS -0.04*WD + 0.08*LODS -2.44*Tmin + 0.48*Tmax + 46.9 [11]

Table 5-7 shows the details of the values generated when building the model with the most relevant and uncorrelated variables.

Table 5- 7: Details of the values generated when building the ultimate model

Coefficients:	Estimate	Std. Error	t value	Pr(>|t|)
(Intercept)	46.986946	14.685182	3.200	0.00384**
CUS	0.007790	0.006202	1.256	0.22114
WD	-0.042379	0.036617	-1.157	0.25851
LODS	0.087445	0.059818	1.462	0.15675
Tmin	-2.449482	0.695915	-3.520	0.00175**
Tmax	0.485114	0.602386	0.805	0.42854

Signif. codes: 0 ‘***’ 0.001 ‘**’ 0.01 ‘*’ 0.05 ‘.’ 0.1 ‘ ’ 1
Residual standard error: 0.992 on 24 degrees of freedom
Multiple R-squared: 0.5055, Adjusted R-squared: 0.4025
F-statistic: 4.908 on 5 and 24 DF, p-value: 0.003109

The coefficient of determination $R^2 = 0.505 \geq 50\%$ is rated as good. Thus, more than 50% of yields can be explained by agroclimatic parameters. Furthermore, the model can predict yam yields with at least 50% accuracy.

5.3.6. Predicting future yam yields according to CMIP 6 scenarios

At this level, CMIP6 models of future precipitation and temperature are used instead of historical data. Future data from climate models and scenarios are used to recalculate the variables retained in the final statistical model equation (Eq 11) over the prediction timeframe.

5.3.6.1. Future yield trends (2025-2054) based on the ssp2-4.5 scenario

Under the ssp2-4.5 scenario, we observed a regressive yam yield over time. This decreasing trend shows fairly interannual variability and ranges from 7.7 t/ha to 5.6 t/ha between 2025 and 2054. The average yield is set at about 6.8 t/ha (**Fig. 5-4**)

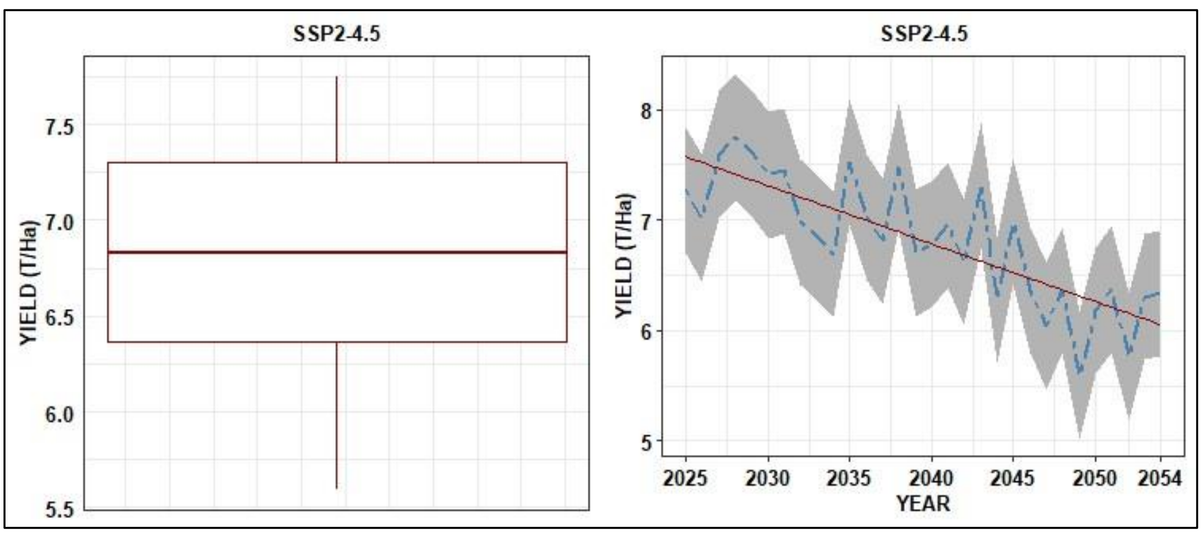

Figure 5- 4: Trend in future yam yields (2025-2054) according to the ssp2-4.5 scenario

5.3.6.2. Future yield trends (2025-2054) based on the ssp5-8.5 scenario

Under the ssp5-8.5 scenario, the future yields fluctuate between 8.2 t/ha to 4.8 t/ha. The figure indicates a downward trend in yield with high interannual variability. The average yield is around 6.4 t/ha (**Fig. 5-5**)

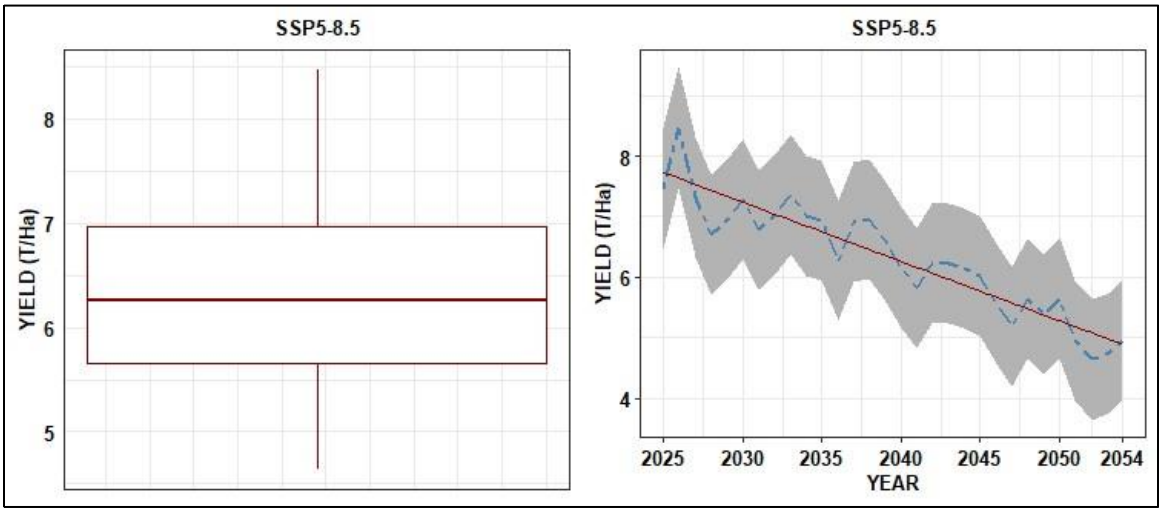

Figure 5- 5: Trend in future yam yields (2025-2054) according to the ssp5-8.5 scenario

5.3.6.3. Relative yield gap

Both climate scenarios (ssp2-4.5; ssp5-8.5) show that yam yields will be lower than in the reference period. Yield variations could vary between -10% to -45% depending on the climate scenario (**Fig. 5-6**). Declines will be characterized by strong interannual fluctuations. According to the relative gap trends in different yields, losses will be more significant in the ssp5-8.5 scenario over the long term.

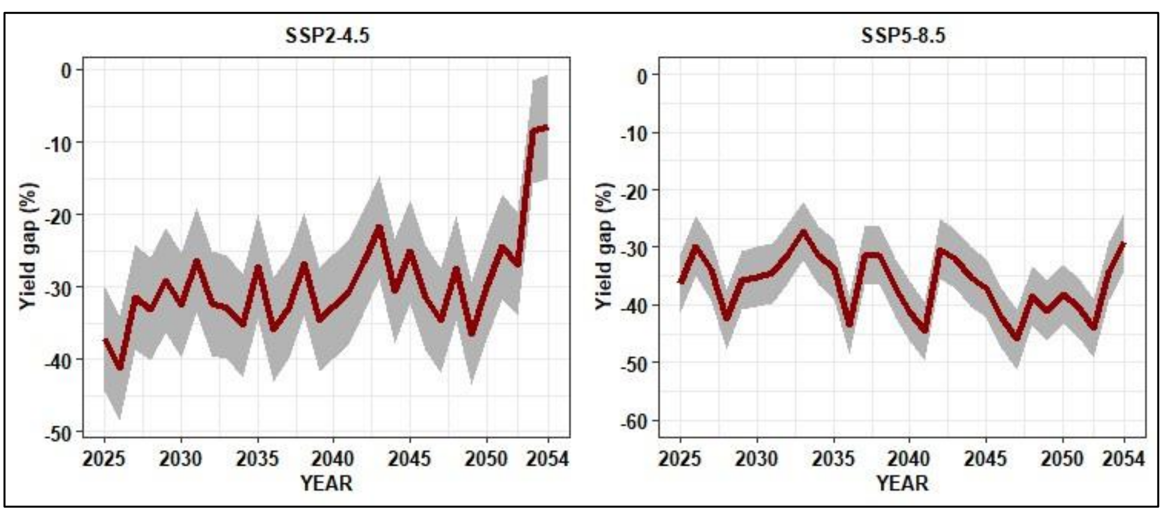

Figure 5- 6: Relative yield gap of the two scenarios (ssp2-4.5; ssp5-8.5) between 2025 and 2054

5.4. Discussion

5.4.1. Impact of agro-climatological characteristics on yam yields.

In yam yield modelling, agro-climatological characteristics play a crucial role in understanding and predicting how different climatic conditions affect yam production. Analysis of Sivakumar's agroclimatology method makes it possible to compute key agroclimatic parameters. Each of these parameters affects yam crop productivity and has a knock-on effect on yield (Alhassane et al., 2013; Kouamé et al., 2018; Nassourou et al., 2018; Owusu Danquah et al., 2022; Sultan et al., 2019). Certain investigations from authors go into further depth on how agroclimatic parameters affect yam yield. This is the case for Sivakumar, (1988); Sultan et al., (2019); and Waongo, (2015), who find that an early onset provides a longer period for yam development, while a late onset may shorten the growing period, potentially reducing yields. Further, an abrupt or early end can force an early harvest, which may result in immature yams with lower yields and poorer quality. Furthermore, they conclude that adequate and well-distributed rainfall supports tuber development, while insufficient or excessive rainfall can cause drought stress or waterlogging, respectively, both of which can reduce yields. In the same way, (Bliefernicht et al., (2021); Ibrahim et al., (2022); Marcos et al., (2009); and Olayiwola Eruola et al., (2012) find that regular wet days ensure consistent moisture availability, critical for yam growth, while periods of dryness within the growing season can stress yam plants, especially during critical growth phases like tuber formation, and prolonged dry spells can significantly reduce yields. These findings corroborate our results, which indicate that the computed variables have a weak correlation ($-0.3<r<0.2$) with yam yield, except for minimum temperature. This reflects (Kouamé et al., (2018), who, while characterizing key agroclimatic parameters of the cropping season in the forest-savanna contact zone of Côte d'Ivoire, revealed that the averages of the fundamental parameters of the two rainy seasons observed for each of the rain gauge stations show more or less significant differences. Indeed, the correlation between Tmin and yam yield is r= -0.6 at the 5% threshold. According to the IPCC's Sixth Assessment Report, climate change might negatively affect the output of tropical food crops such as rice, maize, yams, and cassava if local temperatures rise by 2°C or more (IPCC, 2022). Other studies support this claim by pointing out that because yams are temperature-sensitive, even mild global warming can influence their growth. (FAO, 2021; Marcos et al., 2009). All demonstrate that agroclimatic parameters derived from temperature, as well as precipitation, must be handled to ensure a successful farming season. These parameters are critical, which is why they were computed to analyze their correlation with yam yield and then used to develop our model for future predictions.

5.4.2. Predictive capacity of the model developed and an analysis of the yield simulated

The multiple linear regression (MLR) model developed in this study using agro-climatological characteristics appears to reflect the changing trend in yam yields rather well. Furthermore, statistically, it produced generally satisfactory results. Indeed, relative to actual measurements, the projection somewhat overstated yields from 2001 to 2010. However, the model performed well in reproducing the general patterns, with an $R^2 = 0.50$. Similarly, Dube's study in Pokona et al., (2021) argues that comparing model predictions with data from a real homegrown is the best approach to assess the model's validity, which must show a specific degree of agreement between the calculated findings and the actual observations. Furthermore, a high (R^2) indicates a good fit between a model and observed data (Heumann et al., 2016; Kouassi AM et al., 2014). The established model was further validated by solid findings from specific statistical tests, most notably the Shapiro-Wilk, the Variance Inflation Factor (VIF), Goldfeld-Quandt, and Durbin Watson. The Shapiro-Wilk normality test revealed that the variables were normally distributed because we observed a p-value = 0.1494 > 0.05. Regarding the normality of variables, if p-value ≤ α, the variables are not normally distributed. But if p-value > α, the variables are normally distributed (Hastie et al., 2017). This test is critical since it indicates if the variables are evenly distributed and may be included or not in the model. The VIF test, which assesses the presence (if VIF>5%) or absence (if VIF<5%) of collinearity across variables, yields a score of less than 5% (1.27 < VIF < 2.86) for each selected variable. Collinearity must be avoided for model validation since it decreases the precision and efficiency of parameter estimators (Shrestha, 2020; Voss, 2005). Furthermore, the presence of collinearity between explanatory variables results in significant standard deviations of regression coefficients, which, in this instance, are extremely sensitive to even small variations in the predictor (Shrestha, 2020; Voss, 2005). Similarly, the Goldfeld-Quandt test, which evaluates the homoscedasticity of the model's residuals, yields good findings, with a p-value of 0.7069 above the 5% threshold. Indeed, the homoscedasticity test determines the homogeneity of the residual variances (Sohel Rana et al., 2008). The latter is a fundamental property of the linear regression model's premise, indicating that if the p-value is less than α, then the residuals are heteroscedastic and if the p-value > α, residuals are homoscedastic (Goldfeld & Quandt, 1965). Regarding the Durbin-Watson test, the existence of autocorrelated errors limits a model's relevance to the Durbin-Watson test (Test et al., 1981). The Durbin-Watson test, which determines the existence or absence of autocorrelation of residuals in a linear regression model, found no autocorrelation of residual errors (DW < 1.69). This confirms the model's significance, as the principle accepts the lack of error autocorrelation when the value of this statistic (DW) is near to 2 or between 1.5 and 2.5 (Dufour & Dagenais, 1985; Weber & Monarchi, 1982). Concerning the yield modelling outcomes, it should be noted that the normalized 30-year historical period of the Intergovernmental Panel on Climate Change scenarios extends from 1981 to 2010 and that beyond 2015, the CMIP 6 scenario data are considered the future, this is the reason we picked the timeframe for our data, observation and historical scenario. (Peng et al., 2023; Pu et al., 2020; Rashid et al., 2022). The IPCC separates simulation horizons into short-, medium-, and long-term. The timeframe 2025-2054, over which we made the yam yield projections, fits within the short- to medium-term phase (IPCC, 2023a). Over this period, under the ssp2-4.5 scenario, the yam yield shifts from 7.7 t/ha to 5.6 t/ha, while under the ssp5-8.5 scenario, the yields fluctuate between 8.2 t/ha to 4.8 t/ha. The relative yield gap then computed indicated that yield variations could vary between -10% to -45% depending on the climate scenario. In line with our research, a World Bank study of food crops in Côte d'Ivoire used IPCC Representative Concentration Pathways (RCP) scenarios under Shared Socioeconomic Pathways Three (SSP3) to predict future yam yields. This study demonstrated that the percentage point difference in yield and area of production with different levels of climate change for yams will be reduced negatively in yield under RCP4.5 and RCP8.0 respectively in 2030 and 2050 (RCP4.5: -0.9%; -2.3% and RCP8.0: -1.0%; -2.4%) (World Bank Group, 2019). The following trends can be expected for yam yields in Côte d'Ivoire, especially in the Gontougo region under the SSP2-4.5 scenario from 2025 to 2054. According to numerous research, under the SSP2-4.5 scenario, which represents a middle-of-the-road pathway with moderate climate action and socio-economic development, the future yam yield trends from 2025 to 2054 can be influenced by two key factors: global warming, as yams are sensitive to temperature changes; and changes in rainfall patterns. There will be an urgent need to adapt and employ enhanced seeds. For this goal, continuous improvement in farming practices, development of more resilient yam varieties, and effective implementation of climate adaptation strategies will be crucial to counteract potential negative impacts on yields (Aka et al., 2023; Bobadoye et al., 2016; IPCC, 2022, 2023b, 2023a; Roudier et al., 2011; Sultan et al., 2015).

Then, under the SSP5-8.5 scenario, which represents a pathway characterized by high economic growth, energy-intensive lifestyles, and high greenhouse gas emissions resulting in severe climate change impacts, the future yam yield trends from 2025 to 2054 are likely to be significantly affected. Associated key factors and projected trends include increased frequency and intensity of both droughts and heavy rainfall events (Enders et al., 2023; Guarin et al., 2023; IPCC, 2023a; Liu et al., 2021; Srivastava et al., 2012). Economic growth may not sufficiently offset the negative impacts on agriculture, particularly if environmental degradation continues and adaptation measures lag behind the pace of climate change. As climate impacts become more pronounced, agricultural systems will start to experience significant stress, requiring rapid adaptation and resource allocation to maintain yields.

5.5. Conclusion

This study examines the impact of agro-climatological characteristics on yam and simulated yield using CMIP 6 scenarios. Our analysis demonstrates that future yam yield trends in the Gontougo region from 2025 to 2054 are expected to face significant challenges due to severe climate impacts. While early years might see some variability, the long-term trend points toward declining yields and increased vulnerability. Among all the variables, those that most affect yields are CUS, WD, LODS, Tmin and Tmax. They have a weak correlation ranging from -0.3 to 0.2 except for minimum temperature which has a significant negative correlation with yam yield ($r= -0.6$) at the 5% threshold. Using multiple linear regression (MLR) statistical models to simulate yam yields, the robustness test of the model after validation of the conditions indicates a 50% performance of the model in predicting yam yields in the study area. The statistical results used to validate the model reveal that the error percentages are acceptable for prediction. As a result, these new technologies have the potential to be utilized to establish food safety monitoring and warning systems. In terms of variation, large inter-annual oscillations will characterize declines, while the falling yields are more pronounced in the ssp5 scenario than in the ssp2. Effective and robust adaptation strategies, agricultural innovation, and substantial investment are crucial to mitigate these negative impacts and sustain yam production in the face of rapid climate change. It is worth noting that our study had some limitations including the use of national crop data from the FAOSTAT database to estimate yields instead of actual observation, and then, due to the lack of weather stations, in-situ climate observation data was not used to assess local climate change conditions. In addition to climatic factors, yield prediction can also be linked to pedological, environmental, physiological, phytopathological, and socio-economic aspects. Further investigations should take these considerations into account.

.

GENERAL CONCLUSION

The study's overarching aimed to contribute to achieving food security in Côte d'Ivoire by reducing yam production risks in the Gontougo region. First of all, it examined LULC change analysis and its effects on LST using ML through GEE. We could discriminate six classes: annual crops, perennial crops, savannah, forest, bareland/settlement, and waterbody. The prevailing LULC class is perennial crops. It occupies more than 60% of the area of each LULC map. The NDVI and LST reclassifications correspondence have shown that Non-vegetation land corresponds to very high temperature while low vegetation land corresponds to high temperature. Then, the physicochemical parameters of soil in Tanda's (forest area) and Bondoukou's departments (savannah area) were analyzed. It has been established that the presence of trees improves the physicochemical qualities of soil. Indeed, forest soils contain more physicochemical components than savannah soils for many reasons, including climate, edaphic conditions, and ecology. This is why Bondoukou soil is largely sandy, with coarse sand and a low amount of clay, as opposed to Tanda soil, which is less sandy and contains a lot of clay. Concerning climate analysis and local knowledge aspects, the findings underline the importance of understanding and using weather information while cultivating yam crops and farmers' adaptive reactions to the threats they meet. In the Gontougo region, almost 25% of the time (early years), the growing season began around the 50th day of the year, i.e. around 20 February under the long rainy season, compared to the 220th day of the year (around the end of the first decade of August) under the short rainy season. Furthermore, the typical cessation of the growing season is July 22 to 24 during the long rainy season, and November 20 to 26 during the short rainy season. Concerning perceptions, it is worth noting that farmers' insights into yam production and climate change are crucial in shaping their farming practices. Many farmers recognise the impacts of climate variability on their yam crops, particularly the challenges posed by irregular rainfall, prolonged dry spells and rising temperatures. However, there is often a gap between this awareness and the adoption of adaptive practices. Limited access to information, resources and agricultural extension services hampers the widespread implementation of modern, climate-resilient techniques. Regarding prediction, large inter-annual oscillations will characterize declines, and the falling yield will be more pronounced in the ssp5 scenario than in the ssp2. By the way, the model predictions have resulted between 6 t/ha to 7.2 t/ha of yam yield under the ssp2-4.5 scenario and, under the ssp5-8.5 scenario, the yield declined steadily from 4.5 t/ha to 7.5 t/ha from 2025 to 2054. These results lead us to believe that the sustainability of yam production in the Gontougo region under climate change is doubtful without targeted actions. Addressing the highlighted threats is critical to preserving the local population's food security and economic well-being in the face of present and projected climatic risks.

In sum, Gontougo region experiences a tropical climate with distinct wet and dry seasons. Since yam is a rain-fed crop, it extremely depends on the time and amount of rainfall. Climate change has increased variability in rainfall patterns, with some years seeing lengthy droughts and others seeing heavy rains. These variations not only disturb the growing season but also cause soil erosion and nutrient leaching, which reduces yam yields.

The region's soil is more or less rich, with a loamy-sandy texture in the northern and clay-loamy-sandy in the middle and southern part, allowing for yam farming. However, its fertility is deteriorating due to continual cultivation without adequate nutrient replenishment, resulting in decreasing yields over time. Gontougo's vegetation, which is mostly savannah and mixed forest, also helps to preserve the microclimate and protect the soil from erosion. However, deforestation and soil degradation caused by extensive agriculture (cashew, cocoa, rubber trees, and even yams) without improved land use/cover planning are continuous issues that jeopardize soil health and consequently, yam productivity.

From an economic viewpoint, yams are an important crop in the Gontougo region, providing both a staple food and a source of income for local farmers. The crop's economic importance extends to regional marketplaces where yams are exchanged, assuring farmers' financial security. However, the economic feasibility of yam production is harmed by climate-related hazards such as poor harvests, higher production costs due to soil management and high labour expenses, and a shortage of manpower who have turned to other crops. The economic future of yam crops in Gontougo is thus uncertain, necessitating investments in sustainable agricultural techniques and climate-resistant infrastructure to provide food security and economic stability.

To reduce the hazards associated with climate change, appropriate adaptation methods must be implemented. These might include the creation and spread of climate-resilient yam cultivars, improved farming practices such as soil conservation, and water management, and the introduction of early warning systems to better anticipate and respond to climate-related challenges.

Recommendations

Through the results, we highlight the need to integrate climate change concerns into agricultural policy and food security initiatives. Policymakers need to prioritize expenditure on agricultural research, extension services and infrastructure that promote climate adaptation in yam production.

We must provide the region with a regular rainfall calendar for the growing season, especially for yams, to boost yields. And then strengthen ANADER's staff and establish a special unit dedicated to the yam industry's sustainability and promotion. In addition, strengthening community resilience through education and support programs is crucial. Furthermore, the decision-makers, the state, NGOs, and donors should help farmers by developing hydro-agricultural facilities; Promoting yam festival celebrations in each producing region and rewarding farmers; Making fertilizers, improved climate-resistant yam varieties and farm equipment available to peasants free of charge. Moreover, the combination of agroforestry, in particular the yam-cashew pairing, crop rotation, fallowing and the use of intercropping should be encouraged as a solution to regenerate and increase soil fertility, reduce pressure on biodiversity and increase the flow of ecosystem services. Finally, farmers' perceptions of their vulnerability and exposure to climate change, as well as their endogenous agronomic practices must be considered in actions to increase food security

Limitations and outlooks

As with every scientific research that seeks less boastful, it is always scientifically modest to accept the study's limitations. If we have these wonderful achievements and are happy with what we've achieved so far, it's because of the obstacles and disappointments accompanying our trip. It would thus be wise to recognize these limits and turn them into opportunities to conduct future research.

- ➢ The study's drawbacks include the inability to map the yam crop directly. This would have allowed us to directly analyze how LSTs affected yams. This element will be addressed in future studies, employing very high spatial resolution images or a drone.
- ➢ One of the limitations of our study is the use of national yam data from the FAOSTAT database to estimate yields, instead of actual field observation data. Secondly, due to a shortage of weather stations and reliable data, in situ climate observation data was lacking, so we relied on online climate data to assess local climate change conditions. In light of the above, we will now gather climate data using reliable rain gauges accessible from locally based agricultural services to examine the characteristics of the growing seasons.
- ➢ In terms of productivity and yield prediction, we will establish yearly monitoring of field samples in each of the region's departments, allowing us to estimate yield directly after harvesting across multiple years and extrapolate to regional scales.

- We also intend to investigate and promote sustainable agronomic practices that increase soil fertility and production, such as integrated soil fertility management, agroforestry, and conservation agriculture. This study will assess the effectiveness of these methods in the specific agroecological context of Gontougo.
- Future research might also focus on developing and testing climate-resistant yam cultivars that are more suited to the changing climatic conditions in the Gontougo region. These include varieties with better drought tolerance, pest resistance, and shorter growth cycles.

In short, future perspectives on yam production hazards in the Gontougo region should use a multidisciplinary approach that considers agronomic, economic, social, and policy aspects. This comprehensive approach will aid in the development of tailored interventions that can successfully minimize risks and strengthen the resilience of the region's yam production systems.

NB: In order to promote the results of this doctoral research and ensure that they are put to good use by farmers, policy-makers, the scientific community and the general public, we will put in place an effective global communication strategy.

- ✓ Firstly, we will produce a concise, easy-to-understand summary of the research results in the form of an infographic highlighting the key points of the findings and disseminate it to the country's agricultural agencies and local authorities.
- ✓ Secondly, to work with agricultural extension services and other outreach organisations to translate our research findings into practical recommendations and resources for farmers.
- ✓ Engage with stakeholders such as farmers' associations, government agencies and food security advocacy groups to share findings and discuss potential applications of our research in practical contexts.
- ✓ Publish in journals widely read by policy makers and the general public to increase the visibility of the work and make it more accessible.
- ✓ Present the results at relevant conferences and events related to our field of study in order to reach a targeted audience of farmers, policy makers and other stakeholders interested in the research topic.
- ✓ Finally, exploit social media platforms to share the research findings and connect with a wider audience and spark conversations around the research topic.

This is how we will implement these strategies to effectively promote the results of our doctoral research.

REFERENCES

A. Faye, I. Camara, M. Noblet, & S. Mboup. (2019). *Evaluation de la vulnérabilité du secteur agricole à la variabilité et aux changements climatiques dans la région de Fatick.* www.climateanalytics.org/publications.

Abubakar, A., Yusoff Ishak, M., Makmom, A. A., & Danhassan, S. S. (2021). Climate Change and Smallholder Farmers in the Sahel: Adaptation and Resilience. *African Scholar Journal of Agriculture and Agricultural Tech. (JAAT-1*.

Abulibdeh, A. (2021). Analysis of urban heat island characteristics and mitigation strategies for eight arid and semi-arid gulf region cities. *Environmental Earth Sciences*, *80*(7). https://doi.org/10.1007/s12665-021-09540-7

Adeleke Aturamu, O., Anthony Thompson, O., & Olabimpe Banke, A. (2021). FORECASTING THE EFFECT OF CLIMATE VARIABILITY ON YAM YIELD IN RAIN FOREST AND GUINEA SAVANNAH AGRO-ECOLOGICAL ZONE OF NIGERIA. *Original Research Article Journal of Global Agriculture and Ecology*, *11*(4), 1–12. https://www.researchgate.net/publication/354282449

Adeyeri, O. E., Zhou, W., Wang, X., Zhang, R., Laux, P., Ishola, K. A., & Usman, M. (2022). The trend and spatial spread of multisectoral climate extremes in CMIP6 models. *Scientific Reports*, *12*(1). https://doi.org/10.1038/s41598-022-25265-4

Adifon, F. H., Atindogbé, G., Orou Bello, D., Balogoun, I., Yabi, I., Dossou, J., Ahoton, L., & Saïdou, A. (2020). Effect of Climate Variability on Yams Production in Central and Northern Benin. *American Journal of Climate Change*, *09*(04), 423–440. https://doi.org/10.4236/ajcc.2020.94027

Adifon, F. H., Yabi, I., Vissoh, P., Balogoun, I., Dossou, J., & Saïdou, A. (2019). Yam: ecology, cropping systems and food uses in tropical Africa. A literature review. In *Cahiers Agricultures* (Vol. 28). EDP Sciences. https://doi.org/10.1051/cagri/2019022

Agbazo, M. N., Adéchinan, J. A., N'gobi, G. K., & Bessou, J. (2021). Analysis and Predictability of Dry Spell Lengths Observed in Synoptic Stations of Benin Republic (West Africa). *American Journal of Climate Change*, *10*(04), 597–618. https://doi.org/10.4236/ajcc.2021.104030

Aighewi, Asiedu, R., Maroya, N., & Balogun, M. (2015). Improved propagation methods to raise the productivity of yam (Dioscorea rotundata Poir.). *Food Security*, *7*(4), 823–834. https://doi.org/10.1007/s12571-015-0481-6

Aighewi, B., Maroya, N., Kumar, P. L., Balogun, M., Aihebhoria, D., Mignouna, D., & Asiedu, R. (2021). Seed yam production using high-quality minitubers derived from plants established with vine cuttings. *Agronomy*, *11*(5). https://doi.org/10.3390/agronomy11050978

Aka, K. S. R., Akpavi, S., & Dibi, N. H. (2024). Yam Production-Related Agro-climatological Risks and Yam Yield Modeling in Côte d'Ivoire: A Review. *Journal of Agricultural Science*, *16*(5), 42. https://doi.org/10.5539/jas.v16n5p42

Aka, K. S. R., Akpavi, S., Dibi, N. H., Kabo-Bah, A. T., Gyilbag, A., & Boamah, E. (2023). Toward understanding land use land cover changes and their effects on land surface temperature in yam production area, Côte d'Ivoire, Gontougo Region, using remote sensing and machine learning tools (Google Earth Engine). *Frontiers in Remote Sensing*, *4*. https://doi.org/10.3389/frsen.2023.1221757

Aka, K. S. R., Dibi, H. N., Koffi, J. N., & Bohoussou, C. N. (2022). Land Cover Dynamics and Assessment of the Impacts of Agricultural Pressures on Wetlands Based on Earth Observation Data: Case of the Azagny Ramsar Site in Southern Côte d'Ivoire. *Journal of Geoscience and Environment Protection*, *10*(05), 43–61. https://doi.org/10.4236/gep.2022.105004

Akinsanola, A. A., Ogunjobi, K. O., Abolude, A. T., & Salack, S. (2021). Projected changes in wind speed and wind energy potential over West Africa in CMIP6 models. *Environmental Research Letters*, *16*(4). https://doi.org/10.1088/1748-9326/abed7a

Akomolafe, G. F., & Rosazlina, R. (2022). Land use and land cover changes influence the land surface temperature and vegetation in Penang Island, Peninsular Malaysia. *Scientific Reports*, *12*(1). https://doi.org/10.1038/s41598-022-25560-0

Akoroda, M. O. (1993). Yams, Dioscorea spp. In *Genetic Improvement of Vegetable Crops* (pp. 717–733). Elsevier. https://doi.org/10.1016/B978-0-08-040826-2.50053-9

Alhassane, A., Salack, S., Ly, M., Lona, I., Traoré, S. B., & Sarr, B. (2013). Évolution des risques agroclimatiques associés aux tendances récentes du régime pluviométrique en Afrique de l'Ouest soudano-sahélienne. *Science et Changements Planetaires - Secheresse*, *24*(4), 282–293. https://doi.org/10.1684/sec.2013.0400

Amani, M., Ghorbanian, A., Ahmadi, S. A., Kakooei, M., Moghimi, A., Mirmazloumi, S. M., Moghaddam, S. H. A., Mahdavi, S., Ghahremanloo, M., Parsian, S., Wu, Q., & Brisco, B. (2020). Google Earth Engine Cloud Computing Platform for Remote Sensing Big Data Applications: A Comprehensive Review. *IEEE Journal of Selected Topics in Applied Earth Observations and Remote Sensing*, *13*. https://doi.org/10.1109/JSTARS.2020.3021052

Anatole, B. G., Fréderic, K. K., & Maxime, B. N. K. (2017). Culture de l'igname au Centre-Est de la Côte d'ivoire : contraintes, caractéristiques sociodémographiques et agronomiques. *Journal of Applied Biosciences*, *110*(1), 10701. https://doi.org/10.4314/jab.v110i1.1

Andres, C., AdeOluwa, O. O., & Bhullar, G. S. (2016). Yam (Dioscorea spp.). In *Encyclopedia of Applied Plant Sciences* (Vol. 3, pp. 435–441). Elsevier Inc. https://doi.org/10.1016/B978-0-12-394807-6.00177-5

Aniah, P., Bawakyillenuo, S., Codjoe, S. N. A., & Dzanku, F. M. (2023). Land use and land cover change detection and prediction based on CA-Markov chain in the savannah ecological zone of Ghana. *Environmental Challenges*, *10*. https://doi.org/10.1016/j.envc.2022.100664

Anogbro P. (2015). *Variabilité climatique et culture de l'igname dans le perimètre agricole de Bouaké-commune. Mémoire de Master, Université Alassane Ouattara, Bouaké-Côte d'Ivoire. 105p.*

Anogbro Pascal. (2015). *VARIABILITE CLIMATIQUE ET CULTURE DE L'IGNAME DANS LE PERIMETRE AGRICOLE DE BOUAKE-COMMUNE*. UNIVERSITE ALASSANE OUATTARA.

Aprile, F., & Lorandi, R. (2012). Evaluation of Cation Exchange Capacity (CEC) in Tropical Soils Using Four Different Analytical Methods. *Journal of Agricultural Science*, *4*(6). https://doi.org/10.5539/jas.v4n6p278

Ashane, & Senanayake. (2023). Developing a two-decadal time-record of rice field maps using Landsat-derived multi-index image collections with a random forest classifier: A Google Earth Engine based approach. *Information Processing in Agriculture*, *23*, 1–35. https://doi.org/10.1016/j.inpa.2023.02.009

Asselin, O., Leduc, M., Paquin, D., Winger, K., Luca, A. Di, Bukovsky, M., Music, B., & Giguère, M. (2022). *Climate Response to Severe Forestation: A Regional Climate Model Intercomparison Study*. https://doi.org/10.5194/egusphere-2022-291

B. DABIN, N. L. et G. RIOU. (1960). *ORSTOM: CARTE PEDOLOGlQUE DE LA COTE D'IVUIRE 1-2.000.800 PUBLIEE PAR LE SECRETARIAT D'ETAT A L'AGRICULTURE.*

Banko, G. (1998). *A Review of Assessing the Accuracy of Classifications of Remotely Sensed Data and of Methods Including Remote Sensing Data in Forest Inventory*. www.iiasa.ac.at

BARI, A. S. M. F., LAMB, D., MACFARLANE, G. R., & RAHMAN, M. M. (2022). Influence of soil properties, particle size fraction and mineralogy on leaching potential of arsenic and antimony in abandoned mine soils. *Pedosphere*, *33*(5), 744–753. https://doi.org/10.1016/j.pedsph.2022.07.005

Barriguinha, A., Jardim, B., de Castro Neto, M., & Gil, A. (2022). Using NDVI, climate data and machine learning to estimate yield in the Douro wine region. *International Journal of Applied Earth Observation and Geoinformation*, *114*. https://doi.org/10.1016/j.jag.2022.103069

Batjes, N. H. (1996). Total carbon and nitrogen in the soils of the world. *European Journal of Soil Science*, *47*(2), 151–163. https://doi.org/10.1111/j.1365-2389.1996.tb01386.x

BCEAO. (2017). *Banque Centrale des Etats de l'Afrique de l'Ouest. Annuaire Statistique 2017 de renforcement de la disponibilité de l'information statistique dans les pays de l'Union Economique et Monétaire Ouest Africaine (UEMOA). ISSN 0850 57 05.*

Benmecheta, A. (2016). *Estimation de la température de surface a partir de l'imagerie satellitale; validation sur une zone côtière d'Algérie*. https://tel.archives-ouvertes.fr/tel-01565894

Bi, D., Dix, M., Marsland, S., O'farrell, S., Sullivan, A., Bodman, R., Law, R., Harman, I., Srbinovsky, J., Rashid, H. A., Dobrohotoff, P., Mackallah, C., Yan, H., Hirst, A., Savita, A., Dias, F. B., Woodhouse, M., Fiedler, R., & Heerdegen, A. (2020). Configuration and spin-up of ACCESS-CM2, the new generation Australian Community Climate and Earth System Simulator Coupled Model. *Journal of Southern Hemisphere Earth Systems Science*, *70*(1), 225–251. https://doi.org/10.1071/ES19040

Bintou, D. (2010). *Perceptions endogenes, analyses agroclimatiques et stratégies d'adaptation aux variabilités et changements climatiques des populations dans trois zones climatiques du burkina faso. Mémoire de fin d'étude d'ingenieur en Agrométéorologie, AGRHYMET. 51P.*

Bliefernicht, J., Salack, S., Waongo, M., Annor, T., Laux, P., & Kunstmann, H. (2021). Towards a historical precipitation database for West Africa: Overview, quality control and harmonization. *International Journal of Climatology*. https://doi.org/10.1002/joc.7467

Bobadoye, AO., Ogara, WO., Ouma, GO., & Onono, J. (2016). Assessing Climate Change Adaptation Strategies among Rural Maasai pastoralist in Kenya. *American Journal of Rural Development*, *4*(6), 120–128. https://doi.org/10.12691/ajrd-4-6-1

Boucher, O., Servonnat, J., Albright, A. L., Aumont, O., Balkanski, Y., Bastrikov, V., Bekki, S., Bonnet, R., Bony, S., Bopp, L., Braconnot, P., Brockmann, P., Cadule, P., Caubel, A., Cheruy, F., Codron, F., Cozic, A., Cugnet, D., D'Andrea, F., … Vuichard, N. (2020). Presentation and Evaluation of the IPSL-CM6A-LR Climate Model. *Journal of Advances in Modeling Earth Systems*, *12*(7). https://doi.org/10.1029/2019MS002010

Bremner, J. M. (1960). Determination of nitrogen in soil by the Kjeldahl method. In *J. Agric. Sri* (Vol. 55, Issue 1).

Bremner, J. M. (1965). Total Nitrogen. *No. J-4712 of the Iowa Agr. and Home Econ. Exp. Sta., Ames, Iowa. Project No. 1070. Contribution from the Department of Agronomy.*, 1149–1178.

Brou, T., Akindès, F., Télesphore Brou, Y., & Bigot, S. (2005). Étude originale La variabilité climatique en Côte d'Ivoire : entre perceptions sociales et réponses agricoles. *Cahiers Agricultures*, *14*(6), 533–540. https://doi.org/10.13140/2.1.5174.3368

Carlson, T. N., & Riziley, D. A. (1997). *On the Relation between NDVI, Fractional Vegetation Cover, and Leaf Area Index*.

Cedric, L. S., Adoni, W. Y. H., Aworka, R., Zoueu, J. T., Mutombo, F. K., Krichen, M., & Kimpolo, C. L. M. (2022a). Crops yield prediction based on machine learning models: Case of West African countries. *Smart Agricultural Technology, 2*, 100049. https://doi.org/10.1016/j.atech.2022.100049

Cedric, L. S., Adoni, W. Y. H., Aworka, R., Zoueu, J. T., Mutombo, F. K., Krichen, M., & Kimpolo, C. L. M. (2022b). Crops yield prediction based on machine learning models: Case of West African countries. *Smart Agricultural Technology*, *2*, 100049. https://doi.org/10.1016/j.atech.2022.100049

Cheng, M., Zhang, M., Veldhuizen, R. M. van, & Knight, C. W. (2021). Growing Season and Phenological Stages of Small Grain Crops in Response to Climate Change in Alaska. *American Journal of Climate Change*, *10*(04), 490–511. https://doi.org/10.4236/ajcc.2021.104025

Ciesielski, H., Sterckeman, T., Santerne, M., & Willery, J. (1997). *A comparison between three methods for the determination of cation exchange capacity and exchangeable cations in soils*. https://hal.science/hal-00885821

Ciesielski, H., Sterckeman, T., Santerne, M., Willery, J., Sterckeman, T., & Willery, J. P. (1997). *Determination of cation exchange capacity and exchangeable cations in soils by means of cobalt hexamine trichloride. Effects of experimental conditions* (Vol. 17, Issue 1). https://hal.science/hal-00885820

CILSS. (2021). *Permanent Inter-State Committee for Drought Control in the Sahel. An article published by Casimir Djezou on 23 November 2021 at 17:20 on the website fratmat.info; Consulted online on 7 March 2022.* www.fratmat.info/article/216470/conomie/lutte-contre-linsecurite-alimentaire-le-cilss prepare-un-important-projet-pour-quatre-regions-de-la-cote-divoire

Congalton, R. G. (1991). *A Review of Assessing the Accuracy of Classifications of Remotely Sensed Data* (Vol. 37).

Courault, D., Hossard, L., Demarez, V., Dechatre, H., Irfan, K., Baghdadi, N., Flamain, F., & Ruget, F. (2021). STICS crop model and Sentinel-2 images for monitoring rice growth and yield in the Camargue region. *Agronomy for Sustainable Development, 41*(4). https://doi.org/10.1007/s13593-021-00697-w

Croitoru, A. E., Chiotoroiu, B. C., Ivanova Todorova, V., & Torică, V. (2013). Changes in precipitation extremes on the Black Sea Western Coast. *Global and Planetary Change, 102,* 10–19. https://doi.org/10.1016/j.gloplacha.2013.01.004

CUNY, P., PLANCHERON, F., BIO, A., KOUAKOU, E., & MORNEAU, F. (2023). La forêt et la faune de Côte d'Ivoire dans une situation alarmante – Synthèse des résultats de l'Inventaire forestier et faunique national. *BOIS & FORETS DES TROPIQUES*, *355*, 47–72. https://doi.org/10.19182/bft2023.355.a36939

Dahan, K. S., Dibi N'da, H., & Kaudjhis, C. A. (2021). Dynamique spatio-temporelle des feux de 2001 à 2019 et dégradation du couvert végétal en zone de contact foret-savane, Département de Toumodi, Centre de la Côte d'Ivoire. In *Afrique SCIENCE* (Vol. 19, Issue 2). https://ladsweb.modaps.eosdis.nasa.gov/

Dahan, K. S., & Kasei, R. A. (2022). Overview of Researches on Bush Fires for Natural Resources and Environmental Management in Ghana: A Review. *Environment and Natural Resources Research*, *12*(1), 48. https://doi.org/10.5539/enrr.v12n1p48

Dahan, K. S., Kasei, R. A., Husseini, R., Said, M. Y., & Rahman, Md. M. (2023). Towards understanding the environmental and climatic changes and its contribution to the spread of wildfires in Ghana using remote sensing tools and machine learning (Google Earth Engine). *International Journal of Digital Earth*, *16*(1), 1300–1331. https://doi.org/10.1080/17538947.2023.2197263

Danquah, Danquah, F. O., Frimpong, F., Dankwa, K. O., Weebadde, C. K., Ennin, S. A., Asante, M. O. O., Brempong, M. B., Dwamena, H. A., Addo-Danso, A., Nyamekye, D. R., Akom, M., & Opoku, A. Y. (2022). Sustainable Intensification and Climate-Smart Yam Production for Improved Food Security in West Africa: A Review. In *Frontiers in Agronomy* (Vol. 4). Frontiers Media S.A. https://doi.org/10.3389/fagro.2022.858114

Davi, H., Soudani, K., Deckx, T., Dufrene, E., Le Dantec, V., & François, C. (2006). Estimation of forest leaf area index from SPOT imagery using NDVI distribution over forest stands. *International Journal of Remote Sensing*, *27*(5), 885–902. https://doi.org/10.1080/01431160500227896

Davis, C. L., Hoffman, M. T., & Roberts, W. (2016). Recent trends in the climate of Namaqualand, a megadiverse arid region of South Africa. *South African Journal of Science*, *112*(3–4), 1–9. https://doi.org/10.17159/sajs.2016/20150217

de Santana, F. B., Hall, R. L., Lowe, V., Browne, M. A., Grunsky, E. C., Fitzsimons, M. M., Gallagher, V., & Daly, K. (2023). A systematic approach to predicting and mapping soil particle size distribution from unknown samples using large mid-infrared spectral libraries covering large-scale heterogeneous areas. *Geoderma*, *434*. https://doi.org/10.1016/j.geoderma.2023.116491

De Vos, B., Lettens, S., Muys, B., & Deckers, J. A. (2007). Walkley-Black analysis of forest soil organic carbon: Recovery, limitations and uncertainty. *Soil Use and Management*, *23*(3), 221–229. https://doi.org/10.1111/j.1475-2743.2007.00084.x

Degila, J., Tognisse, I. S., Honfoga, A.-C., Calmette, S., Houetohossou, A., Ariel, F., Sodedji, K., Gérard, H., Avakoudjo, G., Peace, S., Tahi, G., & Assogbadjo, A. E. (2023). *A Survey on Digital Agriculture in Five West African Countries*. https://doi.org/10.20944/preprints202304.0831.v1

Dekoula, C. S., Kouame, B., N'goran, E. K., Yao, F. G., Ehounou, J.-N., & Soro, N. (2018). Impact De La Variabilité Pluviométrique Sur La Saison Culturale Dans La Zone De Production Cotonnière En Côte d'Ivoire. *European Scientific Journal, ESJ*, *14*(12), 143. https://doi.org/10.19044/esj.2018.v14n12p143

Delaune, M., Reiffsteck, M., & Feller, C. (1991). L'analyse granulométrique de sols et sédiments à l'aide du microgranulomètre « Sedigraph 5000 ET » Comparaison avec la méthode « pipette Robinson ». *Cah. Orstom, Sér. Pédol., XXVI, no 2,* 183–189.

Diallo, M. , A. ,. (2001). *Statistical analyse of agroclimatic parameters based on regional meteorological database. Technical Report. Centre Régional AGRHYMET,Niamey, Niger.*

Diancoumba, M., MacCarthy, D., Webber, H., Akinseye, F., Faye, B., Noulèkoun, F., Whitbread, A., Corbeels, M., & Worou, N. (2023). Scientific agenda for climate risk and impact assessment of West African cropping systems. In *Global Food Security* (Vol. 38). Elsevier B.V. https://doi.org/10.1016/j.gfs.2023.100710

Diarrassouba, D. (2019). Histoire et techniques de cultures du vivrier en Côte d'Ivoire, de la transformation à la commercialisation : le cas du manioc (1960-2000). *E-Phaïstos, VII–1*. https://doi.org/10.4000/ephaistos.4174

Dibi, E. B. K., Kouame, N., N'Goran, E. K., Kouakou, M. A., Kouame, J. M. Y., Essis, B. S., & N'zue, B. (2021). Response of the Yam Variety Krengle (Dioscorea rotundata) to Organo-mineral Fertilisation at Bouaké in Central of Côte d'Ivoire. *Journal of Agricultural Science*, *13*(6), 123. https://doi.org/10.5539/jas.v13n6p123

Dibi, Kouakou N'guessan, E., Wajda, M. E., Affian, K., & Af, K. (2008). *Apport de la télédétection au suivi de la déforestation dans le Parc National de la Marahoué (Côte d´Ivoire)* (Vol. 8, Issue 1). Breach Scientific Publishers.

Diby, L. N., Hgaza, V. K., Tié, T. B., Assa, A., Carsky, R., Girardin, O., Sangakkara, U. R., & Frossard, E. (2011). How does soil fertility affect yam growth? *Acta Agriculturae Scandinavica Section B: Soil and Plant Science, 61*(5), 448–457. https://doi.org/10.1080/09064710.2010.505578

Diby, L. N., Tie, B. T., Girardin, O., Sangakkara, R., & Frossard, E. (2011). Growth and Nutrient Use Efficiencies of Yams (Dioscorea spp.) Grown in Two Contrasting Soils of West Africa . *International Journal of Agronomy, 2011*, 1–8. https://doi.org/10.1155/2011/175958

Diulyale, K., André, S. B., Yaya, T., Tchoa, K., Nakpalo, S., Noémie, R., Daouda, K., & Mongomaké, K. (2019). Evaluation de la technique de surgreffage pour le rénouvellement des vieillissants vergers d'anacardier [Anacardium occidentale (L.)] dans la région du Gontougo en Côte d'Ivoire. *European Scientific Journal ESJ*, *15*(6). https://doi.org/10.19044/esj.2019.v15n6p304

Dobor, L., Barcza, Z., Hlásny, T., Árendás, T., Spitkó, T., & Fodor, N. (2016). Crop planting date matters: Estimation methods and effect on future yields. *Agricultural and Forest Meteorology, 223*. https://doi.org/10.1016/j.agrformet.2016.03.023

Dodd, D. E. S., & Jolliffe, I. T. (2001). Early detection of the start of the wet season in semiarid tropical climates of Western Africa. *International Journal of Climatology*, *21*(10), 1251–1262. https://doi.org/10.1002/joc.640

Dohrmann, R. (2006). Cation exchange capacity methodology III: Correct exchangeable calcium determination of calcareous clays using a new silver-thiourea method. *Applied Clay Science*, *34*(1–4), 47–57. https://doi.org/10.1016/j.clay.2006.02.010

Döscher, R., Acosta, M., Alessandri, A., Anthoni, P., Arneth, A., Arsouze, T., Bergman, T., Bernardello, R., Bousetta, S., Caron, L.-P., Carver, G., Castrillo, M., Catalano, F., Cvijanovic, I., Davini, P., Dekker, E., Doblas-Reyes, F. J., Docquier, D., Echevarria, P., … Zhang, Q. (2021). The EC-Earth3 Earth System Model for the Climate Model Intercomparison Project 6. *Geoscientific Model Development*. https://doi.org/10.5194/gmd-2020-446

Döscher, R., Acosta, M., Alessandri, A., Anthoni, P., Arsouze, T., Bergman, T., Bernardello, R., Boussetta, S., Caron, L. P., Carver, G., Castrillo, M., Catalano, F., Cvijanovic, I., Davini, P., Dekker, E., Doblas-Reyes, F. J., Docquier, D., Echevarria, P., Fladrich, U., … Zhang, Q. (2022). The EC-Earth3 Earth system model for the Coupled Model Intercomparison Project 6. *Geoscientific Model Development*, *15*(7), 2973–3020. https://doi.org/10.5194/gmd-15-2973-2022

Doumbia, S., Koko, L., & Aman, S. (2014). L'Introduction et la diffusion de la variété d'igname C18 en région centre de Côte d'Ivoire. *Journal of Applied Biosciences*, *80*(1), 7121. https://doi.org/10.4314/jab.v80i1.2

Doumbia, S., Touré, M., & Mahyao, A. (2006). *Étude originale Commercialisation de l'igname en Côte d'Ivoire : état actuel et perspectives d'évolution*.

Dpt Geographie, U. B. (2021). CARACTÉRISTIQUES PÉDO-GÉOLOGIQUES DU PAYSAGE ET APTITUDE CULTURALE DES TERRES A BÉOUMI (COTE D'IVOIRE). *Revue Ivoirienne de Géographie Des Savanes*, *11*(2521–2125), 1–23.

Du, Z., Zhang, X., Xu, X., Zhang, H., Wu, Z., & Pang, J. (2017). Quantifying influences of physiographic factors on temperate dryland vegetation, Northwest China. *Scientific Reports*, *7*. https://doi.org/10.1038/srep40092

Dufour, J.-M., & Dagenais, M. G. (1985). DURBIN-WATSON TESTS FOR SERIAL CORRELATION IN REGRESSIONS WITH MISSING OBSERVATIONS*. In *Journal of Econometrics* (Vol. 27).

Dunne, J. P., Horowitz, L. W., Adcroft, A. J., Ginoux, P., Held, I. M., John, J. G., Krasting, J. P., Malyshev, S., Naik, V., Paulot, F., Shevliakova, E., Stock, C. A., Zadeh, N., Balaji, V., Blanton, C., Dunne, K. A., Dupuis, C., Durachta, J., Dussin, R., … Zhao, M. (2020). The GFDL Earth System Model Version 4.1 (GFDL-ESM 4.1): Overall Coupled Model Description and Simulation Characteristics. *Journal of Advances in Modeling Earth Systems*, *12*(11). https://doi.org/10.1029/2019MS002015

Dzotsi, K. A., Basso, B., & Jones, J. W. (2013). Development, uncertainty and sensitivity analysis of the simple SALUS crop model in DSSAT. *Ecological Modelling*, *260*, 62–76. https://doi.org/10.1016/j.ecolmodel.2013.03.017

Egbebiyi, T. S., Lennard, C., Crespo, O., Mukwenha, P., Lawal, S., & Quagraine, K. (2019). Assessing future spatio-temporal changes in crop suitability and planting season over West Africa: Using the concept of crop-climate departure. *Climate*, *7*(9). https://doi.org/10.3390/cli7090102

Ema, E.-O. S., Obidiegwu, J. E., Chilaka, C. A., & Akpabio, E. M. (2023). Indigenous Food Yam Cultivation and Livelihood Practices in Cross River State, Nigeria. *World*, *4*(2), 314–332. https://doi.org/10.3390/world4020020

Enders, A., Vianna, M., Gaiser, T., Krauss, G., Webber, H., Srivastava, A. K., Seidel, S. J., Tewes, A., Rezaei, E. E., & Ewert, F. (2023). SIMPLACE - a versatile modelling and simulation framework for sustainable crops and agroecosystems. *In Silico Plants*, *5*(1). https://doi.org/10.1093/insilicoplants/diad006

Engdaw, M. M., Ballinger, A. P., Hegerl, G. C., & Steiner, A. K. (2022). Changes in temperature and heat waves over Africa using observational and reanalysis data sets. *International Journal of Climatology*, *42*(2), 1165–1180. https://doi.org/10.1002/joc.7295

Enten François. (2017). *Les Systèmes d'Alerte Précoce (SAP) en éthiopie comme jeux d'acteurs, de normes et d'échelles* [Doctorat]. École des Hautes Études en Sciences Sociales.

FAO. (2015a). *Climate change and food security: risks and responses*. www.fao.org/publications

FAO. (2015b). *INTERGOVERNMENTAL TECHNICAL PANEL ON SOILS: Status of the World's Soil Resources - Main report. FAO, Rome, Italy.*

FAO. (2017). *Évaluation du Programme de la FAO en Côte d'Ivoire*.

FAO. (2019). *Standard operating procedure for soil organic carbon Walkley-Black method Titration and colorimetric method.*

FAO, I. U. W. and W. (2021). The State of Food Security and Nutrition in the World 2021. Transforming food systems for food security, improved nutrition and affordable healthy diets for all. In *The State of Food Security and Nutrition in the World 2021*. FAO, IFAD, UNICEF, WFP and WHO. https://doi.org/10.4060/cb4474en

FAO, IFAD, UNICEF, WFP, & WHO. (2022). The State of Food Security and Nutrition in the World 2022. Repurposing food and agricultural policies to make healthy diets more affordable. Rome, FAO. In *The State of Food Security and Nutrition in the World 2022*. FAO. https://doi.org/10.4060/cc0639en

FAOSTAT. (2023). *Food and Agriculture Organization of the United Nations Statistical Database. Data accessed on March 21, 2023*. https://www.fao.org/faostat/en/#data

Faour, G., Mhawej, M., & Fayad, A. (2016). Detecting changes in vegetation trends in the middle east and north Africa (MENA) region using spot vegetation. *CyberGeo*, *2016*(April). https://doi.org/10.4000/cybergeo.27620

Fayaz, A., Kumar, Y. R., Lone, B. A., Kumar, S., Dar, Z. A., Rasool, F., Abidi, I., Nisar, F., & Kumar, A. (2021). Crop Simulation Models: A Tool for Future Agricultural Research and Climate Change. *Asian Journal of Agricultural Extension, Economics & Sociology*, 146–154. https://doi.org/10.9734/ajaees/2021/v39i630602

Faye, B., Webber, H., Gaiser, T., Müller, C., Zhang, Y., Stella, T., Latka, C., Reckling, M., Heckelei, T., Helming, K., & Ewert, F. (2023). Climate change impacts on European arable crop yields: Sensitivity to assumptions about rotations and residue management. *European Journal of Agronomy*, *142*. https://doi.org/10.1016/j.eja.2022.126670

Félicia, J., Guessan, N. ', Carine, A., Robert, O., Depo, N. ', Robert N'depo, O., Cherif, M., Johnson, F., Fernand, K., Kassi, J.-M., Carina N'guessan, A., Silue, N., Akesse, E. N., Kone, D., & Mauricette N'goran, O. (2017). Inventaire des insectes ravageurs du verger anacardier dans les régions de Bounkani, Gontougo et Indénie-Djablun au Nord-Est en Côted'Ivoire. In *Afrique SCIENCE* (Vol. 13, Issue 2). http://www.afriquescience.info

Felix, F., Danquah Eric, O., Kwesi, A. A., Ama, E. S., Henry, A., & Norbert, M. (2020). Demonstrating the efficacy of existing yam technologies in the Forest-Savannah transition zone of Ghana. *Journal of Agricultural Science and Practice*, *5*(2), 2536–7072. https://doi.org/10.31248/JASP2020.193

Feller, & Christian. (1993). *Organic inputs, soil organic matter and functional soil organic compartments in low-activity clay soils in tropical zones*. https://www.researchgate.net/publication/319542859

Fernández-Ugalde, O., Jones, A., & Meuli, R. G. (2020). Comparison of sampling with a spade and gouge auger for topsoil monitoring at the continental scale. *European Journal of Soil Science*, *71*(2), 137–150. https://doi.org/10.1111/ejss.12862

Filho, W. L. N. O. D. A. L. A. I. da S. (2021). *African Handbook of Climate Change Adaptation* (W. L. N. O. D. A. L. A. I. da S. Filho, Ed.). Springer.

Francou, Cédric. (2003). Stabilisation de la matière organqiue au cours du compostage de déchets urbains: Influence de la nature des déchets et du procédé de compostage - Recherche d'indicateurs pertinents. *Ecole Doctorale ABIES*, *Doctorat*, 289.

Frossard, E., Aighewi, B. A., Aké, S., Barjolle, D., Baumann, P., Bernet, T., Dao, D., Diby, L. N., Floquet, A., Hgaza, V. K., Ilboudo, L. J., Kiba, D. I., Mongbo, R. L., Nacro, H. B., Nicolay, G. L., Oka, E., Ouattara, Y. F., Pouya, N., Senanayake, R. L., … Traoré, O. I. (2017). The challenge of improving soil fertility in yam cropping systems of West Africa. In *Frontiers in Plant Science* (Vol. 8). Frontiers Media S.A. https://doi.org/10.3389/fpls.2017.01953

Funk, C., Peterson, P., Landsfeld, M., Pedreros, D., Verdin, J., Shukla, S., Husak, G., Rowland, J., Harrison, L., Hoell, A., & Michaelsen, J. (2015). The climate hazards infrared precipitation with stations - A new environmental record for monitoring extremes. *Scientific Data*, *2*(June 2016). https://doi.org/10.1038/sdata.2015.66

Geng, J., Tan, Q., Lv, J., & Fang, H. (2024). Assessing spatial variations in soil organic carbon and C:N ratio in Northeast China's black soil region: Insights from Landsat-9 satellite and crop growth information. *Soil and Tillage Research*, *235*(September), 105897. https://doi.org/10.1016/j.still.2023.105897

Georganos, S., Abdi, A. M., Tenenbaum, D. E., & Kalogirou, S. (2017). Examining the NDVI-rainfall relationship in the semi-arid Sahel using geographically weighted regression. *Journal of Arid Environments*, *146*, 64–74. https://doi.org/10.1016/j.jaridenv.2017.06.004

Ghaderizadeh, S., Abbasi-Moghadam, D., Sharifi, A., Tariq, A., & Qin, S. (2022). Multiscale Dual-Branch Residual Spectral-Spatial Network With Attention for Hyperspectral Image Classification. *IEEE Journal of Selected Topics in Applied Earth Observations and Remote Sensing*, *15*, 5455–5467. https://doi.org/10.1109/JSTARS.2022.3188732

Ghayour, L., Neshat, A., Paryani, S., Shahabi, H., Shirzadi, A., Chen, W., Al-Ansari, N., Geertsema, M., Amiri, M. P., Gholamnia, M., Dou, J., & Ahmad, A. (2021). Performance evaluation of sentinel-2 and landsat 8 OLI data for land cover/use classification using a comparison between machine learning algorithms. *Remote Sensing*, *13*(7). https://doi.org/10.3390/rs13071349

Ghosh, S., Kumar, D., & Kumari, R. (2022). Cloud-based large-scale data retrieval, mapping, and analysis for land monitoring applications with Google Earth Engine (GEE). *Environmental Challenges*, *9*. https://doi.org/10.1016/j.envc.2022.100605

Giannini, A., Ilboudo Nébié, E. K., Ba, D., & Ndiaye, O. (2021). Livelihood Strategies Shape Vulnerability of Households' Food Security to Climate in Senegal. *Frontiers in Climate*, *3*. https://doi.org/10.3389/fclim.2021.731036

Gogoi, P. P., Vinoj, V., Swain, D., Roberts, G., Dash, J., & Tripathy, S. (2019). Land use and land cover change effect on surface temperature over Eastern India. *Scientific Reports*, *9*(1). https://doi.org/10.1038/s41598-019-45213-z

Goldfeld, S. M., & Quandt, R. E. (1965). Some Tests for Homoscedasticity. *Journal of the American Statistical Association*, *60*(310), 539–547. https://doi.org/10.1080/01621459.1965.10480811

Gonçalves, E., Castro, J., Araújo, J., & Heineck, T. (2018). A Systematic Literature Review of iStar extensions. *Journal of Systems and Software*, *137*, 1–33. https://doi.org/10.1016/j.jss.2017.11.023

Gou, y., Louis, V., Roberts, J. F., Rodriguez-Veiga P., & da Conceicao Bishopo, P. (2022). Near Real-Time Change Detection System Using Sentinel-2 and Machine Learning_ A Test for Mexican and Colombian Forests _ Enhanced Reader. *Remote Sensing*, *14, 707*.(https://doi.org/10.3390/rs14030707), 1–21.

Guarin, J. R., Martre, P., Ewert, F., Webber, H., Dueri, S., Calderini, D., Reynolds, M., Molero, G., Miralles, D., Garcia, G., Slafer, G. A., Giunta, F., Pequeno, D. N. L., Stella, T., Ahmed, M., Alderman, P. D., Basso, B., Berger, A. G., Bindi, M., … Asseng, S. (2023). A high-yielding traits experiment for modeling potential production of wheat: field experiments and AgMIP-Wheat multi-model simulations. In *Open Data Journal for Agricultural Research* (Vol. 9). https://agmip.org/

Gutjahr, O., Putrasahan, D., Lohmann, K., Jungclaus, J. H., Von Storch, J. S., Brüggemann, N., Haak, H., & Stössel, A. (2019). Max Planck Institute Earth System Model (MPI-ESM1.2) for the High-Resolution Model Intercomparison Project (HighResMIP). *Geoscientific Model Development*, *12*(7), 3241–3281. https://doi.org/10.5194/gmd-12-3241-2019

Guttman, N. B. (1999). Accepting the standardized precipitation index: A calculation algorithm. *Journal of the American Water Resources Association*, *35*(2), 311–322. https://doi.org/10.1111/j.1752-1688.1999.tb03592.x

Gweyi-Onyango, J. P., Sakha, M. A., & Jefwa, J. (2021). Agricultural Interventions to Enhance Climate Change Adaptation of Underutilized Root and Tuber Crops. In *African Handbook of Climate Change Adaptation: With 610 Figures and 361 Tables* (pp. 61–86). Springer International Publishing. https://doi.org/10.1007/978-3-030-45106-6_40

Harouna, N. D. A., Abou-Soufianou, S., & Boubacar, Y. (2019). Insécurité Alimentaire des Ménages Agricoles et Stratégies de Résilience au Sahel : Cas de la Vallée de Goulbi Maradi, Niger. *European Scientific Journal ESJ*, *15*(18). https://doi.org/10.19044/esj.2019.v15n18p96

Harrison, L., Landsfeld, M., Husak, G., Davenport, F., Shukla, S., Turner, W., Peterson, P., & Funk, C. (2022). Advancing early warning capabilities with CHIRPS-compatible NCEP GEFS precipitation forecasts. *Scientific Data*, *9*(1), 1–13. https://doi.org/10.1038/s41597-022-01468-2

Hastie, T., Tibshirani, R., & Friedman, J. (2017). *The Elements of Statistical Learning: Data Mining, Inference, and Prediction* (Trevor Hastie, Robert Tibshirani, & J. Friedman, Eds.; Springer S). Springer Nature. http://www-stat.stanford.edu/ElemStatLearn%0AIt

He, Y., DeSutter, T., Prunty, L., Hopkins, D., Jia, X., & Wysocki, D. A. (2012). Evaluation of 1:5 soil to water extract electrical conductivity methods. *Geoderma, 185–186*, 12–17. https://doi.org/10.1016/j.geoderma.2012.03.022

Heller, O., Kiba, D. I., Zida, K. W.-D., Schneider, K., Valérie Kouame, H. K., Traoré, O. Y. A., Siegrist, M., & Frossard, E. (2022). Interdisciplinary Assessment of Market Oriented Yam Cultivation in Semi-arid Burkina Faso. *Frontiers in Agronomy*, *4*. https://doi.org/10.3389/fagro.2022.828305

Heumann, C., Michael, •, & Shalabh, S. (2016). *Introduction to Statistics and Data Analysis* (Springer International Publishing Switzerland, Ed.). Springer Nature. https://doi.org/DOI 10.1007/978-3-319-46162-5

Hgaza, V. (2010). *How fertilization affects yam (Dioscorea alata L.) growth and tuber yield across the years YAMSYS-Biophysical, institutional and economic drivers of sustainable soil use in yam systems for improved food security in West Africa View project Vision for Change (V4C) : Building Sustainable Cocoa Communities in Côte d'Ivoire View project*. http://regentinstruments.com

HUANG, R., HUANG, J. xi, ZHANG, C., MA, H. yuan, ZHUO, W., CHEN, Y. yi, ZHU, D. hai, WU, Q., & MANSARAY, L. R. (2020). Soil temperature estimation at different depths, using remotely-sensed data. *Journal of Integrative Agriculture*, *19*(1), 277–290. https://doi.org/10.1016/S2095-3119(19)62657-2

Ibrahim, B., Waongo, M., Sidibe, M., Sanfo, S., & Barry, B. (2022). Agroclimatological Characteristics of Rainy Seasons in Southwestern Burkina Faso during the 1970-2013 Period. *Atmospheric and Climate Sciences*, *12*(02), 330–357. https://doi.org/10.4236/acs.2022.122021

Inamdar, D., Leblanc, G., Soffer, R. J., & Kalacska, M. (2018). The correlation coefficient as a simple tool for the localization of errors in spectroscopic imaging data. *Remote Sensing*, *10*(2). https://doi.org/10.3390/rs10020231

IPCC. (2014). *Climate change 2014: Impacts, adaptation, and vulnerability. Working group II contribution to the fifth assessment report of the Intergovernmental Panel on Climate Change. Technical Report. Cambridge University Press, Cambridge, UK / New York, USA.* www.ipcc-wg2.gov/AR5

IPCC. (2022). Technical Summary. Contribution of Working Group II to the Sixth Assessment Report of the Intergovernmental Panel on Climate Change. In *Climate Change 2022 – Impacts, Adaptation and Vulnerability* (pp. 37–118). Cambridge University Press. https://doi.org/10.1017/9781009325844.002

IPCC. (2023a). Future Global Climate: Scenario-based Projections and Near-term Information. In *Climate Change 2021 – The Physical Science Basis* (pp. 553–672). Cambridge University Press. https://doi.org/10.1017/9781009157896.006

IPCC. (2023b). Human Influence on the Climate System. In *Climate Change 2021 – The Physical Science Basis* (pp. 423–552). Cambridge University Press. https://doi.org/10.1017/9781009157896.005

IPCC. (2023c). Ocean, Cryosphere and Sea Level Change. In *Climate Change 2021 – The Physical Science Basis* (pp. 1211–1362). Cambridge University Press. https://doi.org/10.1017/9781009157896.011

Javari, M. (2018). Daily rainfall nearest neighbor pattern using point data series in Iran. *Data in Brief*, *19*, 1432–1440. https://doi.org/10.1016/j.dib.2018.06.021

Jensen J. R. (1986). Introductory Digital Image Processing. A Remote Sensing Perspective, xv 379 pp. Englewood Cliffs: Prentice-Hall. *Geological Magazine*, *124(3)*(ISBN 0 13 500828 X.).

Jones, J. W., Antle, J. M., Basso, B., Boote, K. J., Conant, R. T., Foster, I., Godfray, H. C. J., Herrero, M., Howitt, R. E., Janssen, S., Keating, B. A., Munoz-Carpena, R., Porter, C. H., Rosenzweig, C., & Wheeler, T. R. (2017). Toward a new generation of agricultural system data, models, and knowledge products: State of agricultural systems science. *Agricultural Systems*, *155*, 269–288. https://doi.org/10.1016/j.agsy.2016.09.021

Jones, J. W., Hoogenboom, G., Porter, C. H., Boote, K. J., Batchelor, W. D., Hunt, L. A., Wilkens, P. W., Singh, U., Gijsman, A. J., & Ritchie, J. T. (2003). *The DSSAT cropping system model*. www.elsevier.com/locate/eja

K. F. Kouame. (2021). *Analyse comparative des données satellitaire d'estimation des précipitations en Côte d'Ivoire. These de Doctorat, mention physique. Obtenu au Centre d'Excellence Africain sur le Changement Climatique, la Biodiversité et l'Agriculture Durable (CEA-CCBAD), 151p.*

Kadio, N Hyppolite DIBI, Jephté N'dri Koffi, & Crystel, Bohoussou, N. (2022). Étude comparative de Sentinel-2 et Landsat-8 Oli à l'évaluation de l'occupation du sol du site Ramsar d'Azagny, Sud de la Côte d'Ivoire. In *Afrique SCIENCE* (Vol. 20, Issue 5). http://www.afriquescience.net

Kafi, K. M., Shafri, H. Z. M., & Shariff, A. B. M. (2014). An analysis of LULC change detection using remotely sensed data; A Case study of Bauchi City. *IOP Conference Series: Earth and Environmental Science*, *20*(1). https://doi.org/10.1088/1755-1315/20/1/012056

Kambou Diulyale, Toure Yaya, Kassi M. F., & Tchoa Kone. (2019). Structuration de la population agricole de la filière anacarde (Anacardium occidentale(L.) Anacardiaceae) et caractérisation des plantations dans les régions du Bounkani et du Gontougo en Côte d'Ivoire. *International Journal of Innovation and Applied Studies*, *ISSN 2028-9324 Vol. 26 No. 4 Jul. 2019, pp. 1159–1169*, 2–12.

Kargas, G., Londra, P., & Sotirakoglou, K. (2022). The Effect of Soil Texture on the Conversion Factor of 1:5 Soil/Water Extract Electrical Conductivity (EC1:5) to Soil Saturated Paste Extract Electrical Conductivity (ECe). *Water (Switzerland)*, *14*(4). https://doi.org/10.3390/w14040642

KEITA Djibril Sékou. (2014). *Effets des téguments de fèves de cacao sur la fertilité chimique d'un ferralsol et le rendement du manioc (Manihot esculenta crantz) au sud de la Côte d'Ivoire.* [Memoire de Master]. Université Félix Houphouët-Boigny.

Khan, M. R., de Bie, C. A. J. M., van Keulen, H., Smaling, E. M. A., & Real, R. (2010). Disaggregating and mapping crop statistics using hypertemporal remote sensing. *International Journal of Applied Earth Observation and Geoinformation*, *12*(1), 36–46. https://doi.org/10.1016/j.jag.2009.09.010

Khan, S. N., Khan, A. N., Tariq, A., Lu, L., Malik, N. A., Umair, M., Hatamleh, W. A., & Zawaideh, F. H. (2023). County-level corn yield prediction using supervised machine learning. *European Journal of Remote Sensing*, *56*(1). https://doi.org/10.1080/22797254.2023.2253985

Khee C. Rhee. (2001). *Determination of Total Nitrogen*.

Kim, S., Kwak, J., Kim, H. S., Jung, Y., & Kim, G. (2016). Full access nearest neighbor-genetic algorithm for downscaling of climate change data from GCMs. *Journal of Applied Meteorology and Climatology*, *55*(3), 773–789. https://doi.org/10.1175/JAMC-D-15-0100.1

Kim, Y. U., Webber, H., Adiku, S. G. K., Nóia Júnior, R. de S., Deswarte, J. C., Asseng, S., & Ewert, F. (2024). Mechanisms and modelling approaches for excessive rainfall stress on cereals: Waterlogging, submergence, lodging, pests and diseases. In *Agricultural and Forest Meteorology* (Vol. 344). Elsevier B.V. https://doi.org/10.1016/j.agrformet.2023.109819

Klein Tank, A. M., Zwiers, F. W., & Zhang, X. (2009). *Guidelines on Analysis of extremes in a changing climate in support of informed decisions for adaptation.* http://www.clivar.org/organization/etccdi/etccdi.php

Kohl, C., McIntosh, E. J., Unger, S., Haddaway, N. R., Kecke, S., Schiemann, J., & Wilhelm, R. (2018). Online tools supporting the conduct and reporting of systematic reviews and systematic maps: A case study on CADIMA and review of existing tools. *Environmental Evidence*, *7*(1). https://doi.org/10.1186/s13750-018-0115-5

Konaté, L. M., Ouattara, D. N., Kouamé, F. N., & Bakayoko, A. (2021). Diversity and uses by farmers of cashew (Anacardium occidentale l.) orchards weeds in Côte d'Ivoire. *Ethnobotany Research and Applications*, *21*. https://doi.org/10.32859/era.21.21.1-14

Koné, I., Kouadio, K.-K. H., Kouadio, E. N., Agyare, W. A., Owusu-Prempeh, N., Amponsah, W., & Gaiser, T. (2022). Assessment of soil fertility status in cotton-based cropping systems in Cote d'Ivoire. *Frontiers in Soil Science, 2*. https://doi.org/10.3389/fsoil.2022.959325

Kosamkar, P. K., & Kulkarni, V. Y. (2019). Agriculture Crop Simulation Models Using Computational Intelligence. *International Journal of Computer Engineering and Technology (IJCET)*, *10*(3), 134–140. http://www.iaeme.com/ijcet/issues.asp?JType=IJCET&VType=10&IType=3JournalImpactFactor

Kosari, A., Sharifi, A., Ahmadi, A., & Khoshsima, M. (2020). Remote sensing satellite's attitude control system: rapid performance sizing for passive scan imaging mode. *Aircraft Engineering and Aerospace Technology*, *92*(7), 1073–1083. https://doi.org/10.1108/AEAT-02-2020-0030

Kouadio, Y. H., Kouassi, K. N., Nimaga, D., N'dri, Y. D., & Amani, N. G. (2022). Impacts of Field Harvesting and Conservation Practices on the Physical Quality of Yam "Kponan" (Dioscorea cayenensis-rotundata) of Côte d'Ivoire. *Open Journal of Applied Sciences*, *12*(12), 1979–1994. https://doi.org/10.4236/ojapps.2022.1212138

Kouakou. (2019). Géotraçabilité de l'igname Kponan de Bondoukou. *Revue Des Sciences Sociales RSS-PASRES*. https://www.researchgate.net/publication/345743736

Kouakou, A. M., Yao, G. F., Brice Dibi, K. E., Mahyao, A., Lopez-Montes, A., Essis, B. S., N'zue, B., Kouamé, B., Adebola, P. O., Asfaw, A., & Asiedu, R. (2019). Yam Cropping System in Cote d'Ivoire: Current Practices and Constraints. *European Scientific Journal ESJ*, *15*(30). https://doi.org/10.19044/esj.2019.v15n30p278

Kouakou, K. P., Kouassi, C. A., & Anoh, K. P. (2019). Le Marche De Gros De L'igname Kponan A Abidjan (Côte D'ivoire). *European Scientific Journal ESJ*, *15*(26). https://doi.org/10.19044/esj.2019.v15n26p218

Kouakou, K. P., Kouassi, C. A., & Anoh, K. P. (2019). Le Marche De Gros De L'igname Kponan A Abidjan (Côte D'ivoire). *European Scientific Journal ESJ*, *15*(26). https://doi.org/10.19044/esj.2019.v15n26p218

Kouamé, B., Ehounou, J.-N., Kassin, K. E., Dekoula, C. S., Yao, G. F., N'goran, E. K., Kouakou, B. J., Koné, B., & Soro, N. (2018). Caractérisation Des Paramètres Agroclimatiques Clés De La Saison Culturale En Zone De Contact ForêtSavane De Côte-d'Ivoire. *European Scientific Journal ESJ*, *14*(36). https://doi.org/10.19044/esj.2018.v14n36p243

KOUAME Hgaza Kouassi Valerie. (2012). *Contribution à l'étude de la variabilité de la réponse de l'igname (Dioscorea alata) à la fertilisation minérale Commission du jury THESE Option: Ecophysiologie Végétale Laboratoire de Physiologie Végétale*.

Kouame, K., Kouame, K., Dje, K. B., & Kouadio, K. (2020). *Evaluation of five Satellite Based Precipitation Products over Côte d'Ivoire from 2001 to 2018*. http://www.met.rdg.ac.uk/~tamsat/.

Kouassi AM, Mamadou A, Ahoussi KE, & Biemi J. (2014). CONCEPTION DE MODÈLES STATISTIQUES A VARIABLES HYDROCHIMIQUES POUR LA PRÉDICTION DE LA CONDUCTIVITÉ ÉLECTRIQUE DES EAUX SOUTERRAINES. In *Larhyss Journal* (Vol. 20).

Koudahe, K., Kayode, A. J., Samson, A. O., Adebola, A. A., & Djaman, K. (2017). Trend Analysis in Standardized Precipitation Index and Standardized Anomaly Index in the Context of Climate Change in Southern Togo. *Atmospheric and Climate Sciences*, *07*(04), 401–423. https://doi.org/10.4236/acs.2017.74030

Koulibaly, A., Nicaise, A., Diomandé, M., Konaté, I., Traoré, D., Bill, R., & Kouadio, Y. J. (2016). Conséquences de la culture de l'anacardier (Anacardium occidentale L.) sur les caractéristiques de la végétation dans la région du Parc National de la Comoé (Côte d'Ivoire). *International Journal of Innovation and Applied Studies*, *17*(4), 1416–1426. http://www.ijias.issr-journals.org/

Kouman, K. D., Kabo-bah, A. T., Kouadio, B. H., & Akpoti, K. (2022). Spatio-Temporal Trends of Precipitation and Temperature Extremes across the North-East Region of Côte d'Ivoire over the Period 1981–2020. *Climate*, *10*(5), 74. https://doi.org/10.3390/cli10050074

Kpanou, M., Laux, P., Brou, T., Vissin, E., Camberlin, P., & Roucou, P. (2021). Spatial patterns and trends of extreme rainfall over the southern coastal belt of West Africa. *Theoretical and Applied Climatology*, *143*(1–2), 473–487. https://doi.org/10.1007/s00704-020-03441-8

Kumar, A., Schreiter, I. J., Wefer-Roehl, A., Tsechansky, L., Schüth, C., & Graber, E. R. (2016). Production and Utilization of Biochar From Organic Wastes for Pollutant Control on Contaminated Sites. *Environmental Materials and Waste: Resource Recovery and Pollution Prevention*, 91–116. https://doi.org/10.1016/B978-0-12-803837-6.00005-6

Kumar, Das, G., Shin, H. S., & Patra, J. K. (2017). Dioscorea spp. (A Wild Edible Tuber): A study on its ethnopharmacological potential and traditional use by the local people of similipal biosphere reserve, India. In *Frontiers in Pharmacology* (Vol. 8, Issue FEB). Frontiers Research Foundation. https://doi.org/10.3389/fphar.2017.00052

Kumar, M. (2021). Evaluation of phosphorus availability indices in acid Alfisols. *Annals of Plant and Soil Research*, *23*(4), 390–396. https://doi.org/10.47815/apsr.2021.10089

Langsdorf, S., Löschke, S., Möller, V., & Okem, A. (2022). *Climate Change 2022 Impacts, Adaptation and Vulnerability Working Group II Contribution to the Sixth Assessment Report of the Intergovernmental Panel on Climate Change.* www.ipcc.ch

Laux, P., Dieng, D., Portele, T. C., Wei, J., Shang, S., Zhang, Z., Arnault, J., Lorenz, C., & Kunstmann, H. (2021). A High-Resolution Regional Climate Model Physics Ensemble for Northern Sub-Saharan Africa. *Frontiers in Earth Science*, *9*. https://doi.org/10.3389/feart.2021.700249

Laux, P., Jäckel, G., Tingem, R. M., & Kunstmann, H. (2010). Impact of climate change on agricultural productivity under rainfed conditions in Cameroon-A method to improve attainable crop yields by planting date adaptations. *Agricultural and Forest Meteorology*, *150*(9), 1258–1271. https://doi.org/10.1016/j.agrformet.2010.05.008

Laux, P., Kunstmann, H., & Bárdossy, A. (2008). Predicting the regional onset of the rainy season in West Africa. *International Journal of Climatology*, *28*(3), 329–342. https://doi.org/10.1002/joc.1542

Lebot, & Dulloo. (2021). *Global strategy for the conservation and use of yam genetic resources: A report of the international treaty on plant genetic resources for food and agriculture*.

Lemessa, S. D., Watebaji, M. D., & Yismaw, M. A. (2019). Climate change adaptation strategies in response to food insecurity: The paradox of improved potato varieties adoption in eastern Ethiopia. *Cogent Food and Agriculture*, *5*(1). https://doi.org/10.1080/23311932.2019.1640835

Leng, G., & Hall, J. W. (2020). Predicting spatial and temporal variability in crop yields: An inter-comparison of machine learning, regression and process-based models. *Environmental Research Letters*, *15*(4). https://doi.org/10.1088/1748-9326/ab7b24

Li, L., Yu, Y., Tang, Y., Lin, P., Xie, J., Song, M., Dong, L., Zhou, T., Liu, L., Wang, L., Pu, Y., Chen, X., Chen, L., Xie, Z., Liu, H., Zhang, L., Huang, X., Feng, T., Zheng, W., … Wei, J. (2020). The Flexible Global Ocean-Atmosphere-Land System Model Grid-Point Version 3 (FGOALS-g3): Description and Evaluation. *Journal of Advances in Modeling Earth Systems*, *12*(9). https://doi.org/10.1029/2019MS002012

Liu, L., Danquah, E. O., Weebadde, C., Bessah, E., & Basso, B. (2021). Modeling soil organic carbon and yam yield under different agronomic management across spatial scales in Ghana. *Field Crops Research*, *263*. https://doi.org/10.1016/j.fcr.2020.108018

Mackallah, C., Chamberlain, M. A., Law, R. M., Dix, M., Ziehn, T., Bi, D., Bodman, R., Brown, J. R., Dobrohotoff, P., Druken, K., Evans, B., Harman, I. N., Hayashida, H., Holmes, R., Kiss, A. E., Lenton, A., Liu, Y., Marsland, S., Meissner, K., … Yeung, N. (2022). ACCESS datasets for CMIP6: Methodology and idealised experiments. *Journal of Southern Hemisphere Earth Systems Science*, *72*(2), 93–116. https://doi.org/10.1071/ES21031

Mackio, J. P. (2022). *Micro Catchment Water Harvesting in Arid and Semi-Arid Areas*. https://infonet-biovision.org/AnimalHealth/

Madeira, M., Auxtero, E., & Sousa, E. (2003). Cation and anion exchange properties of Andisols from the Azores, Portugal, as determined by the compulsive exchange and the ammonium acetate methods. *Geoderma*, *117*(3–4), 225–241. https://doi.org/10.1016/S0016-7061(03)00125-3

Malhi, G. S., Kaur, M., & Kaushik, P. (2021). Impact of climate change on agriculture and its mitigation strategies: A review. In *Sustainability (Switzerland)* (Vol. 13, Issue 3, pp. 1–21). MDPI. https://doi.org/10.3390/su13031318

Manikas, I., Ali, B. M., & Sundarakani, B. (2023). A systematic literature review of indicators measuring food security. *Agriculture & Food Security*, *12*(1), 10. https://doi.org/10.1186/s40066-023-00415-7

Marcos, J., Cornet, D., Bussière, F., & Sierra, J. (2011). Water yam (Dioscorea alata L.) growth and yield as affected by the planting date: Experiment and modelling. *European Journal of Agronomy*, *34*(4), 247–256. https://doi.org/10.1016/j.eja.2011.02.002

Marcos, J., Lacointe, A., Tournebize, R., Bonhomme, R., & Sierra, J. (2009). Water yam (Dioscorea alata L.) development as affected by photoperiod and temperature: Experiment and modeling. *Field Crops Research*, *111*(3), 262–268. https://doi.org/10.1016/j.fcr.2009.01.002

Matus, F. J., Escudey, M., Förster, J. E., Gutiérrez, M., & Chang, A. C. (2009). Is the Walkley-Black method suitable for organic carbon determination in Chilean volcanic soils? *Communications in Soil Science and Plant Analysis*, *40*(11–12), 1862–1872. https://doi.org/10.1080/00103620902896746

Mauritsen, T., Bader, J., Becker, T., Behrens, J., Bittner, M., Brokopf, R., Brovkin, V., Claussen, M., Crueger, T., Esch, M., Fast, I., Fiedler, S., Fläschner, D., Gayler, V., Giorgetta, M., Goll, D. S., Haak, H., Hagemann, S., Hedemann, C., … Roeckner, E. (2019). Developments in the MPI-M Earth System Model version 1.2 (MPI-ESM1.2) and Its Response to Increasing CO2. *Journal of Advances in Modeling Earth Systems*, *11*(4), 998–1038. https://doi.org/10.1029/2018MS001400

McKee Thomas B., N. J. D. and J. K. (1993). The Relationship of Drought Frequency and Duration to Time Scales. *Proceedings of the 8th Conference on Applied Climatology, 17–22 January. Anaheim, CA. Boston, MA, American Meteorological Society.*, *105*(8), 818–824. https://doi.org/10.1002/jso.23002

Mcmaster, G. S., & Wilhelm, W. W. (1997). AGRICULTURAL AND FOREST METEOROLOGY Growing degree-days: one equation, two interpretations. *Agricultural and Forest Meteorology*, *87*(1), 300.

Mekbib, F., Shimelis, H., Tewodros, M., Firew, M., Shimelis, H., & Endale, G. (2020). Interrelationship and Path analysis of Tuber yield and related traits in yam (Dioscorea spp.) from Ethiopia. *Research Journal of Pharmacognosy and Phytochemistry*, *12*(4). www.anvpublication.org

Mengist, W., Soromessa, T., & Legese, G. (2020). Ecosystem services research in mountainous regions: A systematic literature review on current knowledge and research gaps. In *Science of the Total Environment* (Vol. 702). Elsevier B.V. https://doi.org/10.1016/j.scitotenv.2019.134581

Miège, J. (1952). L'importance économique des Ignames en Cote d'Ivoire. Répartition des cultures et principales variétés. *Revue Internationale de Botanique Appliquée et d'agriculture Tropicale*, *32*(353), 144–155. https://doi.org/10.3406/jatba.1952.6776

Miller, R. O., & Kissel, D. E. (2010). Comparison of Soil pH Methods on Soils of North America. *Soil Science Society of America Journal*, *74*(1), 310–316. https://doi.org/10.2136/sssaj2008.0047

MINADER. (2017). *Ministère De L'Agriculture et du Développement Rural-Côte d'Ivoire: Recensement des Exploitants et Exploitations Agricoles (REEA) de 2015/2016, synthèse des résultats.*

Missana, A., Missana Gamba, A., Anderson Kimaro, A., & Mark Mtei, K. (2020). Effects of Climate Smart Agricultural practices and Planting Dates on Maize Growth and Nutrient Uptake in Semi-Arid Tanzania. *International Journal of Biosciences | IJB | Innspub.Net*, *16*(5), 98–109. https://doi.org/10.12692/ijb/16.5.98-109

Moctar, T. (2019). *ACTIVATION DU COMPOSTAGE DE PAILLE DE RIZ PAR EFFET DU PHOSPHORE : Valorisation des résidus de récolte* [Mémoire de Master]. Université Félix HOUPHOUET-BOIGNY de Cocody.

Moisa, M. B., Dejene, I. N., & Gemeda, D. O. (2022). Geospatial technology–based analysis of land use land cover dynamics and its effects on land surface temperature in Guder River sub-basin, Abay Basin, Ethiopia. *Applied Geomatics*, *14*(3), 451–463. https://doi.org/10.1007/s12518-022-00445-z

Moisa, M. B., Dejene, I. N., Merga, B. B., & Gemeda, D. O. (2022). Impacts of land use/land cover dynamics on land surface temperature using geospatial techniques in Anger River Sub-basin, Western Ethiopia. *Environmental Earth Sciences*, *81*(3). https://doi.org/10.1007/s12665-022-10221-2

Moisa, M. B., Gabissa, B. T., Hinkosa, L. B., Dejene, I. N., & Gemeda, D. O. (2022). Analysis of land surface temperature using Geospatial technologies in Gida Kiremu, Limu, and Amuru District, Western Ethiopia. *Artificial Intelligence in Agriculture*, *6*, 90–99. https://doi.org/10.1016/j.aiia.2022.06.002

Morawitz, D. F., Blewett, T. M., Cohen, A., & Alberti, M. (2006). Using NDVI to assess vegetative land cover change in Central Puget Sound. *Environmental Monitoring and Assessment*, *114*(1–3), 85–106. https://doi.org/10.1007/s10661-006-1679-z

Mosunmola, I. A., Samaila, I. K., Emmanuel, B., & Adolphus, I. (2020). Evaluation of Onset and Cessation of Rainfall and Temperature on Maize Yield in Akure, Ondo State, Nigeria. *Atmospheric and Climate Sciences*, *10*(02), 125–145. https://doi.org/10.4236/acs.2020.102006

Müller, C., Jägermeyr, J., Franke, J. A., Ruane, A. C., Balkovic, J., Ciais, P., Dury, M., Falloon, P., Folberth, C., Hank, T., Hoffmann, M., Izaurralde, R. C., Jacquemin, I., Khabarov, N., Liu, W., Olin, S., Pugh, T. A. M., Wang, X., Williams, K., … Elliott, J. W. (2024). Substantial Differences in Crop Yield Sensitivities Between Models Call for Functionality-Based Model Evaluation. *Earth's Future*, *12*(3). https://doi.org/10.1029/2023EF003773

Müller, W. A., Jungclaus, J. H., Mauritsen, T., Baehr, J., Bittner, M., Budich, R., Bunzel, F., Esch, M., Ghosh, R., Haak, H., Ilyina, T., Kleine, T., Kornblueh, L., Li, H., Modali, K., Notz, D., Pohlmann, H., Roeckner, E., Stemmler, I., … Marotzke, J. (2018). A Higher-resolution Version of the Max Planck Institute Earth System Model (MPI-ESM1.2-HR). *Journal of Advances in Modeling Earth Systems*, *10*(7), 1383–1413. https://doi.org/10.1029/2017MS001217

Mustapha, A. A., Abdu, N., Oyinlola, E. Y., & Nuhu, A. A. (2023). Evaluating Different Methods of Organic Carbon Estimation on Nigerian Savannah Soils. *Journal of Soil Science and Plant Nutrition*, *23*(1), 790–800. https://doi.org/10.1007/s42729-022-01082-6

Nacro, H. B., Benest, D., & Abbadie, L. (1996). Distribution of microbial activities and organic matter according to particle size in a humid savanna soil (Lamto, Cote d'Ivoire). *Soil Biology and Biochemistry*, *28*(12), 1687–1697. https://doi.org/10.1016/S0038-0717(96)00246-5

Nassourou, L. M., Sarr, B., Alhassane, A., Traoré, S., & Abdourahamane, B. (2018). Perception et observation : les principaux risques agro-climatique de l'agriculture pluviale dans l'ouest du Niger. *VertigO*, *Volume 18 numéro 1*. https://doi.org/10.4000/vertigo.20003

N'doufou, G. H. C., Nangah, K. Y., & Kouadio, K. H. (2022). Comparative Study of Physico-Chemical Properties of Sediments from Two Sectors Close to Bandama in Northern Côte D'Ivoire (Sinematiali and Niakaramadougou). *Journal of Geoscience and Environment Protection*, *10*(02), 33–46. https://doi.org/10.4236/gep.2022.102003

Neina, D. (2021). Ecological and Edaphic Drivers of Yam Production in West Africa. In *Applied and Environmental Soil Science* (Vol. 2021). Hindawi Limited. https://doi.org/10.1155/2021/5019481

New, M., Hewitson, B., Stephenson, D. B., Tsiga, A., Kruger, A., Manhique, A., Gomez, B., Coelho, C. A. S., Masisi, D. N., Kululanga, E., Mbambalala, E., Adesina, F., Saleh, H., Kanyanga, J., Adosi, J., Bulane, L., Fortunata, L., Mdoka, M. L., & Lajoie, R. (2006). Evidence of trends in daily climate extremes over southern and west Africa. *Journal of Geophysical Research Atmospheres*, *111*(14), 1–11. https://doi.org/10.1029/2005JD006289

N'guessan, L., Ab, D., Kouamé, V., Ac, H., Bi, T., Assa, A., Carsky, R., Girardin, O., & Frossard, E. (2009). Productivity of yams (Dioscorea spp.) as affected by soil fertility. In *Journal of Animal & Plant Sciences* (Vol. 5). http://www.biosciences.elewa.org/JAPS;ISSN2071-7024

Nindjin, C., Konan, G., Agbo, N., Otokore, D., Bricas, N., Farah, Z., & Girardin, O. (2009). Les variétés d'igname (Dioscorea spp) Rencontrées sur les marches en Côte d'Ivoire et leur préférence culinaire. *Annales Des Sciences Agronomiques*, *9*(2). https://doi.org/10.4314/asab.v9i2.43231

Njoku, E. A., & Tenenbaum, D. E. (2022). Quantitative assessment of the relationship between land use/land cover (LULC), topographic elevation and land surface temperature (LST) in Ilorin, Nigeria.

Remote Sensing Applications: Society and Environment, *27*. https://doi.org/10.1016/j.rsase.2022.100780

Njoya, H. M., Matavel, C. E., Msangi, H. A., Wouapi, H. A. N., Löhr, K., & Sieber, S. (2022). Climate change vulnerability and smallholder farmers' adaptive responses in the semi-arid Far North Region of Cameroon. *Discover Sustainability*, *3*(1). https://doi.org/10.1007/s43621-022-00106-6

Noufé, D., Lidon, B., Mahé, G., Servat, E., Yao, T. B., Zueli, K. B., & Chaléard, J. L. (2011). Climate variability and rainfed maize production in the eastern Ivory Coast: Variabilité climatique et production de maïs en culture pluviale dans l'est ivoirien. *Hydrological Sciences Journal*, *56*(1), 152–167. https://doi.org/10.1080/02626667.2010.545247

Odame Appiah, D., Akondoh, A. C. K., Tabiri, R. K., & Donkor, A. A. (2018). Smallholder farmers' insight on climate change in rural Ghana. *Cogent Food and Agriculture*, *4*(1). https://doi.org/10.1080/23311932.2018.1436211

Oka, E., Floquet, A., Dao, D., Hounnakoun, C. O., & Mongbo, R. L. (2021). Diversity of Yam-Based Production Systems and Sustainable Soil Management: the Case of Tiéningboué in Ivory Coast. *Managementjournal.Usamv.Ro*, *21*(3), 16. http://managementjournal.usamv.ro/pdf/vol.21_3/Art69.pdf

Olayiwola Eruola, A., Bello, N., Ufoegbune, G., Makinde, A. A., Eruola, A. O., Bello, N. J., Ufoegbune, G. C., & Makinde, A. A. (2012). Application of Rainfall-Potential Evapotranspiration Model for Determining Optimum Planting Date of Yam (Dioscorea rotundata) in a Tropical Wet-and-Dry Climate. *International Journal of Plant Research*, *2012*(2), 36–40. https://doi.org/10.5923/j.plant

Olofsson, P., Foody, G. M., Stehman, S. V., & Woodcock, C. E. (2013). Making better use of accuracy data in land change studies: Estimating accuracy and area and quantifying uncertainty using stratified estimation. *Remote Sensing of Environment*, *129*, 122–131. https://doi.org/10.1016/j.rse.2012.10.031

Olsen, S. R. and Sommers, L. E. (1982). Phosphorus. In F. W. L. Collins (Ed.), *Methods of soil analysis: Part 2. Chemical and microbiological properties* (2nd ed, Vol. 9, Issue 9, pp. 403–430). Agron. Mongr. and SSSA, Madison, WI. https://doi.org/10.1055/b-0035-119305

Ostrowska, A., & Porębska, G. (2015). Assessment of the C/N ratio as an indicator of the decomposability of organic matter in forest soils. *Ecological Indicators*, *49*, 104–109. https://doi.org/10.1016/j.ecolind.2014.09.044

Ouattara, Z. A., Kabo-Bah, A. T., Dongo, K., & Akpoti, K. (2023). A Review of sewerage and drainage systems typologies with case study in Abidjan, Côte d'Ivoire: failures, policy and management techniques perspectives. *Cogent Engineering*, *10*(1). https://doi.org/10.1080/23311916.2023.2178125

Owusu Danquah, E., Frimpong, F., Yeboah, S., Tetteh, E. N., Weebadde, C., Ennin, S. A., Agyeman, K., Amankwaa-Yeboah, P., Akley, E. K., Hayford, P., & Snapp, S. (2022). Pigeonpea (Cajanus cajan) and white yam (Dioscorea rotundata) cropping system: Improved resource use and productivity in Ghana. *Annals of Agricultural Sciences*, *67*(1), 60–71. https://doi.org/10.1016/j.aoas.2022.05.001

Pedersen, I. F., Munkholm, L. J., Lemming, C., Mäenpää, M., & Rubæk, G. H. (2023). Additional phosphorus intensity analysis needed to identify phosphorus requirement on acid sandy soils with high Olsen-P contents. *Field Crops Research*, *300*. https://doi.org/10.1016/j.fcr.2023.109004

Peng, S., Wang, C., Li, Z., Mihara, K., Kuramochi, K., Toma, Y., & Hatano, R. (2023). Climate change multi-model projections in CMIP6 scenarios in Central Hokkaido, Japan. *Scientific Reports*, *13*(1), 1–18. https://doi.org/10.1038/s41598-022-27357-7

Peng, X., Wu, W., Zheng, Y., Sun, J., Hu, T., & Wang, P. (2020). Correlation analysis of land surface temperature and topographic elements in Hangzhou, China. *Scientific Reports*, *10*(1). https://doi.org/10.1038/s41598-020-67423-6

Penyelidikan, J. (2006). SAMPLE SIZE ESTIMATION USING KREJCIE AND MORGAN AND COHEN STATISTICAL POWER ANALYSIS: A COMPARISON. *Jurnal Penyelidikan IPBL*, *7*, 78–86.

Perez Melo, S. (2014). *Statistical Analysis of Meteorological Data* [Florida International University]. https://doi.org/10.25148/etd.FI14071147

Pérez-Cutillas, P., Pérez-Navarro, A., Conesa-García, C., Zema, D. A., & Amado-Álvarez, J. P. (2023). What is going on within google earth engine? A systematic review and meta-analysis. In *Remote Sensing Applications: Society and Environment* (Vol. 29). Elsevier B.V. https://doi.org/10.1016/j.rsase.2022.100907

Pervez, S., McNally, A., Arsenault, K., Budde, M., & Rowland, J. (2021). Vegetation Monitoring Optimization With Normalized Difference Vegetation Index and Evapotranspiration Using Remote Sensing Measurements and Land Surface Models Over East Africa. *Frontiers in Climate*, *3*. https://doi.org/10.3389/fclim.2021.589981

Phalke, A. R., Özdoğan, M., Thenkabail, P. S., Erickson, T., Gorelick, N., Yadav, K., & Congalton, R. G. (2020). *ISPRS Journal of Photogrammetry and Remote Sensing Mapping croplands of Europe, Middle East, Russia, and Central Asia using Landsat, Random Forest, and Google Earth Engine*. https://doi.org/10.5067/MEaSUREs/GFSAD/GFSAD30EUCEARUMECE.001

Phan, P., Chen, N., Xu, L., Dao, D. M., & Dang, D. (2021). Ndvi variation and yield prediction in growing season: A case study with tea in tanuyen vietnam. *Atmosphere*, *12*(8). https://doi.org/10.3390/atmos12080962

Phan, T. N., Kappas, M., & Tran, T. P. (2018). Land surface temperature variation due to changes in elevation in Northwest Vietnam. *Climate*, *6*(2). https://doi.org/10.3390/cli6020028

Pokona, E. P., Yaka, P., & Ndione, J. A. (2021). Modélisation épidémiologique des pathologies climato-dépendantes au nord-Togo: Cas de la Fièvre Aphteuse dans la région des Savanes. In *Rev. Mar. Sci. Agron. Vét* (Vol. 9, Issue 4). www.agrimaroc.org

Polakowski, C., Makó, A., Sochan, A., Ryżak, M., Zaleski, T., Beczek, M., Mazur, R., Nowiński, M., Turczański, K., Orzechowski, M., Smólczyński, S., Kassai, P., & Bieganowski, A. (2023). Recommendations for soil sample preparation, pretreatment, and data conversion for texture classification in laser diffraction particle size analysis. *Geoderma*, *430*. https://doi.org/10.1016/j.geoderma.2023.116358

Pontes, F. V. M., Carneiro, M. C., Vaitsman, D. S., da Rocha, G. P., da Silva, L. I. D., Neto, A. A., & Monteiro, M. I. C. (2009). A simplified version of the total kjeldahl nitrogen method using an ammonia extraction ultrasound-assisted purge-and-trap system and ion chromatography for analyses of geological samples. *Analytica Chimica Acta*, *632*(2), 284–288. https://doi.org/10.1016/j.aca.2008.11.011

Pouya, N., Hgaza, V. K., Kiba, D. I., Bomisso, L., Aighewi, B., Aké, S., & Frossard, E. (2022). Water Yam (Dioscorea alata L.) Growth and Tuber Yield as Affected by Rotation and Fertilization Regimes across an Environmental Gradient in West Africa. *Agronomy*, *12*(4), 792. https://doi.org/10.3390/agronomy12040792

Pu, Y., Liu, H., Yan, R., Yang, H., Xia, K., Li, Y., Dong, L., Li, L., Wang, H., Nie, Y., Song, M., Xie, J., Zhao, S., Chen, K., Wang, B., Li, J., & Zuo, L. (2020). CAS FGOALS-g3 Model Datasets for the CMIP6 Scenario Model Intercomparison Project (ScenarioMIP). *Advances in Atmospheric Sciences*, *37*(10), 1081–1092. https://doi.org/10.1007/s00376-020-2032-0

Pušnik, Ž., Mraz, M., Zimic, N., & Moškon, M. (2022). Review and assessment of Boolean approaches for inference of gene regulatory networks. In *Heliyon* (Vol. 8, Issue 8). Elsevier Ltd. https://doi.org/10.1016/j.heliyon.2022.e10222

QIU, W., HU, W., CURTIN, D., & MOTOI, L. (2021). Soil particle size range correction for improved calibration relationship between the laser-diffraction method and sieve-pipette method. *Pedosphere*, *31*(1), 134–144. https://doi.org/10.1016/S1002-0160(20)60055-8

R. Michel and G. Apata. (2017). *Diagnostic des systèmes d'information et de suivi et évaluation en Côte d'Ivoire en vue de la mise en place d'une Plateforme Nationale d'Information pour la Nutrition (PNIN). Montpellier, France: Agropolis International, Unité d'appui international pour l'initiative NIPN*. http://www.nipn-nutrition-platforms.org/IMG/pdf/info-systemes-cote-ivoire.pdf

Raes, D., Steduto, P., Hsiao, T. C., & Fereres, E. (2018). *Chapter 1 FAO crop-water productivity model to simulate yield response to water AquaCrop Reference manual*. www.fao.org/publications

Rajendran, P., & Mani, D. K. (2015). Estimation of Spatial Variability of Land Surface Temperature using Landsat 8 Imagery. *The International Journal Of Engineering And Science (IJES)* ||, *4*(11), 19–23. www.theijes.com

Rashid, H. A., Sullivan, A., Dix, M., Bi, D., Mackallah, C., Ziehn, T., Dobrohotoff, P., O'farrell, S., Harman, I. N., Bodman, R., & Marsland, S. (2022). Evaluation of climate variability and change in ACCESS historical simulations for CMIP6. *Journal of Southern Hemisphere Earth Systems Science*, *72*(2), 73–92. https://doi.org/10.1071/ES21028

Raymundo, R., Asseng, S., Cammarano, D., & Quiroz, R. (2014). Potato, sweet potato, and yam models for climate change: A review. In *Field Crops Research* (Vol. 166, pp. 173–185). Elsevier. https://doi.org/10.1016/j.fcr.2014.06.017

RCI-Code Forestier. (2019a). *Code forestier LOI N2019-675 DU 23 JUILLET 2019 , PORTANT CODE FORESTIER EN COTE D'IVOIRE*.

RCI-Code Forestier. (2019b). *www.droit-afrique.com Côte d'Ivoire Code forestier*. www.droit-afrique.com

Recena, R., García-López, A. M., Quintero, J. M., Skyttä, A., Ylivainio, K., Santner, J., Buenemann, E., & Delgado, A. (2022). Assessing the phosphorus demand in European agricultural soils based on the Olsen method. *Journal of Cleaner Production*, *379*. https://doi.org/10.1016/j.jclepro.2022.134749

République de Côte d'Ivoire. (2019). *Constat d'Impact Environnemental et Social (CIES) des travaux de Reprofilage Lourd et de Traitement de Points Critiques de 60 km de routes rurales dans la Région du Gontougo – Rapport provisoire*.

RGPH-CI. (2021). *REPUBLIQUE DE COTE D'IVOIRE: RECENSEMENT GENERAL DE LA POPULATION ET DE L'HABITAT* (RCI). INS.

Rojas, O., & Senay, G. (2021). *remote sensing Next Generation Agricultural Stress Index System (ASIS) for Agricultural Drought Monitoring*. https://doi.org/10.3390/rs

Ross, D. S., & Ketterings, Q. (2011). Recommended Methods for Determining Soil Cation Exchange Capacity. In *Recommended Soil Testing Procedures for the Northeastern United States* (493rd ed., pp. 75–86). Cooperative Bulletin.

Roudier, P., Sultan, B., Quirion, P., & Berg, A. (2011). The impact of future climate change on West African crop yields: What does the recent. literature say? *Global Environmental Change*, *21*(3), 1073–1083. https://doi.org/10.1016/j.gloenvcha.2011.04.007

Rwanga, S. S., & Ndambuki, J. M. (2017). Accuracy Assessment of Land Use/Land Cover Classification Using Remote Sensing and GIS. *International Journal of Geosciences*, *08*(04), 611–622. https://doi.org/10.4236/ijg.2017.84033

Sáez-Plaza, P., Navas, M. J., Wybraniec, S., Michałowski, T., & Asuero, A. G. (2013). An Overview of the Kjeldahl Method of Nitrogen Determination. Part II. Sample Preparation, Working Scale, Instrumental Finish, and Quality Control. *Critical Reviews in Analytical Chemistry*, *43*(4), 224–272. https://doi.org/10.1080/10408347.2012.751787

Sahoo, S. K., Mishra, K. N., Panda, N., Sethi, D., & Dey, P. (2023). Carbon and Nitrogen Mineralization Kinetics in Soil Under Differential Nutrient Management Regimes in Inceptisols of Coastal India. *Communications in Soil Science and Plant Analysis*, *54*(20), 2782–2799. https://doi.org/10.1080/00103624.2023.2241500

Salack, S., Muller, B., Gaye, A. T., Hourdin, F., & Cisse, N. (2012). Analyses multi-échelles des pauses pluviométriques au Niger et au Sénégal. *Science et Changements Planetaires - Secheresse*, *23*(1), 3–13. https://doi.org/10.1684/sec.2012.0335

Salack, S., Sarr, B., Sangare, S. K., Ly, M., Sanda, I. S., & Kunstmann, H. (2015). Crop-climate ensemble scenarios to improve risk assessment and resilience in the semi-arid regions of West Africa. *Climate Research*, *65*, 107–121. https://doi.org/10.3354/cr01282

Sanogo, T., Sokemawu, K., & Karembe, M. (2023). Risks and Influences of Climate Hazards for Agro-Pastoral Development and Strategies Adopted by Agro-Pastoralist Communities in the Bougouni District, Mali. *American Journal of Climate Change*, *12*(02), 244–267. https://doi.org/10.4236/ajcc.2023.122012

Schär, C., Ban, N., Fischer, E. M., Rajczak, J., Schmidli, J., Frei, C., Giorgi, F., Karl, T. R., Kendon, E. J., Tank, A. M. G. K., O'Gorman, P. A., Sillmann, J., Zhang, X., & Zwiers, F. W. (2016). Percentile indices for assessing changes in heavy precipitation events. *Climatic Change*, *137*(1–2), 201–216. https://doi.org/10.1007/s10584-016-1669-2

Schmugge, T., French, A., Ritchie, J. C., Rango, A., & Pelgrum, H. (2020). *Temperature and emissivity separation from multispectral thermal infrared observations*. www.elsevier.com/locate/rse

Seland, Ø., Graff, L. S., Olivié, D., Toniazzo, T., Gjermundsen, A., Debernard, J. B., Kumar Gupta, A., He, Y., Kirkevåg, A., Schwinger, J., Tjiputra, J., Aas, K. S., Bethke, I., Fan, Y., Griesfeller, J., Grini, A., Guo, C., Helene, I., Karset, H., … Schulz, M. (2020). The Norwegian Earth System Model, NorESM2-Evaluation of the CMIP6 DECK and historical simulations. *Geoscientific Model Development*. https://doi.org/10.5194/gmd-2019-378

Setiya, P., Satpathi, A., & Nain, A. S. (2023). Predicting rice yield based on weather variables using multiple linear, neural networks, and penalized regression models. *Theoretical and Applied Climatology*, *154*(1–2), 365–375. https://doi.org/10.1007/s00704-023-04563-5

Sharifi, A. (2018). Estimation of biophysical parameters in wheat crops in Golestan province using ultra-high resolution images. *Remote Sensing Letters*, *9*(6), 559–568. https://doi.org/10.1080/2150704X.2018.1452058

Sharifi, A., & Amini, J. (2015). *Forest biomass estimation using synthetic aperture radar polarimetric features Downloaded From: http://remotesensing.spiedigitallibrary.org/ on 07/17/2015 Terms of Use: http://spiedl.org/terms Forest biomass estimation using synthetic aperture radar polarimetric features*. https://doi.org/10.1117/1

Sharifi, A., Amini, J., & Tateishi, R. (2016). Estimation of forest biomass using multivariate relevance vector regression. *Photogrammetric Engineering and Remote Sensing*, *82*(1), 41–49. https://doi.org/10.14358/PERS.83.1.41

Shi, H., Wang, X., Xu, M., Zhang, H., & Luo, Y. (2017). Characteristics of soil C:N ratio and δ13C in wheat-maize cropping system of the North China Plain and influences of the Yellow River. *Scientific Reports*, *7*(1), 1–9. https://doi.org/10.1038/s41598-017-17060-3

Shrestha, N. (2020). Detecting Multicollinearity in Regression Analysis. *American Journal of Applied Mathematics and Statistics*, *8*(2), 39–42. https://doi.org/10.12691/ajams-8-2-1

Siddique, K. H. M., Bolan, N., Rehman, A., & Farooq, M. (2024). Enhancing crop productivity for recarbonizing soil. *Soil and Tillage Research*, *235*(April 2023), 105863. https://doi.org/10.1016/j.still.2023.105863

Šimek, M., & Cooper, J. E. (2002). The influence of soil pH on denitrification: Progress towards the understanding of this interaction over the last 50 years. *European Journal of Soil Science*, *53*(3), 345–354. https://doi.org/10.1046/j.1365-2389.2002.00461.x

Šinkovičová, M., Igaz, D., Kondrlová, E., & Jarošová, M. (2017). Soil Particle Size Analysis by Laser Diffractometry: Result Comparison with Pipette Method. *IOP Conference Series: Materials Science and Engineering*, *245*(7). https://doi.org/10.1088/1757-899X/245/7/072025

Sivakumar, M. V. (1988). PREDICTING RAINY SEASON POTENTIAL FROM THE ONSET OF RAINS IN SOUTHERN SAHELIAN AND SUDANIAN CLIMATIC ZONES OF WEST AFRICA*. In *Agricultural and Forest Meteorology* (Vol. 42).

Skjemstad, J. O., & Taylor, J. A. (1999). Does the Walkley-Black method determine soil charcoal? *Communications in Soil Science and Plant Analysis*, *30*(15–16), 2299–2310. https://doi.org/10.1080/00103629909370373

Snyder, H. (2019). Literature review as a research methodology: An overview and guidelines. *Journal of Business Research*, *104*, 333–339. https://doi.org/10.1016/j.jbusres.2019.07.039

Sobrino, J. A., Jiménez-Muñoz, J. C., & Paolini, L. (2004). Land surface temperature retrieval from LANDSAT TM 5. *Remote Sensing of Environment*, *90*(4), 434–440. https://doi.org/10.1016/j.rse.2004.02.003

Sohel Rana, M., Midi, H., & Rahmatullah Imon, A. (2008). A Robust Modification of the Goldfeld-Quandt Test for the Detection of Heteroscedasticity in the Presence of Outliers. *Journal of Mathematics and Statistics*, *4*(4), 277–283.

Srivastava, A. K., & Gaiser, T. (2010). Simulating biomass accumulation and yield of yam (Dioscorea alata) in the Upper Ouémé Basin (Benin Republic)- I. Compilation of physiological parameters and calibration at the field scale. *Field Crops Research*, *116*(1–2), 23–29. https://doi.org/10.1016/j.fcr.2009.10.018

Srivastava, A. K., Gaiser, T., Cornet, D., & Ewert, F. (2012). Estimation of effective fallow availability for the prediction of yam productivity at the regional scale using model-based multiple scenario analysis. *Field Crops Research*, *131*, 32–39. https://doi.org/10.1016/j.fcr.2012.01.012

Srivastava, A. K., Gaiser, T., Paeth, H., & Ewert, F. (2012). The impact of climate change on Yam (Dioscorea alata) yield in the savanna zone of West Africa. *Agriculture, Ecosystems and Environment*, *153*, 57–64. https://doi.org/10.1016/j.agee.2012.03.004

Steinfurth, K., Hirte, J., Morel, C., & Buczko, U. (2021). Conversion equations between Olsen-P and other methods used to assess plant available soil phosphorus in Europe – A review. *Geoderma*, *401*. https://doi.org/10.1016/j.geoderma.2021.115339

Sufardi, S., Arabia, T., Khairullah, K., Rusdi, M., Khalil, M., Ilyas, I., Zainabun, Z., & Abdullah, U. (2023). Assessment of carbon and nitrogen distribution on several soil orders for sustainable management in dryland farming: A Case Study in Aceh Besar Regency, Indonesia. *IOP Conference Series: Earth and Environmental Science*, *1230*(1), 012062. https://doi.org/10.1088/1755-1315/1230/1/012062

Sultan, B., Defrance, D., & Iizumi, T. (2019). Evidence of crop production losses in West Africa due to historical global warming in two crop models. *Scientific Reports*, *9*(1). https://doi.org/10.1038/s41598-019-49167-0

Sultan, B., Lalou, R., Sanni, A., Oumarou, A., & Soumaré, M. A. (2015). *Les sociétés rurales face aux changements climatiques et environnementaux en Afrique de l'Ouest*.

Sultan, B., Roudier, P., Quirion, P., Alhassane, A., Muller, B., Dingkuhn, M., Ciais, P., Guimberteau, M., Traore, S., & Baron, C. (2013). Assessing climate change impacts on sorghum and millet yields in the Sudanian and Sahelian savannas of West Africa. *Environmental Research Letters*, *8*(1). https://doi.org/10.1088/1748-9326/8/1/014040

Suraj Poudel. (2020). Organic Matter determination (Walkley-Black method). *Agriculture and Forestry University*. https://doi.org/10.13140/RG.2.2.22043.00807

Suryono, H., Kuswanto, H., & Iriawan, N. (2021). Rice phenology classification based on random forest algorithm for data imbalance using Google Earth engine. *Procedia Computer Science*, *197*, 668–676. https://doi.org/10.1016/j.procs.2021.12.201

Svensson, D. N., Messing, I., & Barron, J. (2022). An investigation in laser diffraction soil particle size distribution analysis to obtain compatible results with sieve and pipette method. *Soil and Tillage Research*, *223*. https://doi.org/10.1016/j.still.2022.105450

Syawalina, R. K., Ratihmanjari, F., & Saputra, R. A. (2022). *Identification of The Relationship Between LST And NDVI On Geothermal Manifestations In A Preliminary Study Of Geothermal Exploration Using Landsat 8 OLI/TIRS Imagery Data Capabilities: Case Study Of Toro, Central Sulawesi*.

Tamiminia, H., Salehi, B., Mahdianpari, M., Quackenbush, L., Adeli, S., & Brisco, B. (2020). Google Earth Engine for geo-big data applications: A meta-analysis and systematic review. In *ISPRS Journal of Photogrammetry and Remote Sensing* (Vol. 164, pp. 152–170). Elsevier B.V. https://doi.org/10.1016/j.isprsjprs.2020.04.001

Tariq, A., Yan, J., Gagnon, A. S., Riaz Khan, M., & Mumtaz, F. (2022). Mapping of cropland, cropping patterns and crop types by combining optical remote sensing images with decision tree classifier and random forest. *Geo-Spatial Information Science*. https://doi.org/10.1080/10095020.2022.2100287

Tchein, G., Kodjo, T. A., Komi, A., Manguilibè, T., & Komla, S. (2019). Perceptions Paysannes des Déterminants de la Faible Productivité des Ignames (Dioscorea spp) et de Leurs Niveaux de Gravité au Sud-Ouest des Savanes Sèches au Togo (Afrique de l'Ouest). *European Scientific Journal ESJ*, *15*(27). https://doi.org/10.19044/esj.2019.v15n27p256

Télesphore Brou, Y. (2009). IMPACTS DES MODIFICATIONS BIOCLIMATIQUES ET DES L'AMENUISEMENT DES TERRES FORESTIèRES DANS LES PAYSANNERIES IVOIRIENNES : QUELLES SOLUTIONS POUR UNE AGRICULTURE DURABLE EN CôTE D'IVOIRE. *Cuadernos Geográicos*, *45*(2), 13–29.

Teluguntla, P., Thenkabail, P., Oliphant, A., Xiong, J., Gumma, M. K., Congalton, R. G., Yadav, K., & Huete, A. (2018). A 30-m landsat-derived cropland extent product of Australia and China using random forest machine learning algorithm on Google Earth Engine cloud computing platform. *ISPRS Journal of Photogrammetry and Remote Sensing*, *144*, 325–340. https://doi.org/10.1016/j.isprsjprs.2018.07.017

Test, D.-W., Bartels, R., & Goodhew, J. (1981). The Robustness of the. In *Source: The Review of Economics and Statistics* (Vol. 63, Issue 1).

Thiex, N. J., Manson, H., Anderson, S., & Persson, J. Å. (2002). Determination of crude protein in animal feed, forage, grain, and oilseeds by using block digestion with a copper catalyst and steam distillation into boric acid: Collaborative study. *Journal of AOAC International*, *85*(2), 309–317. https://doi.org/10.1093/jaoac/85.2.309

Thomas, G. W. (1996). *Soil pH and Soil Acidity* (M. Segoe Rd., Ed.; 677 S.). Soil Science Society of America and American Society of Agronomy.

Tran, B., Van Der Kwast, J., Seyoum, S., Uijlenhoet, R., Jewitt, G., & Mul, M. (2023). Uncertainty Assessment of Satellite Remote Sensing-based Evapotranspiration Estimates: A Systematic Review of Methods and Gaps. *EGUsphere Preprint Repository*, *https://doi.org/10.5194/egusphere-2023-725*, 1–40. https://doi.org/10.5194/egusphere-2023-725

ud din, S., Al-Dousari, A., Ramdan, A., & Al Ghadban, A. (2008). Site-specific precipitation estimate from TRMM data using bilinear weighted interpolation technique: An example from Kuwait. *Journal of Arid Environments*, *72*(7), 1320–1328. https://doi.org/10.1016/j.jaridenv.2007.12.013

Ufoegbune, G., Adekunle Makinde, A., Eruola, A., Ufogbune, G., Makinde, A., & Kassim, H. (2014). Effect of Planting Season on Phenology and Accumulated Heat Units in Relation to Yield of White Yam in the Tropical Wet-and-Dry Climate. In *Jordan Journal of Agricultural Sciences* (Vol. 10, Issue 4). https://www.researchgate.net/publication/279974961

Van Noije, T., Bergman, T., Le Sager, P., O'Donnell, D., Makkonen, R., Gonçalves-Ageitos, M., Döscher, R., Fladrich, U., Von Hardenberg, J., Keskinen, J. P., Korhonen, H., Laakso, A., Myriokefalitakis, S., Ollinaho, P., Pérez Garciá-Pando, C., Reerink, T., Schrödner, R., Wyser, K., & Yang, S. (2021). EC-Earth3-AerChem: A global climate model with interactive aerosols and atmospheric chemistry participating in CMIP6. *Geoscientific Model Development*, *14*(9), 5637–5668. https://doi.org/10.5194/gmd-14-5637-2021

Volodin, E., & Gritsun, A. (2018). Simulation of observed climate changes in 1850-2014 with climate model INM-CM5. *Earth System Dynamics*, *9*(4), 1235–1242. https://doi.org/10.5194/esd-9-1235-2018

Volodin, E. M., Mortikov, E. V., Kostrykin, S. V., Galin, V. Y., Lykossov, V. N., Gritsun, A. S., Diansky, N. A., Gusev, A. V., Iakovlev, N. G., Shestakova, A. A., & Emelina, S. V. (2018). Simulation of the modern climate using the INM-CM48 climate model. *Russian Journal of Numerical Analysis and Mathematical Modelling*, *33*(6), 367–374. https://doi.org/10.1515/rnam-2018-0032

Voss, D. S. (2005). Multicollinearity. *Encyclopedia of Social Measurement*, 759–770. https://doi.org/10.1016/B0-12-369398-5/00428-X

Walkley, A. & Black, I. A. (1934). An Examination of the Degtjareff Method for Determining Soil Organic Matter, A Proposed Modification of the Chromic Acid Titration Method. *Soil Science*, *37*(1), 29–38.

Wallach, D., Makowski, D., Jones, J. W., & Brun, F. (2014). Data Assimilation for Dynamic Models. In *Working with Dynamic Crop Models* (pp. 311–343). Elsevier. https://doi.org/10.1016/b978-0-12-397008-4.00008-3

Walworth, J. L. (2023). Soil Sampling and Analysis. *College of Agriculture and Life Sciences, University of Arizona (Tucson, AZ)*, 1–5. http://hdl.handle.net/10150/239610

Wang, M., Wang, J., Chen, D., Duan, A., Liu, Y., Zhou, S., Guo, D., Wang, H., & Ju, W. (2019). Recent recovery of the boreal spring sensible heating over the Tibetan Plateau will continue in CMIP6 future projections. *Environmental Research Letters*, *14*(12). https://doi.org/10.1088/1748-9326/ab57a3

Waongo, M. (2015). *Optimizing Planting Dates for Agricultural Decision-Making under Climate Change over Burkina Faso/West Africa. Ph.D. doctorate at Augsburg university, Germany. 133p.*

Waongo, M., Laux, P., & Kunstmann, H. (2015). Adaptation to climate change: The impacts of optimized planting dates on attainable maize yields under rainfed conditions in Burkina Faso. *Agricultural and Forest Meteorology*, *205*, 23–39. https://doi.org/10.1016/j.agrformet.2015.02.006

Weber, J. E., & Monarchi, D. E. (1982). Performance of the Durbin-Watson test and WLS estimation when the disturbance term includes serial dependence in addition to first-order autocorrelation. *Journal of the American Statistical Association*, *77*(377), 117–128. https://doi.org/10.1080/01621459.1982.10477774

Weijer, W., Cheng, W., Garuba, O. A., Hu, A., & Nadiga, B. T. (2020). CMIP6 Models Predict Significant 21st Century Decline of the Atlantic Meridional Overturning Circulation. *Geophysical Research Letters*, *47*(12). https://doi.org/10.1029/2019GL086075

Wickham, H., & Grolemund, G. (2017). *R for Data Science* (Marie Beaugureau & Mike Loukides, Eds.; O'Reilly). O'Reilly Media, Inc., 1005 Gravenstein Highway North, Sebastopol, CA 95472. www.allitebooks.com

WMO. (2012). *Guide d'utilisation de l'indice de précipitations normalisé. OMM-N 1090.*

WMO. (2020). *État du climat en Afrique* (WMO-N° 1275).

World Bank Group. (2019). *Cote d'Ivoire Climate-Smart Agriculture Investment Plan. World Bank, Washington, DC. © World Bank. https://openknowledge.worldbank.org/handle/10986/32745 License: CC BY 3.0 IGO."*. www.worldbank.org

World Bank Group. (2024). *Climate Change Knowledge Portal for Development Practitioners and Policy Makers.* www.climateknowledgeportal.worldbank.org

Wu, H., Hayes, M. J., Weiss, A., & Hu, Q. (2001). An evolution of the standardized precipitation index, the China-Z index and the statistical Z-score. *International Journal of Climatology*, *21*(6), 745–758. https://doi.org/10.1002/joc.658

Wu, Y., Zhou, G., Song, Y., Ren, S., Geng, J., Zhao, H., & Song, X. (2023). A Simulation Study on Optimization of Sowing Time of Maize (Zea mays L.) for Maximization of Growth and Yield in the Present Context of Climate Change under the North China Plain. *Agronomy*, *13*(2). https://doi.org/10.3390/AGRONOMY13020385

Wu, Z., Yu, L., Zhang, X., Du, Z., & Zhang, H. (2019). Satellite-based large-scale vegetation dynamics in ecological restoration programmes of Northern China. *International Journal of Remote Sensing*, *40*(5–6), 2296–2312. https://doi.org/10.1080/01431161.2018.1519286

Wumbei, A., Kengni Nerlus Gautier, S., Kwowura Kwodaga, J., Fovo Joseph, D., & Joseph Hubert Galani, Y. (2022). *State of the Art of Yam Production* (Prashant Kaushik, Ed.; IntechOpen). Advances in Root Vegetables Research . https://doi.org/10.5772/intechopen.106504

Xu, X., Thornton, P. E., & Post, W. M. (2013). A global analysis of soil microbial biomass carbon, nitrogen and phosphorus in terrestrial ecosystems. *Global Ecology and Biogeography*, *22*(6), 737–749. https://doi.org/10.1111/geb.12029

Yan, X., Li, J., Yang, D., Li, J., Ma, T., Su, Y., Shao, J., & Zhang, R. (2022). A Random Forest Algorithm for Landsat Image Chromatic Aberration Restoration Based on GEE Cloud Platform—A Case Study of Yucatán Peninsula, Mexico. *Remote Sensing*, *14*(20). https://doi.org/10.3390/rs14205154

Yao, K. L., Kouakou, K. E., Kouassi, A. M., Deguy, A. J. -P., & Camara, M. (2023). Analysis of Land Use Change in the N'ZI Watershed of Côte d'Ivoire Using Landsat Satellite Images. *Earth and Space Science*, *10*(3). https://doi.org/10.1029/2022ea002744

Yates, D., Gangopadhyay, S., Rajagopalan, B., & Strzepek, K. (2003). A technique for generating regional climate scenarios using a nearest-neighbor algorithm. *Water Resources Research*, *39*(7), 1–15. https://doi.org/10.1029/2002WR001769

Yimam, D. A., & Holvoet, N. (2023). Assessing climate change vulnerability of smallholder farmers in northwest Ethiopia: application of a household intrinsic vulnerability index. *International Journal of Climate Change Strategies and Management*, *15*(4), 537–560. https://doi.org/10.1108/IJCCSM-02-2022-0019

Yin, Y., Chen, H., Wang, G., Xu, W., Wang, S., & Yu, W. (2021). Characteristics of the precipitation concentration and their relationship with the precipitation structure: A case study in the Huai River basin, China. *Atmospheric Research*, *253*(February). https://doi.org/10.1016/j.atmosres.2021.105484

Zeleke, T., Beyene, F., Deressa, T., Yousuf, J., & Kebede, T. (2023). Smallholder farmers' perception of climate change and choice of adaptation strategies in East Hararghe Zone, Eastern Ethiopia.

International Journal of Climate Change Strategies and Management, *15*(4), 515–536. https://doi.org/10.1108/IJCCSM-01-2022-0014

Zhang, T., Li, L., & Zheng, B. (2013). Estimation of agricultural soil properties with imaging and laboratory spectroscopy. *Journal of Applied Remote Sensing*, *7*(1), 073587. https://doi.org/10.1117/1.jrs.7.073587

Zhang, Yang, J., Leng, P., Ma, Y., Wang, H., & Song, Q. (2023). Crop type mapping with temporal sample migration. *International Journal of Remote Sensing*. https://doi.org/10.1080/01431161.2023.2192881

Zhao, Feng, S., Xie, F., Zhu, S., & Zhang, S. (2023). Extraction of long time series wetland information based on Google Earth Engine and random forest algorithm for a plateau lake basin – A case study of Dianchi Lake, Yunnan Province, China. *Ecological Indicators*, *146*. https://doi.org/10.1016/j.ecolind.2022.109813

Zhao, M., Golaz, J. C., Held, I. M., Guo, H., Balaji, V., Benson, R., Chen, J. H., Chen, X., Donner, L. J., Dunne, J. P., Dunne, K., Durachta, J., Fan, S. M., Freidenreich, S. M., Garner, S. T., Ginoux, P., Harris, L. M., Horowitz, L. W., Krasting, J. P., … Xiang, B. (2018). The GFDL Global Atmosphere and Land Model AM4.0/LM4.0: 1. Simulation Characteristics With Prescribed SSTs. *Journal of Advances in Modeling Earth Systems*, *10*(3), 691–734. https://doi.org/10.1002/2017MS001208

Zhao, X., Arshad, M., Li, N., Zare, E., & Triantafilis, J. (2020). Determination of the optimal mathematical model, sample size, digital data and transect spacing to map CEC (Cation exchange capacity) in a sugarcane field. *Computers and Electronics in Agriculture*, *173*. https://doi.org/10.1016/j.compag.2020.105436

Zheng, S., Cao, C., Dang, Y., Xiang, H., Zhao, J., Zhang, Y., Wang, X., & Guo, H. (2014). Retrieval of forest growing stock volume by two different methods using Landsat TM images. *International Journal of Remote Sensing*, *35*(1), 29–43. https://doi.org/10.1080/01431161.2013.860567

Zhou, Z., Zhang, L., Chen, J., She, D., Wang, G., Zhang, Q., Xia, J., & Zhang, Y. (2023). Projecting Global Drought Risk Under Various SSP-RCP Scenarios. *Earth's Future*, *11*(5), 1–20. https://doi.org/10.1029/2022EF003420

Zougmoré, R. B., Partey, S. T., Ouédraogo, M., Torquebiau, E., & Campbell, B. M. (2018). Facing climate variability in sub-saharan africa: Analysis of climate-smart agriculture opportunities to manage climate-related risks. In *Cahiers Agricultures* (Vol. 27, Issue 3). EDP Sciences. https://doi.org/10.1051/cagri/2018019

Zro, B. G. F., Guéi, A. M., Nangah, K. Y., Soro, D., & Bakayoko, S. (2016). Statistical approach to the analysis of the variability and fertility of vegetable soils of Daloa (Côte d'Ivoire). *African Journal of Soil Science*, *4*(4), 328–338.

APPENDICES

A. farmers' perception questionnaire

PhD SURVEYS TO COLLECT YAM FARMERS' PERCEPTIONS ON RISKS PRODUCTION UNDER CLIMATE CHANGE IN GONTOUGO REGION

Date and Time

yyyy-mm-dd hh:mm

Localities

- ◯ Hiango
- ◯ Kouassi-Seranou
- ◯ Srambli
- ◯ Goli
- ◯ Kouassi-Datekro
- ◯ KoffiKokorekro
- ◯ Senande
- ◯ Yayego
- ◯ Djipoumdouo
- ◯ Djikparedouo
- ◯ Dokanou
- ◯ Tanokoffikro
- ◯ Tambi
- ◯ Nafabeni
- ◯ Sandegue
- ◯ Kohodio
- ◯ Sangabili
- ◯ Bandole
- ◯ Nagafou
- ◯ Petit Bondoukou
- ◯ Koulkitedouo
- ◯ Broffouedou
- ◯ Kouassia-Niaguini
- ◯ Kouakou-Tanokro
- ◯ Saleye
- ◯ Kouakoukankro
- ◯ Namassi
- ◯ Amanvi
- ◯ Others localities

Others localities

____

Departments

- ◯ Bondoukou
- ◯ Koun-Fao
- ◯ Sandegue
- ◯ Tanda
- ◯ Transua

Location

latitude (x.y °)

longitude (x.y °)

altitude (m)

accuracy (m)

1.1- Gender

- ◯ Male
- ◯ Female

1.2- Age

- ◯ 1 < years < 15
- ◯ 15 < years old < 25
- ◯ 25 < years old < 35
- ◯ 35 < years old < 45
- ◯ 45 < years old < 55
- ◯ Over 55 years old

1.3- Marital status

- ◯ Married
- ◯ Single
- ◯ Cohabiting

1.4- Number of children

- ◯ 00
- ◯ 1 to 3
- ◯ 3 to 5
- ◯ 5 to 10
- ◯ More than 10

1.5- How long have you been producing yams?

- ◯ Less than 5 years
- ◯ Between 5 and 10
- ◯ Between 10 and 20
- ◯ Between 20 and 30
- ◯ More than 30 years

2.1- Causes of vegetations cover losses?

- ☐ Logging
- ☐ Gold panning
- ☐ Bush fires
- ☐ Drying out of vegetation
- ☐ Cashew production
- ☐ Expansion of the savannah
- ☐ Yam production
- ☐ Urbanization
- ☐ Others

Others, please specify

____

2.2- Which of these causes lead to the largest clearings?

- ◯ Logging
- ◯ Gold panning
- ◯ Bush fires
- ◯ Drying out of vegetation
- ◯ Cashew production
- ◯ Expansion of the savannah
- ◯ Yam production
- ◯ Urbanization
- ◯ Others

3.1- Which yam varieties do you regularly grow in this area ?

- ☐ Kponan
- ☐ Krenglè
- ☐ Assawa
- ☐ Bètè bètè
- ☐ Lokpa
- ☐ Florido
- ☐ Others

Others, please specify

____

3.2- How long is the crop cycle?

- ◯ 5 months
- ◯ 6 months
- ◯ 7 months
- ◯ 8 months
- ◯ 9 months
- ◯ 10 months
- ◯ 11 to 12 months

3.3- Growing method

- ◯ Slash and burn
- ◯ Intensive cultivation
- ◯ Extensive cultivation
- ◯ Rotational cultivation

If rotational: How long do you allow to rest formerly cultivated plots?

- ◯ 1 year
- ◯ 2 years
- ◯ 3 years
- ◯ 4 years
- ◯ 5 years
- ◯ More than 5 years

3.4- On what estimated area do you produce yam each year?

- ◯ Area<1 ha
- ◯ Between 1 and 3ha
- ◯ Between 3 and 5ha
- ◯ Between 5 and 10ha
- ◯ Area>10 Ha

3.5- What production (in tonnes) could you harvest for less than 1 ha?

____

3.5- What production (in tonnes) could you harvest between 1 and 3 ha?

____

3.5- What production (in tonnes) could you harvest between 3 and 5 ha?

____

3.5- What production (in tonnes) could you harvest between 5 and 10 ha?

____

3.5- What production (in tonnes) could you harvest for more 10 ha?

____

3.6- In which type of environment do you regularly grow yams?

- [ ] Fallows land
- [ ] Shrubby & herbaceous savannah
- [ ] Trees savannah
- [ ] Forest (degraded, islet, gallery)
- [ ] Shallow areas
- [ ] In association with cashew

3.7 What are the reasons for this choice?

- [ ] Fertility and adaptability of the soil to the crop
- [ ] Suitable for the variety I grow
- [ ] Land availability
- [ ] Accessibility
- [ ] Cultural/traditional habits
- [ ] Others

Others, please specificy

3.8- Do you use chemical fertilizers?

○ No

○ Yes

If yes, which ones?

- [ ] Herbicide
- [ ] Insecticide
- [ ] NPK soil fertilizers
- [ ] Others

Others, please specificy

3.9- Do you take into account the rainy season before planting yams?

○ Yes

○ No

If no, why?

- Rainy season not too necessary
- Cultivation habit
- Personal experience
- Not reliable with rain
- Endogenous knowledge of rainy days
- Other

3.10- When are the mounds made?

- November
- December
- January
- February
- March
- April
- May
- Others

Others, please which month?

____

3.11- When is the yam put in the mound?

- The same day after making the mound
- One to two days at most after mounding
- One to two days after a rain
- Without a rainfall
- After a heavy dew due to harmattan
- One month after mounding
- Others

Others, please specificy

____

Why? Please, justify your answer

- [ ] To reduce the temperature inside the mound
- [ ] To avoid seed rot
- [ ] Acceleration of germination
- [ ] Decomposition of organic and mineral matter in the mound
- [ ] Others

Others, please specificy

3.12- At what stage of yam production does the yam need more water?

- ○ Mounding time
- ○ During planting
- ○ Vegetative period
- ○ Harvesting
- ○ Others

Others, please specificy

Why? Please, justify your answer

- [ ] To reduce the temperature inside the mound
- [ ] To avoid seed rot
- [ ] To accelerate germination
- [ ] Decompose organic and mineral matter in the mound
- [ ] Allow rapid growth of the bud
- [ ] Waterlogging of stems and leaves to enlarge the tuber
- [ ] Strong rooting
- [ ] Others

Others, please specificy

3.13- According to your knowledge, at what stage of yam production does it rain the most in your area?

- ◯ Mounding time
- ◯ Seed planting
- ◯ Vegetative stage
- ◯ harvesting
- ◯ Others

Others, please specificy

____

3.14- When do you start harvesting?

- ☐ June for Early variety
- ☐ July for Early variety
- ☐ August for Early variety
- ☐ December for Late variety
- ☐ January for Late variety
- ☐ February for Late variety
- ☐ Others

Which dekad of June

- ◯ 1st dekad
- ◯ 2nd dekad
- ◯ 3rd dekad

Which dekad of July

- ◯ 1st dekad
- ◯ 2nd dekad
- ◯ 3rd dekad

Others, please specificy the month and the dekad

____

3.15- Does the harmattan coolness have an impact on yam production?

- ◯ No
- ◯ Yes

If yes, which ones?

- Moisten the soil to start the mounds
- Moistens the mounds to start the planting
- Dries the soil
- Dries the seed in the mound
- Others

Others, please specificy

3.16- Do you have a crop calendar for yam in the region?

- No
- Yes

If no, Would you like to have a monthly/annual rainfall report for yam cropping?

- Yes
- No
- Others

If yes, Is it reliable?

- Yes
- No

Others, please provide more accuracy

4.1- Do high land surface temperatures (LST) have an impact on yam production?

- No
- Yes

4.2- If yes, what are these impacts?

- [ ] Yam seed rot
- [ ] Inhibits microorganism's actions in the soil
- [ ] Delays bud growth
- [ ] Increases pests in the mound
- [ ] Slims down tubers
- [ ] Compacts and reduces soil porosity
- [ ] Others

Others, please specificy

5.1- What solutions have you found to deal with these impacts?

- [ ] Plan replacement seedlings
- [ ] Controlling the yam growing season
- [ ] Master the rainy season
- [ ] Controlling endogenous knowledge
- [ ] Replace the variety or species with another one in the next season
- [ ] Others

Others, please specificy

5.2- Which of these cultivation techniques do you use in yam production?

- [ ] ANADER
- [ ] CNRA
- [ ] SODEXAM
- [ ] Traditional Habits
- [ ] Endogenous knowledge
- [ ] Others

Others, please specificy

5.3- How do you predict crop failure?

- [ ] Staggered cropping periods between them
- [ ] Cultivation on soils of different texture
- [ ] Technical assistance
- [ ] Diversification of activities
- [ ] Diversification of yam varieties by DIOSCOREA ALATA
- [ ] Diversification of yam varieties by DIOSCOREA CYENINSIS
- [ ] Others

Which activities? please, be specific

Others, please specificy

B. Statistics on the physico-chemical characteristics of soils in the two sampling areas

B1. Table of raw values from laboratory

		% Organic matter			(ppm)	Complexe Absorbent (Cmol*kg-1)					% Particles size				
	pH	**C**	**N**	**C/N**	**P**	**CEC**	**Ca2+**	**Mg2+**	**K+**	**Na+**	**Clay**	**f-Silt**	**c-Silt**	**f-Sand**	**c-Sand**
Forest soil (Tanda)	5.4	1.17	0.12	9.93	94	12.4	1.131	0.60	0.123	0.097	10	6.6	22.24	21.5	40.15
	5.7	1.26	0.16	8.05	79	13.4	1.206	0.623	0.146	0.101	7	8.48	26.4	13.6	44.35
	5.6	1.28	0.13	9.54	119	15	1.168	0.578	0.087	0.089	8	12	15.6	23.2	40.95
	5.7	1.11	0.14	7.93	70	13	1.181	0.595	0.120	0.078	8.2	11	23.2	16.6	41.20
Savannah soil (Bondoukou)	5.7	0.40	0.11	3.79	24	3.6	0.775	0.398	0.428	0.121	6.1	6	12.2	16.8	58.11
	5.6	0.27	0.08	3.43	47	4	0.744	0.388	0.125	0.076	6.03	8	12.6	18.2	55.14
	5.6	0.50	0.12	4.24	53	4.6	0.976	0.499	0.099	0.068	6.2	12	16.8	18.0	45.74
	5.5	0.27	0.07	3.87	33	2	0.623	0.332	0.083	0.062	6	10	14	19.6	50.34

B2. Qualitatives appreciation of the soils contents

Property	**Forest soil (Tanda)**	**Savannah soil (Bondoukou)**
Texture (Particles size)	Often high in organic matter and clay content, which gives the soil good water-holding capacity and structure.	Often high in sand content, which can lead to poor water-holding capacity and drainage.
Organic matter content	High	Low to moderate
Cation exchange capacity (CEC)	High	Low to moderate
pH	Slightly acidic to neutral	Slightly acidic to neutral
Nitrogen	High	Low to moderate
Phosphorus	Moderate to high	Low to moderate
Potassium	Moderate to high	Low to moderate

C. Cover page of articles published

C1. Article published in 'Frontiers in Remote Sensing'

frontiers | Frontiers in Remote Sensing

TYPE Original Research
PUBLISHED 30 August 2023
DOI 10.3389/frsen.2023.1221757

Check for updates

Toward understanding land use land cover changes and their effects on land surface temperature in yam production area, Côte d'Ivoire, Gontougo Region, using remote sensing and machine learning tools (Google Earth Engine)

Kadio S. R. Aka[1,2]*, Semihinva Akpavi[3], N'Da Hyppolite Dibi[4,5], Amos T. Kabo-Bah[6], Amatus Gyilbag[7] and Edward Boamah[8]

[1]Faculty of Human and Social Sciences, University of Lomé, Lomé, Togo, [2]West African Science Service Centre on Climate Change and Adapted Land Use (WASCAL), Climate Change and Disaster Risk Management Program, University of Lomé, Lomé, Togo, [3]Botany and Plant Ecology Laboratory (LBEV), University of Lomé, Lomé, Togo, [4]Natural Environment Laboratory and Biodiversity Conservation, Department of Biosciences, Félix Houphouët-Boigny University, Abidjan, Côte d'Ivoire, [5]Center for Research and Application in Remote Sensing (CURAT), Félix Houphouët-Boigny University, Abidjan, Côte d'Ivoire, [6]Director of International Affairs, University of Energy and Natural Resources, Sunyani, Ghana, [7]3A Environmental Solutions Ltd., Sunyani, Bono Region, Ghana, [8]Digital Earth Africa, Accra, Ghana

OPEN ACCESS

EDITED BY
Nilanchal Patel,
Birla Institute of Technology, Mesra, India

REVIEWED BY
Mobushir Khan,
Charles Sturt University, Australia
Alireza Sharifi,
Shahid Rajaee Teacher Training University, Iran

*CORRESPONDENCE
Kadio S. R. Aka,
aka.k@edu.wascal.org

RECEIVED 12 May 2023
ACCEPTED 18 July 2023
PUBLISHED 30 August 2023

CITATION
Aka KSR, Akpavi S, Dibi NH, Kabo-Bah AT, Gyilbag A and Boamah E (2023), Toward understanding land use land cover changes and their effects on land surface temperature in yam production area, Côte d'Ivoire, Gontougo Region, using remote sensing and machine learning tools (Google Earth Engine).
Front. Remote Sens. 4:1221757.
doi: 10.3389/frsen.2023.1221757

Land use and land cover (LULC) changes are one of the main factors contributing to ecosystem degradation and global climate change. This study used the Gontougo Region as a study area, which is fast changing in land occupation and most vulnerable to climate change. The machine learning (ML) method through Google Earth Engine (GEE) is a widely used technique for the spatiotemporal evaluation of LULC changes and their effects on land surface temperature (LST). Using Landsat 8 OLI and TIRS images from 2015 to 2022, we analyzed vegetation cover using the Normalized Difference Vegetation Index (NDVI) and computed LST. Their correlation was significant, and the Pearson correlation (r) was negative for each correlation over the year. The correspondence of the NDVI and LST reclassifications has also shown that

C2. Article published in 'Journal of Agricultural Science'

Journal of Agricultural Science; Vol. 16, No. 5; 2024
ISSN 1916-9752 E-ISSN 1916-9760
Published by Canadian Center of Science and Education

Yam Production-Related Agro-climatological Risks and Yam Yield Modeling in Côte d'Ivoire: A Review

Kadio Saint Rodrigue Aka[1,2], Sêmihinva Akpavi[3] & N'Da Hyppolite Dibi[4,5]

[1] West African Science Service Centre on Climate Change and Adapted Land Use (WASCAL), Togo

[2] Climate Change and Disaster Risk Management Program, Department of Geography, Université de Lomé, Togo

[3] Faculty of Science, Botany and Plant Ecology Laboratory (LBEV), University of Lomé, Togo

[4] Natural environment laboratory and biodiversity conservation, Department of Biosciences, Félix Houphouët-Boigny University, Abidjan, Côte d'Ivoire

[5] Center for Research and Application in Remote Sensing (CURAT), Félix Houphouët-Boigny University, Abidjan, Côte d'Ivoire

Correspondence: Kadio Saint Rodrigue Aka, West African Science Service Centre on Climate Change and Adapted Land Use (WASCAL), Togo. E-mail: aka.k@edu.wascal.org

Received: September 13, 2023 Accepted: March 13, 2024 Online Published: April 15, 2024
doi:10.5539/jas.v16n5p42 URL: https://doi.org/10.5539/jas.v16n5p42

Abstract

In this paper, we present a review of the agro-climatological-related risk of yam production and models developed for yam yield prediction in Côte d'Ivoire. Four official national platforms (Ministry of Agriculture and Rural Development (MINADER), National Center for Agricultural Research (CNRA), National Agency for Rural Development Support (ANADER), Airport, Aeronautical and Meteorological Exploitation and Development Company (SODEXAM)) and six scientific search engines were investigated in this study including Theses.fr, African Journal Online, Science Direct, Google Scholar, WorldCat and Semantic Scholar. Using the boolean parameters "AND", "OR" and "()" to facilitate and direct our search, we were able to define four key phrases comprising the topic words that were used in the search. Exclusion and inclusion criteria for the selection of documents were also defined in advance, as well as the criteria for reviewing and extracting information from selected documents. The results showed that no work in the field of agro-climatological risks related to yam production and yam yield modeling in Côte d'Ivoire was available on these online research platforms at the time of this literature review. However, other studies similar to the scope of this review on yam exist in several West African countries, particularly Ghana, Benin and Nigeria, and also in the Caribbean. These studies use simulation models such as the Approach for Land Use Sustainability (SALUS) model, the Environmental Policy Integrated Climate (EPIC) model and the Cropping Systems Simulation (CROPSYST) model for growth, yield modeling and the influence of climatic parameters on yam. In addition to these models, artificial intelligence through machine learning models was also seen in this review as an excellent tool for yield prediction for several crops including yams.

Keywords: yam production, agro-climatological risks, yam yield modeling, literature review, Côte d'Ivoire

D. Letter for data collection in the field

D1. Wascal letters of candidate introduction

WASCAL

UNIVERSITÉ DE LOMÉ
FACULTY OF HUMAN AND SOCIAL SCIENCES
DOCTORAL RESEARCH PROGRAM
CLIMATE CHANGE AND DISASTER RISKS MANAGEMENT
Website : www.wascal-togo.org E-mail : wascal@wascal-togo.org

SPONSORED BY THE Federal Ministry of Education and Research

Université de Lomé

Lomé, 14 JUIN 2023

N°126/CC&DRM/D/DA/WASCAL/UL/2022

Prof. Komi BEGEDOU,
WASCAL Programme Deputy Director,
Doctoral Programme in
Climate Change and Disaster Risks
Management, DRP-CC&DRM,
Université de Lomé,
01P.O. Box: 1515
E-mail: prosbeg@gmail.com

TOGO.

To : MONSIEUR LE PREFET DE LA REGION DU GONTOUGO

Dear Sir / Madam,

LETTER OF INTRODUCTION

I am pleased to introduce Mr. Kadio Saint Rodrigue AKA, national of the Republic of Côte d'Ivoire and postgraduate male student in Climate Change and Disaster Risks Management with the West African Science Service Centre on Climate Change and Adapted Land Use (WASCAL), hosted in Université de Lomé, Republic of Togo.

Mr. AKA is pursuing his doctoral programme on the topic : **Yam production risks analysis for food security under Climate Change over Gontougo Region in Ivory Coast, West Africa.**

Kindly grant him the necessary assistance he may need during the course of his research field work.

Thank you for your kind consideration.

Yours sincerely,

UNIVERSITE DE LOME Faculté des Sciences de l'Homme et de la Société THE DEPUTY DIRECTOR DRP-CCDRM / WASCAL

République de Côte d'Ivoire * Préfecture de BONDOUKOU *

21-06-2023

Dr. Komi BEGDOU,
Associate Professor,
WASCAL Togo Deputy Director.

West African Science Service Centre on Climate Change and Adapted Land Use
Centre Ouest Africain de Services Scientifiques sur le Changement Climatique et l'Utilisation Adaptée des Terres

D2. Supervisor letter to the candidate requesting authorisation to access the study area

MINISTÈRE DE L'ENSEIGNEMENT SUPÉRIEUR ET DE LA RECHERCHE SCIENTIFIQUE

UNIVERSITE FELIX HOUPHOUET BOIGNY

Université Félix Houphouët-Boigny d'Abidjan – Cocody

WEST AFRICAN SCIENCE SERVICE CENTRE ON CLIMATE CHANGE AND ADAPTED LAND USE

WASCAL

Federal Ministry of Education and Research

Université de lomé
Faculty of Human and Social Sciences
Doctoral Research Program on Climate Change and Disaster Risk Management

DIBI HYPPOLITHE N'DA
PhD, Télédétection et SIG
Co-Superviseur de la Thèse
Université Félix Houphouët-Boigny
dibihyppoliten@gmail.com
Tél : (+225) 07 07 86 63 34

Abidjan, le 14 Juin 2023

A
Monsieur le Préfet de Région
GONTOUGO

Objet : Demande d'autorisation d'accès à la Région du Gontougo pour collecte de données sur la production de l'igname

Monsieur le Préfet,

Nous venons par la présente, solliciter une autoristaion d'accès à la circonscription administrative dont vous avez la charge, à Monsieur **AKA Kadio Saint Rodrigue**, étudiant ivoirien inscrit en Doctorat à Wascal-Togo sise à l'Université de Lomé au Togo, pour ses travaux de recherche.

En effet, dans le cadre de sa Thèse de Doctorat, Monsieur AKA Kadio conduit un projet intitulé ***« Analyse des risques liés à la production d'ignames pour la sécurité alimentaire face au changement climatique dans la région du Gontougo en Côte d'Ivoire, Afrique de l'Ouest»***

Pour mener à bien ses travaux de recherche, Monsieur AKA Kadio doit conduire des missions de collecte de données sur l'impact du changement climatique, les pratiques culturales et le mécanisme de résilience des producteurs d'ignames dans la région du Gontougo.
Ces missions sont prévues du 01/07/2023 au 31/07/2023.

Vous remerciant d'avance de votre sollicitude, nous vous prions d'agréer, Monsieur le Préfet, l'expression de nos salutations distinguées.

Ampliation :

- Préfet du département de Bondoukou
- Préfet du département de Koun-Fao
- Préfet du département de Sandégué
- Préfet du département de Tanda
- Préfet du département de Transua

Le Co-Superviseur de la Thèse

DR DIBI N'DA HYPPOLITE
MAITRE DE CONFERENCES
Université FHB / UFR Biosciences

Dr. DIBI N'Da Hyppolite
Maître de Conférences

Université Félix Houphouet-Boigny / UFR Biosciences / Laboratoire des Milieux Naturels et Conservation de la Biodiversité22 B.P. 801 Abidjan 22.

République de Côte d'Ivoire * Préfecture de BONDOUKOU

21-06-2023

TABLE OF CONTENTS